UNIVERSIDADE DE SÃO PAULO
Faculdade de Ciências Farmacêuticas
Programa de Pós-Graduação em Ciência dos Alimentos
Área de Bromatologia

Structural-dependent effects of dietary fibers in colon cancer: Focus on dietary fiber naturally changed by the papaya ripening

Samira Bernardino Ramos do Prado

Tese para obtenção do Título de Doutor
Orientador: Prof. Dr. João Paulo Fabi

São Paulo
2019

UNIVERSIDADE DE SÃO PAULO
Faculdade de Ciências Farmacêuticas
Programa de Pós-Graduação em Ciência dos Alimentos
Área de Bromatologia

Structural-dependent effects of dietary fibers in colon cancer: Focus on dietary fiber naturally changed by the papaya ripening

Samira Bernardino Ramos do Prado

Versão original da Tese conforme resolução CoPGr 6018.

Tese para obtenção do Título de Doutor
Orientador: Prof. Dr. João Paulo Fabi

São Paulo
2019

Ficha Catalográfica elaborada eletronicamente pelo autor, utilizando o programa desenvolvido pela Seção Técnica de Informática do ICMC/USP e adaptado para a Divisão de Biblioteca e Documentação do Conjunto das Químicas da USP

Bibliotecária responsável pela orientação de catalogação da publicação: Marlene Aparecida Vieira - CRB - 8/5562

P896s

Prado, Samira Bernardino Ramos do
Structural-dependent effects of dietary fibers in colon cancer: Focus on dietary fiber naturally changed by the papaya ripening / Samira Bernardino Ramos do Prado. - São Paulo, 2019.
327 p.

Tese (doutorado) - Faculdade de Ciências Farmacêuticas da Universidade de São Paulo. Departamento de Alimentos e Nutrição Experimental.
Orientador: Fabi, Joao Paulo

1. Alimentos. 2. Mamão papaia. 3. Fibra alimentar. 4. Câncer de cólon. I. T. II. Fabi, Joao Paulo, orientador.

Samira Bernardino Ramos do Prado

Structural-dependent effects of dietary fibers in colon cancer

Focus on dietary fiber naturally changed by the papaya ripening

Comissão Julgadora
da
Tese para obtenção do Título de Doutor

Prof. Dr.
orientador/presidente

_____
1o. examinador

_____
2o. examinador

_____
3o. examinador

_____
4o. examinador

São Paulo, _____ de _____ de 2019.

'ad astra per aspera'

Acknowledgments

I am grateful for so many things that I passed through to get this thesis done. It was certainly the four years of my life that I have grown as both a human being and at my professional skills. The people that were around me at this time could not be the best, especially my supervisor, the support that I have from my family and the best husband that I could have.

Firstly, I would like to acknowledge Professor João Paulo (a.k.a. Jota), thank you for being an example of human being, professor, supervisor, researcher, and friend. You believed in me since the begging to get this job done, even in the moments that I do not believe in myself, and it means a lot for me. You gave me the opportunity to learn and you were there to support me at the lab experiments when needed, discussing how we could answer our hypothesis, always questioning me and pushing me beyond. Besides that, you always are a good friend. I truly believe that you can make the world a better place by being a better person for those who are around us, and for me, you are one of these good persons making the world a better place. Thank you!

To the other professors of Laboratory of Food Chemistry, Biochemistry and Molecular Biology, Franco, Beatriz, João Roberto, Eduardo, and Neuza, I am very grateful and privileged to be part of this group! Being routinely part of such an excellent group that has different expertise and is very open to discussing science and research was essential to develop my scientific skills. You are all part of my growing and you are people that inspire me to achieve more in life. The seminars and lab meetings encourage me to be stronger in argue my point of views and to not get so nervous in doing presentations (with so many excellent researchers watching and debating). The staff members of the laboratory, Lucia, Tania, Aline, Luciane and Elias, thank you for all kind of support. I am very grateful and feel privileged to living this last seven years (MSc plus PhD time) next to all of you. And also all the colleagues that were not just part of the professional schedule but also in conversations during the coffee times and dinners.

The collaborations with professors Avraham Raz, Nicholas Carpita, Paul de Vos, Paulo Mourão, Christian Hoffmann, and Fernando Moreno were essential to get in this point of the research, thank you! The evaluation committee in my PhD qualification, Fernando Moreno, Beatriz Rosana Cordenunsi-Lysenko and Julio Cesar Madureira de Freitas Junior, thank you for the valuable suggestions and critics made in that point of my work.

The people who make me feel so welcomed at University Medical Center Groningen, Netherlands. Especially Professor Paul de Vos, who accepted to be my advisor there, and gave me the opportunity to learn so much at my time there. All the conversation – even the ones when he comes to São Paulo – making me look into different aspects of the research and from a different point of views. Thank you, Martin, to helps me to fit in the lab and all the assistance during the experiments. The people that I met there, Marijke, Bart, Renate, Susana, Luiz, ChengCheng, Gea, Sandra, Chunli, Marlies, Alexia, Shuxian, Christina and Yuanrui thanks for the great times and for receiving me so well.

I would like to dedicate this whole next paragraph to my lab friend, and most importantly my husband, Victor. You are the best person that I know in this world (and yes, I know how lucky I am to be surrounded by many good people!). These last six years that you are being part of my life daily could not be better. Your partnership and sense on how to conduct life are so much admired by me. I learn with you every day, and at a professional level you are an example of being an independent researcher. Thank you for being part of my agitated (and at the same time, calm) life, you made it better! I am sure that this work is done because of you by my side.

For my family, I am very grateful for having each of you! My parents and sisters that even with the distance, I can feel loved and motivated by you all! The emotional support that I received from you all made me go through this journey, it was not easy, but indeed worth it and was amazing!

RESUMO

PRADO, S. B. R. **Efeitos estrutura-dependente das fibras alimentares no câncer de cólon: foco na fibra alimentar naturalmente modificada durante o amadurecimento do mamão papaia**. 2019. 327f. Tese (Doutorado) – Faculdade de Ciências Farmacêuticas, Universidade de São Paulo, São Paulo, 2019.

O consumo de fibras alimentares (FA) está relacionado com vários benefícios à saúde como a diminuição no risco do desenvolvimento de câncer de cólon. A FA não é digerida pelas enzimas digestivas do trato gastrointestinal sendo fermentada pela microbiota intestinal do cólon. Como subproduto do processo de fermentação há a liberação de ácidos graxos de cadeia curta (SCFA) - como o butirato, o propionato e o acetato. Além do processo de fermentação, a FA pode interagir diretamente com as células epiteliais do intestino, induzindo mecanismos que também podem estar relacionados com os benefícios associados ao consumo de FA. A falta de informação sobre a FA e o câncer de cólon é, em partes, devido à complexidade de ambos, tanto do câncer quanto da estrutura da FA. As FA do mamão papaia são derivadas da parede celular da fruta apresentando diferentes estruturas dependendo do ponto de amadurecimento do fruto. Esse fato ocorre, pois, durante o amadurecimento do mamão papaia, existe uma extensa hidrólise dos polissacarídeos presentes na parede celular, diminuindo rapidamente a firmeza da polpa do fruto. Devido à falta de informações sobre FA e seus efeitos benéficos à saúde humana que são dependentes da sua estrutura, bem como a possibilidade do amadurecimento do mamão papaia naturalmente modificar as FA presentes na polpa dos frutos, a presente tese teve como principais objetivos: 1) avaliar como as enzimas que degradam a parede celular do mamão papaia afetam a solubilização e o peso molecular da parede celular do fruto; 2) investigar os efeitos diretos da pectina derivada de mamões verdes e maduros em linhagens de células de câncer, na interação com a galectina-3, e em células do tipo HEK que expressam receptores de reconhecimento de padrões (RRP); 3) avaliar a fermentação colônica humana *in vitro* utilizando as FA de mamões verdes e maduros; 4) avaliar em ratos com lesões pré-neoplásicas no cólon o efeito do consumo de ração com ou sem FA de mamões papaias verdes e maduros. As endopoligalacturonases foram relacionadas como as principais enzimas que atuam solubilizando a pectina da parede celular do mamão, afetando tanto a firmeza da polpa do fruto quanto a solubilização da pectina durante o amadurecimento. De modo geral, as FA dos mamões exerceram um efeito estrutura–dependente de acordo com a maturação do fruto. Nos experimentos utilizando linhagens de células de câncer, a pectina do mamão papaia maduro apresentou efeitos mais pronunciados na indução da morte e na inibição da migração e da agregação das células, bem como ativando os RRP, como por exemplo, os receptores do tipo toll-like, além de inibir a proteína pró-metastática galectina-3. As FA dos mamões também apresentaram diferentes resultados na fermentação colônica *in vitro* quanto à utilização das FA pelas bactérias do intestino, e também no perfil de crescimento dessas bactérias. Por fim, os animais que receberam a dieta com as FA dos mamões maduros apresentaram menor incidência de focos de criptas aberrantes do que os animais que receberam as FA provenientes de mamões verdes ou de celulose (FA da ração AIN-93G). Portanto, o estudo das FA dos mamões foi efetuado tanto durante o amadurecimento dos mamões quanto dos seus efeitos biológicos *in vitro* e *in vivo*, tendo gerado resultados inéditos relacionando as alterações bioquímicas endógenas dos frutos durante o amadurecimento com os possíveis efeitos benéficos da sua ingestão para a saúde humana.

Palavras-chaves: fibra alimentar; mamão papaia; amadurecimento; parede celular, câncer de cólon; fermentação *in vitro*; foco de cripta aberrante.

ABSTRACT

PRADO, S. B. R. **Structural-dependent effects of dietary fibers in colon cancer: Focus on dietary fiber naturally changed by the papaya ripening**. 2019. 327f. Tese (Doutorado) – Faculdade de Ciências Farmacêuticas, Universidade de São Paulo, São Paulo, 2019.

Dietary fiber (DF) consumption is related with several healthy benefits such as the decreasing risk of colon cancer development. The DF is not digested by the digestive enzymes and reach to colon where is fermented by the colonic microbiota. The fermentation process releases metabolites as short chain fatty acids (SCFA) – such as butyrate, propionate and acetate. Besides the fermentation process, the DF can directly interact with intestinal epithelial cells inducing mechanism that can also be related with the associated DF consumption benefits. The lack of information regarding DF and colon cancer are due to the complexity of both the cancer and the DF structure. The papayas DF are derived from the fruit cell wall, and they are probably naturally modified during ripening through a massive polysaccharide hydrolysis, because papayas show a very fast pulp softening. Due to the lack of information about DF and their beneficial effects to human health as well as the possibility of the natural papaya ripening to modifying the DF presented in the fruit pulp, the present thesis had as the primary objectives: 1) to evaluate how the cell-wall degrading enzymes affect the fruit cell wall solubilization and molecular weight; 2) to investigate the direct effects of the papaya pectin derived from unripe to ripe papayas in cancer cell lines, in galectin-3 interaction and in HEK cells expressing pattern recognition receptors (PRR); 3) to evaluate the human colonic *in vitro* fermentation using DF from unripe and ripe papayas as substrates; 4) to conduct an *in vivo* experiment using rats with pre-neoplastic colon lesions while receiving a diet with DF from unripe and ripe papayas. The endopolygalacturonases were the main enzymes acting on the solubilizing papaya cell wall pectin affecting both the papaya firmness and pectin structure. Overall, the papayas DF showed a ripening dependent structure–effects. In the cancer cell lines experiments, the ripe papayas pectin showed a more pronounced effects in inducing cancer cell death, inhibiting cancer cells migration and aggregation, activating PRR as toll-like receptors and inhibiting the pro-metastatic protein galectin-3. The DF from papayas also showed different aspects in colonic *in vitro* fermentation regarding the DF utilization by the bacteria and the bacteria abundance profile. Lastly, the animals receiving the diet with the DF from ripe papayas had less aberrant crypt foci in colon than the animals that received the DF from unripe papayas or cellulose (AIN-93G DF). Therefore, the study of papaya DF was carried out both during papaya ripening and its biological effects *in vitro* and *in vivo*, generating unprecedented results relating the endogenous biochemical changes of the fruits during maturation with the possible beneficial effects of their ingestion for health human.

Keywords: dietary fiber; papaya, fruit cell wall; fruit ripening; colon cancer; *in vitro* fermentation, aberrant crypt foci.

TABLE OF CONTENTS

	Rationale and outline of the thesis	19
Chapter 1	*Introduction part I: papaya ripening physiology*	
	Fast and Furious: Ethylene-Triggered Changes in the Metabolism of Papaya Fruit during Ripening	23
Chapter 2	*Papaya cell wall modification during ripening*	
	Physiological degradation of pectin in papaya cell walls: release of long chains galacturonans derived from insoluble fractions during postharvest fruit ripening	53
Chapter 3	*Introduction part II: dietary fiber and healthy effects*	
	Ingestion of non-digestible carbohydrates from plant-source foods and decreased risk of colorectal cancer: A review on the biological effects and the mechanisms of action	81
Chapter 4	*Most soluble citrus and papaya dietary fiber effects on cancer cell lines*	
	Part I: Migration and proliferation of cancer cells in culture are differentially affected by molecular size of modified citrus pectin	123
	Part II: Ripening-induced chemical modifications of papaya pectin inhibit cancer cell proliferation	165
Chapter 5	*Going further to try to understand the mechanisms behind the biological effects*	
	Ripening processes in papaya creates unique pectin structures with differential signaling effects on pattern recognition receptors	213
Chapter 6	*The less soluble pectin (chelate-soluble fraction) effects on cancer cells and galectin-3 interaction*	
	Chelate-soluble pectin fraction from papaya pulp interacts with galectin-3 and inhibits colon cancer cell proliferation	239
Chapter 7	*Unripe and ripe papayas dietary fiber in vitro fermentation*	
	Dietary fiber from unripe and ripe papaya differentially regulate microbiota composition: Evidence from an in vitro colonic fermentation study	267

Chapter 8 *In vivo: Unripe and ripe papayas dietary fiber used to feed rats with colon pre-neoplastic lesions*

Structure-dependent chemopreventive effects of dietary fiber from papaya in rats with colon pre-neoplastic lesions 293

Concluding remarks and perspectives 311

Appendices 315

Rationale and outline of the thesis

The present thesis is divided into chapters and this topic aims to explain the rationale that guided the work. The knowledge regarding the structure of dietary fibers has been growing in the last few years, and the structures that once appear to be responsible for minor effects on human intestine are now being related to distinct structure-dependent beneficial biological effects. In the present thesis, most of the chapters aim to explore different perspectives that together help on elucidate whether changes in the structure of dietary fiber from papaya cell wall during ripening influence its biological effects, focusing mainly on the effects of these dietary fibers on colon cancer.

Little is known about the effects of ripening on the structure of the dietary fiber derived from papaya cell wall, and even less about whether the changes in the structure of dietary fiber influences it effects on health. Thus, to gain further insight into these intriguing questions, we evaluated both the physiology of papaya fruit during ripening and the biological effects of its dietary fibers obtained at different ripening time points. These biological effects comprise mainly (1) effects on cancer cell lines treated directly with dietary fibers from papaya, (2) the colonic *in vitro* fermentation of dietary fibers from papaya, and (3) the *in vivo* effects of dietary fibers from papaya in rats with colon pre-neoplastic lesions. Overall, the idea is that the data described in the thesis help on contribute to a better understanding of the structure-function relationship of dietary fibers, as well as on contributing to the development of new concepts regarding the quality of dietary fibers for consumption as dietary supplements or through introducing specific dietary fiber rich-foods into the diet.

As the understanding regarding papaya ripening is crucial for this study, in **Chapter 1** we reviewed the physiology of papaya fruit during ripening, focusing mainly on the effects of ethylene on metabolism - which is one of the main responsible for triggering changes in cell wall (dietary fiber) structure during ripening. This review describes that a massive change in the cell wall during papaya ripening occurs resulting in fruit softness, with the role of cell wall degrading enzymes during papaya ripening being not fully understood, though. Therefore, on **Chapter 2** we explored the dynamics between the expression of the main enzymes responsible for cell wall degradation during papaya ripening and the changes of dietary fiber during papaya ripening. The results of this research article suggest that polygalacturonases massively act on papaya cell wall between

two and three days after harvesting, reducing the molecular size and increasing the solubilization of less soluble pectin. As the main changes in papaya cell wall during ripening appear to occur in pectin, we focused mainly on the study of papaya pectin fraction in the following parts of this thesis.

The recent advances regarding the effects of non-digestible carbohydrates (dietary fibers) from plant-source foods and their relationship with decreased risk of colorectal cancer were reviewed in **Chapter 3**. We described the dietary fiber-related health effects that can be divided into physicochemical effects, fermentation-related effects, and direct effects. In this review, we also included data that is presented detailed on the further chapters. This review provides insights not only to a better understating of the structure-function relationship between the intake of dietary fibers and the reduction in colon cancer risk but also to point aspects for improving nutritional recommendations for dietary fiber consumption. Finally, we highlighted that much more work still needs to be done in order to relate the structure of dietary fiber with their health effects to human consumption.

In the following chapters, we focus on the characterization of the most soluble dietary fibers from unripe and ripe papaya, as well as on their direct effects on colon cancer cell lines. However, as citrus pectin is one of the most studied dietary fiber, and only appears to have pronounced effects when its chemical structure is modified by chemical, enzymatic or thermic treatments, we decided to start exploring some biological effects of citrus pectin rather than start with papaya pectin (**Chapter 4 - part I**). Although the biological effects of modified citrus pectin on colon cancer are relatively well known, there was a lack of information regarding the biological effects of the modified citrus pectin fractions with distinct molecular size. Thus, we fractionated the modified citrus pectin according to their molecular size aiming to isolate the more active fraction, and therefore fulfill this missing information on literature regarding the well-known modified citrus pectin. We observed that modified citrus pectin fractions with smaller molecular size exerted more pronounced effects in of colon cancer cells death, as well as in inhibiting their migration. In **Chapter 4 (part II)** we studied the probable similar effects showed for the modified citrus pectin but using the papaya pectin obtained at distinct ripening time points. Papaya pectin fractions had different effects on cancer cell lines, which appear to be a structure-dependent effect. Papaya pectin from ripe (but not very ripe) showed the most pronounced effects on inducing the necroptosis of colon cancer cells and on inhibiting cancer cells migration. Besides not directly compared, the abovementioned results

suggested that while the modified citrus pectin must undergo a thermal treatment to obtain a more functional structure, the pectin from papaya could be naturally modified by cell wall degrading enzymes during the fruit ripening process. As we observed structural-dependent effects of papaya pectin at different ripening time points, we further explored the interaction between these pectin fractions and some cell receptors. The pectin interaction with the intestinal epithelial cells can be through several mechanisms, and as the intestinal cells express pattern recognition receptors, we investigated the interaction with both toll-like receptors (TLR) and nucleotide binding oligomerization domain (NOD)-like receptors. In **Chapter 5** we described the results that demonstrated the ability of papaya pectin to interact with TLR and NOD-like receptors. The activation of some TLR were observed only for the pectin fractions from ripe papayas, whereas the pectin fractions from unripe papayas appear to inhibit the activation of some TLR. At this point, the cell wall modification during papaya ripening lead to the formation of pectin fractions with unique polysaccharides structures, which were derived from less soluble pectin fraction (chelate-soluble) during papaya ripening, as proposed in **Chapter 2**. Since the whole fraction of the plant cell wall is ingested with the fruit, the next question arose was if the chelate-soluble fraction of papaya pectin could also exert different biological effects. This is because the less soluble pectin structures, the ones chelated with calcium through the "egg-boxes" structures, could be release during the digestion process. Therefore, on **Chapter 6** we investigated whether the chelate-soluble pectin (less soluble in water) had effects in cancer cell lines or whether the chelate-soluble could interact with the pro-metastatic protein galectin-3. Confirming our hypothesis, the chelate-soluble pectin extracted from the intermediate ripening point of papaya inhibited colon cancer cell lines proliferation and interacted with galectin-3. This data supports our previous results, which showed that differences in pectin structure resulting from the ripening process influence their direct effects in cancer cells.

In the last two chapters, we used the total cell wall extract (soluble and less soluble total dietary fiber) from unripe and ripe papayas to mimic the consumption and digestion of the whole dietary fiber from papayas instead of a specific fraction. In **Chapter 7** we presented the results from *in vitro* human colonic fermentation using the dietary fibers from unripe and ripe papaya. Besides the production of short chain fatty acids were similar for dietary fiber from both unripe and ripe, they were higher than apple pectin and lactulose (two fermentable polysaccharides used as standards). The bacteria utilization of the papayas dietary fiber within distinct ripening point was different, and the bacteria profile

also had some distinctions after fermentation between unripe and ripe fibers. The last part of this thesis, **Chapter 8**, brings out one of the remaining questions: whether the dietary fibers from the unripe and ripe papaya differently affect the development of pre-neoplastic colon cancer lesions. In this study, rats were chemically induced with azoxymethane to develop pre-neoplastic lesions in the colon and were then feed with dietary fiber from unripe or ripe papaya. The main results were measured by counting the aberrant crypt foci, and the dietary fiber from ripe papaya seemed to inhibit the lesions, especially the ones closer to the proximal part of the colon (closer to the cecum).

Therefore, this study contributed to the lack of information regarding the structure-function relationship between dietary fiber derived from plant sources and their biological effects. More information about the general conclusions and perspectives are available at the end of the thesis, in the 'Concluding remarks and perspectives' topic.

Chapter 1

Fast and Furious: Ethylene-Triggered Changes in the Metabolism of Papaya Fruit during Ripening

João Paulo Fabi[1,2,3*], Samira Bernardino Ramos do Prado[1,2]

[1]Department of Food Science and Experimental Nutrition, School of Pharmaceutical Sciences, University of São Paulo, São Paulo, SP, Brazil
[2]Food Research Center (FoRC), CEPID-FAPESP (Research, Innovation and Dissemination Centers, São Paulo Research Foundation), São Paulo, Brazil
[3]Food and Nutrition Research Center (NAPAN), University of São Paulo, São Paulo, Brazil

Frontiers in Plant Science, Submitted, 2019.

Abstract

Papaya is a climacteric fleshy fruit characterized by a fast ripening after harvest. During the relatively short postharvest period, papaya fruit undergoes several changes in primary metabolism that result in pulp softening and sweetening, as well as the development of a characteristic aroma. Since papaya is one of the most cultivated and appreciated tropical fruit crops worldwide, extensive research has been conducted to not only understand the formation of the quality and nutritional attributes of ripe fruit but also to develop methods for controlling the ripening process. However, most strategies to postpone papaya ripening, and therefore to increase shelf life, have failed to maintain fruit quality. Ethylene blockage precludes carotenoid biosynthesis, while cold storage can induce chilling injury and negatively affect the volatile profile of papaya. As a climacteric fruit, the fast ripening of papaya is triggered by ethylene biosynthesis. The generation of the climacteric ethylene positive feedback loop is elicited by the expression of a specific transcription factor that leads to an up-regulation of 1-*aminocyclopropane-1-carboxylic acid* (ACC) *synthase* (ACS) and *ACC-oxidase* (*ACO*) expression, triggering the system II ethylene biosynthesis. The ethylene burst occurs about three to four days after harvest and induces pectinase expression. The disassembling of the papaya cell wall appears to help in fruit sweetness, while glucose and fructose are also produced by acidic invertases. The increase in ethylene production also results in carotenoid accumulation due to the induction of cyclases and hydroxylases, leading to yellow and red/orange colored pulp phenotypes. Moreover, the production of volatile terpene linalool, an important biological marker for papaya sensorial quality, is also induced by ethylene. All these mentioned processes are related to papaya sensorial and nutritional quality. We describe the understanding of ethylene-triggered events that influence papaya quality and nutritional traits, as those characteristics are a consequence of an accelerated primary metabolism during fruit ripening.

Key-words: papaya; climacteric fruits; ethylene; primary metabolism; cell wall; sugars; carotenoids, volatiles.

Abbreviations: ACC, 1-aminocyclopropane-1-carboxylic acid; AI, acid invertase; ACO, 1-aminocyclopropane-1-carboxylic acid oxidase; ACS, 1-amino cyclopropane-1-carboxylic acid synthase; BFF, β-fructofuranosidase; ZDS, ζ-carotene desaturase; CHYB, carotene hydroxylases; GC-O, chromatography-olfactometry; ERFs, ethylene response factors; GalA, galacturonic acid; GPP, geranyl diphosphate; Glc, glucose; HG, homogalacturonan; LIS, linalool synthase; LCY-β, lycopene β-cyclases; 1-MCP, 1-methylcyclopropene; MEP, 2-C-methyl-D-erythritol 4-phosphate; PL, pectate lyases; PME, pectin methyl esterases; PG, polygalacturonases; PDS, phytoene desaturase; RG-I, rhamnogalacturonan type I; RG-II, Rhamnogalacturonan type II; SAM, S-adenosyl methionine; SPS, Sucrose phosphate synthase; STP, sugar transporter; SS, sucrose synthase; UDP-Glc, diphosphate glucose; UTR3, UDP-galactose transporter 3; XG, xylogalacturonans; XYL, xyloglucan; Xyl, xylose.

Introduction

Papaya (*Carica papaya* L.) is a typical climacteric fleshy fruit that is appreciated worldwide because of the sweetness and characteristic flavor of its soft yellow or orange/red pulp [1,2]. Tropical countries from Asia are the main producers of papaya, accounting for 56% of worldwide production. However, countries from South America (16%), Africa (10%), and Central America (9%) are also important producers of papaya (Food and agriculture Organization of the United Nations [FAOSTAT], 2017). As papayas have a relatively short shelf life compared to other fruits, maintaining fruit quality during transport from producing countries to consumer centers (e.g., USA and Europe) is a challenge. In 2016 the main countries that produced papayas for exportation were Mexico (47%), Guatemala (14%), and Brazil (11%; FAOSTAT, 2017), with Mexico being the main supplier to the United States and Brazil the main supplier to Europe [5].

European recommendations for papaya exporting countries take into account fruit softening as a determinant factor in fruit shelf life [6], since the fast softening during papaya ripening facilitates physical injury during handling and transportation. Thus, as the susceptibility of papayas to disease increases proportionally with softening [7], the recommendation for exportation is to maintain the fruit at 10 ºC during shipping to prevent overripening due to heat [6]. However, as will be discussed later, low temperatures negatively impact some fruit quality attributes of ripe papayas.

The ripening of fleshy fruits is a physiological process that alters appearance, texture, flavor, and aroma. These changes function to attract seed-dispersing organisms [8]. In climacteric fruit, such as tomatoes, bananas, and papayas, the onset of ripening coincides with an increase in respiration and ethylene production, the latter being essential to induce molecular mechanisms responsible for accelerating senescence and for the physiological changes that occur during ripening [9,10]. The ripening process in climacteric fruits induces changes in both sensorial and nutritional qualities that are essential for consumer acceptability. Some climacteric fruits are harvested unripe and treated with exogenous ethylene or ethylene-derived molecules to precipitate ripening. Thus, ethylene appears to be the main hormone responsible for regulating the molecular pathways that influence the development of the sensorial and nutritional attributes of climacteric fruits [11]. It has long been known that the safe and effective control of ethylene-mediated responses could extend

the postharvest shelf life of climacteric fruits [12]. However, interfering with natural ethylene-mediated responses during ripening could also negatively impact fruit quality.

While the mechanism by which ethylene is involved in fruit ripening has been thoroughly studied, efforts are still needed to fully understand this process. The ethylene burst in climacteric fruit is controlled by an autocatalytic mechanism, named system II, that synthesizes ethylene [13,14]. Ethylene synthesis involves the conversion of S-adenosyl methionine (SAM) to 1-aminocyclopropane-1-carboxylic acid (ACC) by the action of 1-amino cyclopropane-1-carboxylic acid synthase (ACS), in which ACC is converted to ethylene by ACC oxidase (ACO) [15]. ACS and ACO enzymes have already been identified in papayas, and their responses are increased with ethylene production and reduced when ethylene is blocked [16]. A decrease in ACS and ACO occurs in papayas stored at low temperatures, but levels are restored after exogenous ethylene treatment [17]. The ethylene downstream cascade involves multiple transcription factors, including ethylene response factors (ERFs), that are involved in the control of plant growth, defense, responses to the environment, and plant hormones [18], including those involved in the papaya ripening process [19]. Transcription factors of the MADS-box, NAC and AP2/ERF gene families are also involved in the control of papaya ripening [20]. More recently a NAC transcription factor, rather than MADS transcription factors, was found to regulate ACS and ACO expression during papaya ripening [11]. Papaya has not undergone whole-genome duplication, unlike other climacteric fruits where this process has been utilized to duplicate the MADS transcription factors that form the ripening circuits [21,22]. NAC is one of the largest plant-specific transcription factor families, with members involved in many developmental processes such as senescence, stress, cell wall formation, and embryo development [11]. Lü et al. (2018) have suggested that instead of neofunctionalization of the duplicated MADS genes, plants without whole genome duplication may have repurposed their carpel senescence NAC to generate a positive feedback loop where ethylene regulates ripening, as is the case with papayas. They also suggested that ethylene generated by this feedback loop is autocatalytic. A NAC transcription factor expressed in climacteric fruits, such as papayas and peaches, binds to the promoter regions of some of the key ripening-related genes stimulating their expression in pigment accumulation, volatile secondary metabolite production, cell wall softening, and sugar accumulation [11].

Therefore, the ethylene-mediated effects in fruit metabolism that influence the softening, sweetness, flavor, and color of papaya pulp during ripening will be further discussed.

1. Pulp softening is the main biochemical modification that occurs during papaya ripening

In climacteric fleshy fruits, researches and producers give special attention to ethylene-induced textural changes during ripening, as changes in peel and pulp influence softening, crispness, and juiciness [23] but also increase postharvest losses [7]. In fact, textural changes in most of the fleshy fruits result from complex mechanisms that primarily influence plant cell wall architecture, whose breakdown is considered as the major factor responsible for the pulp softening process [24].

The cell wall architecture of fleshy fruits is comprised of complex polysaccharides, such as pectin, hemicellulose, and cellulose, as well as minor components including proteins and phenolic compounds [25]. Cellulose is comprised of long, rigid, and inextensible microfibrils of 1,4-β-D-glucose (Glc) residues, which are bound tightly together by hydrogen bonds [24]. Hemicelluloses represent a diverse range of structural polymers that constitute the plant cell wall within fruit pulp [26]. In dicotyledonous plants, such as papayas, xyloglucan (XYL) is the major hemicellulose [27]. As with cellulose, XYL consists of a backbone of 1,4-β-D-Glc residues such as cellulose, but smaller and substituted with 1-6-α-D-xylose (Xyl) side chains. Furthermore, these Xyl side chains can be substituted at the O-2 position with β-galactose (Gal) or α-arabionse (Ara; Scheller and Ulvskov, 2010). Pectin is a complex and heterogeneous polysaccharide that is mainly comprised of α-1,4-D-galacturonic acid (GalA) residues that have varying degrees of acetyl and methyl esterification, and these residues are called homogalacturonan (HG). Xylosylation may further modify HG into xylogalacturonans (XG). Pectin also contains structures made up of repeating units of intercalated GalA (1,4-α-D-GalpA) and rhamnose (1,2-α-L-Rhap) called rhamnogalacturonan type I (RG-I). These structures have side groups of arabinose (arabinan), galactose (galactan), and type I arabinogalactan at the O-4 position of the Rha residues [28,29]. Rhamnogalacturonan type II (RG-II) structures are less common in papayas and are composed of HG molecules with side groups of up to 13 different sugars and more than 20 types of glycosidic linkages [28,30]. The firmness of fleshy fruits results from turgor pressure maintenance by the cell wall while also

maintaining cellular adhesion [31]. Pulp softening occurs by the water dissolution of the majority of these polysaccharides from the primary cell wall and middle lamella, with pectin being the main one [32].

Structural changes that occur in the cell wall during ripening are regulated by hydrolases responsible for degrading cell wall polysaccharides [9,33], whose expression is generally regulated by ethylene production [27]. Fruit softening is a complex event that involves several enzymes including pectinases and hemicellulases; however, pectinases, such as polygalacturonases (PGs), pectate lyases (PLs), and pectin methyl esterases (PMEs) appear to be the major enzymes that act on fleshy fruit softening. Polygalacturonases remove the galacturosyl residues from pectin [34], PLs cleave de-esterified pectin [35], and PMEs hydrolyze methyl-groups of esterified polyuronides [36]. Furthermore, side chains of pectin can be degraded by other glycosidases, such as β-galactosidases, which remove the galactosyl residues from pectin and from XYL [37]; α-arabinofuranosidases, which remove arabinosyl from pectin [38,39]; and rhamnogalacturonases, which remove α-1,2 linkages between galacturonosyl and rhamnosyl residues [40].

Despite multiple glycoside hydrolases seeming to be responsible for papaya softening, the main enzymes that play a central role in pulp softening are the PGs [41]. Some contribution of hemicellulose degradation to pulp softening appears to occur as an increase in endoxylanase expression occurs during papaya ripening [42]. Furthermore, β-galactanases are also related to papaya pulp softening through the hydrolysis of both the pectic and the hemicellulosic fractions [41,43]. In order to understand the role of ethylene in the expression of cell wall-degrading enzymes, researchers have treated papayas with 1-methylcyclopropene (1-MCP), an ethylene antagonist. As expected, this had a strong effect on pulp softening [1]. The pulp firmness of 1-MCP-treated papayas decreased marginally during ripening, although not enough to reach an edible state, and there was no detectable PG activity. Notably, 1-MCP-treated papayas were unable to soften at the same rate as untreated papayas [1,44,45]. Treatment with 1-MCP also reduced endoxylanase protein levels [42].

To confirm that ethylene affects PG activity and, therefore, pulp softening during papaya ripening, Fabi et al. (2009) found that treatment with exogenous ethylene had induced PGs expression with a concomitant increase in pulp softening. Furthermore, agroinfiltration of PG1 in 1-MCP-treated papayas significantly enhanced pulp softening compared with 1-MCP-treated papayas that were agroinfiltrated with an empty vector [41].

Papaya cell wall structural changes during ripening involve pectin with the solubilization of long chains of galacturonans and a decrease in the molecular weight of polysaccharides [7,46,47]. Polygalacturonases act on papaya pulp softening by mobilizing high molecular weight pectin from less soluble to more soluble cell wall fractions, especially pectin that is tightly bound to cellulose/hemicellulose, and pectin that are bound to each other by calcium bridges [48]. Furthermore, the degree of methyl esterification in papaya pectin changes during ripening since unripe papaya pectin has a lower degree of methyl esterification compared to ripe papaya pectin [7,49–51]. This variation during papaya ripening was firstly associated to higher PME activity [7]. However, no increase in gene expression of PME appears to occur during papaya ripening [20,41,48,52], and the activity of PG does not require the simultaneous removal of methyl-esterified groups from pectin [41]. Therefore, recent studies support the hypothesis that the increase in the degree of methyl esterification during papaya ripening is a result of the enrichment of the water-soluble pectin fraction that comes from the insoluble fraction due to the massive action of PG rather than an association with increased PME activity (**Figure 1**; Fabi et al., 2014; Prado et al., 2016, 2017). The resulted high methylated low-molecular pectin found in ripe papayas showed anticancer effects in diverse *in vitro* tests [49,50].

Although the use of MCP-1 is useful in gaining further insight into the role of ethylene in papaya softening, cold storage is another way to decrease ethylene action after harvesting. This latter approach is useful as a postharvest technique as it decreases fruit ripening rates and, therefore, pulp softening [53]. The storage of 'Golden' papaya at 10 °C for 10 days had been found to be effective in reducing ethylene production and fruit ripening. Notably, after a 10-day cold storage, fruits can be stored at room temperature to restore ethylene production and pulp softening [53]. However, when cold storage occurs for a longer period (e.g., 20 days at 11 °C), ethylene production did not recover when the fruit was subsequently stored at ambient temperatures [54]. It seems that the prolonged inhibition of ethylene, either by the inhibition of receptor sites (1-MCP) or by prolonged

storage at low temperatures, strongly affects the recovery of the ethylene-mediated response, which negatively influences the pulp softening that is crucial to the quality of the ripe fruit.

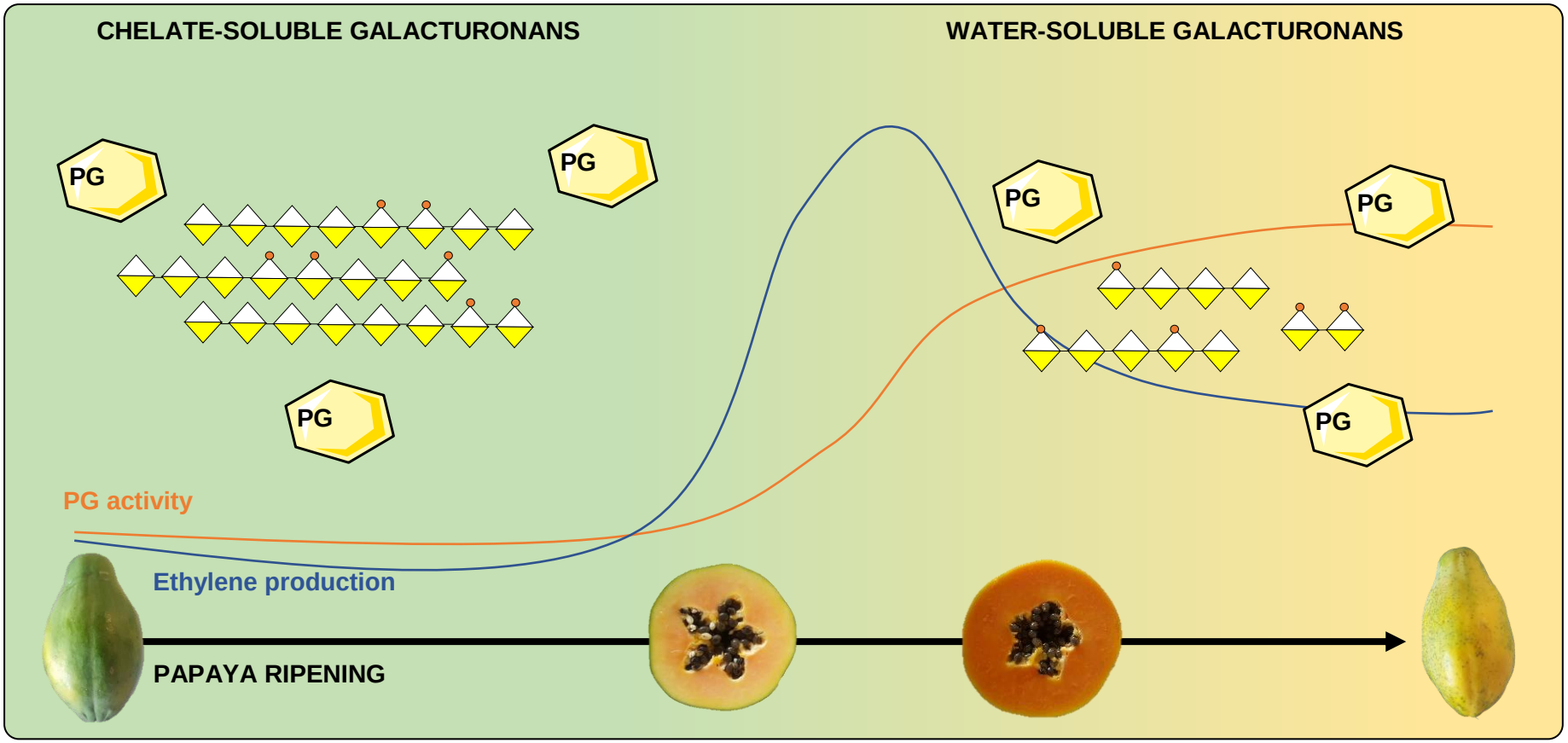

Figure 1. Ethylene production and PG activity during papaya ripening: papaya pectin cell wall solubilization. Ethylene triggers PGs that massively solubilize high molecular weight pectin by action in the non-methylated areas and releasing the low molecular weight fractions that will be enriched in methylated fractions due to the lower activity of PME in ripe papayas. PG: polygalacturonase.

2. Pulp sweetness as a result of papaya primary metabolism

The qualitative and quantitative composition of primary soluble sugars is crucial to papaya sweetness, although fruit firmness also plays a role as there is a correlation between pulp softening and the perception of sweetness during consumption [55]. Thus, it is necessary to understand the key regulatory enzymes involved in the metabolism of soluble sugars, as well as the endogenous and exogenous factors that influence these biochemical pathways, so as to improve both preharvest management and postharvest handling to increase the final sensorial quality of ripe papayas. In papayas, the increment in soluble sugars occurs mainly during fruit growth while still attached to the plant [56].

In most fleshy fruits, there are three main enzymes that have a key regulatory role in the accumulation of soluble sugars: Sucrose phosphate synthase (SPS), sucrose synthase (SS), and acid invertase (AI; Zhou and Paull, 2001). In papayas, sugar accumulation begins after seed maturation and is accompanied by increased activity of SS during fruit development. Acid invertase also appears to increase throughout papaya development [56], and its expression is reduced in harvested unripe papayas. Another increase in AI expression has also been observed after the onset of ethylene production during ripening [57]. Sucrose phosphate synthase activity remains low throughout papaya development however [56]. After harvesting, SPS activity follows the tendency of sucrose formation, since the ratio between SPS activity and sucrose content is constant throughout the papaya ripening process [55]. SPS is a highly conserved glycosyltransferase in dicots that catalyzes the transfer of glucose from uridine diphosphate glucose (UDP-Glc) to D-fructose-6-phosphate, thereby forming D-sucrose-6-phosphate [58]. As SPS also catalyzes the reversible reaction, it is considered as a key control point of sucrose biosynthesis in both monocots and dicots [59]. Sucrose synthase is also a glycosyltransferase, but it catalyzes the reversible formation of UDP-Glc and D-fructose from UDP and D-sucrose [60]. Although SS could act in Glc linked to other nucleotide diphosphate sugars than UDP, such as adenosine diphosphate glucose (ADP-Glc), UDP is the preferred substrate in plants [61]. Finally, AI can control the balance between sucrose, glucose and fructose in fleshy climacteric fruits by an irreversible reaction that cleaves sucrose [62].

Climacteric fruits, such as bananas, commonly increase soluble sugars content after harvesting through starch degradation, which directly correlates with pulp sweetening (Shiga et al., 2011; Aquino et al., 2016). Since unripe papayas have low starch content (less

than 3% by fresh weight; Oboh et al., 2015), most of the soluble sugars in papayas accumulate during fruit development. However, there is also an increase in sucrose, glucose, and fructose, as well as a pattern of expression and activity of both AI and SPS during ripening [55,57]. These results suggest a possible role for ethylene-mediated effects on soluble sugar accumulation in ripe papayas. This hypothesis was confirmed by a previous study of our group [1], which demonstrated that 1-MCP-treated papaya have a distinct pattern of sucrose synthesis during ripening compared to untreated papayas. More recently, Shen et al. (2017) showed that other genes related to soluble sugar metabolism, including *UDP-galactose transporter 3* (*UTR3*), *sugar transporter* (*STP*), and *β-fructofuranosidase* (*BFF*), were induced during the ripening of ethylene-treated papaya and reduced in 1-MCP-treated papaya. However, despite ethylene appearing to be important in enhancing *UTR3*, *STP*, and *BFF* expression, it is unknown whether ethylene-induced changes in the expression pattern of these enzymes affect soluble sugar metabolism during ripening and, therefore, the sensorial quality of papaya.

During papaya ripening, the sucrose content appears to reduce after the onset of ethylene production, which is in agreement with the increase in AI expression [55,67]. In contrast, 1-MCP-treated papayas have been found to have a 10-fold higher level of sucrose compared to untreated ripe fruit [1]. Thus, as AI activity appears to be strongly regulated by ethylene during papaya ripening (**Figure 2**), exogenous treatments or conditions that affect ethylene production may affect the ratios between sucrose, glucose and fructose, thereby influencing pulp sweetness.

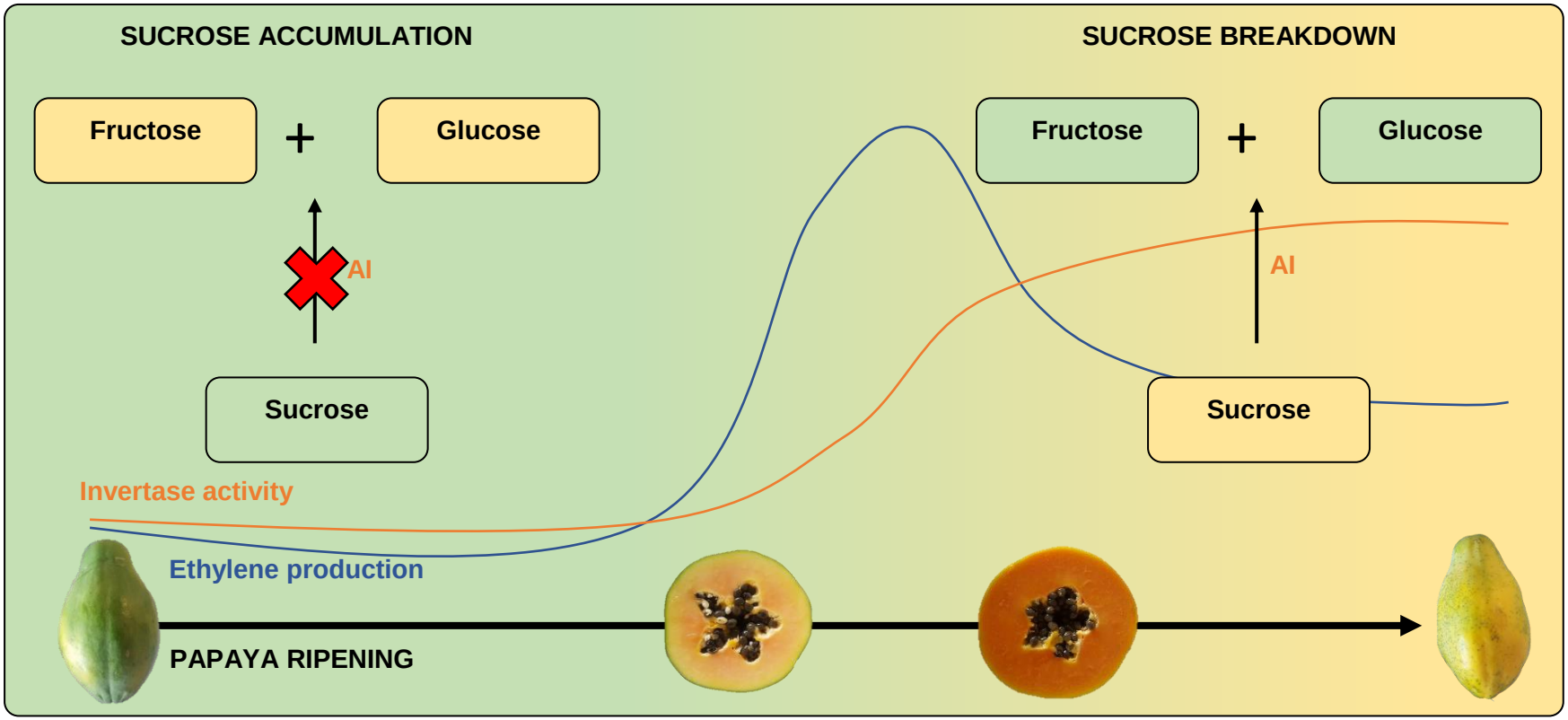

Figure 2. Ethylene production and invertase activity during papaya ripening: papaya sucrose breakdown. Invertase activity is regulated by ethylene burst since sucrose is higher in unripe papayas or in papayas that ethylene perception were blocked, with a subsequent increase in fructose and glucose after ripening/ethylene production. AI: acid invertase.

The use of gamma irradiation in fleshly fruits such as guavas [68] and tomatoes [69] could represent an effective method for fruit decontamination thus reducing postharvest losses [70]. Depending on the intensity of the applied gamma irradiation, the sensorial quality of fruits could be negatively affected because of irradiation-induced changes in fruit metabolism. In papaya, the application of standard irradiation intensities between 0.5 and 1.0 kGy in unripe fruit did not appear to negatively influence fruit ripening [71]. However, analysis of fruit metabolism revealed that these gamma irradiation intensities could reduce soluble sugars content in ripe papayas. This reduction appears to be related to a decrease in AI activity, and these changes are associated with reduced ethylene production throughout the ripening of the irradiated fruit [57].

In addition to gamma irradiation, ozone application has been proposed as a method for fruit decontamination. Furthermore, ozone treatment is used to extend shelf life by reducing oxygen concentrations during fruit storage and shipping, thereby delaying the ripening of climacteric fruits [72]. Thus, as ozone influences fruit respiration and therefore the onset of ethylene production in climacteric fruits, it is expected that this postharvest treatment will also affect soluble sugar metabolism during papaya ripening. Although a previous study did not report significant differences between the total soluble solid content of ozone-treated and untreated papayas [73], the soluble sugars ratio between sucrose and glucose/fructose in ripe fruits could be altered. Recently, the treatment of unripe papaya with plant extracts, such as Neem (*Azadirachta indica* Juss), has been proposed as an alternative for maintaining food quality for a longer postharvest period [74]. However, as with ozone treatment, the observation of fruit quality maintenance for a longer period was not accompanied by an evaluation of soluble sugar metabolism. Therefore, further studies are needed to confirm the effects of ozone as well as other postharvest treatments that may affect ethylene production, since there is a clear role of ethylene on enzymes that orchestrate the metabolism of soluble sugars during papaya ripening.

3. Climacteric alteration of papaya flavor

Papayas have a characteristic sweet flavor that has been studied for more than half a century [75,76]. The volatile profile of papaya consists of a mixture of compounds including esters, terpenes, alcohols, and ketones [77–81]. Although there is great heterogeneity among the volatile profiles of distinct papaya varieties [78,80,82], some compounds appear to be characteristic of the papaya aroma. In this context, linalool and

their oxidative derivatives are generally regarded as the main volatile compounds in most of the distinct cultivars of papaya [53,83,84] along with low molecular weight esters, including ethyl butanoate and methyl butanoate [77,85,86]. Considering that the increase in volatile esters is significantly higher in harvested papayas compared to fruit that is still attached to the plant [81], and considering the magnitude of difference between the volatile profiles of unripe and ripe papayas [53,81], it appears that ethylene plays an important role in the development of flavor during papaya ripening.

Balbontín et al. (2007) suggested that most of the volatile esters synthesized during papaya ripening are derived from primary metabolism compounds, such as fatty acids and amino acid. The release of these compounds is stimulated by ethylene treatment [87,88]. Ethyl acetate, ethyl octanoate, and methyl hexanoate were also found to not be induced in 1-MCP-treated papayas, whereas ethylene-induced papayas increased the amounts of these volatile esters throughout ripening [86]. Interestingly, volatile esters with a higher molecular weight, including butyl hexanoate and octyl acetate, reached higher values in 1-MCP-treated papayas compared to both untreated and ethylene-treated papayas. These results suggests that only the synthesis of the main esters related to aroma quality in ripe papaya—which are those volatile compounds with lower molecular weight produced from C1 and C2 alcohols and C6 and C8 acyl-coenzyme A—were enhanced during the onset of ethylene production [86].

The volatile profile of ripe papayas also consists of branched-chain volatiles [84,89] derived mainly from the amino acid precursors isoleucine and valine, which are responsible for the formation of ethyl-2-methyl and butyl-2-methyl esters. The synthesis of these branched-chain volatiles also appears to be regulated by ethylene, as 1-MCP treated papayas have reduced ethyl-2-methyl butanoate levels [86].

The abovementioned results regarding the synthesis of volatile compounds during ripening provide insights into the development of aroma in ripe papayas. However, little is known about the relationships among the metabolism of these volatile compounds and the sensorial quality of the ripe fruit. In this context, a recent study applied a gas chromatography-olfactometry (GC-O) assisted approach to optimize the extraction and detection of the main volatile compounds responsible for the aroma of ripe papayas [89]. In GC-O a panel of human assessors describes the aroma of each of the volatile compounds from a sample that has been previously separated through gas chromatography, allowing

the identification of the main peaks responsible for the overall aroma of the sample [90]. In summary, GC-O refers to the use of human assessors as a sensitive and selective detector of odor-active compounds [91], and it is a useful tool to assess the contribution of each volatile compound to a fruit's aroma. Studies have successfully applied GC-O-assisted approaches or aroma dilution analysis to assess the volatile profile of papayas [77,89,92]. Jirovetz et al. (2003) and Pino (2014) found linalool as the major compound in papaya flavor. However, the major compounds considered as odor-active and contributors to the typical papaya aroma found in other studies were δ-octalactone (sweet and herbal), benzyl isothiocyanate (papaya), methyl butanoate (fruity), and ethyl butanoate (fruity; Pino 2014; Rocha et al., 2017).

Gomes et al. (2016) explored the volatile profile of papayas in response to cold storage, which clearly affects ethylene production [54]. The authors explored if the cold storage of papayas at temperatures in which the fruit is resistant to cold injury influenced the volatile profile in ripe papayas. The authors found that when papayas were left at 10 °C for 10 days and then subsequently at ambient temperature to complete the ripening process, the fruits were able to restore ethylene production, as well as the development of the loss of green color and the increase in pulp softening to a similar extent to that of fruit stored at ambient temperature, but the process was postponed by a few days. However, there were striking differences between the volatile profiles of the two groups. Interestingly, the synthesis of linalool, regarded in GC-O as one of the main volatile compounds in papaya, was affected by cold storage. These reduced linalool levels in cold-stored papayas appeared to be related to the downregulation of *linalool synthase* (*LIS*) expression [53]. Façanha (2016) also found reduced levels of linalool throughout the ripening of 1-MCP-treated papayas and increased levels of this volatile compound in ethylene-treated papayas. Thus, as LIS uses geranyl diphosphate (GPP) to synthesize linalool in a single step reaction [94], the reduced *LIS* expression, and therefore reduced levels of linalool in both cold storage papayas and in 1-MCP-treated papayas, strongly suggests a possible role of ethylene in linalool biosynthesis through modulation of *LIS* expression.

GPP originates from the plastid-localized 2-C-methyl-D-erythritol 4-phosphate (MEP) pathway, which is important not only in the biosynthesis of linalool and other volatile compounds, including β-ionone and 6-methyl-5-hepten-2-one, but also in

carotenoid biosynthesis and in the development of the characteristic of pulp color in ripe papayas.

4. Pulp color changes in ripening papayas as a consequence of carotenoid synthesis

The characteristic color of ripe papaya pulp (yellow or orange/red) is due to different types of carotenoids. Carotenoids are molecules with a general structure that consists of a 40-carbon acyclic polyene chain containing 9–11 conjugated double bonds and with or without terminating rings, and they are classified as carotenes (hydrocarbons) or as xanthophylls (oxygenated derivatives; Khoo et al., 2011). Distinct papaya varieties have different pulp colors depending mainly on their carotenoid metabolism during ripening. In general, orange/red varieties have relatively high amounts of lycopene, which is a central compound in the metabolism of carotenoids during papaya ripening and is responsible for the red color not only in papayas [96] but also in tomatoes [97], guavas [98], and watermelons [99].

Most of the over 600 naturally occurring carotenoids [100] originate from the MEP pathway (**Figure 3A**), which starts with a reaction between pyruvate and glyceraldehyde-3-phosphate, resulting in the downstream production of isopentenyl diphosphate (IPP) and dimethyl allyl diphosphate (DMAPP; Ruiz-Sola and Rodríguez-Concepción, 2012; Yang and Guo, 2014). Then, three IPP molecules and one DMAPP molecule are used as substrates by geranyl-geranyl diphosphate (GGPP) synthase for the synthesis of GGPP, a 20-carbon molecule [103]. In addition to the presence of relatively high levels of lycopene, orange/red papayas present lower amounts of carotenoids that are synthesized downstream to lycopene in the MEP pathway, such as β-carotene, β-cryptoxanthin, and zeaxanthin [104]. For both papaya cultivars ‘Golden’ and ‘Sunrise Solo’, all-trans-lycopene was the main carotenoid in early stages and all-trans-β-cryptoxanthin was the main carotenoid in overripe fruits [105].

Yellow pulp varieties are characterized by the presence of these last carotenoids with very low to no detectable levels of lycopene [106]. As the metabolism of papaya carotenoids starts from phytoene and occurs in a well-known cascade process (**Figure 3B**), it is possible to establish a relationship between the pattern of enzymes that acts downstream to phytoene and the color of papaya pulp during ripening. Geranyl-geranyl

diphosphate is the precursor of chlorophylls, ubiquinones, and tocopherols. Phytoene synthase (PSY) uses two molecules of GGPP to produce phytoene, a colorless 40-carbon acyclic polyene molecule, which is the first step in carotenoid biosynthesis in the MEP pathway. Phytoene can be further used as a substrate by phytoene desaturase (PDS) to produce ζ-carotene, which can be a substrate for ζ-carotene desaturase (ZDS) for the synthesis of lycopene, a bright red carotenoid widely found in the pulp of orange/red papaya [107]. In yellow papayas there is no significant accumulation of lycopene because of the conversion of phytoene by PDS and ZDS and by both lycopene β-cyclases (LCY-β) and carotene hydroxylases (CHYB). These enzymes rapidly convert lycopene into xanthophylls and β-carotene [106,108]. In orange/red papayas, the initial stages of ripening are characterized mainly by the presence of xanthophylls, including β-cryptoxanthin, which are synthesized from lycopene downstream by lycopene β-cyclase (LCY-β; Blas et al., 2010; Schweiggert et al., 2011). However, after the onset of ethylene production in red/orange papayas, the conversion of lycopene into cyclic carotenoids appears to be strongly decreased due to lycopene accumulation in pulp [96,106]. The accumulation of lycopene in orange/red papayas compared to yellow papayas seems to occur both by a frame shift mutation in the *LCY-β2* gene, which results in a dysfunctional enzyme phenotype, and by other LCY genes (e.g., *LCY-β* and *LCY-ε*) that are downregulated during orange/red papaya ripening [66]. The ζ-carotene desaturase enzyme responsible for converting phytoene into lycopene shows a different pattern of expression during ripening and also between the cultivars ‘Golden’ and ‘Sunrise Solo’, while the lycopene β-cyclase gene, responsible for converting lycopene to β-carotene, is up-regulated in both cultivars [105].

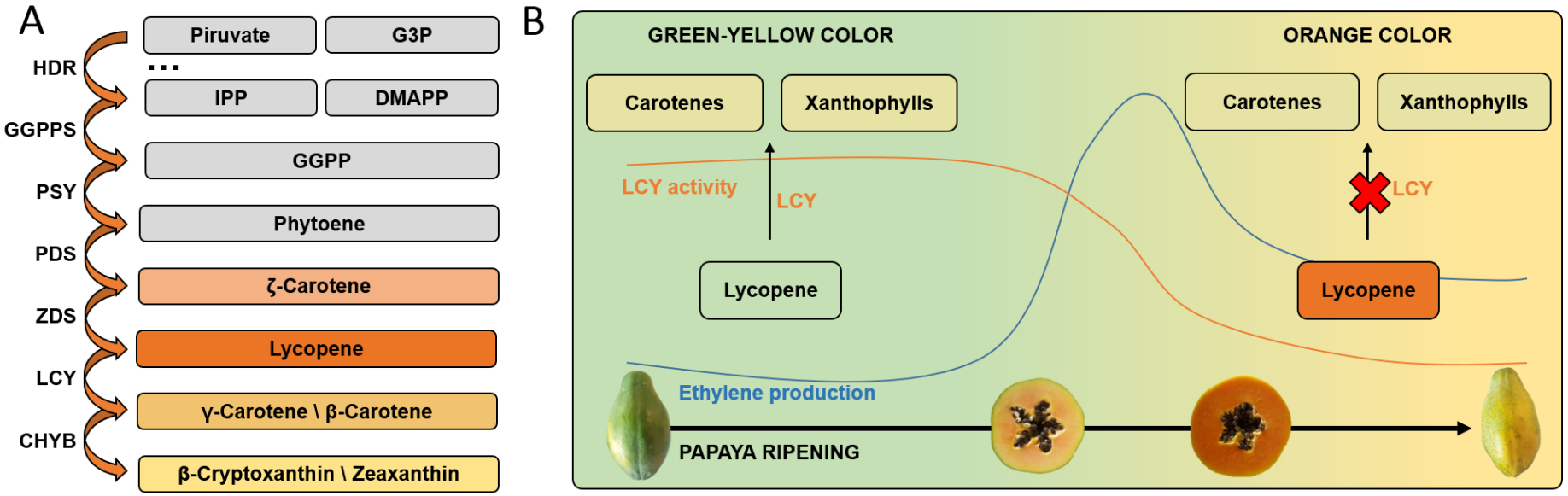

Figure 3. Ethylene production and carotenoids accumulation (LCY activity) during papaya ripening: papayas green/yellow color changing to orange/red color. A) Carotenoids derivated from MEP pathway. B) Papaya LCY activity during ripening drives the lycopene accumulation and pulp color changes through the decreased conversion of lycopene in carotenes and xanthoplylls. G3P: glyceraldehyde-3-phosphate; IPP: isopentenyl diphosphate; DMAPP: dimethyl allyl diphosphate; GGPP: geranyl-geranyl diphosphate; HDR: 4-hydroxy-3-methylbut-2-enyl diphosphate reductase; GGPPS: geranyl-geranyl diphosphate synthase; PSY: Phytoene synthase; PDS: phytoene desaturase; ZDS: ζ-carotene desaturase; LCY: lycopene cyclase; CHYB: carotene hydroxylase.

Interestingly, both ethylene- and 1-MCP-treated papayas had lower levels of minor carotenoids as compared to those of untreated papaya, similarly to what was previously reported for the major carotenoids [1,96]. Furthermore, the treatment of distinct papaya varieties with 1-MCP significantly reduced the carotenoid content in fruit pulp throughout ripening [1,96,109]. Barreto et al. (2011) suggested that the impairment on carotenoid accumulation in papaya pulp by 1-MCP could occur either by the consumption of early carotenoid precursors including GGPP, or by inhibiting PSY or PDS activity. The latter hypothesis was confirmed by Fu et al. (2016), who revealed that a transcription factor (CpNAC1) induced by ethylene enhances the expression of PDS genes (e.g., *CpPDS2* and *CpPDS4*). Recently, Fu et al. (2017) provided new insights into the role of other transcription factors that regulate ethylene responses and are involved in the regulation of several genes related to carotenoid biosynthesis. Therefore, as with pulp softening, sweetness, and the development of flavor, the carotenoid content in papayas is also regulated by ethylene-mediated responses during fruit ripening. Thus, while further studies are needed to define the specific genes whose expression relates to changes in the carotenoid content in papaya pulp, it is known that the reduction of ethylene production at low temperatures influences the composition of carotenoids in ripe papaya pulp [112].

5. Conclusions

Changes in the primary metabolism of papaya are mainly dependent on ethylene, whose onset burst occurs two to three days after the harvest of unripe fruit. Ethylene-triggered events during papaya ripening include an increase in PG and AI expression that are related to pulp softening and sweetening, respectively, as well as changes in carotenoid metabolism that influence both aroma and color, thereby leading to the formation of the expected quality attributes in ripe papaya. As ethylene-triggered events clearly affect the final quality of ripe papayas, studies have investigated the regulatory mechanisms that regulate ethylene function in papaya. Despite recent findings that highlight the ethylene-triggered events during papaya ripening, more efforts are needed to fully understand the key downstream regulators of ethylene in papaya pulp to better develop pre- and postharvest practices to extend papaya shelf life without resulting in losses in quality and nutritional aspects.

References

[1] J.P. Fabi, B.R. Cordenunsi, G.P. de Ma. Barreto, A.Z. Mercadante, F.M. Lajolo, J.R.O. Do Nascimento, Papaya Fruit Ripening: Response to Ethylene and 1-Methylcyclopropene (1-MCP), J. Food Agric. Food Chem. 55 (2007) 6118–6123.

[2] J.P. Fabi, F.H.G. Peroni, M.L.P.A. Gomez, Papaya, mango and guava fruit metabolism during ripening: postharvest changes affecting tropical fruit nutritional content and quality, Fresh Prod. 4 (2010) 56–66.

[3] Food and agriculture Organization of the United Nations (FAOSTAT), Food and agriculture Organization of the United Nations, Crop Downloads. (2017). http://www.fao.org/faostat/en/#data/QC.

[4] FAOSTAT, Food and agriculture Organization of the United Nations, Crop Downloads. (2017).

[5] E.A. Evans, F.H. Ballen, An Overview of Global Papaya Production, Trade, and Consuption, 2012.

[6] CBI Ministry of Foreign Affairs, Exporting fresh papayas to Europe, 2018.

[7] G.D. Manrique, F.M. Lajolo, Cell-wall polysaccharide modifications during postharvest ripening of papaya fruit (Carica papaya), Postharvest Biol. Technol. 33 (2004) 11–26. doi:10.1016/j.postharvbio.2004.01.007.

[8] J.J. Giovannoni, Genetic Regulation of Fruit Development and Ripening, Plant Cell. 16 (2004) S170–S180. doi:10.1105/tpc.019158.

[9] N.E. Gapper, R.P. McQuinn, J.J. Giovannoni, Molecular and genetic regulation of fruit ripening., Plant Mol. Biol. 82 (2013) 575–91. doi:10.1007/s11103-013-0050-3.

[10] F.B. Abeles, P.W. Morgan, M.E.J. Saltveit, Ethylene in plant biology, San Diego, 1992. doi:10.1016/B978-0-7506-1198-5.50126-0.

[11] P. Lü, S. Yu, N. Zhu, Y.R. Chen, B. Zhou, Y. Pan, D. Tzeng, J.P. Fabi, J. Argyris, J. Garcia-Mas, N. Ye, J. Zhang, D. Grierson, J. Xiang, Z. Fei, J. Giovannoni, S. Zhong, Genome encode analyses reveal the basis of convergent evolution of fleshy fruit ripening, Nat. Plants. 4 (2018) 784–791. doi:10.1038/s41477-018-0249-z.

[12] R.H. Wills, T. Lee, D. Graham, W. McGlasson, E. Hall, Postharvest: An Introduction to the Physiology and Handling of Fruit and Vegetables, Westport, CT, 1981. doi:10.1017/CBO9781107415324.004.

[13] E.J. McMurchie, W.B. McGlasson, I.L. Eaks, Treatment of fruit with propylene gives information about the biogenesis of ethylene, Nature. 237 (1972) 235–236.

doi:10.1038/239137a0.

[14] M.T. McManus, The plant hormone ethylene, Wiley–Blackwell, Hoboken, NJ, 2012.

[15] S.F. Yang, N.E. Hoffman, Ethylene biosynthesis and its regulation in higher plants, Annu. Rev. Plant Physiol. 35 (1984) 155–189.

[16] M. Razali, Z.M. Ali, R. Othman, Effects of 1-methylcyclopropene on activities of ethylene biosynthesis and cell wall degrading enzyme during ripening of papaya ' Sekaki ,' J. Trop. Agric. Fd. Sc. 41 (2013) 1–13.

[17] Y. Zou, L. Zhang, S. Rao, X. Zhu, L. Ye, W. Chen, X. Li, The relationship between the expression of ethylene-related genes and papaya fruit ripening disorder caused by chilling injury, PLoS One. 9 (2014) 1–24. doi:10.1371/journal.pone.0116002.

[18] X.L. Xie, X.R. Yin, K.S. Chen, Roles of APETALA2/Ethylene-Response Factors in Regulation of Fruit Quality, CRC. Crit. Rev. Plant Sci. 35 (2016) 120–130. doi:10.1080/07352689.2016.1213119.

[19] X. Li, X. Zhu, J. Mao, Y. Zou, D. Fu, W. Chen, W. Lu, Isolation and characterization of ethylene response factor family genes during development, ethylene regulation and stress treatments in papaya fruit, Plant Physiol. Biochem. 70 (2013) 81–92. doi:10.1016/j.plaphy.2013.05.020.

[20] J.P. Fabi, G.B. Seymour, N.S. Graham, M.R. Broadley, S.T. May, F.M. Lajolo, B.R. Cordenunsi, J.R. Oliveira do Nascimento, Analysis of ripening-related gene expression in papaya using an Arabidopsis-based microarray, BMC Plant Biol. 12 (2012) 242. doi:10.1186/1471-2229-12-242.

[21] T.H. Lee, H. Tang, X. Wang, A.H. Paterson, PGDD: A database of gene and genome duplication in plants, Nucleic Acids Res. 41 (2013) 1152–1158. doi:10.1093/nar/gks1104.

[22] C. Périn, M. Gomez-Jimenez, L. Hagen, C. Dogimont, J.-C. Pech, A. Latché, M. Pitrat, J.-M. Lelièvre, Molecular and genetic characterization of a non-climacteric phenotype in melon reveals two loci conferring altered ethylene response in fruit, Plant Physiol. 126 (2002) 300–309. doi:10.1104/pp.010613.therefore.

[23] J. Chaïb, M.F. Devaux, M.G. Grotte, K. Robini, M. Causse, M. Lahaye, I. Marty, Physiological relationships among physical, sensory, and morphological attributes of texture in tomato fruits, J. Exp. Bot. 58 (2007) 1915–1925. doi:10.1093/jxb/erm046.

[24] D. a. Brummell, Cell wall disassembly in ripening fruit, Funct. Plant Biol. 33 (2006) 103. doi:10.1071/FP05234.

[25] N.C. Carpita, D.M. Gibeaut, Structural models of primary cell walls in flowering plants: consistency of molecular structure with the physical properties of the walls during growth, Plant J. 3 (1993) 1–30.

[26] H.V. Scheller, P. Ulvskov, Hemicelluloses, Annu. Rev. Plant Biol. 61 (2010) 263–289. doi:10.1146/annurev-arplant-042809-112315.

[27] G. Tucker, X. Yin, A. Zhang, M. Wang, Q. Zhu, X. Liu, X. Xie, K. Chen, D. Grierson, Ethylene† and fruit softening, Food Qual. Saf. 1 (2017) 253–267. doi:10.1093/fqsafe/fyx024.

[28] D. Mohnen, Pectin structure and biosynthesis, Curr. Opin. Plant Biol. 11 (2008) 266–277. doi:10.1016/j.pbi.2008.03.006.

[29] E.G. Maxwell, N.J. Belshaw, K.W. Waldron, V.J. Morris, Pectin – An emerging new bioactive food polysaccharide, Trends Food Sci. Technol. 24 (2012) 64–73. doi:10.1016/j.tifs.2011.11.002.

[30] M. Bar-Peled, B.R. Urbanowicz, M.A. O'Neill, The Synthesis and Origin of the Pectic Polysaccharide Rhamnogalacturonan II - Insights from Nucleotide Sugar Formation and Diversity., Front. Plant Sci. 3 (2012) 92. doi:10.3389/fpls.2012.00092.

[31] D. Wang, T.H. Yeats, S. Uluisik, J.K.C. Rose, G.B. Seymour, Fruit Softening: Revisiting the Role of Pectin, Trends Plant Sci. 23 (2018) 302–310. doi:10.1016/j.tplants.2018.01.006.

[32] D. a Brummell, M.H. Harpster, Cell wall metabolism in fruit softening and quality and its manipulation in transgenic plants., Plant Mol. Biol. 47 (2001) 311–40. http://www.ncbi.nlm.nih.gov/pubmed/11554479.

[33] I. Balic, T. Ejsmentewicz, D. Sanhueza, C. Silva, T. Peredo, P. Olmedo, M. Barros, J.C. Verdonk, R. Paredes, C. Meneses, H. Prieto, A. Orellana, B.G. Defilippi, R. Campos-vargas, Biochemical and physiological study of the firmness of table grape berries, Postharvest Biol. Technol. 93 (2014) 15–23.

[34] R.G. Atkinson, K.M. Bolitho, M.A. Wright, T. Iturriagagoitia-Bueno, S.J. Reid, G.S. Ross, Apple ACC-oxidase and polygalacturonase: Ripening-specific gene expression and promoter analysis in transgenic tomato, Plant Mol. Biol. 38 (1998) 449–460. doi:10.1023/A:1006065926397.

[35] M.C. Marín-Rodríguez, J. Orchard, G.B. Seymour, Pectate lyases, cell wall

degradation and fruit softening, J. Exp. Bot. 53 (2002) 2115–2119. doi:10.1093/jxb/erf089.

[36] K. Wakabayashi, T. Hoson, D.J. Huber, Methyl de-esterification as a major factor regulating the extent of pectin depolymerization during fruit ripening: A comparison of the action of avocado (Persea americana) and tomato (Lycopersicon esculentum) polygalacturonases, J. Plant Physiol. 160 (2003) 667–673. doi:10.1078/0176-1617-00951.

[37] D.L. Smith, J. a Abbott, K.C. Gross, Down-Regulation of Tomato 13-Galactosidase 4 Results in Decreased Fruit Softening1, 129 (2014) 1755–1762. doi:10.1104/pp.011025.juice.

[38] G.O. Sozzi, L.C. Greve, G. a Prody, J.M. Labavitch, Gibberellic acid, synthetic auxins, and ethylene differentially modulate alpha-L-Arabinofuranosidase activities in antisense 1-aminocyclopropane-1-carboxylic acid synthase tomato pericarp discs, Plant Physiol. 129 (2002) 1330–1340. doi:10.1104/pp.001180.1330.

[39] A. Itai, K. Ishihara, J.D. Bewley, Characterization of expression, and cloning, of β-D-xylosidase and α-L-arabinofuranosidase in developing and ripening tomato (Lycopersicon esculentum Mill.) fruit, J. Exp. Bot. 54 (2003) 2615–2622. doi:10.1093/jxb/erg291.

[40] D. Wong, Enzymatic deconstruction of backbone structures of the ramified regions in pectins, Protein J. 27 (2008) 30–42. doi:10.1007/s10930-007-9105-0.

[41] J.P. Fabi, S.G. Broetto, S.L.G.L. Da Silva, S. Zhong, F.M. Lajolo, J.R.O. Nascimento, Analysis of Papaya Cell Wall-Related Genes during Fruit Ripening Indicates a Central Role of Polygalacturonases during Pulp Softening, PLoS One. 9 (2014) e105685. doi:10.1371/journal.pone.0105685.

[42] J.Á. Huerta-Ocampo, J.A. Osuna-Castro, G.J. Lino-López, A. Barrera-Pacheco, G. Mendoza-Hernández, A. De León-Rodríguez, A.P. Barba de la Rosa, Proteomic analysis of differentially accumulated proteins during ripening and in response to 1-MCP in papaya fruit, J. Proteomics. 75 (2012) 2160–2169. doi:https://doi.org/10.1016/j.jprot.2012.01.015.

[43] H. Lazan, S.-Y. Ng, L.-Y. Goh, Z.M. Ali, Papaya beta-galactosidase/galactanase isoforms in differential cell wall hydrolysis and fruit softening during ripening., Plant Physiol. Biochem. 42 (2004) 847–53. doi:10.1016/j.plaphy.2004.10.007.

[44] J.P. Fabi, B.R. Cordenunsi, G.B. Seymour, F.M. Lajolo, J.R.O. do Nascimento, Molecular cloning and characterization of a ripening-induced polygalacturonase

related to papaya fruit softening, Plant Physiol. Biochem. 47 (2009) 1075–81. doi:10.1016/j.plaphy.2009.08.002.

[45] J.A. Sañudo-Barajas, J. Labavitch, C. Greve, T. Osuna-Enciso, D. Muy-Rangel, J. Siller-Cepeda, Cell wall disassembly during papaya softening: Role of ethylene in changes in composition, pectin-derived oligomers (PDOs) production and wall hydrolases, Postharvest Biol. Technol. 51 (2009) 158–167. doi:10.1016/j.postharvbio.2008.07.018.

[46] T.M. Shiga, J.P. Fabi, J.R.O. do Nascimento, C.L.D.O. Petkowicz, L.C. Vriesmann, F.M. Lajolo, B.R. Cordenunsi, Changes in cell wall composition associated to the softening of ripening papaya: evidence of extensive solubilization of large molecular mass galactouronides, J. Agric. Food Chem. 57 (2009) 7064–71. doi:10.1021/jf900073b.

[47] H. Lazan, M.K. Selamat, Z.M. Ali, β-Galactosidase, polygalacturonase and pectinesterase in differential softening and cell wall modification during papaya fruit ripening, Physiol. Plant. 95 (1995) 106–112. doi:10.1111/j.1399-3054.1995.tb00815.x.

[48] S.B.R. do Prado, P.R. Melfi, V.C. Castro-Alves, S.G. Broetto, E.S. Araújo, J.R.O. do Nascimento, J.P. Fabi, Physiological Degradation of Pectin in Papaya Cell Walls: Release of Long Chains Galacturonans Derived from Insoluble Fractions during Postharvest Fruit Ripening, Front. Plant Sci. 7 (2016) 1120. doi:10.3389/fpls.2016.01120.

[49] S.B.R. do Prado, G.F. Ferreira, Y. Harazono, T.M. Shiga, A. Raz, N.C. Carpita, J.P. Fabi, Ripening-induced chemical modifications of papaya pectin inhibit cancer cell proliferation, Sci. Rep. 7 (2017) 16564. doi:10.1038/s41598-017-16709-3.

[50] S. Prado, G.R. Santos, P. Mourão, J. Fabi, Chelate-soluble pectin fraction from papaya pulp interacts with galectin-3 and inhibits colon cancer cell proliferation, Int. J. Biol. Macromol. 126 (2019) 170–178. doi:10.1016/j.ijbiomac.2018.12.191.

[51] G.D. Manrique, F.M. Lajolo, FT-IR spectroscopy as a tool for measuring degree of methyl esterification in pectins isolated from ripening papaya fruit, Postharvest Biol. Technol. 25 (2002) 99–107. doi:10.1016/S0925-5214(01)00160-0.

[52] J.P. Fabi, L.R.B.C. Mendes, F.M. Lajolo, J.R.O. do Nascimento, Transcript profiling of papaya fruit reveals differentially expressed genes associated with fruit ripening, Plant Sci. 179 (2010) 225–233. doi:10.1016/j.plantsci.2010.05.007.

[53] B.L. Gomes, J.P. Fabi, E. Purgatto, Cold storage affects the volatile profile and

expression of a putative linalool synthase of papaya fruit, Food Res. Int. 89 (2016) 654–660. doi:10.1016/j.foodres.2016.09.025.

[54] I.U. Bron, A.P. Jacomino, Ethylene action blockade and cold storage affect ripening of “Golden” papaya fruit, Acta Physiol. Plant. 31 (2009) 1165–1173. doi:10.1007/s11738-009-0336-x.

[55] M. Gomez, F. Lajolo, B. Cordenunsi, Evolution of soluble sugars during ripening of papaya fruit and its relation to sweet taste, J. Food Sci. 67 (2002) 442–447. doi:10.1111/j.1365-2621.2002.tb11426.x.

[56] L. Zhou, R.E. Paull, Sucrose Metabolism During Papaya (Carica papaya) Fruit Growth and Ripening, J. Am. Soc. Hortic. Sci. . 126 (2001) 351–357.

[57] L. Gomez, F. Lajolo, B. Cordenunsi, Influence of gamma radiation on carbohydrates metabolism of ripening papaya (Carica papaya L. cv. Solo), Food Sci. Technol. 19 (1999) 246–252.

[58] C.K. Castleden, N. Aoki, V.J. Gillespie, E.A. MacRae, W.P. Quick, P. Buchner, C.H. Foyer, R.T. Furbank, J.E. Lunn, Evolution and Function of the Sucrose-Phosphate Synthase Gene Families in Wheat and Other Grasses, Plant Physiol. 135 (2004) 1753 LP-1764. doi:10.1104/pp.104.042457.

[59] S.C. Huber, J.L. Huber, Role and regulation of sucrose phosphate synthase in higher plants, Annu. Rev. Plant Physiol. Plant Mol. Biol. 47 (1996) 431–444. doi:10.1146/annurev.arplant.47.1.431.

[60] Y. Zheng, S. Anderson, Y. Zhang, R.M. Garavito, The Structure of Sucrose Synthase-1 from Arabidopsis thaliana and Its Functional Implications, J. Biol. Chem. . 286 (2011) 36108–36118. doi:10.1074/jbc.M111.275974.

[61] L.A. Kleczkowski, M. Geisler, I. Ciereszko, H. Johansson, UDP-Glucose Pyrophosphorylase. An Old Protein with New Tricks, Plant Physiol. 134 (2004) 912 LP-918. doi:10.1104/pp.103.036053.

[62] T. Moriguchi, K. Abe, T. Sanada, S. Yamaki, Levels and Role of Sucrose Synthase, Sucrose-phosphate Synthase, and Acid Invertase in Sucrose Accumulation in Fruit of Asian Pear, J. Am. Soc. Hortic. Sci. . 117 (1992) 274–278.

[63] C. Aquino, L. Salomão, S. Rebeiro, D. Siqueira, P. Cecon, Carbohydrates, phenolic compounds and antioxidant activity in pulp and peelof 15 banana cultivars, Rev. Bras. Frutic. 38 (2016) 1–11. doi:http://dx.doi.org/10.1590/0100-29452016090.

[64] T.M. Shiga, C.A. Soares, J.R. Nascimento, E. Purgatto, F.M. Lajolo, B.R.

Cordenunsi, Ripening-associated changes in the amounts of starch and non-starch polysaccharides and their contributions to fruit softening in three banana cultivars, J. Sci. Food Agric. 91 (2011) 1511–1516. doi:10.1002/jsfa.4342.

[65] G. Oboh, A.O. Ademosun, M. Akinleye, O.S. Omojokun, A.A. Boligon, M.L. Athayde, Starch composition, glycemic indices, phenolic constituents, and antioxidative and antidiabetic properties of some common tropical fruits, J. Ethn. Foods. 2 (2015) 64–73. doi:https://doi.org/10.1016/j.jef.2015.05.003.

[66] Y.H. Shen, B.G. Lu, L. Feng, F.Y. Yang, J.J. Geng, R. Ming, X.J. Chen, Isolation of ripening-related genes from ethylene/1-MCP treated papaya through RNA-seq., BMC Genomics. 18 (2017) 671. doi:10.1186/s12864-017-4072-0.

[67] S.B. Nogueira, C.A. Labate, F.C. Gozzo, E.J. Pilau, F.M. Lajolo, J.R. Oliveira do Nascimento, Proteomic analysis of papaya fruit ripening using 2DE-DIGE, J. Proteomics. 75 (2012) 1428–1439. doi:https://doi.org/10.1016/j.jprot.2011.11.015.

[68] J. Zhao, J. Ma, M. Wu, X. Jiao, Z. Wang, F. Liang, G. Zhan, Gamma radiation as a phytosanitary treatment against larvae and pupae of Bactrocera dorsalis (Diptera: Tephritidae) in guava fruits, Food Control. 72 (2017) 360–366. doi:https://doi.org/10.1016/j.foodcont.2016.02.029.

[69] D. Guerreiro, J. Madureira, T. Silva, R. Melo, P.M.P. Santos, A. Ferreira, M.J. Trigo, A.N. Falcão, F.M.A. Margaça, S. Cabo Verde, Post-harvest treatment of cherry tomatoes by gamma radiation: Microbial and physicochemical parameters evaluation, Innov. Food Sci. Emerg. Technol. 36 (2016) 1–9. doi:https://doi.org/10.1016/j.ifset.2016.05.008.

[70] J. Farkas, C. Mohácsi-Farkas, History and future of food irradiation, Trends Food Sci. Technol. 22 (2011) 121–126. doi:https://doi.org/10.1016/j.tifs.2010.04.002.

[71] R.E. Paull, Response of Tropical Horticultural Commodities To Insect Disinfestation Treatments., HortScience . 27 (1992) 569.

[72] A. Chrysargyris, Postharvest ozone application for the preservation of fruits and vegetables AU - Tzortzakis, Nikos, Food Rev. Int. 33 (2017) 270–315. doi:10.1080/87559129.2016.1175015.

[73] M. Bataller, J.E. González, E. Veliz, L.A. Fernández, Ozone Applications in the Post-Harvest of Papaya (Carica papaya L.): An Alternative to Amistar Fungicide AU - Bataller, Mayra, Ozone Sci. Eng. 34 (2012) 151–155. doi:10.1080/01919512.2012.662728.

[74] R. Freitas, P. Souza, R. Ferreira Senhor, C. Moura, F. Costa, Post-harvest storage

of papaya fruits coated with extracts of leaves and fruits of Neem, Rev. Caatinga. 31 (2018) 290–296.

[75] R.A. Flath, R.R. Forrey, Volatile components of papaya (Carica papaya L., Solo variety), J. Agric. Food Chem. 25 (1977) 103–109. doi:10.1021/jf60209a051.

[76] D.B. Katague, E.R. Kirch, Chromatographic analysis of the volatile components of papaya fruit, J. Pharm. Sci. 54 (1965) 891–894. doi:10.1002/jps.2600540616.

[77] J.A. Pino, Odour-active compounds in papaya fruit cv. Red Maradol., Food Chem. 146 (2014) 120–126. doi:10.1016/j.foodchem.2013.09.031.

[78] H. Kelebek, S. Selli, H. Gubbuk, E. Gunes, Comparative evaluation of volatiles, phenolics, sugars, organic acids and antioxidant properties of Sel-42 and Tainung papaya varieties., Food Chem. 173 (2015) 912–919. doi:10.1016/j.foodchem.2014.10.116.

[79] J.A. Pino, K. Almora, R. Marbot, Volatile components of papaya (Carica papaya L., Maradol variety) fruit, Flavour Fragr. J. 18 (2003) 492–496. doi:10.1002/ffj.1248.

[80] G. Jing, T. Li, H. Qu, Z. Yun, Y. Jia, X. Zheng, Y. Jiang, Carotenoids and volatile profiles of yellow- and red-fleshed papaya fruit in relation to the expression of carotenoid cleavage dioxygenase genes, Postharvest Biol. Technol. 109 (2015) 114–119. doi:https://doi.org/10.1016/j.postharvbio.2015.06.006.

[81] P. Fuggate, C. Wongs-Aree, S. Noichinda, S. Kanlayanarat, Quality and volatile attributes of attached and detached ‘Pluk Mai Lie’ papaya during fruit ripening, Sci. Hortic. (Amsterdam). 126 (2010) 120–129. doi:https://doi.org/10.1016/j.scienta.2010.06.019.

[82] D. Ulrich, C. Wijawa, Volatile patterns of different papaya (Carica papaya L.) varieties, J. Appl. Bot. Food Qual. 83 (2010) 128–132.

[83] L.C. Devitt, T. Sawbridge, T.A. Holton, K. Mitchelson, R.G. Dietzgen, Discovery of genes associated with fruit ripening in Carica papaya using expressed sequence tags, Plant Sci. 170 (2006) 356–363. doi:https://doi.org/10.1016/j.plantsci.2005.09.003.

[84] V.M. Lieb, P. Esquivel, E. Cubero Castillo, R. Carle, C.B. Steingass, GC–MS profiling, descriptive sensory analysis, and consumer acceptance of Costa Rican papaya (Carica papaya L.) fruit purees, Food Chem. 248 (2018) 238–246. doi:https://doi.org/10.1016/j.foodchem.2017.12.027.

[85] K. Almora, J.A. Pino, M. Hernández, C. Duarte, J. González, E. Roncal,

Evaluation of volatiles from ripening papaya (Carica papaya L., var. Maradol roja), Food Chem. 86 (2004) 127–130. doi:https://doi.org/10.1016/j.foodchem.2003.09.039.

[86] C. Balbontín, C. Gaete-Eastman, M. Vergara, R. Herrera, M.A. Moya-León, Treatment with 1-MCP and the role of ethylene in aroma development of mountain papaya fruit, Postharvest Biol. Technol. 43 (2007) 67–77. doi:https://doi.org/10.1016/j.postharvbio.2006.08.005.

[87] B.G. Defilippi, A.M. Dandekar, A.A. Kader, Relationship of ethylene biosynthesis to volatile production, related enzymes, and precursor availability in apple peel and flesh tissues., J. Agric. Food Chem. 53 (2005) 3133–3141. doi:10.1021/jf047892x.

[88] Y. Li, H. Qi, Y. Jin, X. Tian, L. Sui, Y. Qiu, Role of ethylene in biosynthetic pathway of related-aroma volatiles derived from amino acids in oriental sweet melons (Cucumis melo var. makuwa Makino), Sci. Hortic. (Amsterdam). 201 (2016) 24–35. doi:https://doi.org/10.1016/j.scienta.2015.12.053.

[89] R.F.J. Rocha, Í.M. da S. Araújo, S.M. Freitas, D.D.S. Garruti, Optimization of headspace solid phase micro-extraction of volatile compounds from papaya fruit assisted by GC-olfactometry, J. Food Sci. Technol. 54 (2017) 4042–4050. doi:10.1007/s13197-017-2871-6.

[90] M. Brattoli, G. de Gennaro, V. de Pinto, A.D. Loiotile, S. Lovascio, M. Penza, Odour detection methods: olfactometry and chemical sensors, Sensors (Basel). 11 (2011) 5290–5322. doi:10.3390/s110505290.

[91] C.M. Delahunty, G. Eyres, J.-P. Dufour, Gas chromatography-olfactometry., J. Sep. Sci. 29 (2006) 2107–2125.

[92] L. Jirovetz, G. Buchbauer, M. Shahabi, Aroma compounds of mango and papaya from Cameroon. Solid phase microextraction analyses of these important fruits - Mangifera indica L. and Carica papaya L., Perfum. Flavorist. 28 (2003) 40–52.

[93] V. Façanha, Study of the relationship between ethylene and 1-methylcyclopropene (1-MCP) in “Golden” papayas, University of São Paulo, 2016.

[94] M. Gutensohn, I. Orlova, T.T.H. Nguyen, R. Davidovich-Rikanati, M.G. Ferruzzi, Y. Sitrit, E. Lewinsohn, E. Pichersky, N. Dudareva, Cytosolic monoterpene biosynthesis is supported by plastid-generated geranyl diphosphate substrate in transgenic tomato fruits, Plant J. 75 (2013) 351–363. doi:10.1111/tpj.12212.

[95] H.E. Khoo, K.N. Prasad, K.W. Kong, Y. Jiang, A. Ismail, Carotenoids and their isomers: Color pigments in fruits and vegetables, Molecules. 16 (2011) 1710–

1738. doi:10.3390/molecules16021710.

[96] G.P.M. Barreto, J.P. Fabi, V. V. De Rosso, B.R. Cordenunsi, F.M. Lajolo, J.R.O. do Nascimento, A.Z. Mercadante, Influence of ethylene on carotenoid biosynthesis during papaya postharvesting ripening, J. Food Compos. Anal. 24 (2011) 620–624. doi:10.1016/j.jfca.2011.02.006.

[97] R. Arias, T.-C. Lee, L. Logendra, H. Janes, Correlation of Lycopene Measured by HPLC with the L*, a*, b* Color Readings of a Hydroponic Tomato and the Relationship of Maturity with Color and Lycopene Content, J. Agric. Food Chem. 48 (2000) 1697–1702. doi:10.1021/jf990974e.

[98] C. Rojas-Garbanzo, M. Gleichenhagen, A. Heller, P. Esquivel, N. Schulze-Kaysers, A. Schieber, Carotenoid Profile, Antioxidant Capacity, and Chromoplasts of Pink Guava (Psidium guajava L. Cv. 'Criolla') during Fruit Ripening, J. Agric. Food Chem. 65 (2017) 3737–3747. doi:10.1021/acs.jafc.6b04560.

[99] P. Perkins-Veazie, J.K. Collins, A.R. Davis, W. Roberts, Carotenoid Content of 50 Watermelon Cultivars, J. Agric. Food Chem. 54 (2006) 2593–2597. doi:10.1021/jf052066p.

[100] G.T. Sigurdson, P. Tang, M.M. Giusti, Natural Colorants: Food Colorants from Natural Sources, Annu. Rev. Food Sci. Technol. 8 (2017) 261–280. doi:10.1146/annurev-food-030216-025923.

[101] J. Yang, L. Guo, Biosynthesis of β-carotene in engineered E. coli using the MEP and MVA pathways, Microb. Cell Fact. 13 (2014) 160. doi:10.1186/s12934-014-0160-x.

[102] M.Á. Ruiz-Sola, M. Rodríguez-Concepción, Carotenoid biosynthesis in Arabidopsis: a colorful pathway, Arab. B. 10 (2012) e0158–e0158. doi:10.1199/tab.0158.

[103] E. Majer, B. Llorente, M. Rodríguez-Concepción, J.-A. Daròs, Rewiring carotenoid biosynthesis in plants using a viral vector, Sci. Rep. 7 (2017) 41645.

[104] R.M. Schweiggert, C.B. Steingass, E. Mora, P. Esquivel, R. Carle, Carotenogenesis and physico-chemical characteristics during maturation of red fleshed papaya fruit (Carica papaya L.), Food Res. Int. 44 (2011) 1373–1380. doi:https://doi.org/10.1016/j.foodres.2011.01.029.

[105] G.F. Martins, J.P. Fabi, A.Z. Mercadante, V.V. de Rosso, The ripening influence of two papaya cultivars on carotenoid biosynthesis and radical scavenging capacity, Food Res. Int. 81 (2016) 197–202. doi:10.1016/j.foodres.2015.11.027.

[106] Y.H. Shen, F.Y. Yang, B.G. Lu, W.W. Zhao, T. Jiang, L. Feng, X.J. Chen, R. Ming, Exploring the differential mechanisms of carotenoid biosynthesis in the yellow peel and red flesh of papaya, (2019) 1–11.

[107] N. Nisar, L. Li, S. Lu, N.C. Khin, B.J. Pogson, Carotenoid Metabolism in Plants, Mol. Plant. 8 (2015) 68–82. doi:https://doi.org/10.1016/j.molp.2014.12.007.

[108] A.L. Blas, R. Ming, Z. Liu, O.J. Veatch, R.E. Paull, P.H. Moore, Q. Yu, Cloning of the papaya chromoplast-specific lycopene beta-cyclase, CpCYC-b, controlling fruit flesh color reveals conserved microsynteny and a recombination hot spot., Plant Physiol. 152 (2010) 2013–2022. doi:10.1104/pp.109.152298.

[109] M.A. Moya-León, M. Moya, R. Herrera, Ripening of mountain papaya (Vasconcellea pubescens) and ethylene dependence of some ripening events, Postharvest Biol. Technol. 34 (2004) 211–218. doi:https://doi.org/10.1016/j.postharvbio.2004.05.005.

[110] C.-C. Fu, Y.-C. Han, Z.-Q. Fan, J.-Y. Chen, W.-X. Chen, W.-J. Lu, J.-F. Kuang, The Papaya Transcription Factor CpNAC1 Modulates Carotenoid Biosynthesis through Activating Phytoene Desaturase Genes CpPDS2/4 during Fruit Ripening., J. Agric. Food Chem. 64 (2016) 5454–5463. doi:10.1021/acs.jafc.6b01020.

[111] C. Fu, Y. Han, J. Kuang, J. Chen, W. Lu, Papaya CpEIN3a and CpNAC2 Co-operatively Regulate Carotenoid Biosynthesis-Related Genes CpPDS2/4, CpLCY-e and CpCHY-b During Fruit Ripening, Plant Cell Physiol. 58 (2017) 2155–2165. doi:10.1093/pcp/pcx149.

[112] D.M. Rivera-Pastrana, E.M. Yahia, G.A. Gonzalez-Aguilar, Phenolic and carotenoid profiles of papaya fruit (Carica papaya L.) and their contents under low temperature storage., J. Sci. Food Agric. 90 (2010) 2358–2365. doi:10.1002/jsfa.4092.

Chapter 2

Physiological Degradation of Pectin in Papaya Cell Walls: Release of Long Chains Galacturonans Derived from Insoluble Fractions during Postharvest Fruit Ripening

Samira B. R. do Prado[1], Paulo R. Melfi[1], Victor C. Castro-Alves[1], Sabrina G. Broetto[1], Elias S. Araújo[1], João R. O. do Nascimento[1,2,3] and João P. Fabi[1,2,3]

[1] Department of Food Science and Experimental Nutrition, School of Pharmaceutical Sciences, University of São Paulo,
São Paulo, Brazil
[2] University of São Paulo – NAPAN – Food and Nutrition Research Center, São Paulo, Brazil
[3] Food Research Center, CEPID-FAPESP (Research, Innovation and Dissemination Centers, São Paulo Research Foundation), São Paulo, Brazil

Frontiers in Plant Science, v. 7, p. 1120, 2016.

Abstract

Papaya (*Carica* papaya L.) is a fleshy fruit that presents a rapid pulp softening during ripening. However, the timeline on how papaya pectinases act in polysaccharide solubilization and the consequent modification of the cell wall fractions during ripening is still not clear. In this work, the gene expression correlations between, on one hand, 16 enzymes potentially acting during papaya cell wall disassembling and, on the other hand, the monosaccharide composition of cell wall fractions during papaya ripening were evaluated. In order to explain differences in the ripening of papaya samplings, the molecular mass distribution of polysaccharides from water-soluble and oxalate-soluble fractions (WSF and OSF, respectively), as well as the oligosaccharide profiling from the WSF fraction, were evaluated by high performance size exclusion chromatography coupled to a refractive index detector and high performance anion-exchange chromatography coupled to pulse amperometric detection analyses, respectively. Results showed that up-regulated polygalacturonase and b-galactosidase genes were positively correlated with some monosaccharide profiles. In addition, an overall increase in the retention time of high molecular weight (HMW) and low molecular weight (LMW) polysaccharides in WSF and OSF was shown. The apparent disappearance of one HMW peak of the OSF may result from the conversion of pectin that were crosslinked with calcium into more soluble forms through the action of PGs, which would increase the solubilization of polysaccharides by lowering their molecular weight. Thus, the results allowed us to propose a detailed process of papaya cell wall disassembling that would affect sensorial properties and post-harvesting losses of this commercially important fruit.

Keywords: papaya ripening, galacturonan, cell wall disassembly, pectin depolymerization, fruit softening

Abbreviations: AGAL, a-galactosidases; ASF, alkali-soluble fraction; ARF, a-L-arabinofuranosidase; Ara, arabinose; BGAL, b-galactosidases; CELL, cellulase; DAH, days after harvesting; Fuc, fucose;GalA, galacturonic acid; GlcA, glucuronic acid; Gal, galactose; Glc, glucose; HPSEC-RID, high performance size exclusion chromatography coupled to a refractive index detector; HPAEC-PAD, high performance anion-exchange chromatography coupled to pulse amperometric detector; HMWP, high molecular weight polysaccharides; IF, insoluble fraction; LMWP, low molecular weight polysaccharides;Man, mannose; OSF, oxalate-soluble fraction; PCA, Principal component analysis; PG, polygalacturonases; PL, pectate lyase; PME, pectinesterases; Rha, rhamnose; TCW, total cell wall fraction; WSF, water-soluble fraction; Xyl, xylose; XYL, xylan endohydrolase; XTH, xyloglucan endotransglycosylase.

Introduction

The softening of fruit pulp is a major change that occurs during ripening, and pulp softening is mainly caused by cell wall disassembly [1]. The plant cell wall is composed of a matrix of cellulose microfibrils crosslinked to hemicelluloses and embedded with pectin, which also can be bound to cellulose [1,2]. Pulp softening is likely to occur by a reduction of cell-to-cell adhesion as a consequence of the dissolution of polysaccharides of the primary cell wall and middle lamella [3] by the action of hydrolases [1,4]. Different methods to identify those polysaccharides are based on plant cell wall fractionation, sugar composition, and molecular weight distribution to predict the possible biochemical modifications [5].

Papaya (*Carica* papaya L.) is a fleshy fruit that presents rapid pulp softening during ripening, which contributes to making the fruit edible but also increases post-harvest losses [6]. The softening of papaya fruit pulp is an ethylene dependent process likely resulting from the action of several cell wall-related enzymes on the polysaccharide components of the plant cell wall and middle lamella. Previous works had indeed identified a critical subset of genes involved in cell-wall disassembly [7–9]. However, despite the relevance of this process to fruit quality, the role played by each enzyme, the polysaccharides affected, and the time course of the structural changes are not clear. Apparently, there is solubilization of large molecular mass galacturonans from pectins during ripening [10]; however, from which component of the cell wall the water-soluble galacturonans are derived and the degree of hydrolysis achieved remain elusive. At the same time, the upregulation of PG, b-galactanases, and an endoxylanase have been associated with papaya softening [11], but it is not clear how and when these enzymes act on the structural polysaccharides.

In this way, the present study aimed to investigate the correlations between 16 genes of cell wall-related enzymes identified in previous works [9,12,13] and the changes in the monosaccharide composition of polysaccharides from the water-soluble, chelate-soluble, and ASFs of the cell wall during papaya ripening. As expected for other fleshy fruits, papaya WSF would correspond to the most soluble polysaccharides, including pectins, whereas the OSF would represent less soluble polysaccharides, mainly pectins that are tightened together by calcium bridges. On the other hand, the ASF would include celluloses, hemicelluloses, and even pectins bound to matrix glycans [1]. In addition, ripening-associated changes in molecular mass distribution of the water-soluble and

chelate-soluble fractions and the presence of oligomers were investigated by size exclusion and anion-exchange chromatography. This is the first time a systematized mobilization of polysaccharides has been proposed in 'Golden' papaya pulp softening during ripening, and the cause of the cell wall disassembly caused by pectinase expression can open new perspectives on the mechanisms of papaya pulp softening.

Materials and methods

Plant Material

Papaya fruits (C. papaya L. cv. 'Golden') were acquired from a producer in Aracruz (Espírito Santo, Brazil). Fruits were harvested from distinct plants at color break to one-fourth yellow (around 150 days post-anthesis) and were stored in 240-L chambers with controlled temperature and humidity (25 0.1 ºC and 95%, respectively). Daily analyses were performed on, at least, six fruits until complete ripening. Carbon dioxide, ethylene, and pulp firmness were measured according to methods of Fabi et al. (2007). The fruits were individually placed in airtightsealed jars and left at 25 C for 1 h. After that, air samples for ethylene and CO2 analysis (10 mL and 1 mL, respectively) were collected, and the composition of gasses was determined by gas chromatography using a flame ionization detector (FID) and a thermal conductivity detector (TCD) for ethylene and CO_2 analysis, respectively (Agilent Technologies, model HP-6890). The column used was a HP-Plot Q (30 meters, I.D. 0.53 mm, Agilent Technologies) and the injector and detector temperatures were 250 ºC with an isothermal run at 30 ºC. Helium was used as gas carrier (1 mL min^{-1} for ethylene and 4 mL min^{-1} for CO2) and injections were performed in splitless pulse mode for ethylene and split mode for CO_2 analysis (50:1). Ethylene and CO_2 external standards in synthetic air (Air Liquid) were used for calibration curves. The remaining pulp following physiological analysis each day was pooled as two distinct biological replicates (at least three fruits each replicate), frozen in liquid N_2, and stored at -80 ºC until analyses.

Gene Expression Analyses of Papaya

Cell Wall-Degrading Enzymes

Gene expression of papaya cell wall-degrading enzymes were measured according to methods of Fabi et al. (2014) and following the "Minimum Information for Publication of Quantitative Real-Time PCR Experiments – MIQE" [14]. The primer sequences for genes are depicted in Supplementary Table S1 (PG – *PG1* and *PG2*; PG 3 "QRT2" – *PG3*; PL – *PL1*; PL family – *PL2*; AGAL – *AGAL1* and *AGAL3*; BGAL – *BGAL1* and *BGAL3*; PME – *PME1*, *PME2*, and *PME3*; ARF – *ARF*; XYL – *XYL*; CELL – *CELL*; and XTH [ext/EXGTA1] – *XTH*). Internal controls (reference genes) were the actin (ACT), the elongation factor 1-a (*EF1*), and the ubiquitin (*UBQ*) genes, as previously reported [11,15], and RNA expression levels did not influence data, as suggested by the GeNorm analyses [16]. The geometrical means of the threshold cycle (Ct) values were achieved for the analysis of relative expression [16]. Expressions of one new gene for an a-galactosidase (*AGAL3*, located on chromosome LG7 contig 16621 – GenBank accession number ABIM01016598.1) and another gene for a β-galactosidase (*BGAL3*, located on chromosome Un contig 26518 – GenBank accession number ABIM01026480.1) were also analyzed. All amplicons were sub-cloned and sequenced in order to confirm gene identity. Real-time PCR was performed using a four-channel Rotor-Gene 3000 multiplexing system (Corbett Research, Sydney, NSW, Australia). The melting curves of amplicons and non-template controls were continuously checked in all experiments. The Ct values (four technical replicates from two biological replicates) were computed using the Rotor-Gene 3000 software, and quantification was performed using the relative standard curve method [17]. Results of the standard curves calculations are shown in Supplementary Table S3.

Papaya Cell Wall Polysaccharide Extraction

Polysaccharide extraction scheme is summarized in Supplementary Figure S1. Total Cell Wall Polysaccharides The frozen papaya pulp was triturated and extracted three times with chloroform:methanol (1:1, v/v) for enzyme inactivation and protein/pigment removal. Residues were washed with three volumes of 80% boiling ethanol for monosaccharide removal and were also washed with three volumes of acetone for drying purposes. Finally, residues were dried and weighed, resulting in a TCW.

Water-Soluble, Oxalate-Soluble, and Alkali-Soluble Cell Wall Polysaccharides

The TCW were extracted three times with 20 mL deionized water under constant magnetic stirring for 20 min at 25 ºC and centrifuged (10000 *g*, 20 min, 25 ºC). The supernatant, or WSF, was lyophilized and weighed. Residues of WSF were extracted according to methods of Taboada et al. (2010) [18], with modifications. Briefly, residues were extracted three times with 150 mL of 0.08 M $(NH_4)_2C_2O_4H_2O$ (pH 4.5) under constant magnetic stirring for 30 min at 25 ºC and centrifuged (1500 *g*, 10 min, 25 ºC). The supernatant, or OSF, was dialyzed against continuously replaced distilled water for 3 days using Millipore dialysis membranes (MWCO 3.5 kDa; Billerica, MA, USA), lyophilized, and weighed. Finally, remnant residues of WSF and OSF were extracted three times with 4 M NaOH and 0.2 M $NaBH_4$ under an N_2 stream and constant magnetic stirring overnight at 25 ºC and centrifuged (1500 *g*, 10 min, 25 ºC). The supernatant, or ASF, was dialyzed against continuously replaced distilled water for 3 days using Millipore dialysis membranes (MWCO 3.5 kDa), lyophilized, and weighed. The remnant, or IF, was lyophilized and weighed. The yield was calculated for all fractions in relation (%) to papaya pulp fresh weight.

Papaya Cell Wall Polysaccharide Composition

Hydrolyzed monosaccharides were generated by trifluoroacetic acid and H_2SO_4 hydrolysis [10]. The supernatants obtained were analyzed for neutral sugars and uronic acids by HPAEC-PAD according to methods of Shiga et al. (2009). Briefly, 1 mg of polysaccharides obtained by extractions (WSF and OSF) was hydrolyzed with 1 mL of 2 M TFA at 120 ºC for 60 min in a screw-capped conical vial and centrifuged (2000 *g*, 5 min, 25 ºC). Supernatants were transferred to new vials, dried under an N_2 stream, and separated for analysis. The same procedure was applied for ASF and IF, but the precipitates that resulted from TFA hydrolysis (the cellulose-rich residues) were dried under an N_2 stream and rehydrolyzed with 0.9 mL of 2 M H_2SO_4 at 120 ºC for 90 min. After hydrolysis, supernatants were neutralized with 0.1 mL of 50% NaOH (w/w) and analyzed in a DX 500 HPAEC-PAD system (Dionex, Sunnyvale, CA, USA). Neutral sugars (L-arabinose, D-galactose, D-glucose, D-fucose, D-mannose, L-rhamnose, and D-xylose) and uronic acids (Dglucuronic and D-galacturonic acid) were used as standards (Sigma; St. Louis, MO, USA).

Papaya Cell Wall Polysaccharide

Homogeneity and Molecular Weight

Molecular mass distribution of the papaya polysaccharides was analyzed by HPSEC-RID via a 1250 Infinity system (Agilent, Santa Clara, CA, USA). Samples were diluted with water (0.5 mg/mL), injected (25 mL) and separation was conducted through two PL aquagel-OH MIXED-M (300 mm 7.5 mm, 8 mm) columns (Agilent). The eluent was 0.2 M $NaNO_3$ at 35 ºC with a flow of 0.6 mL/min. Molecular weights were estimated using dextran T-series (5, 12, 25, 50, 80, 150, 410, and 750 kDa) (Sigma; St. Louis, MO, USA) as external standards.

Papaya Cell Wall Oligosaccharide Profiling

The low molecular weight peaks from WSF at 1 and 5 DAH were separated by ultrafiltration using Millipore Amicon Ultra-4 centrifugal filter units (MWCO 30 kDa). The oligosaccharide profiles were analyzed using a DX 500 HPAEC-PAD system (Dionex, Sunnyvalle, CA, USA) as described by Jonathan et al. (2012) [19]. Briefly, samples were diluted in 500 mL of water, injected (25 mL) and their profiles were analyzed in a CarboPac PA-1 column (2 mm 250 mm) (Dionex). Oligomers derived from neutral sugars were eluted (0.3 mL/min) with a linear gradient of 0.02–0.05 M NaOH for 3 min and 0.05–0.075 M NaOH for 10 min, followed by isocratic elution of 0.1 M NaOH for 2 min. Oligomers derived from uronic acids were then eluted with a gradient of 0–1 M NaOAc in 0.1 M NaOH for 50 min. Finally, the column was washed with 1 M NaOAc in 0.1 M NaOH for 7 min followed by 0.1 M NaOH for 3 min. Equilibration was done by eluting 0.02 M NaOH for 20 min. Standards sugars (L-arabinose, D-galactose, D-glucose, D-fucose, D-mannose, L-rhamnose, D-xylose, D-galacturonic acid, and digalacturonic acid) and oligosaccharides (maltotriose, maltopentaose, maltohexaose, and trigalacturonic acid) were used as external standards (Sigma).

Statistics

The results were expressed as the mean standard deviation (SD) obtained from, at least, two technical and two biological replicates. We did not conduct an analysis of variance since it would not lead to statistically valid results (low number of biological replicates). Data were analyzed using GraphPad Prism version 6.0 software (GraphPad Software, San Diego, CA, USA). To perform Pearson linear correlations and PCA data

were transformed by log, to obtain homogeneity of variance. The Pearson correlation coefficients were calculated using the quadruplicates of genes and monosaccharide values and the heat maps were done in GENE-E version 3.0.204 (Broad Institute, Inc., Cambridge, MA, USA). Twenty five variables were submitted to a PCA, adopting the genes and monosaccharide as columns and the 5 DAH, in quadruplicate, as rows. Eigenvalues higher than 1.0 were adopted to explain the projection of the samples on the two-dimensional graph.

Results

During the 5 DAH, there was appreciable softening of the pulp of papayas (**Figure 1A**). Although the extraction yield of total cell wall material from the fruit pulp appeared not changed during ripening, the specific yields of some fractions were quite different, as the WSF and IF clearly increased through ripening, whereas the OSF and ASF decreased (**Figure 1B**).

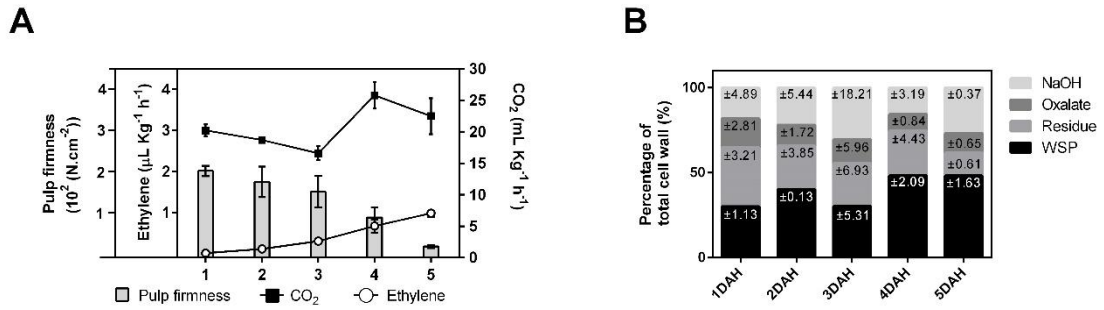

Fig. 1. Ripening of papaya fruit. A) The amount of CO2 produced by respiration (black squares – mg.Kg-1.h-1), the production of ethylene (open circles - µL.Kg-1.h-1), and the pulp firmness (bars – 102(N.cm-2)) were examined during ripening. Error bars indicate SDs of the mean for, at least, six fruits (n=6). **B)** Yield of cell wall fractions in the pulp of ripening papayas, based on fresh weight basis (percentage of each cell wall fraction using total cell wall as 100%) (B). Standard deviation values (duplicate for each biological replicate, n=4) are depicted in each corresponding cell wall fraction bars. DAH: days after harvesting.

The monosaccharide composition of the cell wall fractions was investigated and revealed GalA, followed by Gal, was the most abundant monosaccharide in the WSF and OSF. In contrast, neutral sugars, such as Gal, Glc, Man, and Xyl, predominated in the ASF, while Gal and Rha were more abundant in the IF (**Figure 2**). There was an overall increase

in acid and neutral sugars in the WSF during ripening, which was inversely correlated to a monosaccharide decrease in the OSF. The expression analysis of 16 cell wall-related enzymes (**Figure 3**) showed different up-regulated and down-regulated genes during papaya ripening. Interestingly, *PG*, galactosidase, and *XYL* genes showed the most significant changes in relative expression. The *PGs* and *BGAL1* seemed to increase during ripening, while the *ARF* and *PLs* seemed to decrease. It was noteworthy that *BGAL1* and *BGAL3* increased after day 2 and maintained higher values comparing with day 1 and 2. Generally, *PL1*, *PL2*, and *ARF* showed lower values starting from day 2. *PME1* and *PME2* expression peaked at day 3, and *XYL* peaked at day 3 with higher values even at day 4. A correlation matrix was obtained for the gene expression and the monosaccharides of WSF, OSF, and ASF during ripening (**Figure 4**). Overall, *PGs* and *BGALs* were positively correlated to uronic acids and most of the neutral sugars in the WSF but were negatively correlated in the OSF. Negative correlations of *PGs* and *BGALs* were also noticed in the ASF but were limited to GalA, Gal, Ara, and Rha. Regarding *XYL*, which was also significantly up-regulated, negative correlations with uronic acids and neutral sugars were observed in the WSF and ASF, especially Gal, Glc, and GlcA.

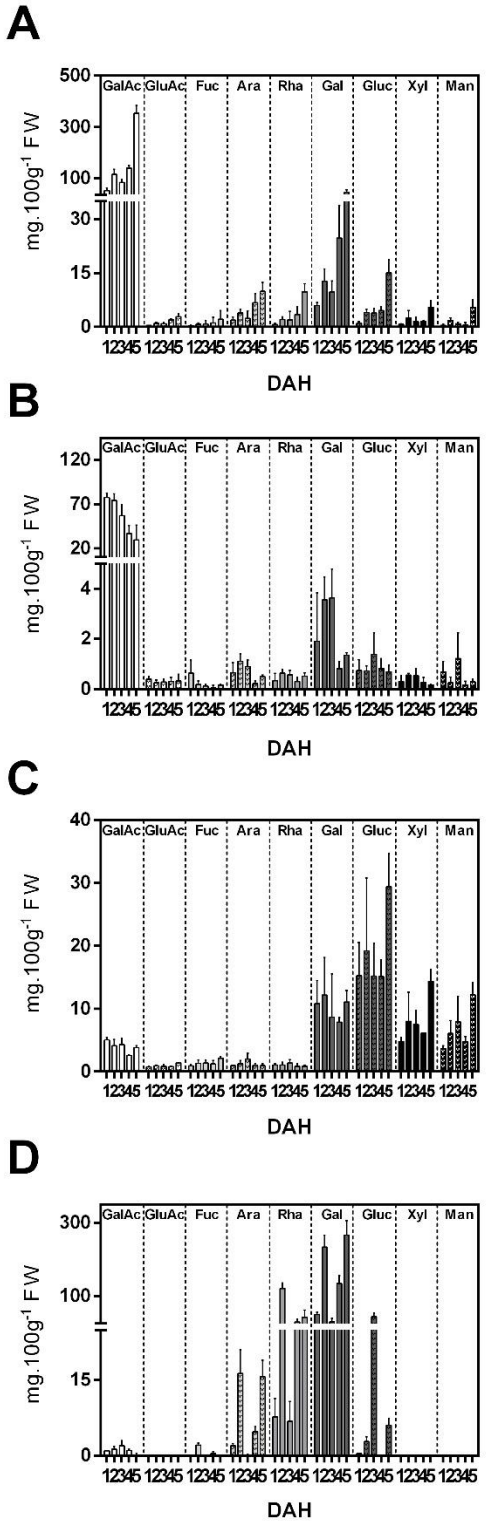

Fig. 2. Monosaccharide composition (mg.100g-1 Fresh Weight) of cell wall fractions isolated from papaya during 5 days after harvesting. A) Water Soluble Fraction. **B)** Oxalate Soluble Fraction. **C)** Alkali Soluble Fraction. **D)** Insoluble fraction. Galacturonic acid (GalA), glucuronic acid (GlcA), fucose (Fuc), arabinose (Ara), rhamnose (Rha),

galactose (Gal), glucose (Glc), xylose (Xyl), mannose (Man). Error bars indicate SDs of the mean (duplicate for each biological replicate, n=4).

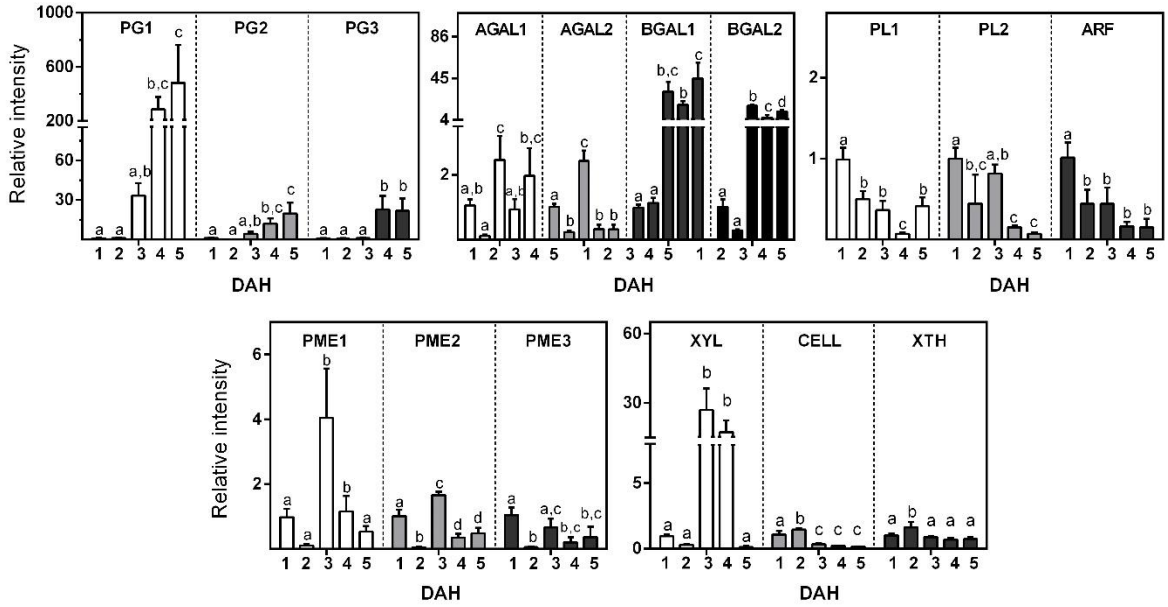

Fig. 3. Gene Expression of enzymes related to cell wall disassembling during papaya ripening. Real-time PCR (qPCR) was used to analyze the mRNA levels of various genes during ripening. The column heights indicate the relative mRNA abundance; the expression values for unripen fruit (first day after harvesting) were set to 1. The error bars on each column indicate the SD of four technical replicates for each biological replicate (n=8). Polygalacturonase 1 (PG1); Polygalacturonase 2 (PG2); Polygalacturonase 3 "QRT2" (PG3); Pectate lyase (PL1); Pectate lyase family (PL2); Alpha-galactosidase (AGAL1); Alpha-galactosidase (AGAL3); Beta-galactosidase (BGAL1); Beta-galactosidase (BGAL3); Pectinesterase (pectin methylesterase) (PME1); Pectinesterase (pectin methylesterase) (PME2); Pectinesterase (pectin methylesterase) (PME3); Alpha-L-arabinofuranosidase (ARF); Xylan endohydrolase (XYL); Cellulase (CELL); and Xyloglucan endotransglycosylase (ext/EXGT-A1) (XTH). The primer sequences and GenBank accession numbers for genes are depicted in Supplementary File 1.

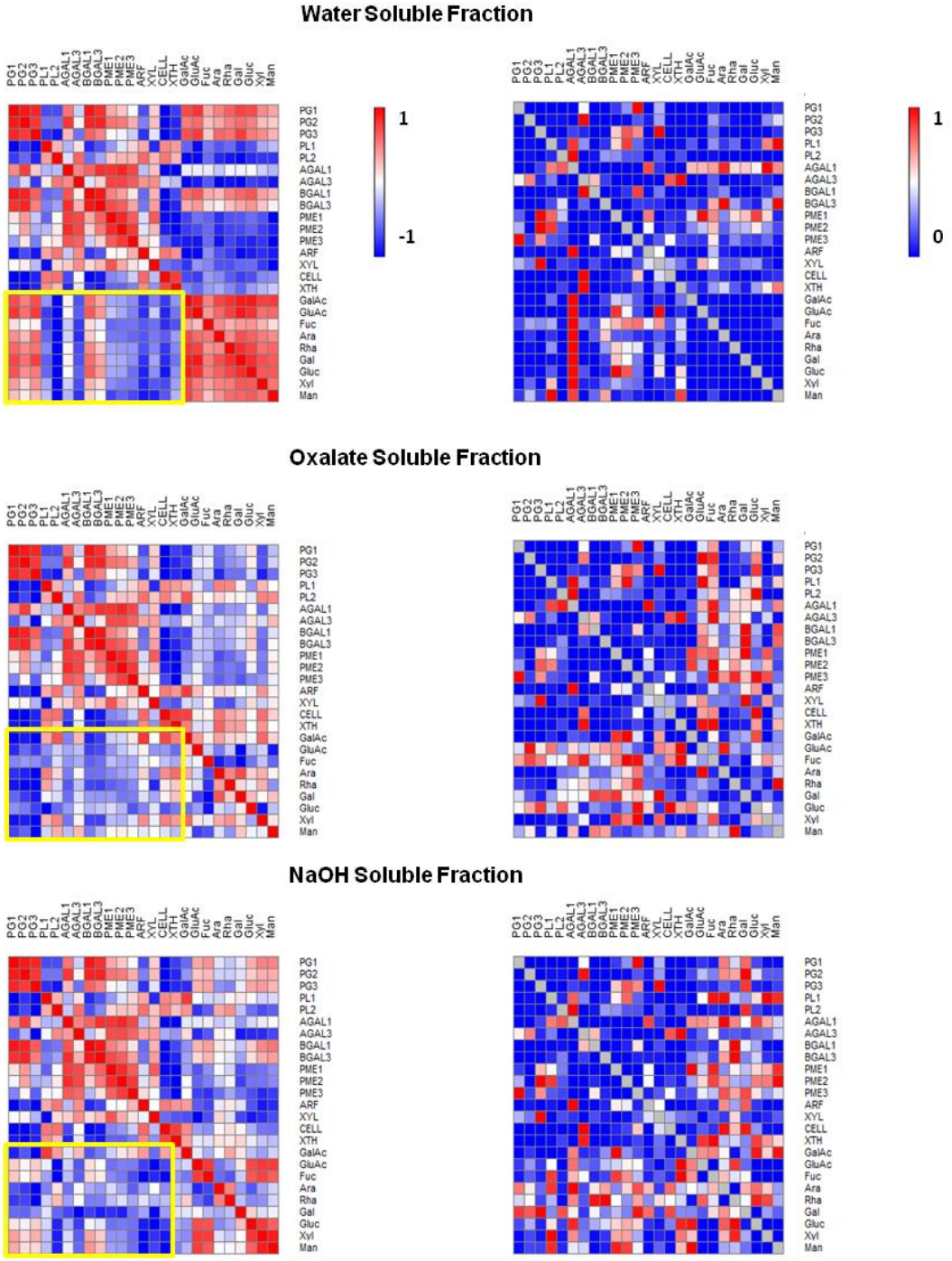

Fig. 4. Pearson correlations and associated p-values of papaya cell wall-related genes and monosaccharides. Pearson correlation of papaya cell wall-related genes and monosaccharides cell wall composition from water-soluble fraction, oxalate-soluble fraction and alkali-soluble fraction were analyzed. SPSS software was used to calculate the Pearson correlation and the corresponding p-values for the 25 combinations using the 16 values of gene expression and 9 values of monosaccharides. Left pics in figure are the heat maps of correlation values described as positive values that were set to red color and

negative values that were set to blue color. Right pics in figure are the heat maps of p values as values near to one that were set to red color and values near to zero that were set to blue color.

The homogeneity and molecular weight distribution of WSF and OSF during papaya ripening were monitored by HPSEC RID (**Figure 5**). In the chromatograms of the WSF, the peak area corresponding to HMWP increased during ripening, while a second peak of LMWP diminished, the same time during which retention time slightly increased. The chromatographic separation of the OSF revealed three peaks, and two of them were significantly affected during ripening. The main peak corresponding to HMWP almost disappeared, while the retention time of the peak of LMWP remarkably increased. The WSF from fruit sampled at day 1 and day 5 were also examined for the presence of oligosaccharides using HPAEC PAD (**Figure 6**), and the chromatograms revealed an increase in the diversity and abundance of oligosaccharides derived from both neutral and acidic sugars at 5 DAH.

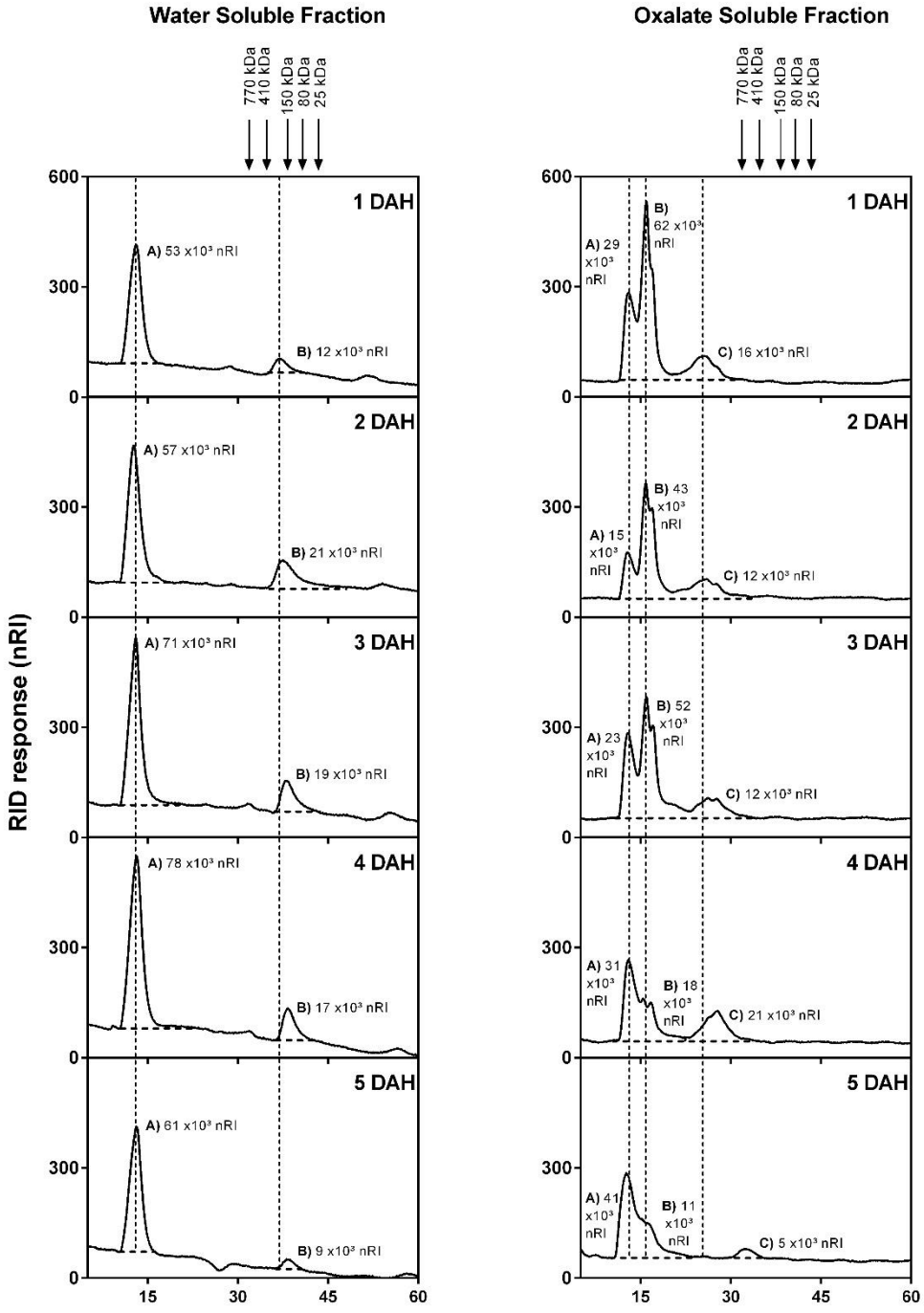

Fig. 5. High performance size exclusion chromatography (HPSEC-RID) elution profile of papaya water-soluble fractions for 1 to 5 DAH. HPSEC coupled to a refractive index detector was used to evaluate the molecular weight distribution in Water Soluble Fraction (WSF) and Oxalate Soluble Fraction (OSF) extracted from total cell wall obtained from papaya pulp. Molecular weights were estimated using a standard curve of dextran T-series (25, 80, 150, 410, and 750 kDa) showed with arrows in the figure. The peaks were marked with dotted lines in order to facilitate retention time comparisons. Peaks were

divided in A) and B) (for WSF) and A), B) and C) (For OSF), and total area values are depicted in graphics. DAH: days after harvesting.

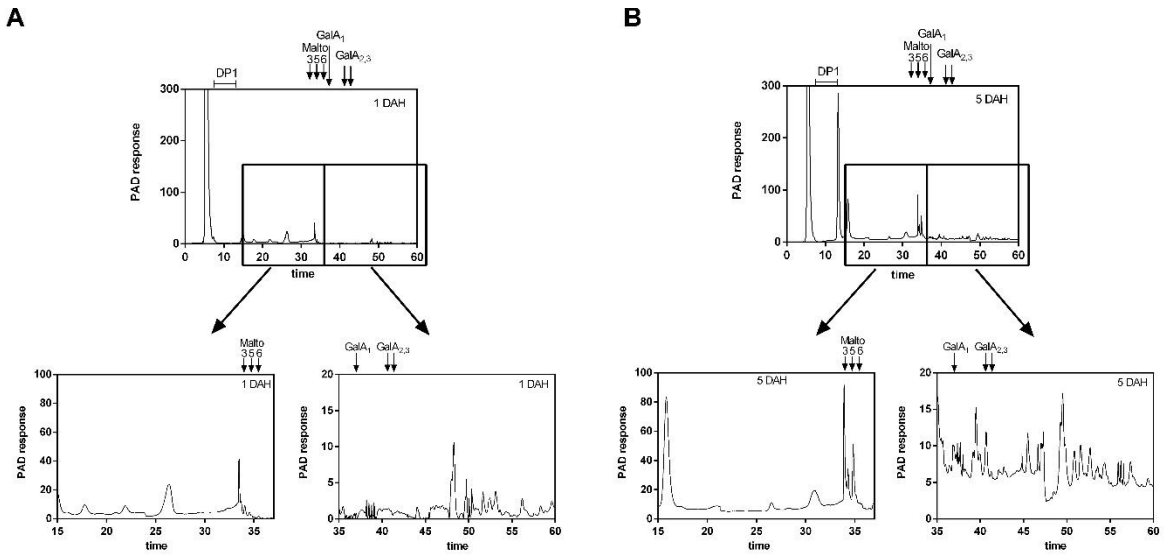

Fig. 6. High Performance Anion Exchange Chromatography (HPAEC) elution profile of papaya oligosaccharides smaller than 30 kDa at 1 and 5 DAH (days after harvest). The low molecular weight oligosaccharides from WSF at 1 and 5 days after harvesting (DAH) were separated by ultrafiltration (<30 kDa) using Millipore Amicon Ultra-4 centrifugal filter units and analyzed using a DX 500 HPAEC coupled with Pulsed Electrochemical Detection (Dionex) in a CarboPac PA-1 column. Oligos derived from neutral sugars were eluted first using a NaOH gradient, while oligos derived from uronic acids were later eluted using NaOAc/NaOH gradient. Maltotriose, maltopentaose and maltohexaose, as well as mono, di and tri-galacturonic acid DAH: days after harvesting.

PCA of the whole dataset revealed that factors 1 and 2 accounted for more than 75% of the variability (**Figure 7**). The combination of Factor 1 and 2 allowed the discrimination between all 5 sampling days. Factor 1 allowed the separation of papaya fruit samples at 1 DAH (quadrant on the left) from 5 DAH (quadrants on the right). GlcA, GalA, *PG1*, and *PG3* were the strongest variables that forced day 5 to get on the right side in the graphic. *PL2* and *ARF* forced day 1 to get on the left size. Day 3 correlates with *AGAL2*, *PME1*, and *PME2* and – less strongly – with *XYL* and *PME3*. Day 4 correlates with Glc and Day 5 with GlcA.

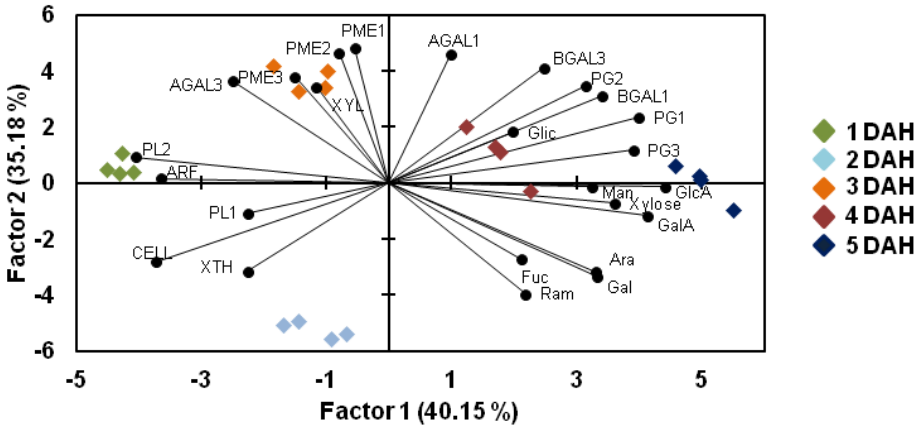

Fig. 7. Principal component analysis (PCA) of papaya samples analysis comparing monosaccharides and genes expression. A PCA analysis was done in order to distinguish the uppermost differences in papaya samples for days from 1 to 5 after harvesting using data from sugars composition and genes expression. PCA revealed that factors 1 and 2 accounted for more than 75% of the variability and separating papaya fruits sampled at 1, 2, and 3 DAH from those at 4 and 5 DAH. The high correlations of *PGs* and *BGALs* to papaya at 5 DAH and of *PMEs*, *XYL*, and *AGAL3* to fruits at 3 DAH were the highest observed discrepancies.

Discussion

In general, climacteric fruit ripening is fast due to ethylene biosynthesis and its self-regulation [1]. The triggering of ethylene-dependent biochemical reactions in papaya ripening, such as pulp softening, affects fruit quality and postharvest handling [6]. Previous works had identified a subset of genes involved in cell-wall disassembly [7,9,13] that were studied in the present work. Despite the importance, it was not clear how and when cell wall-related enzymes act in the solubilization and modification of papaya cell wall fractions. In this way, the following discussion attempted to fill in those gaps.

Polygalacturonases and galactanases are the main factors responsible for galacturonan depolymerization in papaya pulp

Differences in cell wall yield, monosaccharide composition from fractions, and gene expression of cell wall-related enzymes in papayas can provide evidence regarding pectin molecule structure in papaya pulp. These structures would be more or less disposable for biochemical changes that lead to a determined phenotypic characteristic in a short

period of time (soft pulp in ripe fruit). According to the analysis of the papaya cell wall fractions, the softening of the fruit pulp was followed by an apparent increase in the yield of water-soluble polysaccharides. The increase in acid and neutral sugars in the WSF, especially GalA, was inversely correlated to the respective monosaccharide decrease in the OSF, suggesting a massive release of less soluble galacturonans during papaya ripening. Since the changes in Ara, Rha, and Gal contents were similar to that of GalA, it seems that there was solubilization of rhamnogalacturonan I portions of the OSF. The Gal increase in the WSF also would suggest the solubilization of galactans from the OSF during ripening.

The up-regulation of *PG1*, *PG2*, *PG3*, and *XYL* genes, which have been associated previously with papaya pectin disassembly [11], could explain some important changes in monosaccharide composition of the cell wall fractions. The upregulation of *PGs* and *XYL* has been correlated to the release of GalA and Xyl to the WSF, reinforcing the idea of a massive hydrolysis of galacturonans and xylans from the OSF and ASF, respectively, during papaya ripening. The combined action of upregulated PGs and XYL, as well as XTH (slightly increase on day 2), would agree with the proposal of Lazan et al. (2004) [20], who suggested the presence of xyloglucan–pectin linkages in papaya. The disruption of those linkages during ripening would lead to solubilization of the pectin tightly bound to more IF of the papaya cell wall.

The action of PGs on homogalacturonans and the action of GALs on the side chains could have contributed to solubilization of rhamnogalacturonan I portions of the pectins, but not the action of PLs nor ARF. The expression of galactosidases has been associated with papaya pulp softening [11,20,21], and the present research revealed up-regulation of *β-GALs*, including a newly identified *β-GAL* gene (*β-GAL3*). α-GALs had also an apparent up-regulation but not at the higher levels as *β-GALs*, which might have assisted for the significant release of Gal during fruit ripening. Similar biochemical changes were described for ‘Jonagold’ apple, since increases in galactosidase enzyme activity promoted losses of Gal from the side chains of rhamnogalacturonan I, leading to earlier softening during low temperature storage [22]. The presence of GalA in the ASF denoted the occurrence of pectin firmly bound to the IF of the cell wall via the side chains and/or backbone [23,24]. Regarding the fact that methylation of WSF increases during papaya ripening [10,25], the up-regulation of *PMEs* could be related to an increasing in calcium bridges by demethylation that allowed pectins to be continuously tightly bound to the IF besides PGs depolymerization [26].

The increase in Glc amounts in all fractions during ripening (WSF, OSF, and ASF) was noteworthy, which could result from the solubilization of hemicelluloses tightly bound to small pieces of cellulose by the action of XTH and XYL, making more soluble complexes. Although expression of the CELL gene is not suggestive of a relevant role in papaya cell wall degradation, the action of other up-regulated CELLs that have not been identified may not be disregarded. The PCA analysis provided an integrated view of the changes in gene expression and the monosaccharide composition of the cell wall fractions, evidencing the positive correlations between PGs and BGALs and between PMEs and XYL to the changes in neutral and acid sugars during papaya ripening.

Mobilization of high molecular weight polysaccharides from insoluble to soluble fractions is responsible for papaya pulp softening

The decreasing pattern in the OSF and the increasing one in the WSF for GalA, Fuc, Ara, Rha, and Gal quantities suggest that a massive migration of insoluble pectins to more soluble forms occurred during papaya ripening. The correlation values between sugar quantities and cell wall-related gene expression also could support this suggestion, since the pectin molecular weight would decrease due to pectinase action.

The study of polysaccharides by HPSEC-RID analysis showed an overall increase in the retention time of HMW and LMW polysaccharides, which could be attributed to the depolymerizing action of pectinases, mainly PG, in both the WSF and OSF. The apparent disappearance of one HMW peak of the OSF may result from the conversion of pectins that were crosslinked with calcium into more soluble forms through the action of PGs, which would increase the solubilization of polysaccharides by lowering their molecular weight. Therefore, the pectin solubilizing flow from the insoluble parts of papaya cell walls would contribute to papaya softening. In this process, the release of insoluble pectins tightly bound to celluloses, xyloglucans, and xylans would enrich the OSF [26–28], and the continuous depolymerization of pectins tightly bound to each other by calcium bridges (insoluble) would enrich the WSF, making cell wall adhesion weaker and causing tissue softening. Based on the gene expression analysis, it is likely the highly expressed pectinases would act on pectins tightly bound to xyloglucans and xylans [29] that had been depolymerized partially by XYL and XTH [30,31], leading to disruption of cell walls. A similar process had been reported for long-storage carrots, in which the WSF was enriched by degraded

polysaccharides from the chelate-soluble fraction due to enzymatic degradation and solubilization of polysaccharides from chelate-soluble and ASFs [32].

In addition to the release of soluble polysaccharide chains from the cell wall, the massive depolymerization of pectins resulted in high quantities of pectin-derived oligomers in the WSF at day 5, as previously observed for 'Maradol' papayas [33]. The HPAEC-PAD analysis of LMW peaks eluted from HPSEC-RID showed the oligomers had a mixed profile of neutral and acidic sugars. Some oligomers were composed of neutral sugars, and since the technique cannot distinguish between linear and branched oligomers, the detected oligomers may have derived from rhamnogalacturonans. The predominance of peaks eluted after the trigalacturonic acid standard may indicate the release of some oligomers from homogalacturonans by the action of endopolygalacturonases.

In general, climacteric fruits present the expression of *PGs* as the key role in fruit softening despite it is not the only enzyme responsible for this process. Papayas seem to express high quantities of *PGs* transcripts during ripening when compared to other plant species [24] and this is due to variation in the composition of cell walls and the different rate of pulp softening [34]. Papaya contains high molecular weight galacturonans, that probably require high quantities of *PGs* for a rapid pulp softening by solubilizing homogalacturonans and concomitant up-regulation of *β-GALs* could have contributed to solubilization of rhamnogalacturonan I. Apples had higher *PGs* activities only late in ripening and the high β-Gal was a very important event during early ripening [22]. For carrots the mechanisms responsible for the softening may be the disintegration of the network of more IF into shortest molecules (action of *β-Gal*, *α-L-Af* and *PGs* enzymes) and the polymer size increased in WSP [32].

As expected for future works, gene silencing of the three *PGs* genes from papaya (*PG1*, *PG2*, and *PG3*) could abolish the release of homogalacturonan long chains during postharvest fruit ripening showing a central role of *PGs* on pulp softening, unless other set of genes would be highly expressed and responsible for marginal pulp softening (which seems not to be the case of). The study of the cell-wall degrading enzyme activities such as *PGs*, *GALs*, and *XYLs*, that had mRNA levels highly altered during fruit ripening, would reinforce the releasing of galacturonans during papaya ripening. However, one could argue enzyme activity experiments would not account for the expression of specific genes, so it would be important to correlate with gene expression data [11].

The softening of papaya fruit during ripening is a relatively fast and complex process likely resulting from the coordinated action of several enzymes on the polysaccharide structure of the plant cell wall. In this regard, the results of the present research point to the action of pectinases, mainly PG and galactanases, as well as a xylanase as being responsible for the mobilization of HMW pectins from less soluble to more soluble fractions, especially the pectins tightly bound to cellulose/hemicellulose and to each other by calcium bridges. In this way, understanding the biochemical pathways that lead to papaya pulp softening would be of valuable interest, since the fruit could be represented as a model for in vivo rapid cell wall polysaccharide solubilization that instantly alters sensorial properties and post-harvesting losses of this commercially important fruit.

References

[1] N.E. Gapper, R.P. McQuinn, J.J. Giovannoni, Molecular and genetic regulation of fruit ripening., Plant Mol. Biol. 82 (2013) 575–91. doi:10.1007/s11103-013-0050-3.

[2] N.C. Carpita, D.M. Gibeaut, Structural models of primary cell walls in flowering plants: consistency of molecular structure with the physical properties of the walls during growth, Plant J. 3 (1993) 1–30.

[3] D. a Brummell, M.H. Harpster, Cell wall metabolism in fruit softening and quality and its manipulation in transgenic plants., Plant Mol. Biol. 47 (2001) 311–40. http://www.ncbi.nlm.nih.gov/pubmed/11554479.

[4] I. Balic, T. Ejsmentewicz, D. Sanhueza, C. Silva, T. Peredo, P. Olmedo, M. Barros, J.C. Verdonk, R. Paredes, C. Meneses, H. Prieto, A. Orellana, B.G. Defilippi, R. Campos-vargas, Biochemical and physiological study of the firmness of table grape berries, Postharvest Biol. Technol. 93 (2014) 15–23.

[5] F.B. Daher, A.B. Siobhan, How to let go: pectin and plant cell adhesion, Front. Plant Sci. 6 (2015) 1–8. doi:10.3389/fpls.2015.00523.

[6] J.P. Fabi, B.R. Cordenunsi, G.P. de Ma. Barreto, A.Z. Mercadante, F.M. Lajolo, J.R.O. Do Nascimento, Papaya Fruit Ripening: Response to Ethylene and 1-Methylcyclopropene (1-MCP), J. Food Agric. Food Chem. 55 (2007) 6118–6123.

[7] J.P. Fabi, B.R. Cordenunsi, G.B. Seymour, F.M. Lajolo, J.R.O. do Nascimento, Molecular cloning and characterization of a ripening-induced polygalacturonase related to papaya fruit softening, Plant Physiol. Biochem. 47 (2009) 1075–81. doi:10.1016/j.plaphy.2009.08.002.

[8] J.P. Fabi, F.H.G. Peroni, M.L.P.A. Gomez, Papaya, mango and guava fruit metabolism during ripening: postharvest changes affecting tropical fruit nutritional content and quality, Fresh Prod. 4 (2010) 56–66.

[9] J.P. Fabi, G.B. Seymour, N.S. Graham, M.R. Broadley, S.T. May, F.M. Lajolo, B.R. Cordenunsi, J.R. Oliveira do Nascimento, Analysis of ripening-related gene expression in papaya using an Arabidopsis-based microarray, BMC Plant Biol. 12 (2012) 242. doi:10.1186/1471-2229-12-242.

[10] T.M. Shiga, J.P. Fabi, J.R.O. do Nascimento, C.L.D.O. Petkowicz, L.C. Vriesmann, F.M. Lajolo, B.R. Cordenunsi, Changes in cell wall composition associated to the softening of ripening papaya: evidence of extensive solubilization of large molecular mass galactouronides, J. Agric. Food Chem. 57 (2009) 7064–71. doi:10.1021/jf900073b.

[11] J.P. Fabi, S.G. Broetto, S.L.G.L. Da Silva, S. Zhong, F.M. Lajolo, J.R.O. Nascimento, Analysis of Papaya Cell Wall-Related Genes during Fruit Ripening Indicates a Central Role of Polygalacturonases during Pulp Softening, PLoS One. 9 (2014) e105685. doi:10.1371/journal.pone.0105685.

[12] J.P. Fabi, F.M. Lajolo, J.R.O. Do Nascimento, Cloning and characterization of transcripts differentially expressed in the pulp of ripening papaya, Sci. Hortic. (Amsterdam). 121 (2009) 159–165. doi:10.1016/j.scienta.2009.01.036.

[13] J.P. Fabi, L.R.B.C. Mendes, F.M. Lajolo, J.R.O. do Nascimento, Transcript profiling of papaya fruit reveals differentially expressed genes associated with fruit ripening, Plant Sci. 179 (2010) 225–233. doi:10.1016/j.plantsci.2010.05.007.

[14] S. a Bustin, V. Benes, J. a Garson, J. Hellemans, J. Huggett, M. Kubista, R. Mueller, T. Nolan, M.W. Pfaffl, G.L. Shipley, J. Vandesompele, C.T. Wittwer, The MIQE guidelines: minimum information for publication of quantitative real-time PCR experiments., Clin. Chem. 55 (2009) 611–22. doi:10.1373/clinchem.2008.112797.

[15] S.G. Broetto, J.P. Fabi, J.R.O. Nascimento, Cloning and expression analysis of two putative papaya genes encoding polygalacturonase-inhibiting proteins, Postharvest Biol. Technol. 104 (2015) 48–56. doi:10.1016/j.postharvbio.2015.03.002.

[16] J. Vandesompele, K. De Preter, F. Pattyn, B. Poppe, N. Van Roy, A. De Paepe, F. Speleman, Accurate normalization of real-time quantitative RT-PCR data by geometric averaging of multiple internal control genes, Genome Biol. 3 (2002) RESEARCH0034-RESEARCH0034. https://www.ncbi.nlm.nih.gov/pubmed/12184808.

[17] M.W. Pfaffl, A new mathematical model for relative quantification in real-time RT-PCR., Nucleic Acids Res. 29 (2001) e45. http://www.pubmedcentral.nih.gov/articlerender.fcgi?artid=55695&tool=pmcentrez&rendertype=abstract.

[18] E. Taboada, P. Fisher, R. Jara, E. Zúñiga, M. Gidekel, J.C. Cabrera, E. Pereira, A. Gutiérrez-Moraga, R. Villalonga, G. Cabrera, Isolation and characterisation of pectic substances from murta (Ugni molinae Turcz) fruits, Food Chem. 123 (2010) 669–678. doi:10.1016/j.foodchem.2010.05.030.

[19] M.C. Jonathan, J.J.G.C. van den Borne, P. van Wiechen, C. Souza da Silva, H. a. Schols, H. Gruppen, In vitro fermentation of 12 dietary fibres by faecal inoculum from pigs and humans, Food Chem. 133 (2012) 889–897. doi:10.1016/j.foodchem.2012.01.110.

[20] H. Lazan, S.-Y. Ng, L.-Y. Goh, Z.M. Ali, Papaya beta-galactosidase/galactanase isoforms in differential cell wall hydrolysis and fruit softening during ripening., Plant Physiol. Biochem. 42 (2004) 847–53. doi:10.1016/j.plaphy.2004.10.007.

[21] C.-P. Soh, M.A. Zainon, H. Lazan, Characterisation of an α-galactosidase with potential relevance to ripening related texture changes, Phytochemistry. 67 (2006) 242–254. doi:10.1016/j.phytochem.2005.09.032.

[22] S.G. Gwanpua, S. Van Buggenhout, B.E. Verlinden, S. Christiaens, A. Shpigelman, V. Vicent, Z.J. Kermani, B.M. Nicolai, M. Hendrickx, A. Geeraerd, Pectin modifications and the role of pectin-degrading enzymes during postharvest softening of Jonagold apples, Food Chem. 158 (2014) 283–291.

[23] A.W. Zykwinska, M.J. Ralet, C.D. Garnier, Evidence for In Vitro Binding of Pectin Side Chains to Cellulose 1, 139 (2005) 397–407. doi:10.1104/pp.105.065912.1.

[24] D. a. Brummell, Cell wall disassembly in ripening fruit, Funct. Plant Biol. 33 (2006) 103. doi:10.1071/FP05234.

[25] G.D. Manrique, F.M. Lajolo, Cell-wall polysaccharide modifications during postharvest ripening of papaya fruit (Carica papaya), Postharvest Biol. Technol. 33 (2004) 11–26. doi:10.1016/j.postharvbio.2004.01.007.

[26] T. Wang, Y.B. Park, D.J. Cosgrove, M. Hong, Cellulose-Pectin Spatial Contacts Are Inherent to Never-Dried Arabidopsis Primary Cell Walls: Evidence from Solid-State Nuclear Magnetic Resonance, Plant Physiol. 168 (2015) 871–884. doi:10.1104/pp.15.00665.

[27] A. Zykwinska, J.F. Thibault, M.C. Ralet, Competitive binding of pectin and xyloglucan with primary cell wall cellulose, Carbohydr. Polym. 74 (2008) 957–961. doi:10.1016/j.carbpol.2008.05.004.

[28] D.J. Cosgrove, Re-constructing our models of cellulose and primary cell wall assembly, Curr. Opin. Plant Biol. 22 (2014) 122–131. doi:10.1016/j.pbi.2014.11.001.

[29] Z. a. Popper, S.C. Fry, Xyloglucan-pectin linkages are formed intra-protoplasmically, contribute to wall-assembly, and remain stable in the cell wall, Planta. 227 (2008) 781–794. doi:10.1007/s00425-007-0656-2.

[30] A. Manenoi, R.E. Paull, Papaya fruit softening, endoxylanase gene expression, protein and activity., Physiol. Plant. 131 (2007) 470–80. doi:10.1111/j.1399-3054.2007.00967.x.

[31] Y. Han, Q. Zhu, Z. Zhang, K. Meng, Y. Hou, Q. Ban, J. Suo, J. Rao, Analysis of xyloglucan endotransglycosylase/hydrolase (XTH) genes and diverse roles of isoenzymes during persimmon fruit development and postharvest softening, PLoS One. 10 (2015) 1–20. doi:10.1371/journal.pone.0123668.

[32] J. Cybulska, A. Zdunek, A. Koziol, The self-assembled network and physiological degradation of pectins in carrot cell walls, Food Hydrocoll. 43 (2015) 41–50.

[33] J.A. Sañudo-Barajas, J. Labavitch, C. Greve, T. Osuna-Enciso, D. Muy-Rangel, J. Siller-Cepeda, Cell wall disassembly during papaya softening: Role of ethylene in changes in composition, pectin-derived oligomers (PDOs) production and wall hydrolases, Postharvest Biol. Technol. 51 (2009) 158–167. doi:10.1016/j.postharvbio.2008.07.018.

[34] V. Prasanna, T.N. Prabha, R.N. Tharanathan, Fruit Ripening Phenomena–An Overview, Crit. Rev. Food Sci. Nutr. 47 (2007) 1–19. doi:10.1080/10408390600976841.

Supplementaty files

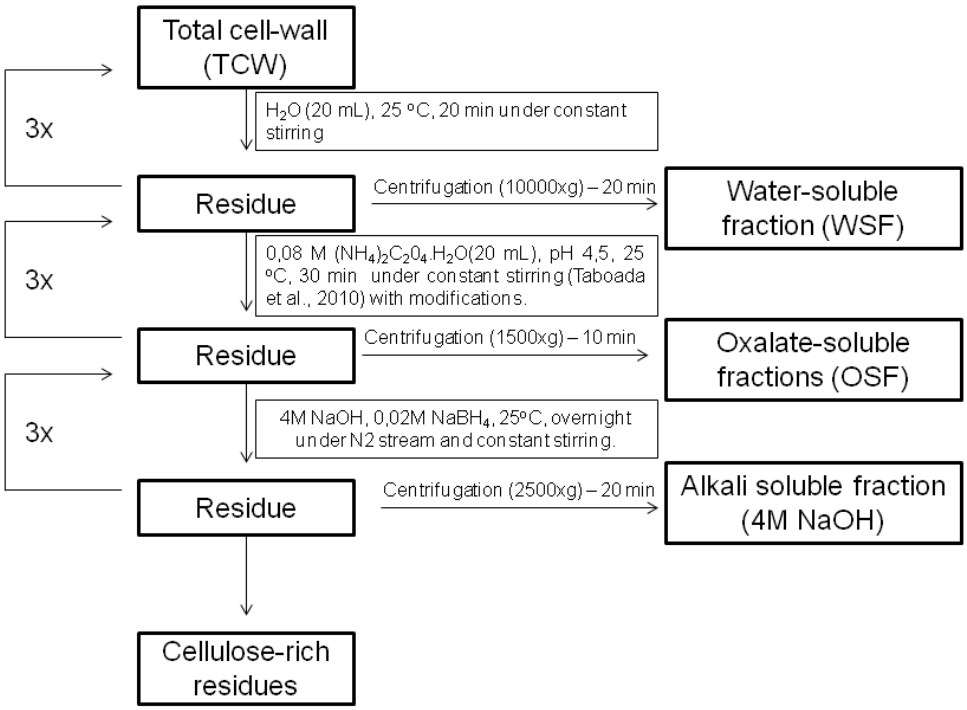

Fig. S1. Schematic sequence of papaya cell wall extraction and fractionation.

Table S1. Nucleotide sequences used in qPCR.

Gene	*Primer name*	*Sequence (5'→3')*
cpPG1	>pg1_f	TGG TGG TGC GTA TAG ATG GA
	>pg1_r	ACA AAA CCC AGT ACC CAC CA
cpPG2	>pg2_f	TCC TGA AGC TCA CCC TTC AT
	>pg2_r	CCT CAA TGC CTT TGA AGC TC
cpPG3	>pg3_f	TTG GAG GGC AGC TTG TTT AG
	>pg3_r	CAC CCA AGC CTT TAT TGT TCC
cpPL1	>pl1_f	TTC CCT GTG GGC TTA CAA TC
	>pl1_r	AGG GAG GTC TGC CAT TAC AT
cpPL2	>pl2_f	CAT GTT CTT GTC CTG CGT GT
	>pl2_r	CCA TCC ACG GCT CTA ATT TC
cpAGAL1	>a-gal1_f	GTA TAG GCG GAA GGT GGA T
	>a-gal1_r	AAG GCC ACC TCT CTG GAT
cpAGAL3	>a-gal3_f	TGT CCG TTG ATC CTT CAG TG
	>a-gal3_r	AGT CCG GAA GAA TGC TGA TG
cpBGAL1	>bgal1_f	GTG CTT GCA ACT ATG CTG GA
	>bgal1_r	ATA GGT TCG CAG TTG GGT TG
cpBGAL3	>bgal3_f	CCA AAG TGG GGA CAT TTG AG
	>bgal3_r	ACA CCC AGA CTT CGA CTT G
cpPME1	>pme1_f	TAT CTT GGT AGG CCC TGG A
	>pme1_r	AGG CCA GTG TTT CGG TAC T
cpPME2	>pme2_f	GTG GTT TGT TCC TCA GCA CA
	>pme2_r	TGG AAC GTA ACT GCA AGT GG
cpPME3	>pme3_f	GCA AGC TTT AGG GGT GTT GA
	>pme3_r	AGG CCT GCA GAG CTT ATT GA
cpARF	>arf_f	AGG TGG CTG TTT TGT TGA GG
	>arf_r	TCT CTT CCC AAG GTC CAA TG
cpXYL	>xyl_f	GCT TCC GCT GTG TTT TAT GG
	>xyl_r	ATG ATT GGA TCG ACC TCA GC
cpCELL	>cell_f	GCC TCC AGA CCC ATT TC TTT
	>cell_r	CAT CGA AGA TGG TGA CAA CG
cpXTH	>xth_f	GCA CTC AGG AGG AAG AGT A
	>xth_r	GTG GGA CCA GAA GGA GTT T
cpACT	>act_f	CGT GAC CTT ACT GAT CAC TTG
	>act_r	GTC AAG GGC AAT GTA AGA CAG
cpEF1	>ef1_f	GTT AAG AAC GTT GCC GTG AAG
	>ef1_r	ATG TGA AGT TGG CTG CTT CCT
cpUBQ	>ubq_f	ACT CAC CGG CAA GAC CAT
	>ubq_r	GTG GAG AGT CGA TTC CTT TTG

Table S2. GenBank Annotations
PG1: FJ007644
PG2: GQ479791
PG3: GQ479794
PL1: DQ660903
PL2: ABIM01001816
AGAL1: ABIM01008846
AGAL3: ABIM01016598
BGAL1: AF064786
BGAL3: ABIM01026480
PME1: GR486204
PME2: ABIM01018702
PME3: ABIM01014785
ARF: GQ479793
XYL: AY138968
CELL: ABIM01009161
XTH: ABIM01014233

Table S3. Calibration curves for relative gene expression.

Name of the gene	*Efficiency (10-slope)*	*y=ax+b*	R^2
cpPG1	1.96	-3.4408x + 22.295	0.9973
cpPG2	1.94	-3.4841x + 27.584	0.9906
cpPG3	1.93	-3.4997x + 28.439	0.9999
cpPL1	1.98	-3.3722x + 23.508	0.9954
cpPL2	1.82	-3.8546x + 35.543	0.9922
cpAGAL1	2.20	-2.9239x + 25.249	0.9872
cpAGAL3	2.17	-2.9673x + 25.612	0.9689
cpBGAL1	2.05	-3.2145x + 24.034	0.9895
cpBGAL3	1.93	-3.4933x + 25.775	0.9992
cpPME1	1.95	-3.4408x + 22.295	0.9993
cpPME2	1.94	-3.4841x + 27.584	0.9906
cpPME3	1.93	-3.4997x + 28.439	0.9999
cpARF	2.00	-3.3321x + 27.523	0.9885
cpXYL	1.94	-3.4742x + 23.389	0.9998
cpCELL	1.86	-3.7239x + 24.695	0.9942
cpXTH	1.74	-4.1503x + 28.827	0.9898
cpACT	2.03	-3.2446x + 21.922	0.9884
cpEF1	1.92	-3.5886x + 25.540	0.9779
cpUBQ	1.89	-3.4841x + 22.049	0.9906

Chapter 3

Ingestion of non-digestible carbohydrates from plant-source foods and decreased risk of colorectal cancer: A review on the biological effects and the mechanisms of action

Samira Bernardino Ramos do Prado[1,2,†], Victor Costa Castro-Alves[1,2,†], Gabrielle Fernandez Ferreira[1], João Paulo Fabi[1,2,3,*]

[1] Department of Food Science and Experimental Nutrition, School of Pharmaceutical Sciences, University of São Paulo, São Paulo, SP, Brazil

[2] Food Research Center (FoRC), CEPID-FAPESP (Research, Innovation and Dissemination Centers, São Paulo Research Foundation), São Paulo, Brazil

[3] Food and Nutrition Research Center (NAPAN), University of São Paulo, São Paulo, Brazil

† These authors have contributed equally to this work

Frontiers in Nutrition, Submitted, 2019.

Abstract

The hypothesis that links the increase in the intake of plant-source foods to a decrease in colorectal cancer (CRC) risk has almost fifty years. Nowadays, systematic reviews and meta-analysis of case-control and cohort studies confirmed the association between dietary patterns and CRC risk, in which the non-digestible carbohydrates (NDC) from plant-source foods are known to play beneficial effects. However, the mechanisms behind the physicochemical properties and biological effects induced by NDC on the decrease of CRC development and progression remain not fully understood. NDC from plant-source foods consist mainly of complex carbohydrates from plant cell wall including pectin and hemicellulose, which vary among foods in structure and in composition, therefore in both physicochemical properties and biological effects. In the present review, we highlighted the mechanisms and described the recent findings showing how these complex NDC from plant-source foods are related to a decrease in CRC risk through induction of both physicochemical effects in the gastrointestinal tract, fermentation-related effects, and direct effects resulting from the interaction between NDC and cellular components including toll-like receptors and galectin-3. Studies support that the definition of the structure-function relationship—especially regarding the fermentation-related effects of NDC, as well as the direct effects of these complex carbohydrates in cells—is crucial for understanding the possible NDC anticancer effects. The dietary recommendations for the intake of NDC are usually quantitative, describing a defined amount of intake per day. However, as NDC from plant-source foods can exert effects that vary widely according to the NDC structure, the dietary recommendations for the intake of NDC plant-source foods are expected to change from a quantitative to a qualitative perspective in the next few years, as occurred for lipid recommendations. Thus, further studies are necessary to define whether specific and well-characterized NDC from plant-source foods induce beneficial effects related to a decrease in CRC risk, thereby improving nutritional recommendations of healthy individuals and CRC patients.

Keywords: Colorectal cancer; Dietary fibre, Fermentation; Galectin-3, Non-digestible carbohydrates, Pattern Recognition Receptors; Pectin; Tool-like receptors.

Abbreviations: AceA, Aceric acid; Ac, Acetylated; Api, Apiose; Ara, Arabinose; CRD, Carbohydrate recognition domain; CLR, C-type lectin receptors; CRC, Colorectal cancer; DAMP, damaged-associated molecular patterns; Fuc, Fucose; Gal, Galactose; GalA, galacturonic acid; Gal-3, Galectin-3; Glc, Glucose; HSP, Heat shock proteins; HDAC, Hystone deacetylases; HG, Homogalacturonan; IEC, Intestinal ephitelial cells; LPS, Lipopolysaccharide; LRR, C-terminal leucine-rich repeat motif; Man, Mannose; MAPK, mitogen-activated protein kinase; Me, Methylated; MCP, Modified citrus pectin; NDC, Non-digestible carbohydrates; NRL, Nucleotide binding oligomerization domain (NOD)-like receptors; PAMP, Pathogen-associated molecular patterns; PRR, Pattern recognition receptors; RIPK, receptor-interacting serine/threonine-protein kinase; RG, Rhamnogalacturonan; Rha, Rhamnose; SCFA, short-chain fatty acids; TLR, Toll-like receptors; Xyl, Xylose;

Introduction

Relationship between the intake of plant-source foods and decrease in colorectal cancer risk

Cancer is one of the leading cause of death globally. Around one-third of cancer-related death are mostly connected to behavioural and dietary habits including tobacco and alcohol use, lack of physical activity, high body mass index, and low intake of fruits and vegetables [1]. Colorectal cancer (CRC) is known to be associated mainly with dietary patterns of the so-called western lifestyle. The incidence of CRC is higher in developing countries and this incidence is increasing fast in both low- and middle-income countries. This is mainly due to a shift in dietary patterns towards a decreased intake of plant-source foods and an increased intake of fat, sugar and animal-source foods [2]. Despite CRC is the second most diagnosed type of cancer in men and the third in women, as well as the third leading cause of all cancer death, only less than 10% of CRC arise from inherited syndromes [3,4]. Thus, studies have systematically pointed out that tackling modifiable risk factors, specially changing the dietary patterns, can substantially reduce CRC-related deaths [5–10].

Recently, a prospective longitudinal study revealed that a dietary pattern characterized by the high intake of plant-source foods is associated to a delayed CRC risk up to 10 years [11]. Systematic reviews and meta-analysis of case-control and cohort studies also reported an inverse association between the intake of plant-source foods and CRC risk [12–14]. Besides scientific data, the traditional knowledge suggests the intake of plant-source foods as adjuvant treatment against CRC [15]. As plant-source foods contain relatively high amounts of biologically active molecules, such as polyphenols and non-digestible carbohydrates (NDC), the adoption of specific nutritional interventions using fruits and vegetables has been taken into consideration to assist cancer therapies [16]. Furthermore, the increased ingestion of dietary fibre from plant-source foods, which are composed mainly by the NDC that constitutes the plant cell wall, is known for a long time to play a pivotal role in the reduction of CRC risk [17–20].

Although NDC are resistant to digestion by human enzymes, these carbohydrates are not a static collection of food components that pass through the gastrointestinal tract without inducing biological effects. Instead, NDC modulate nutrient absorption through binding to organic molecules that induce indirect biological effects acting as substrate for colonic fermentation by the gut microbiota [21]. Furthermore, recent efforts have focused on exploring the direct interaction between NDC and CRC cells that will be described further in this review. However, the composition and chemical structure of NDC may vary depending of plant species and tissues, thereby resulting in great heterogeneity of structure with variability in composition and branching pattern. Thus, although NDC from plant-source foods share common patterns and biological functions, the ingestion of these food components that have great variation in size and structure will result in structure-dependent properties and therefore diverse biological

effects. In this review, we will describe some known mechanisms through which NDC from plant-source foods induce beneficial health effects that relate to a decrease in CRC risk.

Structure of non-digestible carbohydrates from plant-source foods

As the chemical structure strongly influences the physicochemical properties and the biological effects of NDC from plant-source foods, it is necessary to define the main structural patterns of biologically active NDC in CRC models. NDC are comprised mainly by polysaccharides from plant cell wall, such as cellulose, hemicellulose and pectin (**Figure 1)**. Cellulose consists of relatively conserved polysaccharides with long and linear β-(*1,4*)-linked glucose (Glc) residues that vary in size according to plant species and tissue. On the other hand, hemicellulose consists of structurally complex and heterogeneous oligo- and polysaccharides with β-(*1,4*)-linked backbone of xylose (Xyl), Glc, mannose (Man) or galactose (Gal). The hemicellulosic fractions include xylans (glucoronoxylan, arabinoglucoronoxylan, arabinoxylan and other heteroxylans), mannans (acetylated and non-acetylated mannan, galactoglucomannan, galactomannan and glucomannan), galactans (galactan and arabinogalactan), xyloglucans, and mixed-linkage glucans [22], which vary in size and branching pattern.

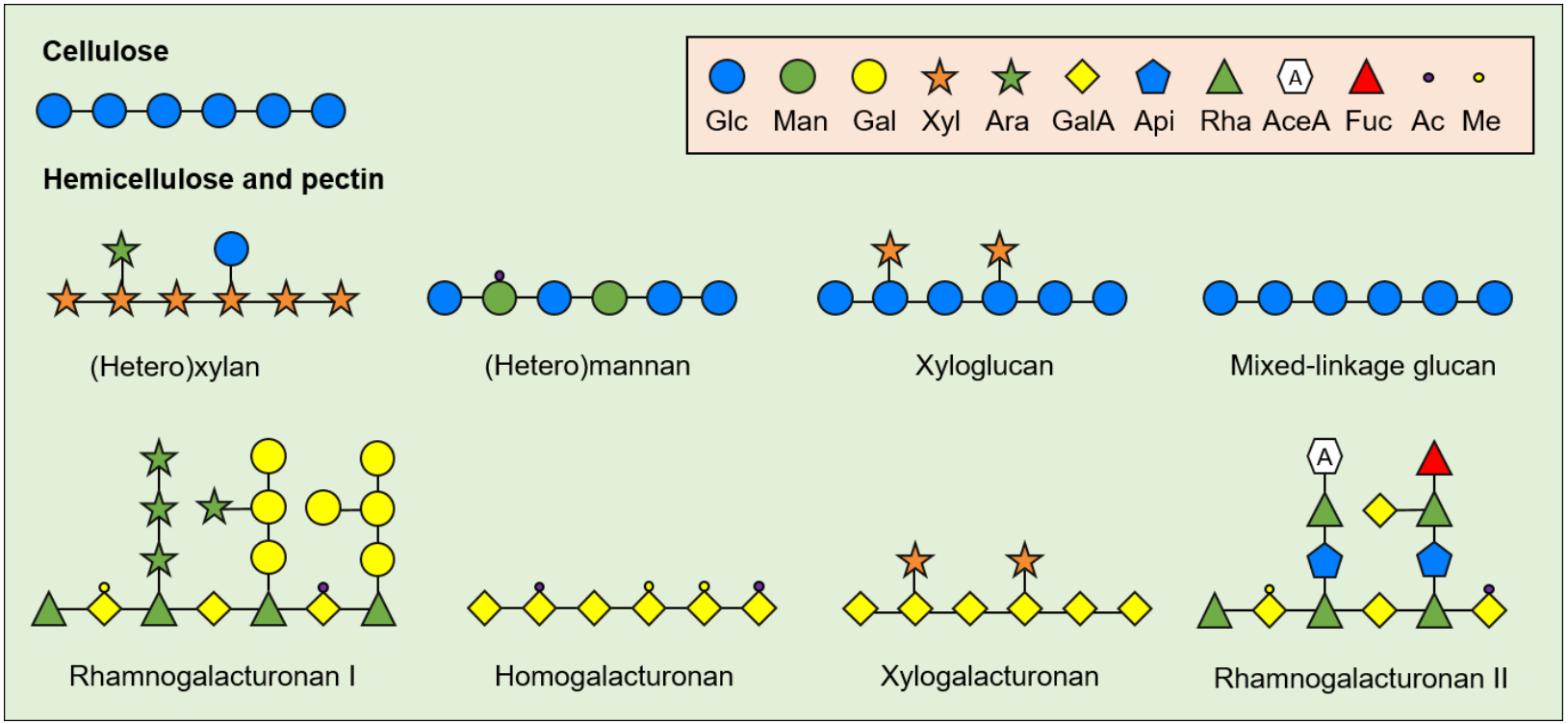

Figure 1. General structure of plant cell wall-derived non-digestible carbohydrates (NDC). Cell-wall derived NDC from plant-source foods include cellulose, hemicelluloses and pectin. Glc, Glucose; Man, Mannose; Gal, Galactose; Xyl, Xylose; Ara, Arabinose; GalA, galacturonic acid; Api, Apiose; Rha, Rhamnose; AceA, Aceric acid; Fuc, Fucose; Ac, Acetylated; Me, Methylated.

Similar to hemicellulose, pectin consists of linear and ramified homo- and heteropolysaccharides; however, pectin contains relatively high amount of acidic monomers compared to hemicellulose including mainly galacturonic acid (GalA). The major fraction of pectin usually consists of linear α-(*1,4*)-linked GalA residues (homogalacturonan, HG) with varying degree of methyl and acetyl esterification. Xylogalacturonan is also a component of pectin and have the same α-(*1,4*)-linked GalA backbone as HG but substituted at C2 and C3 with β-(*1,3*)-linked Xyl residues [23]. The pectic fraction also consists of branched structures named rhamnogalacturonan (RG-) I and II. RG-I is usually pointed out as the second major pectic fraction in plant-source foods and consists of a backbone of alternate α-(*1,4*)-GalA and α-(*1,2*)-rhamnose (Rha), in which the latter can be substituted at O4 mainly by arabinans, galactans and arabinogalactans – although substitutions with Xyl and Glc residues coexist in specific plant-source foods [24]. Finally, RG-II consists of an α-(*1,4*)-linked GalA backbone with complex branches made up of rare monomers (e.g. aceric acid and apiose) with different side chain, size and conformation depending on plant-food source [25–27].

As mentioned above, even though NDC is generally considered as a dietary fibre, the diversity of NDC structure from plant-source foods result in different physicochemical properties, fermentation patterns, and biological effects, thereby making the evaluation of the structure-function relationship challenging. Thus, there is an increasing number of studies exploring which specific structural patterns of NDC induce beneficial biological effects in CRC models [28–30].

Effects of the non-digestible polysaccharides on CRC development and progression

Studies have shown the association between the intake of specific food components and cancer, such as an inverse correlation between the intake of NDC from plant-source foods and CRC development and progression [12,18,31–33]. However, despite the evidence that high intake of NDC could reduce the risk of CRC up to 38% [34], the levels of this evidence is still considered as probable, because of both the broad spectrum of CRC subtypes [35], and the heterogeneity of physical and biological functions of NDC from distinct plant sources [36–38]. Besides that, there are the presence of others dietary components in food matrix that influence the physicochemical properties and biological effects of NDC [39]. Therefore, as some studies did not consider dietary components other than NDC in plant-source foods, such as polyphenols, vitamins, and minerals [34], it is difficult to establish an inverse association between the intake of NDC and CRC risk. A reliable characterization of the complex NDC structure, followed by their isolation, purification and the study of their biological effect, is crucial to reach a desirable structure-function relationship between NDC and the anticancer effects.

There are three main mechanisms in which NDC act against CRC development and progression. The consumption of NDC can induce (A) physicochemical effects in the gastrointestinal tract, (B) fermentation-related effects, and (C) direct effects resulting from the

interaction between NDC and cells, such as intestinal epithelial cells (IEC), immune system cells, and CRC cells (**Figure 2**). Below we summarized the physicochemical and the fermentation-related effects of NDC from plant-source foods, and focused on the recent findings that show the possible mechanisms through which distinct NDC directly interact with cells, thereby suggesting new beneficial effects regarding the intake of NDC and decreased CRC development and progression.

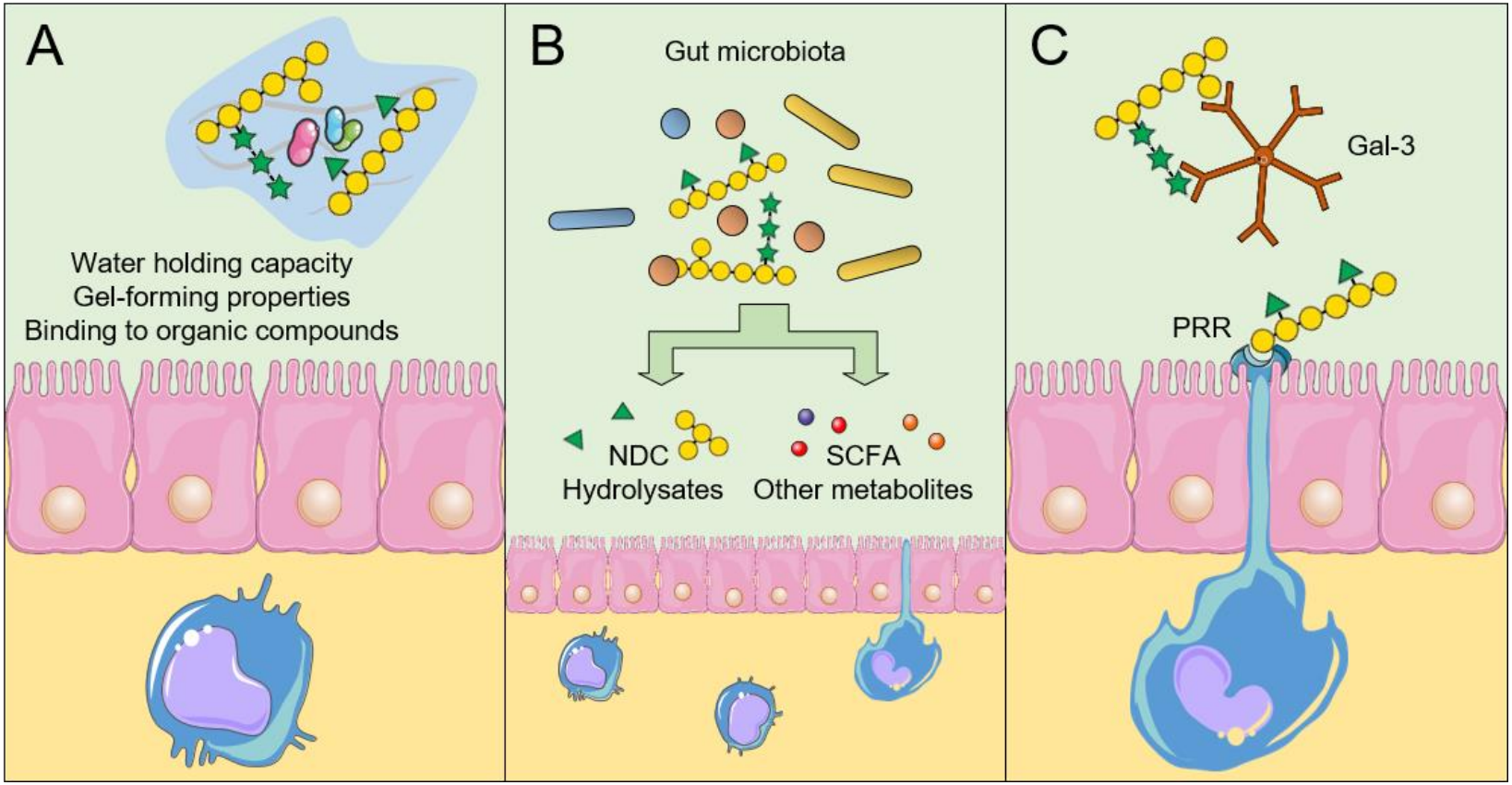

Figure 2. Physicochemical and biological effects of non-digestible carbohydrates (NDC) after the intake. (**A**) The physicochemical properties of NDC influence the absorption of other nutrients and reduce the interaction between carcinogens and the intestinal epithelium. Furthermore, NDC can promote an increase in satiety and stool bulk, as well as reduce the transit time throughout the gastrointestinal tract. (**B**) The fermentation-related effects result in the production of short-chain fatty acids (SCFA) and other metabolites, which can induce biological effects in epithelial intestinal cells, immune system cells and cancer cells. The fermentation of NDC by the gut microbiota can also influence the microbiota profile itself. (**C**) NDC can also interact directly with cellular components, such as the Pattern recognition receptors (PRR) and galectin-3 (Gal-3), thereby inducing downstream signalling pathways in cells and affecting cancer cell adhesion and invasion. The figure was modified from Smart Servier Medical Art (http,//smart.servier.com/), licensed under a Creative Common Attribution 3.0 Unported Licens (https,//creativecommons.org/licenses/by/3.0/).

Physicochemical effects

The physicochemical effects of NDC in the gastrointestinal tract are related to the interaction of these carbohydrates with other components through gel-forming properties, water holding capacity, and the ability of binding to other organic compounds [40].

Both gel-forming properties and water holding capacity result in increased stool bulk, thereby providing satiety [41]. Promising results concerning the effects of specific NDC on satiety have been stimulating industry to reformulate the nutritional composition of foods and community to change their dietary pattern, aiming to reduce obesity trends [42], which is a risk factor for CRC development [11,43]. The increase in stool bulk also contributes to the dilution of possible carcinogens. Furthermore, the reduction in stool transit time, which is a result of gastrointestinal mobility due to increased luminal content, reduces the exposition of IEC cells to carcinogens [44]. NDC can also entrap other food components or metabolites, thereby influencing macronutrient digestibility or metabolite reabsorption (e.g. glucose, lipids, bile acid) [37], and having a positive impact on postprandial insulin levels and glycaemic response. As example, β-glucan from barley, which consists mainly of linear and mixed β-(*1,4*)- and β-(*1,3*)-linked Glc polysaccharides, reduces postprandial glycaemic response improving glycaemic control [45]. Furthermore, β-glucan from distinct barley varieties bind to primary and secondary bile acids in intestine [46] and reduces bile acid reabsorption through the enterohepatic circulation, which is associated to a reduction of serum cholesterol levels [47,48].

The abovementioned physicochemical effects of NDC are dependent on both their macrostructure (e.g., molecular weight, degree of crystallinity, and particle size) and microstructure (e.g., presence of functional groups). In terms of macrostructure, studies suggest that β-glucans from cereals should have a molecular weight above 100 kDa to increase the viscosity of the digestive effluents and to induce a positive effect on postprandial response [49]. However, oat β-glucans with lower molecular weight have also increased bile acid capacity [50]. The overall structure is also a major source of variability in the physicochemical effects, since the threshold for arabinoxylans to induce a similar effect to that of β-glucans on postprandial response is significantly lower—approximately 20 kDa [49]. Furthermore, as the crystallinity of NDC influences their interaction with other components in the gastrointestinal lumen, changes in the crystallinity of NDC have a strong impact in their physicochemical effects. In this context, it was shown that rats fed with distinct celluloses with a degree of crystallinity ranging from 8 to 20% had differences in their faecal water content, which appears to be related to an inverse relationship between crystallinity and water holding capacity [51]. This inverse relationship is not observed only for cellulose [52], but also for other NDC from plant-source foods including galactomannans from coconut flour [53] and fenugreek [54]. The particle size of NDC also influences the physicochemical effects of NDC, as shown by the increase in water holding and lipid binding capacity of NDC from coconut after grinding [55]. However, other studies demonstrated that the reduction in the particle size of NDC decreased

the water holding capacity, as observed for NDC from rice bran [56], wheat bran [57], and citrus [58].

Recent studies that applied distinct processing methods (e.g., micronization, milling and enzymatic degradation) in NDC from plant-source foods also support the relationship between changes in both the degree of crystallinity and particle size with changes in the physicochemical effects [59–61]. For example, the reduction in the particle size of NDC from carrots subjected to high-pressure micronization, but not by ball milling, increases its water holding and lipid binding capacity [56].

In addition to the enzymatic- and physical-induced changes in the microstructure of NDC, studies are also exploring whether the introduction/removal of functional groups influences the physicochemical effects of specific NDC from plant-source foods. The phosphorylation of NDC from soybean does not appear to change its bile acid binding capacity. However, the water holding capacity of the phosphorylated NDC are 1.5-fold higher compared to the native NDC [62]. The degree of esterification also appears to be directly related to the water holding capacity of NDC, as was found for citrus pectin [63] and more recently for NDC extracted from eggplant [64].

Therefore, processing methods that affect the macrostructure or the microstructure of NDC can be applied to control the physicochemical effects of these dietary components. The knowledge and control in NDC characteristics may in turn be useful in for the selection and production of NDC from plant-source foods with desired physicochemical properties that are relates related to a decreased CRC risk.

Fermentation-related effects

The chemical structures of NDC are crucial for colonic fermentation because not all NDC are fermented, and because different metabolites resulting from the fermentation of distinct NDC act on a broad range of downstream signalling pathways in non-cancer cells and in CRC cells [65]. Besides the structure-dependent effects, the fermentation-related effects of NDC in the decrease of CRC risk are dependent of the gut microbiota itself since distinct bacteria profile will result in differentially bioactive metabolites production in a time- and structure-dependent manner [66–68].

Some bacteria from the human gut microbiota possess a large repertoire of enzymes that hydrolyse glycosidic linkages from complex carbohydrates to use the hydrolysates and some metabolites as energy sources [69]. However, the identification of key bacterial species in the gut microbiota that are responsible for the disassembling of specific NDC structural patterns remains somewhat limited [25,28,69–72]. Despite the questions that still need to be answered, the main outcomes of fermentation-related effects that contribute to a decreased CRC risk are the modulation of gut microbiota profile and the production of biologically active

metabolites including short-chain fatty acids (SCFA), such as acetate, propionate and butyrate [73]. The association between SCFA and the reduction of CRC risk was reviewed elsewhere [21,74].

SCFA produced after fermentation of NDC could help to maintain the lumen pH at lower levels, thereby inhibiting pathogens growth and favouring the establishment of a healthy gut microbiota. SCFA, especially butyrate, also stimulate IEC growth by functioning as the primary source of energy for these cells while being metabolized by β-oxidation in the mitochondria. Several mechanisms for SCFA uptake across the apical membrane of IEC had been proposed including transport by monocarboxylate transporter (e.g., MCT1 and SMCT1), counter-transport with bicarbonate, and passive diffusion [75]. These SCFA also act in downstream signalling pathways in CRC cells [76,77] and in non-cancer cells including IEC and immune system cells [78,79] through interaction with G protein coupled receptors (FFAR2/GPR43, FFAR3/GPR41, GPR109a and Olfr78) [80]. Thus, the uptake of SCFA by IEC results not only in the provision of energy to normal metabolic functions but also in the production of interleukin (IL-) 18 [81], involved in the maintenance of epithelial integrity, as well as in the increased secretion of antimicrobial peptides [82]. For example, butyrate reduces pro-inflammatory effects by inhibiting nuclear factor-κB (NF-κB) activation [83], as well as the Wnt signalling pathway, a pro-inflammatory pathway [84] constitutively expressed in some CRC cells [85]. Besides effects in CRC cells, butyrate contributes to the normal turnover of cells in the gastrointestinal tract, as it induces proliferation of IEC at the crypt of the colon and increases apoptosis of IEC at the villus [86]. Notably, this effect on proliferation does not occur at the same extent in CRC cells because cancer cells present a shift from oxidative metabolism to anaerobic glycolysis (the so-called Warburg effect), which results in the accumulation of lactic acid. As CRC cells rely on glucose as their primary energy source instead of butyrate, this shift in the metabolism of CRC cells results in accumulation of butyrate, whose increased intracellular levels inhibits histone deacetylases (HDAC), thereby resulting in cell cycle arrest and further induction of apoptosis in cancer cells [87] (**Figure 3**).

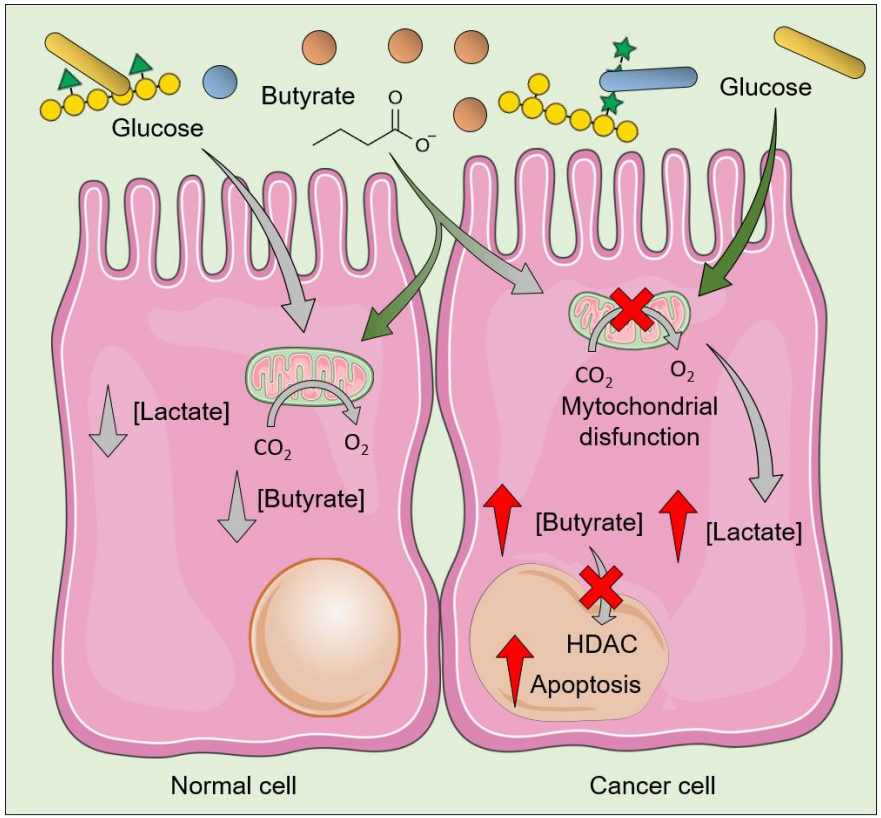

Figure 3. Effects of butyrate in normal cells and colorectal cancer cells (CRC). The butyrate produced during fermentation of non-digestible polysaccharides induces distinct effects in normal cell and CRC cells, as the latter rely on glucose—instead of butyrate—as their primary energy source. Increased glycolysis results in increased intracellular levels of lactate and decreased clearance/utilisation of butyrate, whose increased intracellular levels inhibit histone deacetylases (HDAC) and induce death of CRC cells. As normal cells usually butyrate as the main energy source, relatively low levels of butyrate is accumulated. The figure was modified from Smart Servier Medical Art (http,//smart.servier.com/), licensed under a Creative Common Attribution 3.0 Unported Licens (https,//creativecommons.org/licenses/by/3.0/).

In addition to the induction of IL-18 by IEC, which is also crucial for intestinal immune homeostasis since IL-18 helps maintaining the balance between T helper 17 cells (T_h17) and regulatory T cells (T_{reg}) [88,89], SCFA also interact directly with innate mechanisms of defence. In neutrophils, SCFA modulates recruitment, effector function, and cell survival [90]. Phagocytes including dendritic cells and macrophages also respond to SCFA, which regulates pro-inflammatory cytokine production [91,92].

Thus, despite CRC cells can use SCFA as energy source for proliferation [93], the fermentation-related effects on IEC and immune system cells have a clear relationship with the maintenance of host defence mechanisms and therefore with regulation of inflammatory response. As the molecular pathobiology of CRC usually implicates in pro-inflammatory conditions with an increase in the secretion of cytokines and chemokines that will promote malignant progression, invasion, and metastasis [94], the fermentation-related effects are generally regarded as an essential mechanism through which the intake of NDC relate with reduced inflammation and reduced CRC development and progression. For more detailed reviews regarding these fermentation-related effects of NDC in non-cancer and CRC cells, as well as the interplay between gut microbiota and fermentation-related beneficial effects, the reader is referred to Lam et al. [95], McNabney and Henagan [96], van der Beek et al. [97], and Zhou et al. [98].

Despite the mechanisms through which the fermentation-induced SCFA production relates to a decrease in CRC risk appear to be well known, recent studies have also been conducted to explore how specific NDC affect gut microbiota composition. As bacterial strains have distinct prebiotic properties, changes in the microbiota composition induced by these dietary components may influence SCFA production, thereby influencing CRC risk. A previous study strongly supports this hypothesis by showing changes in the microbiota composition of children from Europe and rural Africa during the transition between breast milk feeding and the introduction of solid diet [99]. The study has shown that differences between the faecal microbiota composition of children from Europe and rural Africa occurred only after the introduction of a solid diet. Children from Europe have reduced consumption of NDC from plant-source foods (e.g., arabinoxylans) compared to children from rural Africa, and this difference appears to induce an enrichment of Bacteroidetes phylum—whose members have specific genes encoding xylanases—in the gut microbiota of children from rural Africa. After this finding, numerous studies have applied *in vivo* analysis of faecal microbiota and/or *in vitro* human faecal fermentation to explore whether specific NDC induce changes in the microbiota composition, providing insights into the relationship between structure of NDC and their prebiotic function, as showed by the structure-dependent effects of NDC in promote the survival of *Lactobacillus* spp [100]. Furthermore, a recent study [101] explored the relationship between the structure of distinct NDC from orange, lemon, lime and sugar beet, and their beneficial effects on the modulation of gut microbiota. Using an *in vitro* colonic fermentation model (TIM-2), the authors had found that the increase in the degree of esterification of HG appears to be the most important parameter in determining beneficial effects on gut microbiota

composition, followed by the composition of neutral sugars (e.g., increase in HG/RG ratio and the presence of arabinose) and the reduction in the degree of branching [101].

Thus, although studies are successfully proving insights into the relationship between the structure and prebiotic function of purified NDC from plant-source foods, the preference of a specific bacterial strain in utilize an NDC from a food matrix appears to be more complex, as the fermentation rate of a single NDC is affected when others NDC and other dietary components (e.g., polyphenols) are present [39]. In this context, it was found that mixing fast-fermenting NDC including HG from citrus pectin and xyloglucan from tamarind reduces their fermentation rate, thereby delaying the prebiotic effect [102]. This reduction in the fermentation rate probably make NDC reach the distal parts of the colon, which is of particular importance in terms of CRC risk. The reduced fermentation rate in the distal part of the colon have been thought as one of the reasons why most of CRC are detected in this region. This delay in the prebiotic effect by mixing different NDC appear to occur because of the hierarchical preference, which refers to the ability of a bacterial strain in prioritize the utilisation of some NDC before others [103]. Studies confirm the hierarchical preference by observing that a bacterial strain can prioritize the fermentation of specific host mucosal glycans [104] or NDC from plant-source foods [105]. Examples of hierarchical preference includes the preference of *Bacteroides thetaiotaomicron* in utilising galactan from potato instead of arabinan from sugar beet [103], as well as the increased ability of *Bacteroides* spp., *Bifdobacterium* spp., *Faecalibacterium* spp., and *Lactobacillus* spp. in utilise fructans with low molecular weight compared to fructans with high molecular weight [106,107]. These hierarchical preferences appear to be strain-specific, as closely related gut bacterial strains (e.g., *B. thetaiotaomicron* and *B. ovatus*, or *L. delbruckii* and *L. paracasei*) prioritize the use of distinct NDC [71,108]. Furthermore, recent studies are focusing on evaluate whether distinct gut microbiota profiles can utilize specific NDC from plant-source foods, such as arabinoxylans from corn and sorghum, and fructans from chicory root [105,109]. Therefore, studies using more complex samples such as the whole food or a mix of NDC instead of using a single NDC, as well as studies comparing the ability of distinct microbiota profiles in utilizing the same NDC—as performed by Yang et al. [110], Chen et al. [105] and Brahma et al. [111]—, are elucidating practical knowledge required to use prebiotic therapy or diet modifications to benefit the function of specific bacterial strains that relates to a decreased CRC risk.

Direct effects

NDC share structural features to lipopolysaccharides and other structural carbohydrate-containing molecules at the surface of bacteria [112,113]. As these carbohydrates from bacteria directly interact with IEC and immune system cells along the gastrointestinal tract, it was hypothesized that NDC from plant-source foods also directly interact with cells in the gut.

The abovementioned hypothesis has been confirmed through *in vitro* studies and most recently through *in vivo* studies [114]. Since pattern-recognition receptors (PRR) in cells are

the main responsible for the recognition of bacterial carbohydrates, efforts have been made mainly on the investigation of the PRR-mediated effects of NDC [115], although some direct but PRR-independent mechanisms have also been described [116,117] and will be pointed out later in this review.

Pattern recognition receptor-mediated effects

PRR existing in IEC and immune system cells regulates epithelial proliferation and intestinal permeability, and maintains gut homeostasis through recognition of harmful organisms and endogenous metabolites [118]. Furthermore, PRR plays an important role in shaping intestinal microbiota in both composition and number by interacting with commensal bacteria [119]. Thus, PRR-mediated signalling pathways result in immune surveillance and in maintenance of host-bacteria interaction alongside the gastrointestinal tract, whose dysregulation is clearly associated with increased CRC risk [98,120]. As NDC influence microbiota profile and therefore the formation of specific metabolites in the gut lumen, the intake of plant-source foods rich in NDC influences the PRR-mediated responses through an indirect mechanism. Interestingly, NDC also directly interacts with PRR in a structure-dependent manner [114,115].

The PRR include RNA helicases (RLR), Nucleotide binding oligomerization domain (NOD)-like receptors (NLR), C-type lectin receptors (CLR) and Toll-like receptors (TLR), which recognize distinct evolutionarily conserved pathogen-associated molecular patterns (PAMP) of microorganisms—such as the carbohydrate-containing molecules at the surface of microorganisms—as well as endogenous damaged-associated molecular patterns (DAMP) [120]. Despite the variety of PRR in human cells, only few PRR has been shown to recognize NDC from plant-source foods (**Table 1**). Most of studies focused in the interaction between NDP from plant-source foods and TLR, but we will also describe some recent findings regarding the effects of NDC from foods through NLR- and CLR-dependent pathways.

Table 1. Pattern-recognition receptors (PRR) that recognizes non-digestible carbohydrates (NDC) from plant-source foods. NLR, Nod-like receptors; CLR, C-type lectin receptors; TLR, Tool-like receptors; HG, Homogalacturonan; RG-II, Rhamnogalacturonan II; AG, Type II arabinogalactan; ME, Methyl esterification; RS, Resistant starch; FOS, Fructooligosaccharides.

PRR	NDC	Plant-source food	Effects	Ref
NLR				
NOD1-2	HG, RG-II and AG-II	Papaya (ripe)	Activation in HEK cells, NF-κB release	[121]
NOD2	Inulin	Chicory root	Activation in HEK cells, NF-κB release	[115]
NLRP3	HG, RG-II and HC	Chayote	Inhibition of NLRP3 priming in macrophage-like cells	[122]
CLR				
Dectin-1	Mixed linkage β-glucan	Barley	Activation in immune cells, NF-κB release, IL-6 and IL-8 release	[123]
Dectin-1	Arabinoxylan	Wheat	Inhibition in HEK cells	[124]
TLR				
TLR2	Inulin	Chicory	Activation in THP-1 cells, NF-κB release	[115]
TLR2	RS2	Maize	Activation in HEK cells, NF-κB release	[125]
TLR2	Maltooligosaccharides	Wheatgrass	Activation in immune cells	[126]
TLR2 and 4	FOS	Rice	Induction of dendritic cell maturation in mice	[127]
TLR2 and 4	HG (varying degree of ME)	Lemon	Activation in T84 cells, maintenance of intestinal epithelial barrier integrity	[128]
TLR2 and 5	RS3	Maize	Activation in HEK cells, NF-κB release	[125]
TLR2, 3, 5, 9	HG, RG-II, AG-II and HC	Papaya (ripe)	Activation in HEK cells, NF-κB release	[121]
TLR2, 3, 9	HG, RG-II, AG-II and HC	Papaya (unripe)	Activation (TLR2) or inhibition (TLR3 and TLR9) in HEK cells	[121]
TLR4	Galactan	Apple	Inhibition of LPS-induced activation in a colitis model	[129]
TLR4	HG (varying degree of ME)	Citrus	Inhibition of LPS-induced activation in a colitis model	[130,131]
TLR4	HG (branched)	Citrus	Inhibition in immune cells	[130]

Continue...

PRR	NDC	Plant-source food	Effects	Ref
TLR4	Levan	Soybean	Cytokine release in mice	[132]
TLR4-8	Inulin	Chicory	Activation in THP-1 cells, NF-κB release	[115]
Heterodimers				
TLR1\TLR2	HG (low degree of ME)	Lemon	Inhibition of intestinal inflammation	[133]
Dectin-1\TLR2	Galactomannan	Guar gum	Inhibition of IEC *in vitro* and in a colitis model	[134]
Dectin-1\TLR2	Galactomannan	Guar gum	Inhibition of IEC in a colitis model	[135]

Nucleotide binding oligomerization domain-like receptor

All NLR have C-terminal leucine-rich repeat motifs (LRR) for ligand sensing, except NLRP10 [136], and a NACHT domain that facilitates protein oligomerization [137]. The presence of the LRR motif and NACHT domain are essential for NLR function, which acts as a scaffolding cytosolic protein that assembles signalling platforms triggering NF-κB and mitogen-activated protein kinase (MAPK) signalling pathways, thereby controlling the activation of several caspases [137]. Thus, the activation of NLR usually results in the assembling of pro-inflammatory complexes termed inflammasomes, which relates not only to NF-κB- and MAPK-mediated secretion of cytokines and chemokines but also to the activation of a myriad of cell death regulators [138]. Therefore, the dysregulation of NLR have been associated with infections, autoimmune diseases, inflammatory disorders and cancer, such as CRC [139,140].

Among the more than 20 NLR that have been identified in human cells [141], NOD1, NOD2 and NLRP3 are pointed out as the most important in terms of relevant biological functions and CRC development [138]. The mechanisms through NLR-mediated effects are associated with increased CRC risk relates mainly to an excessive NLR-induced chronic pro-inflammatory microenvironment [142]. Intriguingly, NLR agonists, specially NOD1 and NOD2 agonists, have been proposed as therapeutic agents in CRC treatment because both experimental studies showed that NOD1 deficiency leads to increased tumorigenesis in mice [143] and the activation of these NLR may regulate the pro-inflammatory effects induced by other PRR [144,145]. Thus, although both beneficial and deleterious effects of NLR activation on CRC remains not fully understood, it seems that punctual activation or inhibition of NLR could differentially induce effects during cancer development, progression, and metastasis.

Despite the relevance of NLR in CRC risk, few studies had focused on exploring the effects of NDC from plant-source foods in the regulation of NLR because they are cytosolic receptors. Phagocytes including macrophages can internalize NDC [146], but the exact mechanism of interaction between NDC and cytosolic receptors is not proven. Furthermore, it is known that IEC can transfer exosome-like vesicles from their apical or basolateral surface to both mesenteric lymph node and gut lumen [147], and these cells can also take up exosomes from foods (e.g., bovine milk exosomes) or produced by immune system cells [148]. However, despite these evidences, it is not possible to assert that vesicle trafficking between cells—or between cells and food components—is responsible for the internalization of NDC. Despite the lack of evidences on the mechanisms through which NDC interact with cytosolic receptors, our research group had recently found that NDC from ripe papaya, but not from unripe papaya, activated both NOD1 and NOD2 in an *in vitro* model using HEK 293 hNOD1 and HEK 293 hNOD2 reporter cells. The distinct effects of NDC from ripe and unripe papaya on NLR activation seem to be related to changes in the structure of NDC that occur during fruit ripening, as ripe papaya had increased proportion of homogalacturonans with higher degree of methylation compared to NDC from unripe papaya [121]. Notably, a similar NDC—also from papaya fruit—inhibited CRC cells proliferation *in vitro* [149]. Furthermore, linear β-(*1*,*2*)-linked fructose

oligosaccharides (inulin) from chicory root also activate NOD2 in HEK 293 hNOD2 reporter cells [115].

On the other hand, NDC from chayote fruit, which consists mainly of pectic homogalacturonan and highly branched RG-II, as well as hemicellulosic material including glucomannan, xyloglucan, and glucurono(arabino)xylan, inhibits NLRP3 inflammasome activation in human THP-1 macrophage-like cells. The effects of this NDC on NLRP3 inflammasome can be considered an indirect effect of the interaction between the NDC and other PRR that are essential to induce priming signals required for NLRP3 inflammasome activation [122]. In fact, cross-talk between PRR may occur through three main mechanisms. It can be a (a) requirement of two or more PRR for a specific biological response, (b) an interaction between PRR for robustness or redundancy of biological response, or (c) a negative regulation between PRR [150]. Thus, although the effects of NDC from chayote were not directly explored in CRC cells, it can be proposed that NDC-mediated effects on the modulation of cytosolic NLR may occur through indirect mechanisms that involve the interaction between NDP and other PRR. Therefore, despite the investigation of NDC-induced effects on NLR is important to gain further insights into the biological effects induced by NDC from plant source foods, further analyses are necessary to explore the interaction between the NDC and other PRR, such as CLR and TLR.

C-type lectin receptors

Unlike NLR that are cytosolic proteins, the main CLR (Dectin-1, Dectin-2, Mannose receptor, and macrophage inducible Ca^{2+}-dependent lectin—Mincle) are trans-membrane PRR widely expressed in myeloid cells. Glycosylated structures are the natural ligands of CLR, which contain conserved carbohydrate-recognition domains (CRD). Thus, it is easy to think that some food-derived carbohydrates interact with CLR. In this regard, studies had explored the interaction between NDC from foods and CLR, especially Dectin-1. However, the effects were investigated mainly using fungal-source foods [151–153] compared to plant-source foods [123,134]. As CLR is expressed mainly in antigen-presenting cells including macrophages and dendritic cells, the study of the interaction between NDC from foods and CLR focused mainly on innate immune responses against pathogens and cancer, including CRC.

Activation of CLR can induce anti-inflammatory effects, as observed by the activation of the heterodimer Dectin-1\TLR2, which increases suppressor of cytokine signalling (SOCS)-1 expression, thereby resulting in anti-inflammatory effects [154]. However, in general, the inhibition of CLR in some CRC cells [155] promotes cell apoptosis [156] and suppresses a pro-inflammatory phenotype, thereby reducing CRC risk [157]. As CLR also facilitates adhesion of head, neck and breast cancer cells to the lymphatic endothelium and thus favour tumour invasiveness [158], NDC-mediated inhibition of CLR may directly impact in the invasiveness of cancer cells. On the other hand, CLR is essential for the recognition of altered glycosylated membrane proteins of CRC cells by immune system cells [159,160]. Thus, as NDC-mediated inhibition is

beneficial in cancer cells but may suppress anticancer response by the innate immune system, further studies using *in vivo* models may elucidate possible benefits on the interaction between NDC from plant-source foods and CLR in decreasing CRC risk.

Among all CLR, Dectin-1 seems to have a major impact in innate immune responses against cancer and are present in CRC cells [155,159]. Dectin-1 is a specific receptor for β-glucan [161,162], which is the most abundant fungal cell wall polysaccharide – and is also a constituent of the bacterial cell wall [163,164]. As β-glucan is a naturally occurring NDC in mushrooms and some plant-source foods, especially in cereal grains [165], Dectin-1 is by far the most studied CLR in terms of interaction with food-derived NDC. Furthermore, as Dectin-1 expression is high in phagocytes such as macrophages and dendritic cells, β-glucan from foods seems to act first through interaction with these innate immune system cells [166].

Phagocytes can extrude their dendrites across the intestinal epithelium into the gastrointestinal lumen and diet-derived β-glucan could interact with them through Dectin-1. Upon activation of Dectin-1, β-glucan induces mainly the Spleen tyrosine kinase (Syk)-dependent pathway, which triggers adaptive immune response in T cells and B cells that results in the inhibition of both tumour growth and metastasis [167]. Despite the inhibition of Dectin-1 induces apoptosis in CRC cells *in vitro* [156], evidence that showed the positive role of Dectin-1 activation in the decrease of CRC risk comes from the findings that a loss of function of this CLR is associated with increased risk of ulcerative colitis [168]. Furthermore, the relationship between the loss of Dectin-1 function due to polymorphism and the increasing risk of inflammatory disorders in the gastrointestinal tract [160], as well as other *in vivo* studies [169,170], supports the beneficial effects of Dectin-1 activation in the reduction of CRC risk.

In this context, a barley-derived β-glucan that consists of linear and mixed β-(*1,4*)- and β-(*1,3*)-linked Glc residues interacts with Dectin-1 and triggers a Syk-dependent pathway that results in the activation of NF-κB of immune system cells, leading to cytokine secretion including IL-6 and IL-8 [123]. Thus, it is possible that some NDC from plant-source foods, especially β-glucans, directly activates Dectin-1 and induces positive effects in the reduction of CRC risk. In addition to enhancing the innate immune response, CRL seems to function together with other PRR, especially with TLR [153,171,172], to regulate the function of IEC. In this context, a recent study showed that guar gum exerted *in vitro* and *in vivo* anti-inflammatory effects in IEC through a Dectin-1\TLR2-dependent pathway [134]. The same mechanism seemed to be related to the anti-inflammatory effects of partially hydrolysed guar gum—which consists of a backbone containing β-(*1,4*)-linked Man residues and short branches containing Gal at C4—in a colitis model [135].

Toll-like receptors (TLR)

TLR are the most studied class of PRR because of both the variety of PAMP and DAMP that interact with these germline-encoded PRR and also because of the biological outcomes that TLR-induction/inhibition could cause in human health [173]. Currently, 13

TLR have been identified in human cells, among intracellular and extracellular receptors [174]. As NLR, TLR are evolutionary conserved PRR-containing LRR motifs for ligand sensing that induces NF-κB and MAPK signalling. Most of TLR activate NF-κB and MAPK mainly through the adaptor myeloid differentiation factor 88 (MyD88), except TLR3, which triggers NF-κB and MAPK through a TIR-domain-containing adapter-inducing interferon-β (TRIF)-dependent pathway [175].

Among all TLR, TLR2 and TLR4 have been the most studied ones concerning the interaction with NDC from plant-food sources [115,128]. TLR2 recognizes different kinds of PAMP including lipoprotein, lipoteichoic acid and peptidoglycan molecules from Gram-positive bacteria, as well as DAMP, such as heat shock proteins (HSP). TLR4 interacts with lipopolysaccharide (LPS) from Gram-negative bacteria and with several DAMP including HSP, fibronectin and heparan sulfate [176].

In the context of CRC, several studies had explored the role of TLR on cancer development, progression, and invasion, as reviewed by Li et al. [177]. Furthermore, results of a recent prospective cohort study suggested that the protective effect of NDC on CRC risk may involve interactions between the NDC and TLR4, and that polymorphisms in TLR2 and TLR4 are associated with increased CRC risk [178]. In fact, CRC development and progression have been correlated with TLR2 and TLR4 overexpression in CRC [179]. CRC cells express both mutated TLR2 and MyD88, thereby resulting in increased activation of TLR2-dependent pathways. Thus, TLR2 inhibitors were proposed as therapeutic agent in CRC [180].

TLR4 is considered the most important inflammatory inducer amongst all TLR, thereby playing a key role in immune response against intestinal pathogens. However, excessive activation of TLR4 may enhance not only immune response but also gives rise to cancer progression through disruption of intestinal immune homeostasis [181]. Excessive TLR4 activation also induces macrophages apoptosis after activation of the receptor-interacting serine/threonine-protein kinase (RIPK) 1 and RIPK3, which induces cell lysis and necroptotic death [182]. Furthermore, enhanced expression of TLR4 in CRC cells promotes cell survival, epithelial-mesenchymal transition [183], and downregulates the expression of the death receptor Fas in cancer cells [184,185]. Thus, excessive activation of TLR4 increases the risk of inflammatory diseases and CRC, and—as occur to TLR2—potential inhibitors of TLR4/NF-κB pathway have also been considered as therapeutic agents in CRC [186].

Despite the abovementioned evidences show that inhibition of TLR4-dependent signaling pathways may reduce CRC risk, some NDC from plant-source foods including citrus pectin and ginseng polysaccharides have potential anticancer effects that seems to be related to TLR4-mediated activation [128,187–189]. The most reasonable explanation is that these NDC from plant-source foods do not activate TLR4 at the same extent as natural PAMP, such as LPS. Therefore, NDC-induced TLR4 activation reduces the interaction of this PRR with more potent ligands [188–190]. Furthermore, TLR-mediated activation can

launch a strong immune response to assist cancer treatments and/or activate TLR-dependent programmed cell death, including apoptosis, autophagy and necroptosis [191].

Apart from the biological relevance of TLR2 and TLR4, TLR3 activation with polyinosinic, polycytidylic acid induces apoptosis of in CRC cells [192], whereas TLR5 activation suppress CRC growth and induce necrosis of cancer cells *in vivo* [193]. Furthermore, TLR9-induced activation in immune system cells promotes cell survival and therefore enhances immune response against cancer; however, the role of TLR9 in CRC remains unclear [177], as CRC cells have reduced expression of TLR9, suggesting a protective role of TLR9 expression against malignant transformation in the gastrointestinal tract [194].

Molecules from plant-source foods including polyphenols [195,196] and NDC have been found to exert effects on TLR-mediated pathways [114,115,133]. In the context of NDC from plant-source foods, it was found that apple galactan suppressed LPS-induced activation of TLR4 downstream signaling in an *in vivo* model of colitis-induced CRC [129]. Furthermore, NDC from apple reduced the migration of CRC cells *in vitro* [197], and enhanced the inhibitory effect of 5-fluorouracil in the growth of CRC cells [198]. Homogalacturonan-rich fractions from lemon pectin with varying degree of methyl esterification also induced TLR2- and TLR4-mediated responses [128]. Authors have showed that the varied degree of methyl esterification in the homogalacturonan residues of lemon pectin strongly influenced TLR2-mediated responses, but did not affect TLR4-mediated response. Furthermore, both low- and high-methoxylated lemon pectin seemed to exert positive effects on the maintenance of intestinal epithelial barrier integrity *in vitro* [128]. Recently, it was found that the inhibitory effect of low-methoxylated pectin from lemon suppressed the pro-inflammatory TLR2\TLR1 pathway while the heterodimerization between TLR2 and TLR6, which induces a tolerogenic effect, was not induced by lemon pectin [133]. Furthermore, authors found that the administration of low-methoxylated pectin from lemon prevented intestinal inflammation *in vivo* in a fermentation-independent manner. Notably, similar TLR-inhibitory effects are in agreement with *in vivo* studies using low- and high-methoxylated citrus pectin, which attenuated both endotoxin shock through a TLR-dependent pathway [130], as well as inflammatory effects in a colitis model [131].

Besides the TLR-mediated effects of NDC from apple and citrus, it was found that inulin from chicory roots with distinct chain-lengths interacted not only with TLR4, but also with TLR5, TLR6, TLR7 and TLR8 in a MyD88-dependent pathway, and had no effects on cytosolic TLR3 and TLR9 [115]. Furthermore, it was found that water-soluble NDC from unripe and ripe papaya differentially regulated TLR3, TLR5 and TLR9. Notably, NDC from ripe papaya activated TLR3, TLR5 and TLR9, whereas NDC from unripe papaya blocked TLR3 and TLR9, and had no effect on TLR5 [121]. Although it is not clear the biological outcome related to the interaction between these NDC and TLR, the observation of TLR-mediated effects by NDC from plant-source foods may support further studies aiming to evaluate the direct effects of these dietary components in CRC development and progression.

Direct interaction with galectin-3

In addition to the direct effects of NDC from plant-food sources through PRR-dependent mechanisms in IEC, immune system cells and CRC cells, NDC can also directly interact with cellular components in a PRR-independent pathway. The main PRR-independent effect seems to be related with the interaction between NDC from plant-source foods and the galectin-3 (Gal-3).

Gal-3 is a protein of the lectin family that has a CRD with strong affinity for β-galactosides. Notably, it has been consistently shown in the past two decades a strong association between increased levels of Gal-3 and several types of cancer including CRC [199,200]. Gal-3 expression had been correlated not only with CRC incidence, but also with CRC severity, as increased levels of Gal-3 are associated with a worse cancer prognostic [199–201]. A recent study supported this correlation by showing that the positive expression rate of Gal-3 in CRC tissues is approximately 5-fold higher compared to cancer-adjacent tissues [200]. Furthermore, authors suggest a direct association between positive expression of Gal-3 and both tumour size and malignant progression.

Gal-3 is present intracellularly—at the cytoplasm or within the nucleus—attached to cell surface, or in the extracellular media as a dimer or as a pentamer [202]. Regardless the localization of Gal-3, the increase in its levels is related with increased CRC risk and severity because this protein is involved in a wide range of cancer-promoting effects including CRC cells adhesion, invasiveness, growth and proliferation [203,204]. Notably, some NDC from plant-source foods bind to the CRD of Gal-3 and therefore inhibits Gal-3-mediated effects, which includes not only attachment to glycan-containing surfaces [205], but also with downstream signalling mechanisms that inhibits both apoptosis and cell cycle arrest in CRC cells [206]. Furthermore, Gal-3 appears to be associated to multiples mechanisms related to chemo-resistance of CRC cells by enhancing drug efflux, DNA repair mechanisms and activating signalling pathways (e.g., Wnt, Hedgehog and Notch) associated with multi-drug resistance [207]. Thus, since the observation of specific bind of NDC from plant-source foods to Gal-3 [208], several studies have been performed to assess the interaction between distinct NDC and Gal-3, as well as the effects of this interaction in CRC progression, as described previously [117].

Among NDC from plant-food sources and Gal-3 inhibition, the modified citrus pectin (MCP) is the most studied one [187,209–211]. MCP is a preparation derived from citrus pectin that is modified by high temperature, alteration of pH and/or pectinase treatment, which result in the partial hydrolysis of glycosidic linkages, thereby generating smaller and less ramified NDC structure. These processes of MCP modification release neutral chains of galactan with high affinity to the CRD of Gal-3 [208,209], which induce a broad range of inhibitory effects that had been extensively studied through *in vitro* and *in vivo* studies [209,212,213].

Modified sugar beet pectin, papaya pectin, and ginseng pectin have structures composed of neutral (*1,4*)-β-galactose residues, which were related to Gal-3 interaction and

inhibition [210,211,214]. As observed for MCP, the binding between these pectin and Gal-3 has been associated with both *in vitro* and *in vivo* effects on CRC [211,215]. Besides the interaction with Gal-3, molecular size-fractionated MCP showed other effects than inhibit Gal-3, as leading CRC cells to apoptosis and inhibiting their migration [216]. NDC from plant-source food also seem to interact with Gal-3 through non-specific binding as suggested by previous study [217]. Since homogalacturonans contain relatively high amounts of charged GalA residues, it is possible that charge-charge interactions between GalA residues and Gal-3 induce a non-specific binding that may exert inhibitory effects on Gal-3 activity. Recently, it was also shown that NDC from plant-source foods can interact with Gal-3 by a combination of homogalacturonan and RG residues acting in concert, as the homogalacturonan seem to interact with RG exposing additional galectin-binding sites of the NDC, thereby enhancing Gal-3-binding properties [218].

As NDC are essentially polyhydroxy molecules, which are often esterified, it is possible that the NDC from plant-source foods interacts with other cellular components. The studies that had shown anticancer effects of NDC through interaction with Gal-3 support further studies aiming the investigation of the interaction between NDC and other signalling mediators related to the decreased CRC risk.

Concluding remarks

The complexity of biological effects resulting from the intake of NDC from plant-source foods and their relationship with decreased CRC risk can be divided into physicochemical effects, fermentation-related effects, and PRR-dependent and PRR-independent direct effects. However, in biological systems, these complex NDC effects occur at the same time in an intricate – and poorly understood – relationship. Although the evaluation of a specific biological effect does not fully answer whether a single NDP from a plant-source food relates to a decreased CRC risk, it can provide further insights to elucidate the structure-function relationship between NDC and their effects in CRC development and progression. Therefore, as recent studies are demonstrating that intrinsic properties of NDC from plant-source foods, as well as individual characteristics among cells and individuals, strongly influence the beneficial effects of NDC on the reduction of CRC risk (**Figure 4**), similarities between the intrinsic properties of NDC from distinct plant-source foods may drive the discovery of new bioactive NDC. Clearly, studies that integrate the structural characterization of NDC from plant-source foods with their physicochemical, fermentation-related, and/or direct effects will provide insights not only for a better understating of the structure-function relationship between the intake of NDC and CRC risk but also for improving nutritional recommendations of NDC for healthy individuals, as well as CRC patients.

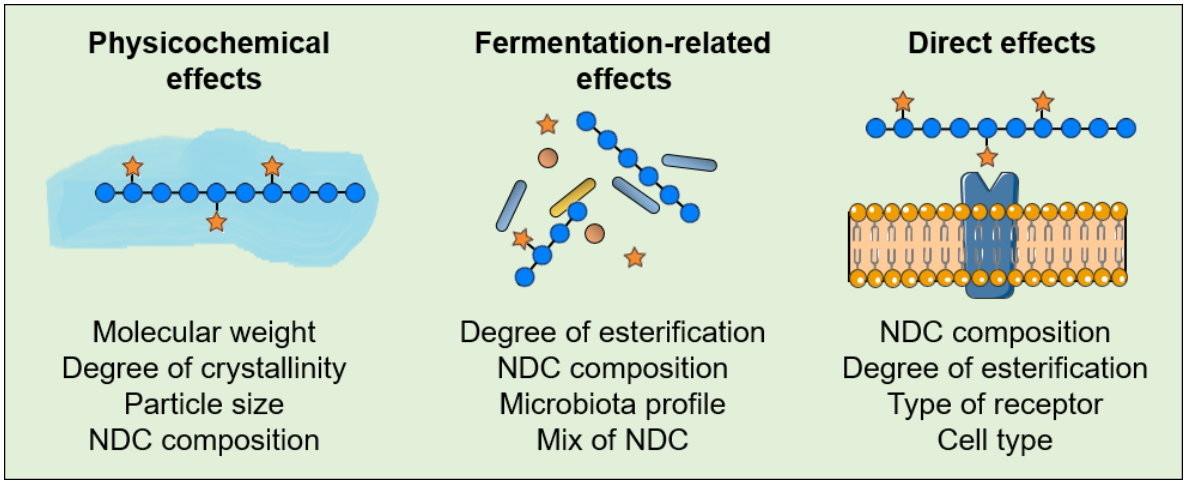

Figure 4. Features that influence the effects of non-digestible carbohydrates (NDC) from plant-source foods in colorectal cancer (CRC). Some of the intrinsic properties of NDC, as well as individual characteristics among cells and individuals, that influences the physicochemical, fermentation-related and direct effects of NDC from plant-source foods on the reduction of CRC risk.

References

[1] M.H. Forouzanfar, et al. Global, regional, and national comparative risk assessment of 79 behavioural, environmental and occupational, and metabolic risks or clusters of risks, 1990–2015: a systematic analysis for the Global Burden of Disease Study 2015, Lancet. 388 (2016) 1659–1724. doi:10.1016/S0140-6736(16)31679-8.

[2] M. Arnold, M.S. Sierra, M. Laversanne, I. Soerjomataram, A. Jemal, F. Bray, Global patterns and trends in colorectal cancer incidence and mortality, Gut. 66 (2017) 683–691. doi:10.1136/gutjnl-2015-310912.

[3] K.W. Jasperson, T.M. Tuohy, D.W. Neklason, R.W. Burt, Hereditary and familial colon cancer, Gastroenterology. 138 (2010) 2044–2058. doi:10.1053/j.gastro.2010.01.054.Hereditary.

[4] E.J. Kuipers, W.M. Grady, D. Lieberman, T. Seufferlein, J.J. Sung, P.G. Boelens, C.J. van de Velde, T. Watanabe, Colorectal cancer, Nat. Rev. 1 (2015) 1–25. doi:10.3109/9781841847481.

[5] H. Brenner, M. Kloor, C.P. Pox, Colorectal cancer, Lancet. 383 (2014) 1490–1502. doi:10.3810/pgm.2000.5.1.1083.

[6] E. Vogtmann, Y.-B. Xiang, H.-L. Li, E.B. Levitan, G. Yang, J.W. Waterbor, J. Gao, H. Cai, L. Xie, Q.-J. Wu, B. Zhang, Y.-T. Gao, W. Zheng, X.-O. Shu, Fruit and vegetable intake and the risk of colorectal cancer: Results from the Shanghai Men's Health Study, Cancer Causes Control. 24 (2013) 1935–1945. doi:10.1016/j.dcn.2011.01.002.

[7] R. Baena, P. Salinas, Diet and colorectal cancer, Maturitas. 80 (2015) 258–264. doi:10.1016/j.maturitas.2014.12.017.

[8] S.K. Bhat, J.E. East, Colorectal cancer: Prevention and early diagnosis, Med. (United Kingdom). 43 (2015) 295–298. doi:10.1016/j.mpmed.2015.03.009.

[9] D. Aune, D.S.M. Chan, R. Lau, R. Vieira, D.C. Greenwood, E. Kampman, T. Norat, Dietary fibre , whole grains , and risk of colorectal cancer: systematic review and dose-response meta-analysis of prospective studies, BMJ. 6617 (2011) 1–20. doi:10.1136/bmj.d6617.

[10] D. Aune, N. Keum, E. Giovannucci, L.T. Fadnes, P. Boffetta, D.C. Greenwood, S. Tonstad, L.J. Vatten, E. Riboli, T. Norat, Whole grain consumption and risk of cardiovascular disease, cancer, and all cause and cause specific mortality: systematic review and dose-response meta-analysis of prospective studies, BMJ. 353 (2016) 1–14. doi:10.1136/bmj.i2716.

[11] R.A. Torres Stone, M.E. Waring, S.L. Cutrona, C.I. Kiefe, J. Allison, C.A. Doubeni, The association of dietary quality with colorectal cancer among normal weight, overweight and obese men and women: A prospective longitudinal study in the USA, BMJ. 7 (2017) 1–11. doi:10.1136/bmjopen-2016-015619.

[12] K.E. Bradbury, P.N. Appleby, T.J. Key, Fruit, vegetable, and fiber intake in relation to cancer risk: findings from the European Prospective Investigation into Cancer and Nutrition (EPIC), Am. J. Clin. Nutr. 100 (2014) 394S–398S. doi:10.3945/ajcn.113.071357.394S.

[13] M. Leenders, P.D. Siersema, K. Overvad, A. Tjønneland, A. Olsen, M.C. Boutron-Ruault, N. Bastide, G. Fagherazzi, V. Katzke, T. Kühn, H. Boeing, K. Aleksandrova, A. Trichopoulou, P. Lagiou, E. Klinaki, G. Masala, S. Grioni, M. Santucci De Magistris, R. Tumino, F. Ricceri, P.H.M. Peeters, E. Lund, G. Skeie, E. Weiderpass, J.R. Quirõs, A. Agudo, M.J. Sánchez, M. Dorronsoro, C. Navarro, E. Ardanaz, B. Ohlsson, K. Jirström, B.

Van Guelpen, M. Wennberg, K.T. Khaw, N. Wareham, T.J. Key, I. Romieu, I. Huybrechts, A.J. Cross, N. Murphy, E. Riboli, H. Bueno-De-Mesquita, Subtypes of fruit and vegetables, variety in consumption and risk of colon and rectal cancer in the European Prospective Investigation into Cancer and Nutrition, Int. J. Cancer. 137 (2015) 2705–2714. doi:10.1002/ijc.29640.

[14] F. Turati, M. Rossi, C. Pelucchi, F. Levi, C. La Vecchia, Fruit and vegetables and cancer risk: A review of southern European studies, Br. J. Nutr. 113 (2015) S102–S110. doi:10.1017/S0007114515000148.

[15] M. Fridlender, Y. Kapulnik, H. Koltai, Plant derived substances with anti-cancer activity: from folklore to practice, Front. Plant Sci. 6 (2015) 1–9. doi:10.3389/fpls.2015.00799.

[16] F. Pistollato, F. Giampieri, M. Battino, The use of plant-derived bioactive compounds to target cancer stem cells and modulate tumor microenvironment, Food Chem. Toxicol. 75 (2015) 58–70. doi:10.1016/j.fct.2014.11.004.

[17] B. Modan, V. Barell, F. Lubin, M. Modan, R.A. Greenberg, S. Graham, Low-fiber intake as an etiologic factor in cancer of the colon, J. Natl. Cancer Inst. 55 (1975) 15–18. doi:10.1093/jnci/55.1.15.

[18] V. Gianfredi, T. Salvatori, M. Villarini, M. Moretti, D. Nucci, S. Realdon, Is dietary fibre truly protective against colon cancer? A systematic review and meta-analysis, Int. J. Food Sci. Nutr. 69 (2018) 904–915. doi:10.1080/09637486.2018.1446917.

[19] D.P. Bukkitt, Epidemiology of cancer of the colon and rectum, Cancer. 28 (1971) 1–11. doi:10.1002/1097-0142(197107)28:1<3::AID-CNCR2820280104>3.0.CO;2-N.

[20] D. Burkitt, RELATED DISEASE—RELATED CAUSE?, Lancet. 294 (1969) 1229–1231. doi:https://doi.org/10.1016/S0140-6736(69)90757-0.

[21] H. Zeng, D. Lazarova, M. Bordonaro, Mechanisms linking dietary fiber, gut microbiota and colon cancer prevention, World J. Gastrointest. Oncol. 6 (2014) 41. doi:10.4251/wjgo.v6.i2.41.

[22] M.C. McCann, P. Knox, Plant cell wall biology: Polysaccharides in architetural and developmental contexts, Annu. Plant Rev. 41 (2011). doi:10.1002/9781119312994.apr0443.

[23] D. Mohnen, Pectin structure and biosynthesis, Curr. Opin. Plant Biol. 11 (2008) 266–277. doi:10.1016/j.pbi.2008.03.006.

[24] J.-P. Ele-Ekouna, C. Pau Roblot, B. Courtois, J. Courtois, Chemical characterization of pectin from green tea (Camellia sinensis), 2011. doi:10.1016/j.carbpol.2010.09.028.

[25] D. Ndeh, A. Rogowski, A. Cartmell, A.S. Luis, A. Baslé, J. Gray, I. Venditto, J. Briggs, X. Zhang, A. Labourel, N. Terrapon, F. Buffetto, S. Nepogodiev, Y. Xiao, R.A. Field, Y. Zhu, M.A. O'Neill, B.R. Urbanowicz, W.S. York, G.J. Davies, D.W. Abbott, M.-C. Ralet, E.C. Martens, B. Henrissat, H.J. Gilbert, Complex pectin metabolism by gut bacteria reveals novel catalytic functions, Nature. (2017). doi:10.1038/nature21725.

[26] M.A. O'Neill, T. Ishii, P. Albersheim, A.G. Darvill, Rhamnogalacturonan II: Structure and function of a borate cross-linked cell wall pectic polysaccharide, Annu. Rev. Plant Biol. 55 (2004) 109–139. doi:10.1146/annurev.arplant.55.031903.141750.

[27] D. Wong, Enzymatic deconstruction of backbone structures of the ramified regions in pectins, Protein J. 27 (2008) 30–42. doi:10.1007/s10930-007-9105-0.

[28] B.R. Hamaker, Y.E. Tuncil, A perspective on the complexity of dietary fiber structures and their potential effect on the gut microbiota., J. Mol. Biol. 426 (2014) 3838–50.

doi:10.1016/j.jmb.2014.07.028.

[29] W. Cheng, J. Lu, B. Li, W. Lin, Z. Zhang, X. Wei, C. Sun, M. Chi, W. Bi, B. Yang, A. Jiang, J. Yuan, Effect of functional oligosaccharides and ordinary dietary fiber on intestinal microbiota diversity, Front. Microbiol. 8 (2017) 1–11. doi:10.3389/fmicb.2017.01750.

[30] E. Maxwell, A.T. Hotchkiss, V.J. Morris, N.J. Belshaw, Rhamnogalacturonan I containing homogalacturonan inhibits colon cancer cell proliferation by decreasing ICAM1 expression, Carbohydr. Polym. 132 (2015) 546–553. doi:10.13140/RG.2.1.3768.1769.

[31] A.T. Kunzmann, H.G. Coleman, W.-Y. Huang, C.M. Kitahara, M.M. Cantwell, S.I. Berndt, Dietary fiber intake and risk of colorectal cancer and incident and recurrent adenoma in the Prostate, Lung, Colorectal, and Ovarian Cancer Screening Trial, Am J Clin Nutr. 102 (2015) 881–890. doi:10.3945/ajcn.115.113282.1.

[32] S.H.J. Jochems, F.H.M. Van Osch, R.T. Bryan, A. Wesselius, F.J. Van Schooten, K.K. Cheng, M.P. Zeegers, Impact of dietary patterns and the main food groups on mortality and recurrence in cancer survivors: A systematic review of current epidemiological literature, BMJ. 8 (2017) 1–12. doi:10.1136/bmjopen-2016-014530.

[33] C. Bamia, Dietary patterns in association to cancer incidence and survival: concept, current evidence, and suggestions for future research, Eur. J. Clin. Nutr. 72 (2018) 818–825. doi:10.1038/s41430-018-0128-8.

[34] A.J. Vargas, P.A. Thompson, Diet and Nutrient Factors in Colorectal Cancer Risk The Natural History of Colorectal Cancer and Opportunities for Dietary Factors With Convincing Evidence as a Factor in Colorectal Cancer The Role of Diet and Colorectal Cancer, Nutr. Clin. Pract. 27 (2012) 613–623. doi:10.1177/0884533612454885.

[35] J. Guinney, R. Dienstmann, X. Wang, A. De Reyniès, A. Schlicker, C. Soneson, L. Marisa, P. Roepman, G. Nyamundanda, P. Angelino, B.M. Bot, J.S. Morris, I.M. Simon, S. Gerster, E. Fessler, F. De Sousa .E Melo, E. Missiaglia, H. Ramay, D. Barras, K. Homicsko, D. Maru, G.C. Manyam, B. Broom, V. Boige, B. Perez-Villamil, T. Laderas, R. Salazar, J.W. Gray, D. Hanahan, J. Tabernero, R. Bernards, S.H. Friend, P. Laurent-Puig, J.P. Medema, A. Sadanandam, L. Wessels, M. Delorenzi, S. Kopetz, L. Vermeulen, S. Tejpar, The consensus molecular subtypes of colorectal cancer, Nat. Med. 21 (2015) 1350–1356. doi:10.1038/nm.3967.

[36] S. Christiaens, S. Van Buggenhout, K. Houben, Z. Jamsazzadeh Kermani, K.R.N. Moelants, E.D. Ngouemazong, A. Van Loey, M.E.G. Hendrickx, Process-Structure-Function Relations of Pectin in Food., Crit. Rev. Food Sci. Nutr. 56 (2016) 1021–1042. doi:10.1080/10408398.2012.753029.

[37] M.M.-L. Grundy, C.H. Edwards, A.R. Mackie, M.J. Gidley, P.J. Butterworth, P.R. Ellis, Re-evaluation of the mechanisms of dietary fibre and implications for macronutrient bioaccessibility, digestion and postprandial metabolism., Br. J. Nutr. 116 (2016) 816–33. doi:10.1017/S0007114516002610.

[38] S.S. Ferreira, C.P. Passos, P. Madureira, M. Vilanova, M.A. Coimbra, Structure-function relationships of immunostimulatory polysaccharides: A review, Carbohydr. Polym. 132 (2015) 378–396. doi:10.1016/j.carbpol.2015.05.079.

[39] T. Pham, K.T. Teoh, B.J. Savary, M.-H. Chen, A. McClung, S.-O. Lee, In Vitro Fermentation Patterns of Rice Bran Components by Human Gut Microbiota., Nutrients. 9 (2017). doi:10.3390/nu9111237.

[40] K.S. Poutanen, P. Dussort, A. Erkner, S. Fiszman, K. Karnik, M. Kristensen, C.F.M. Marsaux, S. Miquel-kergoat, S.P. Pentik, P. Putz, J.L. Slavin, R.E. Steinert, D.J. Mela, A

review of the characteristics of dietary fibers relevant to appetite and energy intake outcomes in human intervention trials, Am. J. Clin. Nutr. 106 (2017) 747–54.

[41] K. Logan, A.J. Wright, H.D. Goff, Correlating the structure and in vitro digestion viscosities of different pectin fibers to in vivo human satiety, Food Funct. 6 (2015) 62–70. doi:10.1039/C4FO00543K.

[42] C.J. Rebello, C.E. O'Neil, F.L. Greenway, Dietary fiber and satiety: the effects of oats on satiety, Nutr. Rev. 74 (2016) 131–147.

[43] Y. Dong, J. Zhou, Y. Zhu, L. Luo, T. He, H. Hu, H. Liu, Y. Zhang, D. Luo, S. Xu, L. Xu, J. Liu, J. Zhang, Z. Teng, Abdominal obesity and colorectal cancer risk: systematic review and meta-analysis of prospective studies., Biosci. Rep. 37 (2017) 1–12. doi:10.1042/BSR20170945.

[44] Y. Ma, M. Hu, L. Zhou, S. Ling, Y. Li, B. Kong, P. Huang, Dietary fiber intake and risks of proximal and distal colon cancers: A meta-analysis, Medicine (Baltimore). 97 (2018) e11678.

[45] S. AbuMweis, S.J. Thandapilly, J. Storsley, N. Ames, Effect of barley β-glucan on postprandial glycaemic response in the healthy human population: A meta-analysis of randomized controlled trials, J. Funct. Foods. 27 (2016) 329–342. doi:https://doi.org/10.1016/j.jff.2016.08.057.

[46] T. Ghaffarzadegan, Y. Zhong, F. Fåk Hållenius, M. Nyman, Effects of barley variety, dietary fiber and β-glucan content on bile acid composition in cecum of rats fed low- and high-fat diets, J. Nutr. Biochem. 53 (2018) 104–110. doi:https://doi.org/10.1016/j.jnutbio.2017.10.008.

[47] E.J. Gallagher, D. LeRoith, Obesity and Diabetes: The Increased Risk of Cancer and Cancer-Related Mortality., Physiol. Rev. 95 (2015) 727–748. doi:10.1152/physrev.00030.2014.

[48] A.A. Moghaddam, M. Woodward, R. Huxley, Obesity and Risk of Colorectal Cancer: A Meta-analysis of 31 Studies with 70,000 Events, Cancer Epidemiol. Biomarkers &Amp; Prev. 16 (2007) 2533 LP-2547. doi:10.1158/1055-9965.EPI-07-0708.

[49] R. Gemen, J.F. de Vries, J.L. Slavin, Relationship between molecular structure of cereal dietary fiber and health effects: focus on glucose/insulin response and gut health., Nutr. Rev. 69 (2011) 22–33. doi:10.1111/j.1753-4887.2010.00357.x.

[50] H.J. Kim, P.J. White, In Vitro Bile-Acid Binding and Fermentation of High, Medium, and Low Molecular Weight β-Glucan, J. Agric. Food Chem. 58 (2010) 628–634. doi:10.1021/jf902508t.

[51] J.C. Hsu, M.H. Penner, Influence of cellulose structure on its digestibility in the rat., J. Nutr. 119 (1989) 872–878. doi:10.1093/jn/119.6.872.

[52] M. Ulbrich, E. Flöter, Impact of high pressure homogenization modification of a cellulose based fiber product on water binding properties, Food Hydrocoll. 41 (2014) 281–289. doi:https://doi.org/10.1016/j.foodhyd.2014.04.020.

[53] X. Du, X. Bai, W. Gao, Z. Jiang, Properties of soluble dietary fibre from defatted coconut flour obtained through subcritical water extraction, Int. J. Food Sci. Technol. 0 (2019). doi:10.1111/ijfs.14071.

[54] F. Rashid, S. Hussain, Z. Ahmed, Extraction purification and characterization of galactomannan from fenugreek for industrial utilization, Carbohydr. Polym. 180 (2018) 88–95. doi:https://doi.org/10.1016/j.carbpol.2017.10.025.

[55] S.N. Raghavendra, S.R. Ramachandra Swamy, N.K. Rastogi, K.S.M.S. Raghavarao, S. Kumar, R.N. Tharanathan, Grinding characteristics and hydration properties of coconut residue: A source of dietary fiber, J. Food Eng. 72 (2006) 281–286. doi:https://doi.org/10.1016/j.jfoodeng.2004.12.008.

[56] Y. Wen, M. Niu, B. Zhang, S. Zhao, S. Xiong, Structural characteristics and functional properties of rice bran dietary fiber modified by enzymatic and enzyme-micronization treatments, LWT. 75 (2017) 344–351. doi:https://doi.org/10.1016/j.lwt.2016.09.012.

[57] K. Zhu, S. Huang, W. Peng, H. Qian, H. Zhou, Effect of ultrafine grinding on hydration and antioxidant properties of wheat bran dietary fiber, Food Res. Int. 43 (2010) 943–948. doi:https://doi.org/10.1016/j.foodres.2010.01.005.

[58] F. Ye, B. Tao, J. Liu, Y. Zou, G. Zhao, Effect of micronization on the physicochemical properties of insoluble dietary fiber from citrus (Citrus junos Sieb. ex Tanaka) pomace., Food Sci. Technol. Int. 22 (2016) 246–255. doi:10.1177/1082013215593394.

[59] G. Yu, J. Bei, J. Zhao, Q. Li, C. Cheng, Modification of carrot (Daucus carota Linn. var. Sativa Hoffm.) pomace insoluble dietary fiber with complex enzyme method, ultrafine comminution, and high hydrostatic pressure, Food Chem. 257 (2018) 333–340. doi:https://doi.org/10.1016/j.foodchem.2018.03.037.

[60] N. Li, Z. Feng, Y. Niu, L. Yu, Structural, rheological and functional properties of modified soluble dietary fiber from tomato peels, Food Hydrocoll. 77 (2018) 557–565. doi:https://doi.org/10.1016/j.foodhyd.2017.10.034.

[61] Z. Feng, W. Dou, S. Alaxi, Y. Niu, L. (Lucy) Yu, Modified soluble dietary fiber from black bean coats with its rheological and bile acid binding properties, Food Hydrocoll. 62 (2017) 94–101. doi:https://doi.org/10.1016/j.foodhyd.2016.07.032.

[62] E. Yamazaki, K. Murakami, O. Kurita, Easy preparation of dietary fiber with the high water-holding capacity from food sources., Plant Foods Hum. Nutr. 60 (2005) 17–23.

[63] A.G.J. Voragen, G.J. Coenen, R.P. Verhoef, H.A. Schols, Pectin, a versatile polysaccharide present in plant cell walls, Struct. Chem. 20 (2009) 263–275. doi:10.1007/s11224-009-9442-z.

[64] M. Kazemi, F. Khodaiyan, S.S. Hosseini, Eggplant peel as a high potential source of high methylated pectin: Ultrasonic extraction optimization and characterization, LWT. 105 (2019) 182–189. doi:https://doi.org/10.1016/j.lwt.2019.01.060.

[65] B.A. Williams, L.J. Grant, M.J. Gidley, D. Mikkelsen, Gut fermentation of dietary fibres: Physico-chemistry of plant cell walls and implications for health, Int. J. Mol. Sci. 18 (2017). doi:10.3390/ijms18102203.

[66] D. Rea, G. Coppola, G. Palma, A. Barbieri, A. Luciano, P. Del Prete, S. Rossetti, M. Berretta, G. Facchini, S. Perdonà, M.C. Turco, C. Arra, Microbiota effects on cancer: from risks to therapies, Oncotarget. 9 (2018) 17915–17927. doi:10.18632/oncotarget.24681.

[67] S.J. Bultman, The microbiome and its potential as a cancer preventive intervention, Semin. Oncol. 43 (2016) 97–106. doi:10.1053/j.seminoncol.2015.09.001.

[68] H. Tilg, T.E. Adolph, R.R. Gerner, A.R. Moschen, The Intestinal Microbiota in Colorectal Cancer, Cancer Cell. 33 (2018) 954–964. doi:https://doi.org/10.1016/j.ccell.2018.03.004.

[69] H.J. Flint, K.P. Scott, S.H. Duncan, P. Louis, E. Forano, Microbial degradation of complex carbohydrates in the gut, (2012) 289–306.

[70] P. Kovatcheva-Datchary, A. Nilsson, R. Akrami, Y.S. Lee, F. De Vadder, T. Arora, A. Hallen, E. Martens, I. Björck, F. Bäckhed, Dietary fiber-induced improvement in glucose

metabolism is associated with increased abundance of prevotella, Cell Metab. 22 (2015) 971–982. doi:10.1016/j.cmet.2015.10.001.

[71] E.C. Martens, E.C. Lowe, H. Chiang, N.A. Pudlo, M. Wu, N.P. McNulty, D.W. Abbott, B. Henrissat, H.J. Gilbert, D.N. Bolam, J.I. Gordon, Recognition and Degradation of Plant Cell Wall Polysaccharides by Two Human Gut Symbionts, PLOS Biol. 9 (2011) e1001221.

[72] W.S.F. Chung, A.W. Walker, P. Louis, J. Parkhill, J. Vermeiren, D. Bosscher, S.H. Duncan, H.J. Flint, Modulation of the human gut microbiota by dietary fibres occurs at the species level, BMC Biol. 14 (2016) 3. doi:10.1186/s12915-015-0224-3.

[73] P. Louis, G.L. Hold, H.J. Flint, The gut microbiota, bacterial metabolites and colorectal cancer, Nat. Rev. Microbiol. 12 (2014) 661–672. doi:10.1038/nrmicro3344.

[74] L. Zitvogel, R. Daillere, M.P. Roberti, B. Routy, G. Kroemer, Anticancer effects of the microbiome and its products., Nat. Rev. Microbiol. 15 (2017) 465–478. doi:10.1038/nrmicro.2017.44.

[75] P. Gonçalves, F. Martel, Regulation of colonic epithelial butyrate transport: Focus on colorectal cancer, Porto Biomed. J. 1 (2016) 83–91. doi:https://doi.org/10.1016/j.pbj.2016.04.004.

[76] B.F. Hinnebusch, S. Meng, J.T. Wu, S.Y. Archer, R.A. Hodin, Nutrition and Cancer The Effects of Short-Chain Fatty Acids on Human Colon Cancer Cell Phenotype Are Associated with Histone Hyperacetylation 1, J. Nutr. 132 (2002) 1012–1017.

[77] U.-H. Jin, Y. Cheng, H. Park, L.A. Davidson, E.S. Callaway, R.S. Chapkin, A. Jayaraman, A. Asante, C. Allred, E.A. Weaver, S. Safe, Short Chain Fatty Acids Enhance Aryl Hydrocarbon (Ah) Responsiveness in Mouse Colonocytes and Caco-2 Human Colon Cancer Cells, Sci. Rep. 7 (2017) 10163. doi:10.1038/s41598-017-10824-x.

[78] J. Tan, C. McKenzie, P.J. Vuillermin, G. Goverse, C.G. Vinuesa, R.E. Mebius, L. Macia, C.R. Mackay, Dietary fiber and bacterial SCFA enhance oral tolerance and protect against food allergy through diverse cellular pathways, Cell Rep. 15 (2016) 2809–2824. doi:10.1016/j.celrep.2016.05.047.

[79] G. Goverse, R. Molenaar, L. Macia, J. Tan, M.N. Erkelens, T. Konijn, M. Knippenberg, E.C.L. Cook, D. Hanekamp, M. Veldhoen, A. Hartog, G. Roeselers, C.R. Mackay, R.E. Mebius, Diet-Derived Short Chain Fatty Acids Stimulate Intestinal Epithelial Cells To Induce Mucosal Tolerogenic Dendritic Cells, J. Immunol. (2017) 1600165. doi:10.4049/jimmunol.1600165.

[80] R. Corrêa-Oliveira, J.L. Fachi, A. Vieira, F.T. Sato, M.A.R. Vinolo, Regulation of immune cell function by short-chain fatty acids, Clin. Transl. Immunol. 5 (2016) e73. doi:10.1038/cti.2016.17.

[81] U. Kalina, N. Koyama, T. Hosoda, H. Nuernberger, K. Sato, D. Hoelzer, F. Herweck, T. Manigold, M.V. Singer, S. Rossol, U. Böcker, Enhanced production of IL-18 in butyrate-treated intestinal epithelium by stimulation of the proximal promoter region, Eur. J. Immunol. 32 (2002) 2635–2643. doi:10.1002/1521-4141(200209)32:9<2635::AID-IMMU2635>3.0.CO;2-N.

[82] Y. Zhao, F. Chen, W. Wu, M. Sun, A.J. Bilotta, S. Yao, Y. Xiao, X. Huang, T.D. Eaves-Pyles, G. Golovko, Y. Fofanov, W. D'Souza, Q. Zhao, Z. Liu, Y. Cong, GPR43 mediates microbiota metabolite SCFA regulation of antimicrobial peptide expression in intestinal epithelial cells via activation of mTOR and STAT3, Mucosal Immunol. 11 (2018) 752–762. doi:10.1038/mi.2017.118.

[83] M.E. Rodríguez-Cabezas, J. Gálvez, M.D. Lorente, A. Concha, D. Camuesco, S. Azzouz, A. Osuna, L. Redondo, A. Zarzuelo, Dietary Fiber Down-Regulates Colonic Tumor Necrosis Factor α and Nitric Oxide Production in Trinitrobenzenesulfonic Acid-Induced Colitic Rats, J. Nutr. 132 (2002) 3263–3271. http://dx.doi.org/10.1093/jn/132.11.3263.

[84] J. Jang, Y. Jung, Y. Kim, E.-H. Jho, Y. Yoon, LPS-induced inflammatory response is suppressed by Wnt inhibitors, Dickkopf-1 and LGK974, Sci. Rep. 7 (2017) 41612. doi:10.1038/srep41612.

[85] K. Uchiyama, T. Sakiyama, T. Hasebe, M.W. Musch, H. Miyoshi, Y. Nakagawa, T.-C. He, L. Lichtenstein, Y. Naito, Y. Itoh, T. Yoshikawa, B. Jabri, T. Stappenbeck, E.B. Chang, Butyrate and bioactive proteolytic form of Wnt-5a regulate colonic epithelial proliferation and spatial development, Sci. Rep. 6 (2016) 32094. https://doi.org/10.1038/srep32094.

[86] D.R. Donohoe, L.B. Collins, A. Wali, R. Bigler, W. Sun, S.J. Bultman, The Warburg effect dictates the mechanism of butyrate-mediated histone acetylation and cell proliferation, Mol. Cell. 48 (2012) 612–626. doi:10.1016/j.molcel.2012.08.033.

[87] J.R. Davie, Inhibition of Histone Deacetylase Activity by Butyrate, J. Nutr. 133 (2003) 2485S–2493S.

[88] S. Omenetti, T.T. Pizarro, The Treg/Th17 Axis: A Dynamic Balance Regulated by the Gut Microbiome , Front. Immunol. . 6 (2015) 639.

[89] O.J. Harrison, N. Srinivasan, J. Pott, C. Schiering, T. Krausgruber, N.E. Ilott, K.J. Maloy, Epithelial-derived IL-18 regulates Th17 cell differentiation and Foxp3+ Treg cell function in the intestine, Mucosal Immunol. 8 (2015) 1226.

[90] S.D. Gomes, C.S. Oliveira, J. Azevedo-Silva, M. Casanova, J. Barreto, H. Pereira, S. Chaves, L. Rodrigues, M. Casal, M. Corte-Real, F. Baltazar, A. Preto, The role of diet-related short-chain fatty acids in colorectal cancer metabolism and survival: prevention and therapeutic implications, Curr. Med. Chem. [Epub ahea (2018). doi:10.2174/0929867325666180530102050.

[91] C. Nastasi, M. Candela, C.M. Bonefeld, C. Geisler, M. Hansen, T. Krejsgaard, E. Biagi, M.H. Andersen, P. Brigidi, N. Ødum, T. Litman, A. Woetmann, The effect of short-chain fatty acids on human monocyte-derived dendritic cells, Sci. Rep. 5 (2015) 16148.

[92] M. Li, B.C.A.M. van Esch, G.T.M. Wagenaar, J. Garssen, G. Folkerts, P.A.J. Henricks, Pro- and anti-inflammatory effects of short chain fatty acids on immune and endothelial cells, Eur. J. Pharmacol. 831 (2018) 52–59. doi:https://doi.org/10.1016/j.ejphar.2018.05.003.

[93] A. Belcheva, T. Irrazabal, S.J. Robertson, C. Streutker, H. Maughan, S. Rubino, E.H. Moriyama, J.K. Copeland, A. Surendra, S. Kumar, B. Green, K. Geddes, R.C. Pezo, W.W. Navarre, M. Milosevic, B.C. Wilson, S.E. Girardin, T.M.S. Wolever, W. Edelmann, D.S. Guttman, D.J. Philpott, A. Martin, Gut microbial metabolism drives transformation of MSH2-deficient colon epithelial cells., Cell. 158 (2014) 288–299. doi:10.1016/j.cell.2014.04.051.

[94] N. Janakiram, C. Rao, The role of inflammation in colon cancer, in: B. Aggarwal, B. Sun, S. Gupta (Eds.), Inflamm. Cancer, 1st ed., Springer, Basel, 2014: pp. 25–52. doi:10.1007/978-3-0348-0837-8_2.

[95] S.Y. Lam, J. Yu, S.H. Wong, M.P. Peppelenbosch, G.M. Fuhler, The gastrointestinal microbiota and its role in oncogenesis, Best Pract. Res. Clin. Gastroenterol. 31 (2017) 607–618. doi:10.1016/j.bpg.2017.09.010.

[96] S.M. McNabney, T.M. Henagan, Short chain fatty acids in the colon and peripheral tissues: A focus on butyrate, colon cancer, obesity and insulin resistance, Nutrients. 9 (2017) 1–28. doi:10.3390/nu9121348.

[97] C.M. van der Beek, C.H. Dejong, F.J. Troost, A.A. Mascle, K. Lenaerts, Role of short-chain fatty acids in colonic inflammation, carcinogenesis, and mucosal protection and healing, Nutr. Rev. 75 (2017) 286–305. doi:10.1093/nutrit/nuw067.

[98] S. Zou, L. Fang, M.H. Lee, Dysbiosis of gut microbiota in promoting the development of colorectal cancer, Gastroenterol. Rep. 6 (2018) 1–12. doi:10.1093/gastro/gox031.

[99] C. De Filippo, D. Cavalieri, M. Di Paola, M. Ramazzotti, J.B. Poullet, S. Massart, S. Collini, G. Pieraccini, P. Lionetti, Impact of diet in shaping gut microbiota revealed by a comparative study in children from Europe and rural Africa, Proc. Natl. Acad. Sci. 107 (2010) 14691 LP-14696. doi:10.1073/pnas.1005963107.

[100] N. Larsen, T.B. Cahú, S.M. Isay Saad, A. Blennow, L. Jespersen, The effect of pectins on survival of probiotic Lactobacillus spp. in gastrointestinal juices is related to their structure and physical properties, Food Microbiol. 74 (2018) 11–20. doi:https://doi.org/10.1016/j.fm.2018.02.015.

[101] N. Larsen, C. Bussolo de Souza, L. Krych, T. Barbosa Cahú, M. Wiese, W. Kot, K.M. Hansen, A. Blennow, K. Venema, L. Jespersen, Potential of Pectins to Beneficially Modulate the Gut Microbiota Depends on Their Structural Properties , Front. Microbiol. . 10 (2019) 223.

[102] Y.E. Tuncil, C.H. Nakatsu, A.E. Kazem, S. Arioglu-Tuncil, B. Reuhs, E.C. Martens, B.R. Hamaker, Delayed utilization of some fast-fermenting soluble dietary fibers by human gut microbiota when presented in a mixture, J. Funct. Foods. 32 (2017) 347–357. doi:https://doi.org/10.1016/j.jff.2017.03.001.

[103] T.E. Rogers, N.A. Pudlo, N.M. Koropatkin, J.S.K. Bell, M. Moya Balasch, K. Jasker, E.C. Martens, Dynamic responses of Bacteroides thetaiotaomicron during growth on glycan mixtures, Mol. Microbiol. 88 (2013) 876–890. doi:10.1111/mmi.12228.

[104] N.A. Pudlo, K. Urs, S.S. Kumar, J.B. German, D.A. Mills, E.C. Martens, Symbiotic Human Gut Bacteria with Variable Metabolic Priorities for Host Mucosal Glycans, MBio. 6 (2015) e01282-15. doi:10.1128/mBio.01282-15.

[105] T. Chen, W. Long, C. Zhang, S. Liu, L. Zhao, B.R. Hamaker, Fiber-utilizing capacity varies in Prevotella- versus Bacteroides-dominated gut microbiota, Sci. Rep. 7 (2017) 2594. doi:10.1038/s41598-017-02995-4.

[106] F. Moens, S. Weckx, L. De Vuyst, Bifidobacterial inulin-type fructan degradation capacity determines cross-feeding interactions between bifidobacteria and Faecalibacterium prausnitzii., Int. J. Food Microbiol. 231 (2016) 76–85. doi:10.1016/j.ijfoodmicro.2016.05.015.

[107] M. Rossi, C. Corradini, A. Amaretti, M. Nicolini, A. Pompei, S. Zanoni, D. Matteuzzi, Fermentation of Fructooligosaccharides and Inulin by Bifidobacteria: a Comparative Study of Pure and Fecal Cultures, Appl. Environ. Microbiol. 71 (2005) 6150 LP-6158. doi:10.1128/AEM.71.10.6150-6158.2005.

[108] Y. Tsujikawa, R. Nomoto, R. Osawa, Difference in Degradation Patterns on Inulin-type Fructans among Strains of Lactobacillus delbrueckii and Lactobacillus paracasei, Biosci. Microbiota, Food Heal. 32 (2013) 157–165. doi:10.12938/bmfh.32.157.

[109] J. Yang, D.J. Rose, The impact of long-term dietary pattern of fecal donor on in vitro fecal fermentation properties of inulin., Food Funct. 7 (2016) 1805–1813.

doi:10.1039/c5fo00987a.

[110] J. Yang, I. Martínez, J. Walter, A. Keshavarzian, D.J. Rose, In vitro characterization of the impact of selected dietary fibers on fecal microbiota composition and short chain fatty acid production, Anaerobe. 23 (2013) 74–81. doi:https://doi.org/10.1016/j.anaerobe.2013.06.012.

[111] S. Brahma, I. Martínez, J. Walter, J. Clarke, T. Gonzalez, R. Menon, D.J. Rose, Impact of dietary pattern of the fecal donor on in vitro fermentation properties of whole grains and brans, J. Funct. Foods. 29 (2017) 281–289. doi:10.1016/j.jff.2016.12.042.

[112] P. V Toukach, K.S. Egorova, Bacterial, plant, and fungal carbohydrate structure databases: daily usage., Methods Mol. Biol. 1273 (2015) 55–85. doi:10.1007/978-1-4939-2343-4_5.

[113] K.S. Egorova, A.N. Kondakova, P. V Toukach, Carbohydrate Structure Database: tools for statistical analysis of bacterial, plant and fungal glycomes., Database (Oxford). 2015 (2015). doi:10.1093/database/bav073.

[114] F. Fransen, N.M. Sahasrabudhe, M. Elderman, M. Bosveld, S. El Aidy, F. Hugenholtz, T. Borghuis, B. Kousemaker, S. Winkel, C. van der Gaast-de Jongh, M.I. de Jonge, M. V Boekschoten, H. Smidt, H.A. Schols, P. de Vos, β2→1-Fructans Modulate the Immune System In Vivo in a Microbiota-Dependent and -Independent Fashion, Front. Immunol. 8 (2017) 154.

[115] L. Vogt, U. Ramasamy, D. Meyer, G. Pullens, K. Venema, M.M. Faas, H.A. Schols, P. de Vos, Immune Modulation by Different Types of β2→1-fructans Is Toll-Like Receptor Dependent, PLoS One. 8 (2013) 1–12. doi:10.1371/journal.pone.0068367.

[116] T. Zhang, Y. Zheng, D. Zhao, J. Yan, C. Sun, Y. Zhou, G. Tai, Multiple approaches to assess pectin binding to galectin-3, Int. J. Biol. Macromol. 91 (2016) 994–1001. doi:10.1016/j.ijbiomac.2016.06.058.

[117] W. Zhang, P. Xu, H. Zhang, Pectin in cancer therapy: A review, Trends Food Sci. Technol. 44 (2015) 258–271. doi:10.1016/j.tifs.2015.04.001.

[118] L.W. Peterson, D. Artis, Intestinal epithelial cells: Regulators of barrier function and immune homeostasis, Nat. Rev. Immunol. 14 (2014) 141–153. doi:10.1038/nri3608.

[119] S. Frosali, D. Pagliari, G. Gambassi, R. Landolfi, F. Pandolfi, R. Cianci, How the Intricate Interaction among Toll-Like Receptors, Microbiota, and Intestinal Immunity Can Influence Gastrointestinal Pathology, J. Immunol. Res. 2015 (2015). doi:10.1155/2015/489821.

[120] M. Fukata, M. Arditi, The role of pattern recognition receptors in intestinal inflammation, Mucosal Immunol. 6 (2013) 451–463. doi:10.1038/mi.2013.13.The.

[121] S.B.R. do Prado, Structural-dependent effects of dietary fibers in colon cancer: Focus on dietary fiber naturally changed by the papaya ripening, University of São Paulo, 2019.

[122] V.C. Castro-Alves, T.M. Shiga, J.R.O. do Nascimento, Polysaccharides from chayote enhance lipid efflux and regulate NLRP3 inflammasome priming in macrophage-like THP-1 cells exposed to cholesterol crystals, Int. J. Biol. Macromol. 127 (2019) 502–510. doi:https://doi.org/10.1016/j.ijbiomac.2019.01.048.

[123] R. Tada, F. Ikeda, K. Aoki, M. Yoshikawa, Y. Kato, Y. Adachi, A. Tanioka, K. Ishibashi, K. Tsubaki, N. Ohno, Barley-derived β-d-glucan induces immunostimulation via a dectin-1-mediated pathway, Immunol. Lett. 123 (2009) 144–148. doi:https://doi.org/10.1016/j.imlet.2009.03.005.

[124] N.M. Sahasrabudhe, H.A. Schols, M.M. Faas, P. de Vos, Arabinoxylan activates Dectin-1

and modulates particulate β-glucan-induced Dectin-1 activation, Mol. Nutr. Food Res. (2015) 458–467. doi:10.1002/mnfr.201500582.

[125] M. Bermudez-Brito, C. Rösch, H.A. Schols, M.M. Faas, P. de Vos, Resistant starches differentially stimulate Toll-like receptors and attenuate proinflammatory cytokines in dendritic cells by modulation of intestinal epithelial cells, Mol. Nutr. Food Res. 59 (2015) 1814–1826. doi:10.1002/mnfr.201500148.

[126] C.-C. Tsai, C.-R. Lin, H.-Y. Tsai, C.-J. Chen, W.-T. Li, H.-M. Yu, Y.-Y. Ke, W.-Y. Hsieh, C.-Y. Chang, C.-Y. Wu, S.-T. Chen, C.-H. Wong, The Immunologically Active Oligosaccharides Isolated from Wheatgrass Modulate Monocytes via Toll-like Receptor-2 Signaling, J. Biol. Chem. . 288 (2013) 17689–17697.

[127] C.C. Lin, H.H. Chen, Y.K. Chen, H.C. Chang, P.Y. Lin, I.-H. Pan, D.-Y. Chen, C.M. Chen, S.Y. Lin, Rice bran feruloylated oligosaccharides activate dendritic cells via Toll-like receptor 2 and 4 signaling., Molecules. 19 (2014) 5325–5347. doi:10.3390/molecules19045325.

[128] L.M. Vogt, N.M. Sahasrabudhe, U. Ramasamy, D. Meyer, G. Pullens, M.M. Faas, K. Venema, H.A. Schols, P. de Vos, The impact of lemon pectin characteristics on TLR activation and T84 intestinal epithelial cell barrier function, J. Funct. Foods. 22 (2016) 398–407. doi:10.1016/j.jff.2016.02.002.

[129] S. Xu, Y. Huang, Y. Xie, T. Lan, K. Le, J. Chen, S. Chen, S. Gao, X. Xu, X. Shen, H. Huang, P. Liu, Evaluation of foam cell formation in cultured macrophages: An improved method with Oil Red O staining and DiI-oxLDL uptake, Cytotechnology. 62 (2010) 473–481. doi:10.1007/s10616-010-9290-0.

[130] K. Ishisono, T. Yabe, K. Kitaguchi, Citrus pectin attenuates endotoxin shock via suppression of Toll-like receptor signaling in Peyer's patch myeloid cells, J. Nutr. Biochem. 50 (2017) 38–45. doi:10.1016/j.jnutbio.2017.07.016.

[131] S. V Popov, P.A. Markov, G.Y. Popova, I.R. Nikitina, L. Efimova, Y.S. Ovodov, Anti-inflammatory activity of low and high methoxylated citrus pectins, Biomed. Prev. Nutr. 3 (2013) 59–63. doi:https://doi.org/10.1016/j.bionut.2012.10.008.

[132] Q. Xu, T. Yajima, W. Li, K. Saito, Y. Ohshima, Y. Yoshikai, Levan (β-2, 6-fructan), a major fraction of fermented soybean mucilage, displays immunostimulating properties via Toll-like receptor 4 signalling: induction of interleukin-12 production and suppression of T-helper type 2 response and immunoglobulin E prod, Clin. Exp. Allergy. 36 (2006) 94–101. doi:10.1111/j.1365-2222.2006.02401.x.

[133] N.M. Sahasrabudhe, M. Beukema, L. Tian, B. Troost, J. Scholte, E. Bruininx, G. Bruggeman, M. van den Berg, A. Scheurink, H.A. Schols, M.M. Faas, P. de Vos, Dietary fiber pectin directly blocks toll-like receptor 2-1 and prevents doxorubicin-induced ileitis, Front. Immunol. 9 (2018) 1–19. doi:10.3389/fimmu.2018.00383.

[134] T. Van Hung, T. Suzuki, Guar gum fiber increases suppressor of cytokine signaling-1 expression via toll-like receptor 2 and dectin-1 pathways, regulating inflammatory response in small intestinal epithelial cells, Mol. Nutr. Food Res. 61 (2017) 1700048. doi:10.1002/mnfr.201700048.

[135] Y. Naito, T. Takagi, K. Katada, K. Uchiyama, M. Kuroda, S. Kokura, H. Ichikawa, J. Watabe, N. Yoshida, T. Okanoue, T. Yoshikawa, Partially hydrolyzed guar gum down-regulates colonic inflammatory response in dextran sulfate sodium-induced colitis in mice, J. Nutr. Biochem. 17 (2006) 402–409. doi:https://doi.org/10.1016/j.jnutbio.2005.08.010.

[136] M.-Y. Su, C.-I. Kuo, C.-F. Chang, C.-I. Chang, Three-Dimensional Structure of Human NLRP10/PYNOD Pyrin Domain Reveals a Homotypic Interaction Site Distinct from Its

Mouse Homologue, PLoS One. 8 (2013) e67843.

[137] L. Franchi, N. Warner, K. Viani, G. Nuñez, Function of Nod-like receptors in microbial recognition and host defense, Immunol. Rev. 227 (2009) 106–128. doi:10.1111/j.1600-065X.2008.00734.x.

[138] M. Saxena, G. Yeretssian, NOD-like receptors: Master regulators of inflammation and cancer, Front. Immunol. 5 (2014) 1–16. doi:10.3389/fimmu.2014.00327.

[139] N. Gagliani, N.W. Palm, M.R. de Zoete, R.A. Flavell, Inflammasomes and intestinal homeostasis: regulating and connecting infection, inflammation and the microbiota, Int. Immunol. 26 (2014) 495–499. doi:10.1093/intimm/dxu066.

[140] S. Huhn, M.I. da Silva Filho, T. Sanmuganantham, T. Pichulik, C. Catalano, B. Pardini, A. Naccarati, V. Polakova-Vymetálkova, K. Jiraskova, L. Vodickova, P. Vodicka, M.W. Löffler, L. Courth, J. Wehkamp, F.V.N. Din, M. Timofeeva, S.M. Farrington, L. Jansen, K. Hemminki, J. Chang-Claude, H. Brenner, M. Hoffmeister, M.G. Dunlop, A.N.R. Weber, A. Försti, Coding variants in NOD-like receptors: An association study on risk and survival of colorectal cancer, PLoS One. 13 (2018) e0199350.

[141] L.C. Freeman, J.P.-Y. Ting, The pathogenic role of the inflammasome in neurodegenerative diseases, J. Neurochem. 136 (2016) 29–38. doi:10.1111/jnc.13217.

[142] C. Lin, J. Zhang, Inflammasomes in Inflammation-Induced Cancer , Front. Immunol. . 8 (2017) 271.

[143] Y. Zhan, S.S. Seregin, J. Chen, G.Y. Chen, Nod1 Limits Colitis-Associated Tumorigenesis by Regulating IFN-γ Production, J. Immunol. 196 (2016) 5121–5129. doi:10.4049/jimmunol.1501822.

[144] S.M.N. Udden, L. Peng, J.-L. Gan, J.M. Shelton, J.S. Malter, L. V Hooper, M.H. Zaki, NOD2 Suppresses Colorectal Tumorigenesis via Downregulation of the TLR Pathways, Cell Rep. 19 (2017) 2756–2770. doi:https://doi.org/10.1016/j.celrep.2017.05.084.

[145] M. V Pashenkov, Y.A. Dagil, B. V Pinegin, NOD1 and NOD2: Molecular targets in prevention and treatment of infectious diseases, Int. Immunopharmacol. 54 (2018) 385–400. doi:https://doi.org/10.1016/j.intimp.2017.11.036.

[146] S. Chen, D.-K. Yin, W.-B. Yao, Y.-D. Wang, Y.-R. Zhang, X.-D. Gao, Macrophage receptors of polysaccharide isolated from a marine filamentous fungus Phoma herbarum YS4108., Acta Pharmacol. Sin. 30 (2009) 1008–14. doi:10.1038/aps.2009.93.

[147] L.E. Smythies, J.R. Smythies, Exosomes in the gut, Front. Immunol. 5 (2014) 104. doi:10.3389/fimmu.2014.00104.

[148] A.T. Xu, J.T. Lu, Z.H. Ran, Q. Zheng, Exosome in intestinal mucosal immunity, J. Gastroenterol. Hepatol. 31 (2016) 1694–1699. doi:10.1111/jgh.13413.

[149] S.B.R. do Prado, G.F. Ferreira, Y. Harazono, T.M. Shiga, A. Raz, N.C. Carpita, J.P. Fabi, Ripening-induced chemical modifications of papaya pectin inhibit cancer cell proliferation, Sci. Rep. 7 (2017) 16564. doi:10.1038/s41598-017-16709-3.

[150] R.S.T. Tan, B. Ho, B.P. Leung, J.L. Ding, TLR Cross-talk Confers Specificity to Innate Immunity, Int. Rev. Immunol. 33 (2014) 443–453. doi:10.3109/08830185.2014.921164.

[151] Y. Masuda, T. Togo, S. Mizuno, M. Konishi, H. Nanba, Soluble β-glucan from Grifola frondosa induces proliferation and Dectin-1/Syk signaling in resident macrophages via the GM-CSF autocrine pathway, J. Leukoc. Biol. 91 (2012) 547–556. doi:10.1189/jlb.0711386.

[152] W.-J. Li, X.-F. Tang, X.-X. Shuai, C.-J. Jiang, X. Liu, L.-F. Wang, Y.-F. Yao, S.-P. Nie,

M.-Y. Xie, Mannose Receptor Mediates the Immune Response to Ganoderma atrum Polysaccharides in Macrophages, J. Agric. Food Chem. 65 (2017) 348–357. doi:10.1021/acs.jafc.6b04888.

[153] N.M. Sahasrabudhe, J. Dokter-Fokkens, P. de Vos, Particulate β-glucans synergistically activate TLR4 and Dectin-1 in human dendritic cells, Mol. Nutr. Food Res. 60 (2016) 2514–2522. doi:10.1002/mnfr.201600356.

[154] M.E. Eberle, A.H. Dalpke, Dectin-1 Stimulation Induces Suppressor of Cytokine Signaling 1, Thereby Modulating TLR Signaling and T Cell Responses, J. Immunol. 188 (2012) 5644 LP-5654. doi:10.4049/jimmunol.1103068.

[155] S. Cohen-Kedar, L. Baram, H. Elad, E. Brazowski, H. Guzner-Gur, I. Dotan, Human intestinal epithelial cells respond to β-glucans via Dectin-1 and Syk, Eur. J. Immunol. 44 (2014) 3729–3740. doi:10.1002/eji.201444876.

[156] C.F. Ji, Y. Bin Ji, Laminarin-induced apoptosis in human colon cancer LoVo cells, Oncol. Lett. 7 (2014) 1728–1732. doi:10.3892/ol.2014.1952.

[157] C. Tang, T. Kamiya, Y. Liu, M. Kadoki, S. Kakuta, K. Oshima, M. Hattor, K. Takeshita, T. Kanai, S. Saijo, N. Ohno, Y. Iwakura, Inhibition of dectin-1 signaling ameliorates colitis by inducing Lactobacillus-mediated regulatory T cell expansion in the intestine, Cell Host Microbe. 18 (2015) 183–197.

[158] D. Ding, Y. Yao, S. Zhang, C. Su, Y. Zhang, C-type lectins facilitate tumor metastasis (Review), Oncol. Lett. 13 (2017) 13–21. doi:10.3892/ol.2016.5431.

[159] S. Chiba, H. Ikushima, H. Ueki, H. Yanai, Y. Kimura, S. Hangai, J. Nishio, H. Negishi, T. Tamura, S. Saijo, Y. Iwakura, T. Taniguchi, Recognition of tumor cells by Dectin-1 orchestrates innate immune cells for anti-tumor responses, Elife. 3 (2014) e04177. doi:10.7554/eLife.04177.

[160] H. Yan, T. Kamiya, P. Suabjakyong, N.M. Tsuji, Targeting C-Type Lectin Receptors for Cancer Immunity , Front. Immunol. . 6 (2015) 408.

[161] G.D. Brown, Dectin-1: a signalling non-TLR pattern-recognition receptor., Nat. Rev. Immunol. 6 (2006) 33–43. doi:10.1038/nri1745.

[162] G.D. Brown, J. Herre, D.L. Williams, J.A. Willment, A.S.J. Marshall, S. Gordon, Dectin-1 mediates the biological effects of β-glucans, J. Exp. Med. 197 (2003) 1119–1124. doi:10.1084/jem.20021890.

[163] M. McIntosh, B.A. Stone, V.A. Stanisich, Curdlan and other bacterial (1→3)-β-d-glucans, Appl. Microbiol. Biotechnol. 68 (2005) 163–173. doi:10.1007/s00253-005-1959-5.

[164] G. Camilli, G. Tabouret, J. Quintin, The Complexity of Fungal β-Glucan in Health and Disease: Effects on the Mononuclear Phagocyte System , Front. Immunol. . 9 (2018) 673.

[165] M.S. Mikkelsen, M.G. Jensen, T.S. Nielsen, Barley beta-glucans varying in molecular mass and oligomer structure affect cecal fermentation and microbial composition but not blood lipid profiles in hypercholesterolemic rats, Food Funct. 8 (2017) 4723–4732. doi:10.1039/C7FO01314K.

[166] H.S. Kim, J.T. Hong, Y. Kim, S.-B. Han, Stimulatory Effect of β-glucans on Immune Cells, Immune Netw. 11 (2011) 191–195. doi:10.4110/in.2011.11.4.191.

[167] S.H.A. and J. Yan, The Effects of Glucans on Dendritic Cells and Implications for Cancer Therapy, Anticancer. Agents Med. Chem. 13 (2013) 689–698. doi:http://dx.doi.org/10.2174/1871520611313050003.

[168] I.D. Iliev, V.A. Funari, K.D. Taylor, Q. Nguyen, C.N. Reyes, S.P. Strom, J. Brown, C.A. Becker, P.R. Fleshner, M. Dubinsky, J.I. Rotter, H.L. Wang, D.P.B. McGovern, G.D. Brown, D.M. Underhill, Interactions Between Commensal Fungi and the C-Type Lectin Receptor Dectin-1 Influence Colitis, Science (80-.). 336 (2012) 1314 LP-1317. doi:10.1126/science.1221789.

[169] Y. Zhao, X. Chu, J. Chen, Y. Wang, S. Gao, Y. Jiang, X. Zhu, G. Tan, W. Zhao, H. Yi, H. Xu, X. Ma, Y. Lu, Q. Yi, S. Wang, Dectin-1-activated dendritic cells trigger potent antitumour immunity through the induction of Th9 cells, Nat. Commun. 7 (2016) 12368.

[170] M. Liu, F. Luo, C. Ding, S. Albeituni, X. Hu, Y. Ma, Y. Cai, L. McNally, M.A. Sanders, D. Jain, G. Kloecker, M. Bousamra, H. Zhang, R.M. Higashi, A.N. Lane, T.W.-M. Fan, J. Yan, Dectin-1 Activation by a Natural Product β-Glucan Converts Immunosuppressive Macrophages into an M1-like Phenotype, J. Immunol. 195 (2015) 5055 LP-5065. doi:10.4049/jimmunol.1501158.

[171] M. Yadav, J.S. Schorey, The beta-glucan receptor dectin-1 functions together with TLR2 to mediate macrophage activation by mycobacteria, Blood. 108 (2006) 3168–3175. doi:10.1182/blood-2006-05-024406.

[172] K.M. Dennehy, G. Ferwerda, I. Faro-Trindade, E. Pyz, J.A. Willment, P.R. Taylor, A. Kerrigan, S.V. Tsoni, S. Gordon, F. Meyer-Wentrup, G.J. Adema, B.J. Kullberg, E. Schweighoffer, V. Tybulewicz, H.M. Mora-Montes, N.A.R. Gow, D.L. Williams, M.G. Netea, G.D. Brown, Syk kinase is required for collaborative cytokine production induced through Dectin-1 and Toll-like receptors, Eur. J. Immunol. 38 (2008) 500–506. doi:10.1002/eji.200737741.

[173] M.T. Abreu, M. Fukata, M. Arditi, TLR Signaling in the Gut in Health and Disease, J. Immunol. 174 (2005) 4453 LP-4460. doi:10.4049/jimmunol.174.8.4453.

[174] Z. Shi, Z. Cai, A. Sanchez, T. Zhang, S. Wen, J. Wang, J. Yang, S. Fu, D. Zhang, A novel toll-like receptor that recognizes vesicular stomatitis virus, J. Biol. Chem. 286 (2011) 4517–4524. doi:10.1074/jbc.M110.159590.

[175] M.J. Jimenez-Dalmaroni, M.E. Gerswhin, I.E. Adamopoulos, The critical role of toll-like receptors--From microbial recognition to autoimmunity: A comprehensive review., Autoimmun. Rev. 15 (2016) 1–8. doi:10.1016/j.autrev.2015.08.009.

[176] Y. Sato, Y. Goto, N. Narita, D.S.B. Hoon, Cancer Cells Expressing Toll-like Receptors and the Tumor Microenvironment, Cancer Microenviron. 2 (2009) 205–214. doi:10.1007/s12307-009-0022-y.

[177] T.T. Li, S. Ogino, Z.R. Qian, Toll-like receptor signaling in colorectal cancer: Carcinogenesis to cancer therapy, World J. Gastroenterol. 20 (2014) 17699–17708. doi:10.3748/wjg.v20.i47.17699.

[178] T.I. Kopp, U. Vogel, A. Tjonneland, V. Andersen, Meat and fiber intake and interaction with pattern recognition receptors (TLR1, TLR2, TLR4, and TLR10) in relation to colorectal cancer in a Danish prospective, case-cohort study, Am. J. Clin. Nutr. 107 (2018) 465–479.

[179] Y. Nihon-Yanagi, K. Terai, T. Murano, T. Matsumoto, S. Okazumi, Tissue expression of Toll-like receptors 2 and 4 in sporadic human colorectal cancer., Cancer Immunol. Immunother. 61 (2012) 71–77. doi:10.1007/s00262-011-1085-4.

[180] A.H. Kuo, F.A. Scheeren, Cell-intrinsic TLR2/MyD88 pathway in breast and colon cancer, Cell Cycle. 13 (2014) 3785–3786. doi:10.4161/15384101.2014.989947.

[181] J. Li, F. Yang, F. Wei, X. Ren, The role of toll-like receptor 4 in tumor microenvironment,

Oncotarget. 8 (2017) 66656–66667. doi:10.18632/oncotarget.19105.

[182] M. Najjar, D. Saleh, M. Zelic, S. Nogusa, S. Shah, A. Tai, J.N. Finger, A. Polykratis, P.J. Gough, J. Bertin, M.J. Whalen, M. Pasparakis, S. Balachandran, M. Kelliher, A. Poltorak, A. Degterev, RIPK1 and RIPK3 Kinases Promote Cell-Death-Independent Inflammation by Toll-like Receptor 4, Immunity. 45 (2016) 46–59. doi:10.1016/j.immuni.2016.06.007.

[183] Y.H. Chung, D. Kim, Enhanced TLR4 Expression on Colon Cancer Cells After Chemotherapy Promotes Cell Survival and Epithelial-Mesenchymal Transition Through Phosphorylation of GSK3beta., Anticancer Res. 36 (2016) 3383–3394.

[184] B. Huang, J. Zhao, H. Li, K.-L. He, Y. Chen, S.-H. Chen, L. Mayer, J.C. Unkeless, H. Xiong, Toll-like receptors on tumor cells facilitate evasion of immune surveillance., Cancer Res. 65 (2005) 5009–5014. doi:10.1158/0008-5472.CAN-05-0784.

[185] M.J. Gunter, R. Stolzenberg-Solomon, A.J. Cross, M.F. Leitzmann, S. Weinstein, R.J. Wood, J. Virtamo, P.R. Taylor, D. Albanes, R. Sinha, A prospective study of serum C-reactive protein and colorectal cancer risk in men., Cancer Res. 66 (2006) 2483–2487. doi:10.1158/0008-5472.CAN-05-3631.

[186] W. Gao, Y. Xiong, Q. Li, H. Yang, Inhibition of Toll-Like Receptor Signaling as a Promising Therapy for Inflammatory Diseases: A Journey from Molecular to Nano Therapeutics , Front. Physiol. . 8 (2017) 508.

[187] L. Leclere, P. Van Cutsem, C. Michiels, Anti-cancer activities of pH- or heat-modified pectin, Front. Pharmacol. 4 (2013) 128. doi:10.3389/fphar.2013.00128.

[188] S.E. Byeon, J. Lee, J.H. Kim, W.S. Yang, Y.S. Kwak, S.Y. Kim, E.S. Choung, M.H. Rhee, J.Y. Cho, Molecular mechanism of macrophage activation by red ginseng acidic polysaccharide from Korean red ginseng, Mediators Inflamm. 2012 (2012) 7–9. doi:10.1155/2012/732860.

[189] D. Cheng, X. Zhang, M. Meng, L. Han, C. Li, L. Hou, W. Qi, C. Wang, Inhibitory effect on HT-29 colon cancer cells of a water-soluble polysaccharide obtained from highland barley, Int. J. Biol. Macromol. 92 (2016) 88–95.

[190] V.C. Castro-Alves, M. Sansone, A.B. Sansone, J.R.O. Nascimento, Polysaccharides from raw and cooked chayote modulate macrophage function, Food Res. Int. 81 (2016) 171–179. doi:10.1016/j.foodres.2016.01.017.

[191] X. Cen, S. Liu, K. Cheng, The Role of Toll-Like Receptor in Inflammation and Tumor Immunity, Front. Pharmacol. 9 (2018) 1–8. doi:10.3389/fphar.2018.00878.

[192] M. Taura, R. Fukuda, M.A. Suico, A. Eguma, T. Koga, T. Shuto, T. Sato, S. Morino-Koga, H. Kai, TLR3 induction by anticancer drugs potentiates poly I:C-induced tumor cell apoptosis, Cancer Sci. 101 (2010) 1610–1617. doi:10.1111/j.1349-7006.2010.01567.x.

[193] S.H. Rhee, E. Im, C. Pothoulakis, Toll-Like Receptor 5 Engagement Modulates Tumor Development and Growth in a Mouse Xenograft Model of Human Colon Cancer, Gastroenterology. 135 (2008) 518–528.e3. doi:https://doi.org/10.1053/j.gastro.2008.04.022.

[194] I. Furi, F. Sipos, T.M. Germann, A. Kalmár, Z. Tulassay, B. Molnár, G. Muzes, Epithelial toll-like receptor 9 signaling in colorectal inflammation and cancer: Clinico-pathogenic aspects, World J. Gastroenterol. 19 (2013) 4119–4126. doi:10.3748/wjg.v19.i26.4119.

[195] E.-H. Byun, T. Omura, K. Yamada, H. Tachibana, Green tea polyphenol epigallocatechin-3-gallate inhibits TLR2 signaling induced by peptidoglycan through the polyphenol sensing molecule 67-kDa laminin receptor, FEBS Lett. 585 (2011) 814–820. doi:10.1016/j.febslet.2011.02.010.

[196] M. Rahimifard, F. Maqbool, S. Moeini-Nodeh, K. Niaz, M. Abdollahi, N. Braidy, S.M. Nabavi, S.F. Nabavi, Targeting the TLR4 signaling pathway by polyphenols: A novel therapeutic strategy for neuroinflammation, Ageing Res. Rev. 36 (2017) 11–19. doi:https://doi.org/10.1016/j.arr.2017.02.004.

[197] D. Zhang, Y. Li, M. Mi, F.-L. Jiang, Z. Yue, Y. Sun, L. Fan, J. Meng, X. Zhang, L. Liu, Q.-B. Mei, Modified apple polysaccharides suppress the migration and invasion of colorectal cancer cells induced by lipopolysaccharide., Nutr. Res. 33 (2013) 839–48. doi:10.1016/j.nutres.2013.06.004.

[198] Y. Li, L. Fan, Y. Niu, W. Mian, F. Zhang, M. Xie, Y. Sun, Q. Mei, An apple oligogalactan enhances the growth inhibitory effect of 5-fluorouracil on colorectal cancer, Eur. J. Pharmacol. 804 (2017) 13–20. doi:https://doi.org/10.1016/j.ejphar.2017.04.001.

[199] H. Lahm, S. Andre, A. Hoeflich, J.R. Fischer, B. Sordat, H. Kaltner, E. Wolf, H.J. Gabius, Comprehensive galectin fingerprinting in a panel of 61 human tumor cell lines by RT-PCR and its implications for diagnostic and therapeutic procedures., J. Cancer Res. Clin. Oncol. 127 (2001) 375–386.

[200] L. Tao, L. Jin, L. Dechun, Y. Hongqiang, K. Changhua, L. Guijun, Galectin-3 expression in colorectal cancer and its correlation with clinical pathological characteristics and prognosis, Open Med. 12 (2017) 226–230. doi:10.1515/med-2017-0032.

[201] K. Endo, S. Kohnoe, E. Tsujita, A. Watanabe, H. Nakashima, H. Baba, Y. Maehara, Galectin-3 expression is a potent prognostic marker in colorectal cancer, Anticancer Res. 25 (2005) 3117–21. http://www.ncbi.nlm.nih.gov/pubmed/16080575.

[202] P. Nangia-Makker, V. Balan, A. Raz, Regulation of tumor progression by extracellular galectin-3, Cancer Microenviron. 1 (2008) 43–51. doi:10.1007/s12307-008-0003-6.

[203] A. Fortuna-Costa, A.M. Gomes, E.O. Kozlowski, M.P. Stelling, M.S.G. Pavão, Extracellular galectin-3 in tumor progression and metastasis, Front. Oncol. 4 (2014) 138. doi:10.3389/fonc.2014.00138.

[204] P.P. Ruvolo, Galectin 3 as a guardian of the tumor microenvironment, Biochim. Biophys. Acta - Mol. Cell Res. 1863 (2016) 427–437. doi:https://doi.org/10.1016/j.bbamcr.2015.08.008.

[205] N.A. Kamili, C.M. Arthur, C. Gerner-Smidt, E. Tafesse, A. Blenda, M. Dias-Baruffi, S.R. Stowell, Key regulators of galectin-glycan interactions, Proteomics. 16 (2016) 3111–3125. doi:10.1002/pmic.201600116.

[206] Y. Wang, P. Nangia-Makker, L. Tait, V. Balan, V. Hogan, K.J. Pienta, A. Raz, Regulation of prostate cancer progression by galectin-3., Am. J. Pathol. 174 (2009) 1515–23. doi:10.2353/ajpath.2009.080816.

[207] P. Nangia-Makker, V. Hogan, A. Raz, Galectin-3 and cancer stemness, Glycobiology. 28 (2018) 172–181. doi:10.1093/glycob/cwy001.

[208] A.P. Gunning, R.J.M. Bongaerts, V.J. Morris, Recognition of galactan components of pectin by galectin-3., FASEB J. 23 (2009) 415–24. doi:10.1096/fj.08-106617.

[209] V. V. Glinsky, A. Raz, Modified citrus pectin anti-metastatic properties: one bullet, multiple targets, Carbohydr. Res. 344 (2009) 1788–1791. doi:10.1016/j.carres.2008.08.038.

[210] T. Zhang, Y. Lan, Y. Zheng, F. Liu, D. Zhao, K.H. Mayo, Y. Zhou, G. Tai, Identification of the bioactive components from pH-modified citrus pectin and their inhibitory effects on galectin-3 function, Food Hydrocoll. 58 (2016) 113–119. doi:10.1016/j.foodhyd.2016.02.020.

[211] E.G. Maxwell, I.J. Colquhoun, H.K. Chau, A.T. Hotchkiss, K.W. Waldron, V.J. Morris, N.J. Belshaw, Modified sugar beet pectin induces apoptosis of colon cancer cells via an interaction with the neutral sugar side-chains, Carbohydr. Polym. 136 (2016) 923–929. doi:10.1016/j.carbpol.2015.09.063.

[212] E.G. Maxwell, N.J. Belshaw, K.W. Waldron, V.J. Morris, Pectin – An emerging new bioactive food polysaccharide, Trends Food Sci. Technol. 24 (2012) 64–73. doi:10.1016/j.tifs.2011.11.002.

[213] M. Azémar, B. Hildenbrand, B. Haering, M.E. Heim, C. Unger, Clinical Benefit in Patients with Advanced Solid Tumors Treated with Modified Citrus Pectin: A Prospective Pilot Study, Clin. Med. Oncol. 1 (2007) CMO.S285. doi:10.4137/CMO.S285.

[214] S. Prado, G.R. Santos, P. Mourão, J. Fabi, Chelate-soluble pectin fraction from papaya pulp interacts with galectin-3 and inhibits colon cancer cell proliferation, Int. J. Biol. Macromol. 126 (2019) 170–178. doi:10.1016/j.ijbiomac.2018.12.191.

[215] S. Chen, Z. Wang, Y. Huang, S.A. O'Barr, R.A. Wong, S. Yeung, M.S.S. Chow, Ginseng and anticancer drug combination to improve cancer chemotherapy: A critical review, Evidence-Based Complement. Altern. Med. 2014 (2014). doi:10.1155/2014/168940.

[216] S.B.R. do Prado, T.M. Shiga, Y. Harazono, V.A. Hogan, A. Raz, N.C. Carpita, J.P. Fabi, Migration and proliferation of cancer cells in culture are differentially affected by molecular size of modified citrus pectin, Carbohydr. Polym. 211 (2019) 141–151. doi:https://doi.org/10.1016/j.carbpol.2019.02.010.

[217] V.J. Morris, A. Gromer, A.R. Kirby, R.J.M. Bongaerts, A. Patrick Gunning, Using AFM and force spectroscopy to determine pectin structure and (bio) functionality, Food Hydrocoll. 25 (2011) 230–237. doi:10.1016/j.foodhyd.2009.11.015.

[218] T. Zhang, M.C. Miller, Y. Zheng, Z. Zhang, H. Xue, D. Zhao, J. Su, K.H. Mayo, Y. Zhou, G. Tai, Macromolecular assemblies of complex polysaccharides with galectin-3 and their synergistic effects on function, Biochem. J. 474 (2017) 3849–3868. doi:10.1042/BCJ20170143.

Chapter 4

Part I: Migration and proliferation of cancer cells in culture are differentially affected by molecular size of modified citrus pectin

Samira Bernardino Ramos do Prado[1], Tânia Misuzu Shiga[1], Yosuke Harazono[2,3], Victor A. Hogan[2], Avraham Raz[2], Nicholas C. Carpita[4], João Paulo Fabi[1,5,6]

[1]Department of Food Science and Experimental Nutrition, School of Pharmaceutical Sciences, University of São Paulo, São Paulo, SP, Brazil.
[2]Departments of Oncology and Pathology, School of Medicine, Wayne State University, and Karmanos Cancer Institute, Detroit, MI, USA.
[3]Department of Maxillofacial Surgery, Tokyo Medical and Dental University, Bunkyo-ku, Tokyo, 113–8510, Japan.
[4]Department of Botany & Plant Pathology, Purdue University, West Lafayette, IN, USA.
e Food and Nutrition Research Center (NAPAN), University of São Paulo, São Paulo, SP, Brazil.
[5]Food Research Center (FoRC), CEPID-FAPESP (Research, Innovation and Dissemination Centers, São Paulo Research Foundation), São Paulo, SP, Brazil.

Carbohydrate Polymers, v. 211, p. 141-151, 2019.

Abstract

While chemically and thermally modified citrus pectin (MCP) has already been studied for health benefits, it is unknown how size-fractionated oligo- and polysaccharides differentially affect cancer cell behavior. We produced thermally MCP and fractionated it by molecular size to evaluate the effect these polymers have on cancer cells. MCP30/10 (between 30 and 10 kDa) had more esterified homogalacturonans (HG) and fewer rhamnogalacturonans (RG-I) than MCP and MCP30 (higher than 30 kDa), while MCP10/3 (between 10 and 3 kDa) showed higher amounts of type I arabinogalactans (AGI) and lower amounts of RG-I. MCP3 (smaller than 3 kDa) presented less esterified HG and the lowest amount of AGI and RG-I. Our data indicate that the enrichment of de-esterified HG oligomers and the AGI and RG-I depletions in MCP3, or the increase of AGI and loss of RGI in MCP30/10, enhance the anticancer behaviors by inhibiting migration, aggregation, and proliferation of cancer cells.

Key-words: pectin, modified pectin, citrus, cancer cells

Abbreviations: AGI, type I arabinogalactan; AGII, type II arabinogalactan; Ara, arabinose; ATR, attenuated total reflectance; BAMEC, bovine adrenal medullary endothelial cells; BSA, bovine serum albumin; CP, citrus pectin; DF, dietary fiber; DMEM, Dulbecco's modified Eagle's medium; DTGS, deuterated triglycine sulfate; ECM, extracellular matrix; EMEM, Earle's Minimal Essential Medium; f, furanose; FBS, fetal bovine serum; FTIR, Fourier Transform Infrared; Fuc: fucose; Gal, galactose, GalA, galacturonic acid; Glc, glucose; GlcA, glucuronic acid; HG, homogalacturonan; LDH, lactate dehydrogenase; LSD, Least Significant Difference; Man, mannose; MCP, modified citrus pectin; MTT, 3-(4,5-Dimethyl-2-thiazolyl)-2,5-diphenyl-2H-tetrazolium bromide; p, pyranose; PMAA, partially methylated alditol acetates; RG-I, rhamnogalacturonan-I; RG-II, rhamnogalacturonan-II; Rha, rhamnose; SCFA, short chain fatty acids; SD, standard deviation; t, terminal; V_e, elution volume; V_o, void volume; XGA, xylogalacturonans; Xyl: xylose.

Introduction

Previous studies have supported an association between a dietary fiber (DF)-rich diet and a reduced risk of colorectal cancer [1,2]. However, the biological mechanism for how DF acts to reduce the chance of intestinal cells altering to cancerous phenotypes is not fully understood.

DF is mainly composed of carbohydrates that are resistant to digestion and, therefore, are not absorbed by the small intestine. Thus, DF can interact directly with cells throughout the gastrointestinal tract before reaching the colon. DF can be largely metabolized by the gut microbiota in the colon, thereby reducing the size of these carbohydrates and producing short chain fatty acids (SCFA) [3]. This SCFA release is one of the main mechanisms for the beneficial effects associated with a DF-rich diet. However, although the anticancer effects of SCFA are well known [4], the mechanisms through which DF can directly interact with cancer cells is poorly understood.

Plant DF is mainly comprised of cell wall polysaccharides that are a complex network of cellulose, hemicellulose and pectin [5]. Pectin is comprised of two types of polysaccharides: homogalacturonan (HG) and rhamnogalacturonan-I (RG-I). HG is composed of α-1,4-D-galacturonic acid (Gal*p*A) residues with varying degrees of acetyl and methyl esterification [5,6], and it can be further modified by xylosylation into xylogalacturonans (XGA) or the highly complex rhamnogalacturonan-II (RG-II; Mohnen, 2008). The RG-I backbone is made of repeating units of [→4)-α-D-Gal*p*A-(1→2)-α-L-Rha*p*-(1→] that have side groups of arabinan, galactan, and type I arabinogalactan (AGI) at the O-4 position of the rhamnose (Rha*p*) residues [5,6]. The molecular size, monosaccharide composition, and linkage pattern of HG and RG-I vary substantially during the development of any plant species and organ, which results in a large degree of pectin heterogeneity in fruits and vegetables [7]. This structural diversity within a single pectin fraction makes it challenging to establish a structure-function relationship between pectin and intestinal cells.

Water-soluble citrus pectin (CP), which is mainly formed by HG (~65%) and RG-I (~35%), is the most studied DF from plant food sources with respect to anticancer effects [6]. Previous studies have shown that CP exhibits no or low inhibitory effects on cancer cell

proliferation and migration unless it is modified thermally, in which case stronger effects are observed (Hao et al., 2013; Jackson et al., 2007; Leclere, Cutsem, & Michiels, 2013; Leclere et al., 2015; Platt & Raz, 1992). This thermal modification normally involves autoclaving CP at 121ºC for 30 min to 1 h (Jackson et al., 2007). Modified citrus pectin (MCP) altered through this thermal process has been demonstrated to induce apoptosis of prostate cancer cells, while the effects of CP have been minimal or absent. Lung and liver cell death have also been induced by MCP [10], as has the inhibition of colon cancer cell proliferation [11]. Other studies have found that MCP inhibits cancer cell aggregation through interaction with galectin-3, where galectin-3-mediated interactions are reduced between cells and between cells and the extracellular matrix (ECM) [14,15]. The enhanced anticancer effects of CP that has been thermally modified have mostly been attributed to a reduction in molecular size, which allows the MCP to access and bind galectin-3 [14]. This enhances the apoptotic activity (Jackson et al., 2007). While thermal modification of CP represents an inexpensive method to produce these biologically active molecules, the structural modifications and the explanation of a possible structure-function relationship still need to be elucidated. The characterization of MCP fractions will provide new insights into the relationship between the structure of MCP fragments and their effects on different cancer cells.

In the present study, thermally generated MCPs were separated into four fractions with a range of molecular size from greater than 30 kDa to less than 3 kDa. We ascertained the linkage structure of each fraction to determine the relative enrichment of HG, RG-I, and AGI. We then investigated each fraction for its anticancer properties through cell proliferation, migration and aggregation inhibitions. These different fractions have different anticancer properties, and structure- and cell-dependent effects.

Material and methods

Chemicals and reagents

Heat-inactivated fetal bovine serum (FBS), trypsin/EDTA and Dulbecco's modified Eagle's medium (DMEM) containing penicillin (100 UI/mL) and streptomycin (100 µg/mL) were from Gibco (Grand Island, NY) or Cultilab (Campinas, Brazil). Earle's Minimal Essential Medium (EMEM) was purchased from Invitrogen (Carlsbad, CA).

Vybrant DiO and DiI Cell-Labeling Solution were purchased from Thermo Scientific (Waltham, MA). Antibodies for p-Akt (sc-7985-R), p-Erk (sc-7383) and Erk 1/2 (sc - 135900) were purchased from Santa Cruz Biotechnology (Santa Cruz, CA). Antibodies for Akt (#9272), p21 (2946S), PARP (#9542), cleaved caspase-3 (#9661) and p-JNK (#9255S) were purchased from Cell Signaling Technology (Beverly, MA). Rat monoclonal anti-Gal-3 antibody was obtained from the hybridoma cell line TIB-166 of the American Type Culture Collection (ATCC, Manassas, VA). Water was collected from a Milli-Q purification system from EMD Millipore (Bedford, USA). Unless stated otherwise, remaining reagents and chemicals were purchased from Sigma-Aldrich (St. Louis, USA).

Preparation of modified citrus pectin (MCP)

Pectin from citrus peel (CP; P9561 Sigma-Aldrich; ≥ 85% esterified; ≥ 74% of GalA; dextran equivalent molecular size 184.6 ± 3.1 kDa; purity 99% - ash, starch, proteins and phenolic compounds analysis) was thermally treated to produce MCP. Briefly, CP (20 grams in 1.5 L in water, pH ~ 5.0, triplicate) was autoclaved (121 °C; 1 h) and MCP was recovered from solution after precipitation with cold ethanol (80% v/v final solution) overnight. MCP precipitate was extensively washed with 80% ethanol and washed twice with acetone. After acetone evaporation at 50 ºC, MCP was left on a desiccator for further analysis. The MCP samples (triplicate) were water-solubilized and fractionated according to different molecular size by sequential ultrafiltration using 30, 10 and 3 kDa MWCO Amicon Ultra-4 Centrifugal Filters (Millipore). Then, extracts were lyophilized resulting in four MCP fractions: (1) MCP higher than 30 kDa (MCP30); (2) MCP between 30 and 10 kDa (MCP30/10); (3) MCP between 10 and 3 kDa (MCP10/3); and (4) MCP lower than 3 kDa (MCP3).

Structural characterization

Monosaccharide analysis

MCP fractions were carboxyl-reduced with $NaBD_4$ after carbodiimide activation [16,17]. Then, alditol acetates were prepared [18] and analyzed in a gas-chromatography mass-spectrometry (GC-MS) system (Hewlett-Packard, Palo Alto, CA) equipped with a SP-2330 column (0.25 mm × 30 m; 0.20 µm; Supelco, Bellefonte, PA). After injection

(splitless mode), the oven temperature was held at 80 °C (1 min), then increased to 170 °C at 25 °C/min, and then to 240 °C at 5 °C/min with a 10 min hold at the upper temperature. Helium was used as the carrier gas (1 mL/min). The electron impact-MS was performed at 70 eV with the temperature source at 250 °C. Pairs of diagnostic fragments (m/z 187/189, 217/219 and 289/291) were used to calculate the proportion of 6,6-dideuteriogalactosyl as described previously [17]. MCP values were achieved by all MCP fractions values corrected by their total yield in percentage.

Linkage analysis

MCP fractions were per-O-methylated as described previously [18]. The same GC-MS system and column used for monosaccharide analysis were used for the analysis of partially methylated alditol acetates (PMAA). After injection (splitless mode), the oven temperature was held at 80 °C (1 min), then increased to 160 °C at 25 °C/min, to 210 °C at 2 °C/min and then to 240 °C at 5 °C/min with a 5 min hold at the upper temperature. PMAA structures were confirmed by their MS fragmentation pattern and relative retention time based on the retention time of myo-inositol (internal standard; Kim & Carpita, 1992). MCP monosaccharide percentages were based on the relative amounts of material collected in each fraction. MCP values were achieved by all MCP fractions values corrected by their total yield in percentage.

Homogeneity and average molecular size

MCP and MCP fractions were analyzed by high performance size exclusion chromatography coupled to a refractive index detector (HPSEC-RID) using a 1250 Infinity system (Agilent, Santa Clara, CA) equipped with four PL-aquagel-OH columns (60, 50, 40 and 30; 300 × 7.5 mm; Agilent) connected in tandem. The eluent was 0.2 M $NaNO_3$/0.02% NaN_3 (0.6 mL/min) and the RID temperature was set at 30 °C. Dextran equivalent average molecular size was calculated using a standard curve of dextrans (MW 5–1800 kDa). The void volume (V_o) was the elution time of the heavier molecule (blue dextran; ~1800 kDa), and the elution volume (V_e) was the release time of lighter molecule (glucose).

Determination of the degree of O-Methyl Esterification

Fourier Transform Infrared (FTIR) spectroscopy was applied to determine the degree of *O*-methyl esterification [19]. MCP and MCP fractions were analyzed using an Alpha FTIR spectrometer (Bruker Optic, Ettlingen, Germany) equipped with a deuterated triglycine sulfate (DTGS) detector and a single bounce attenuated total reflectance (ATR) accessory (diamond crystal). FTIR–ATR spectra were obtained with a resolution of 4 cm^{-1} and 50 scans. GRAMS/AI 9.1 software (Thermo Scientific) was used for spectra analysis. Methyl esterified and free uronic acids correspond to bands at 1749 cm^{-1} and 1630 cm^{-1}, respectively, and the degree of *O*-methyl esterification was calculated using a standard curve of commercially available pectin with known degrees of *O*-methyl esterification (28%, 64%, 91%) and their mixtures (14%, 46%, 78%).

Cancer cell lines

HCT116 and HT29 colon and PC3 prostate cancer cell lines were purchased from ATCC and were cultured according ATCC guidelines. Briefly, cells were cultured in DMEM containing penicillin and streptomycin with 10% FBS at 37 °C in a humidified atmosphere of 5% CO_2. Cells were passed to new culture plates by using by using trypsin/EDTA when they reached 70–90% of confluence. Before treatments, cells were added to the culture plates at the desired concentration and left overnight on the incubator. After incubation, culture media was replaced by DMEM containing MCP/MCP fractions at 0.2, 0.5 or 1.0% or lactose (galetin-3 binding sugar) or sucrose (galectin-3 non-binding sugar; osmolality control) at 10, 33 or 100 mM. Cells were continuous tested for mycoplasma contamination. Cancer cells were treated with citrus pectin at a higher concentration to evaluate a cytotoxicity effect and no differences in cell proliferation were observed compared to the control (non-treated - results not shown).

MTT assay

Cells (1×10^4 cells/well; 96-well plate) were treated or not with MCP, MCP fractions, lactose, sucrose or 0.02% Triton X-100 (cell death control) for 24, 48, 72 and 96 h. After incubation, MTT solution in DMEM (0.5 mg/mL) was added and cells were incubated for further 3 h. Then, the supernatant was removed, formazan crystals were

solubilized with DMSO and the absorbance was read at 490 nm using a Benchmark Plus Microplate Reader (Bio-Rad, Hercules, CA). Cell viability (%) was expressed in relation to the control (untreated cells).

LDH assay

The lactate dehydrogenase (LDH) was evaluated using the "Cytotoxicity Detection Kit" (Roche, Mannheim, Germany) following the manufacturer's instructions and accordingly to Prado et al. (2017).

Homotypic aggregation assay

Cells were detached from monolayer of culture plates by using 0.02% EDTA in Calcium-Magnesium free PBS (CMF-PBS) and suspended (1×10^6 cells/ mL) in CMF-PBS containing or not 20 g/mL asialofetuin and treatments. Aggregation inhibition was done accordingly to Nangia-Makker, Vitaly, & Avraham (2012) and Prado et al. (2017).

Migration assay

Migration assay was performed as previously described (Nangia-Makker et al., 2012; Prado et al., 2017). Briefly, bovine adrenal medullary endothelial cells (BAMEC) maintained in EMEM containing 10% FBS were pre-labeled with DiL (green) and incubated in one well of a 2-well culture-insert chamber (2.4×10^4 cells/well). HCT116, HT29 or PC3 cells prelabeled with DiO (red) were incubated in the other wells of the culture-insert chamber (2.4×10^4 cells/well). After 12 h, the cells were washed with PBS and the culture-insert chamber was removed. Cells were treated or not with MCP, MCP fractions or lactose for 24 h. Migration of co-cultures toward each other was observed after 24 h using a LSM 510 META LNO Laser Scanning Microscope (Carl Zeiss, Oberkochen, Germany; The Wayne State University Microscopy and Imaging Core Facility) and migration was compared to the co-culture before treatment (0 h).

Wound healing assay

Wound healing assay was performed as described previously [21]. Cancer cells were plated (2×10^5 cells/35-mm cell culture plate) and a wound was made by scratching the monolayer culture with a sterile micropipette tip. Then, cells were washed with PBS to remove floating cells and treated or not with MCP, MCP fractions or lactose for 24 h. Migration of cells towards gap closing was observed after 24 h using an inverted microscope (Carl Zeiss) and compared to the wound before treatment (0 h).

Extracellular matrix proteins (ECM) assay

ECM interaction was performed according to Nangia-Makker et al. (2012). Firstly, 96-well plates were coated with serially diluted laminin from mouse Engelbreth-Holm-Swarm (EHS) sarcoma, collagen type IV or fibronectin (10 - 0 µg) and incubated for 1 h at 37 °C. Then cell culture plates were blocked with 1% bovine serum albumin (BSA) and washed with PBS. Then, cancer cells were transferred and incubated (4.0×10^4 cells/well) in the plates containing the ECM for 16 h. Then, plates were washed to remove non-adherent cells and fluorescence levels obtained after incubation with Alamar blue (3 h) was used to define the concentration of each ECM that retained the highest number of cancer cells. After define the best concentration of each ECM (1 µg EHS laminin, 0.5 µg collagen IV and 2.5 µg fibronectin), the same experiment described above was done, but using media containing or not MCP, MCP fractions or lactose. Cells treated or not with MCP, MCP fractions or lactose were also incubated in non-coated plates (positive control) and 0.1% BSA-coated plates (negative control).

Apoptosis assay

Apoptosis was evaluated by flow cytometry using PE Annexin V Apoptosis Detection Kit I (BD Biosciences, San Diego, CA) according to the manufacturer's instructions. Briefly, cells (2.0×10^5 cells/well; 24-well plate) were treated or not with MCP, MCP fractions or lactose for 24 h. After incubation, cells were washed with 2% BSA in PBS and suspended in the Binding Buffer (1.0×10^6 cells /mL). Then, cell suspension (100 µL) was incubated with FITC Annexin V and 7AAD for 15 min protected from light. Finally, analysis was performed using a FACSVerse flow cytometer (BD Biosciences, San

Diego, CA). Controls of unstained cells and staining only with FITC Annexin V or 7AAD were used. Data analysis was performed with FlowJo software (BD Biosciences).

Western blot

Cells (5.0×10^5 cells/well; 6-well plate) were treated or not with MCP, MCP fractions or lactose and incubated for 24 h. Then, cells were washed with PBS and lysed with RIPA buffer (50 mM Tris-HCl pH 7.4, 1% NP-40, 0.5% Na-deoxycholate, 0.1% SDS, 150 mM NaCl, 2 mM EDTA, 50 mM NaF and 0.2 mM Na_3VO_4) containing protease and phosphate inhibitors (Roche). Proteins were quantified using the Pierce BCA Protein Assay Kit (Thermo Scientific). Protein separation, transfer and detection were performed accordingly to Prado et al (2017).

Hemagglutination assay inhibition with galectin-3

Recombinant galectin-3 was produced as described Nangia-Makker et al. (2012). The inhibition of hemagglutination was done as described previously [22,23]. Briefly, erythrocyte was isolated from rabbit blood and a final suspension of 4% was used in experiment. In each well of a V plate was add 50 µL of 1% BSA, 50 µL of PBS 1× or the sample diluted in PBS 1× and/or 10 µg/mL galectin-3, and 25 µL of rabbit erythrocyte. After, the plate was incubated on room temperature for 90 min.

Statistical analysis

The results were expressed as the mean ± standard deviation (SD) and the images were representative of at least three independent experiments, except for WB analysis, which were performed in duplicate. Data were analyzed using GraphPad Prism 6.0 software (GraphPad Software, San Diego, CA). One-way ANOVA with Tukey's (to assess differences between all groups) or Dunnett's (to assess differences between the control and two or more groups) were used as post hoc tests, and Least Significant Difference (LSD) was used to compare means at 0.0001. Significance was set at $p < 0.05$.

Results and Discussion

Thermal modification leads to structural differences among MCP fractions

The yield of MCP fractions was based on the total MCP that was separated. The MCP30 fraction was the most abundant (68 ± 1% w/w), followed by MCP 30/10 (15 ± 1% w/w), MCP10/3 (10 ± 0% w/w), and MCP3 (7 ± 0% w/w). HPSEC-RID confirmed sequential ultrafiltration of the separated MCP fractions according to their molecular size (**Table 1**). The dextran equivalent average molecular sizes were calculated using three replicates of MCP30, MCP30/10, MCP10/3 and MCP3 fractions and the results of the main peaks were 35.2 kDa, 27.5 kDa, 10.2 kDa, and 5.1 kDa, respectively (**Table 1**). We also calculated the maximum and minimum values at half height for each analysis (**Supplemental Figure S1**).

Monosaccharide analysis showed that galacturonic acid GalA was the most abundant monosaccharide in all the MCP fractions, followed by galactose (Gal; **Table 1**). Among the MCP fractions, MCP10/3 had the highest level of Gal and the lowest level of GalA. Degrees of esterification were similar for fractions of larger molecular size, ranging from 79 - 85%, whereas degree of esterification was 54% in MCP3 (**Table 1**)**.** Linkage analysis showed that the most prevalent form of GalA in all the fractions was *4*-GalA (**Figure 1; Supplemental Table S1**), indicating that all MCP was mostly HG. The presence of a small amount of *3,4*-GalA and the corresponding *t*-Xyl residues demonstrated that XGA was also part of the HG fraction. Smaller amounts of *2*-Rha, *2,4*-Rha and an equal amount of *4*-GalA indicated the presence of RG-I. The *4*-Gal and *3,4*-Gal, and a corresponding amount of *t*-Ara*f* equal to the branch points were taken as evidence for the presence of AGI. Similar results between the monosaccharide composition and linkage patterns of MCP, MCP30 and MCP30/10 were found. Notably, MCP10/3 and MCP3 showed a strong decrease in GalA : *t*-GalA, consistent with a decreased molecular size (**Supplemental Table S2**). MCP10/3 had higher proportions of *4*-Gal, *3,4*-Gal, and the corresponding *t*-Araf, as well as enrichment of Gal, indicating higher amounts of AGI compared to the other MCP fractions. When some linkages were gathered into the probable polysaccharide structures, HG (*4*-GalA and *t*-GalA) fragments become the dominant ones with a decrease in MCP10/3 due to AGI increase (*4*-Gal, *3,4*-Gal, *4,6*-Gal and *t*-Ara*f*). Minor changes between MCP fractions were observed for: RG-I (*2*-Rha, *2,4*-Rha, *3,4*-GalA and *4*-GalA), type II arabinogalactan (AGII - *3*-Gal, *6*-Gal, *2*-Ara, *3,6*-Gal, *3,4,6*-Gal, *t*-Rha, *t*-Ara), heteroxylan (e.g. glucuronoarabinoxylan; *4*-Xyl, *2,4*-Xyl, *3,4*-Xyl, *2,3,4*-Xyl, *t*-GlcA, *t*-Ara), heteromannan (e.g. glucomannan; *4*-Man, *4,6*-Man, *4*-Glc, *4,6*-Glc, *t*-Gal), arabinan (*5*-Ara, *2,5*-Ara, *3,5*-Ara, *t*-Ara) and xyloglucan (*4,6*-Glc, *4*-Glc, *2*-Xyl, *2*-Gal, *t*-

Fuc, *t*-Xyl). Others partially methylated alditol acetate residues did not change between MCP fractions (*t*-Ara*p*, *3*-Araf, Ara(OAc)5, Xyl(OAc)5, Man(OAc)6, *2,4*-Gal, *2,4,6*-Gal, Gal(OAc)6, *4,6*-GalA, *2,4*-GalA, *3,4*-Glc, Glc(OAc)6) [24].

MCP, MCP30 and MCP30/10 are mainly composed of highly esterified HG and similar proportions of RG-I and AGI. The MCP10/3 fraction was also characterized by highly esterified HG, but with higher quantities of AGI, while MCP3 had fewer branched structures (RG-I and AGI) with lesser degree of esterification and a smaller molecular size. The characteristics of smaller but high-methylated MCP10/3 fraction and the smaller but low-methylated MCP3 fraction may result in differences in biological effects [25]. MCP10/3 fraction possesses promising biologically active structures since methylated structures, the HG:RG-I ratio and the higher AGI quantity are requisites in enhancing the anticancer effects [26].

Table 1. Molecular size, degree of esterification (DE) and monosaccharide composition of MCP and MCP fractions.

			Monosaccharide composition (g/100 g)*								
	Molecular size[†]	**DE**[‡]	**Rha**	**Fuc**	**Ara**	**Xyl**	**Man**	**Gal**	**GalA**	**Glc**	**GlcA**
MCP	22.2	79.8 ± 4.3	3.1 ± 0.2	0.1 ± 0.0	2.5 ± 0.6	1.5 ± 0.4	0.9 ± 0.2	11.5 ± 1.4	75.8 ± 2.5	1.5 ± 0.4	3.1 ± 0.2
MCP30	35.2	84.2 ± 4.8	3.5 ± 0.2	0.1 ± 0.1	3.2 ± 0.8	1.9 ± 0.5	0.9 ± 0.2	10.8 ± 0.9	74.7 ± 2.5	1.7 ± 0.5	3.2 ± 0.3
MCP30/10	27.5	85.0 ± 5.6	2.7 ± 0.0	0.0 ± 0.0	1.1 ± 0.0	0.5 ± 0.0	0.5 ± 0.0	11.2 ± 0.0	80.0 ± 0.2	1.6 ± 0.2	2.4 ± 0.1
MCP10/3	10.2	78.9 ± 2.1	2.0 ± 0.0	0.0 ± 0.0	0.9 ± 0.1	1.1 ± 0.1	1.4 ± 0.1	20.7 ± 7.8	69.7 ± 7.3	0.7 ± 0.2	3.5 ± 0.4
MCP3	5.1	53.7 ± 6.0	1.7 ± 0.0	0.1 ± 0.0	0.8 ± 0.0	0.6 ± 0.3	1.2 ± 0.1	5.5 ± 0.1	86.0 ± 0.1	1.0 ± 0.2	3.2 ± 0.0

* Results represents mean ± SD ($n \geq 7$).

[†] Molecular size is dextran equivalent. The maximum and minimum values at half height for each analysis are represented in Figure S1.

[‡] DE: degree of esterification. DE values were calculated using the calibration curve ($R^2 = 0.9798$) and results are expressed in mean ± SD (n=3). GlcA: glucuronic acid; Glc: glucose; GalA: galacturonic acid; Gal: galactose; Man: mannose; Xyl: xylose; Ara: arabinose; Fuc: fucose; Rha: rhamnose. MCP: modified citrus pectin.

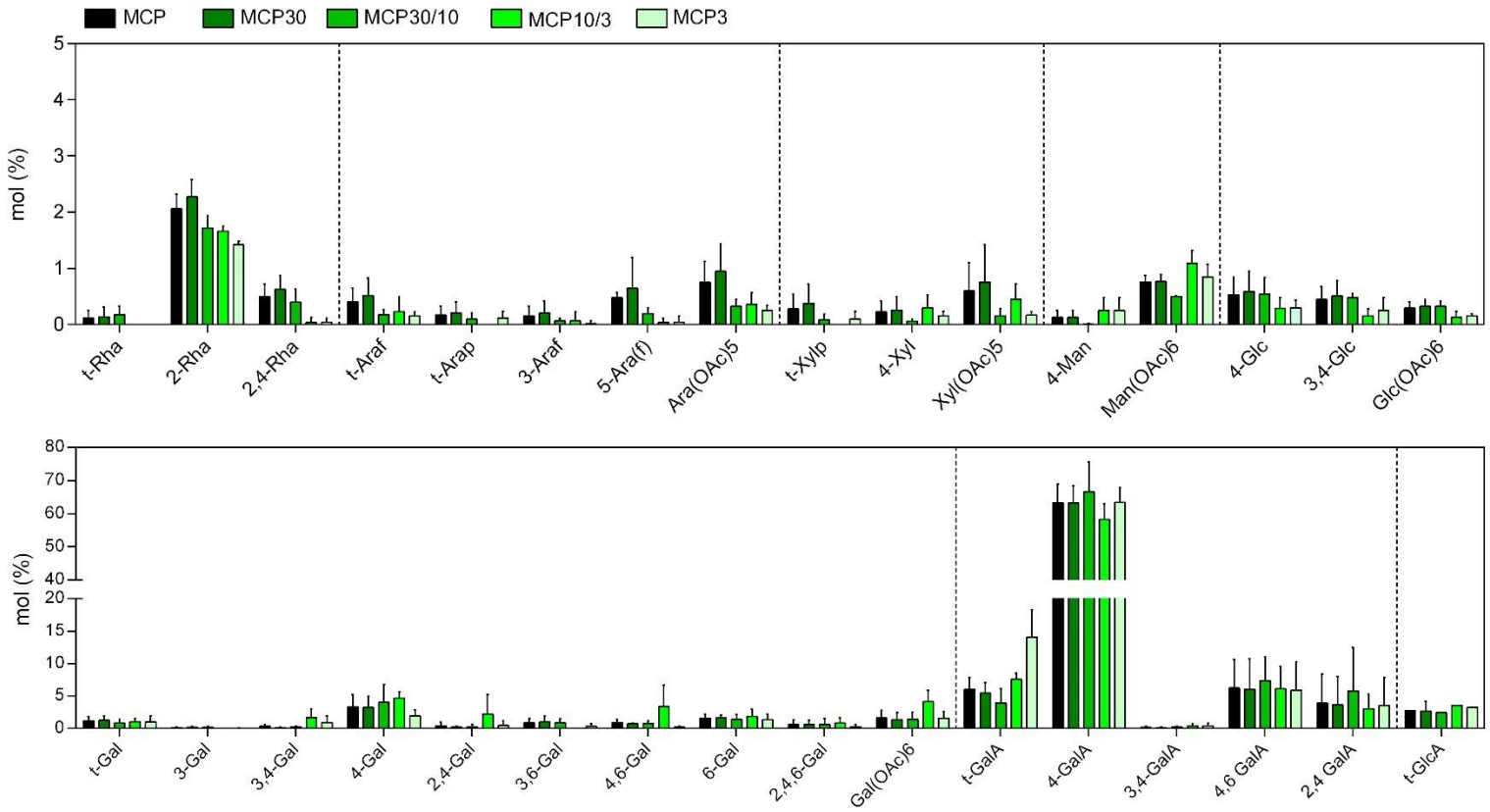

Figure 1. Linkage analysis of MCP and MCP fractions. The table of linkage results is presented in Supplemental Table 1. Rhamnose (Rha); fucose (Fuc); arabinose (Ara); xylose (Xyl); mannose (Man); galactose (Gal); Galacturonic acid (GalA); glucose (Glc); glucuronic acid (GlcA); terminal (t); pyranose (p); furanose (f). MCP: modified citrus pectin.

MCP fractions differentially regulate cancer cells proliferation, migration, and aggregation

Three cell lines were used to observe how different cancer cell mutations responded to treatment with MCP fractions with respect to necrosis, necroptosis, apoptosis, viability, and cytotoxicity. HCT116 and HT29 are colon cancer cell lines, while PC3 is a prostate cancer cell line. Initial screening was made to investigate the effects of MCP and MCP fractions on cell viability using sucrose, lactose and CP as controls (**Supplemental Figure S2**). Viability was measured by 3-(4,5-Dimethyl-2-thiazolyl)-2,5-diphenyl-2H-tetrazolium bromide (MTT) and sucrose and lactose were used as a control of galectin-3 non-binding and galectin-3 binding carbohydrates, respectively [27]. The screening for a loss in cancer cell viability (compared with a control without treatment) showed that after a 24 h-incubation with sucrose and lactose at 100 mM, a loss of cancer cell viability was observed (**Supplemental Figure S2**). No loss in cell viability was seen with a treatment of CP. Lactose at 100 mM is widely used for galectin-3 inhibition since it is non-cytotoxic [28,29]. In the same manner as the simpler carbohydrates, cells treated with MCP and MCP fractions at 1.0% also exhibited reduced cell viability (**Figure 2**).

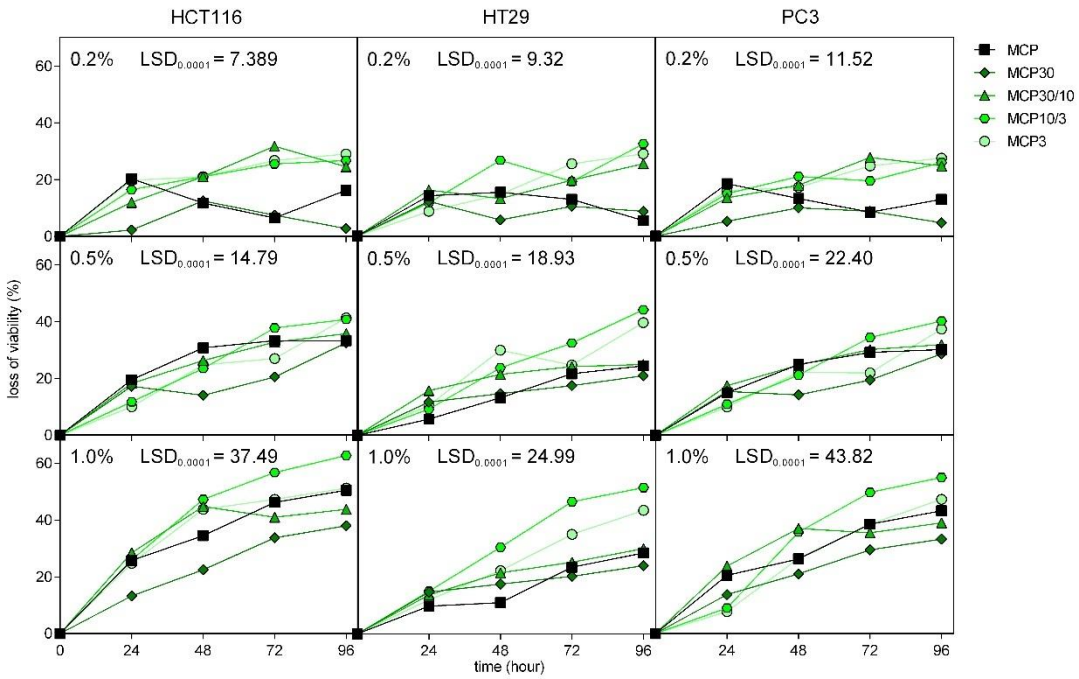

Figure 2. Cell viability loss after MCP and MCP fractions treatment. The loss of viability was calculated based on control (without treatment) as 100%. Cells were treated with MCP and MCP fractions at different concentrations (0.2%, 0.5% and 1%) and the higher concentrations and the lower fractions precluded cells growth. Data were shown as mean values. One-way ANOVA with the Least Significant Difference (LSD) test was used to compare means at 0.0001. Significant mean values are those with differences larger than the LSD value showed in each graphic. The results were from three independent experiments, with each performed in triplicate. The complete data are presented in Table S3.

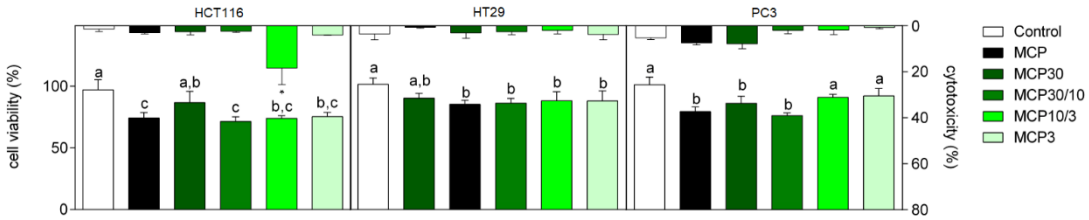

Figure 3. Cell viability by MTT assay (left x axis) and cells cytotoxicity after 24 h of treatment by LDH assay (right x axis). Effects on cell viability of the higher

concentration of MCP and MCP fractions (1%) at t=24 h are shown on lower graphic. Data are shown as mean ± SD. Tukey's test (*$p < 0.05$) was performed. Different letters represent significant differences between the treatments. Cytotoxicity by LDH assay after 24 h of incubation is shown in upper graphic. Data are expressed as percentage of cell viability compared to control (no treatment) of each time. Results are represented as mean ± SD of three independent experiments, with each performed in triplicate. *$p < 0.05$ vs control, according to Dunnetts's test.

Thus, for comparison experiments, a 24 h-incubation period was used with 1.0% MCP and MCP fractions and 100 mM of lactose and sucrose. To determine if the reduction in cell viability was a result of cytotoxicity, the lactate dehydrogenase (LDH) assay was performed. Results showed that a significant cytotoxicity was observed only for HCT116 cells after treatment with MCP10/3 (**Figure 3**), highlighting that MCP fractions may have distinct effects in different cancer cells with respect to cell death, but these mechanisms need to be further investigated.

Annexin V is a protein that binds to the negative heads of phosphatidylserine in the external monolayer of the membrane. When this protein is conjugated with a fluorochrome, the cellular fraction that increases the translocation of negative phospholipids to the outer monolayer of the membrane can be determined. The fluorescent DNA marker 7-AAD intercalates within DNA, and it requires a prior permeabilization of the plasma membrane. The translocation of phospholipids in the outer monolayer of the membrane is considered an early event in the triggering of cell death by apoptosis (quadrant Q1). The permeabilization of the membrane only occurs during necrotic processes (quadrant Q3), and when both events happen it could be indicative of late apoptosis/necroptosis (quadrant Q2). The MCP30/10 and MCP10/3 fractions induced necrosis (Q1) and necroptosis (Q2) in HCT116 and PC3 cells but not in HT29 cells (**Figure 4; Supplemental Figure S3**). It has been suggested that MCP30/10 and MCP10/3 have the same esterification degree and the lowest molecular size of the other fractions except for MCP3.

These chemical and structural differences could explain why MCP30/10 and MCP10/3 increased necroptosis in HCT116 cells while MCP3 did not, since the higher the degree of esterification the better the programmed cell death activation on cancer cells (Jackson et al., 2007).

Because the size and number of cancer cell aggregates have been found to correlate with cell survival [30] and because cancer cells that form aggregates in suspension cultures have been found to exhibit significantly lower levels of death than single cells [31], MCP and MCP fractions were evaluated for the inhibition of cancer cell aggregation. In the aggregation assay, asialofetuin was used to induce cell aggregation, and lactose, which inhibits lectins-dependent aggregation, was used as a positive control. The inhibition of aggregation induced by MCP3 was similar to lactose in all three cell lines (**Figure 5**). Similar effects compared to lactose were also found for MCP30/10 and MCP10/3 in HT29 cells (**Supplemental Figure S4**).

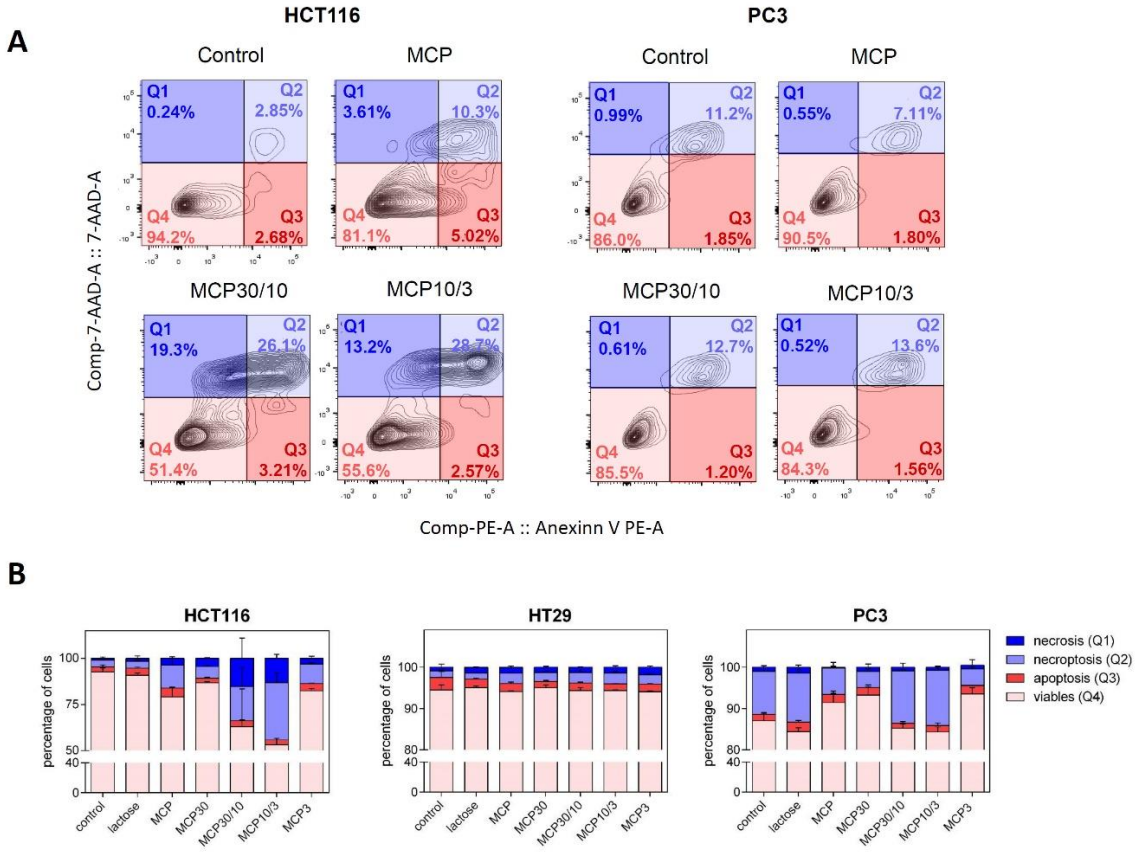

Figure 4. Effects of MCP and MCP fractions in HCT116, HT29 and PC3 apoptosis by flow cytometry. Cancer cells were induced to late apoptosis/necroptosis after MCP and MCP fractions treatment for 24 h. **A)** Q1: necrosis quadrant; Q2: necroptosis quadrant; Q3: apoptopsis quadrant; Q4: viable cells quadrant. The most significant differences in graphics are shown in the figure (HCT116 and PC3 cells treatment). **B)** The results were expressed in percentage of cells in comparison with control (no treatment). Results were represented as mean ± SD of two independent experiments, with each performed in triplicate.

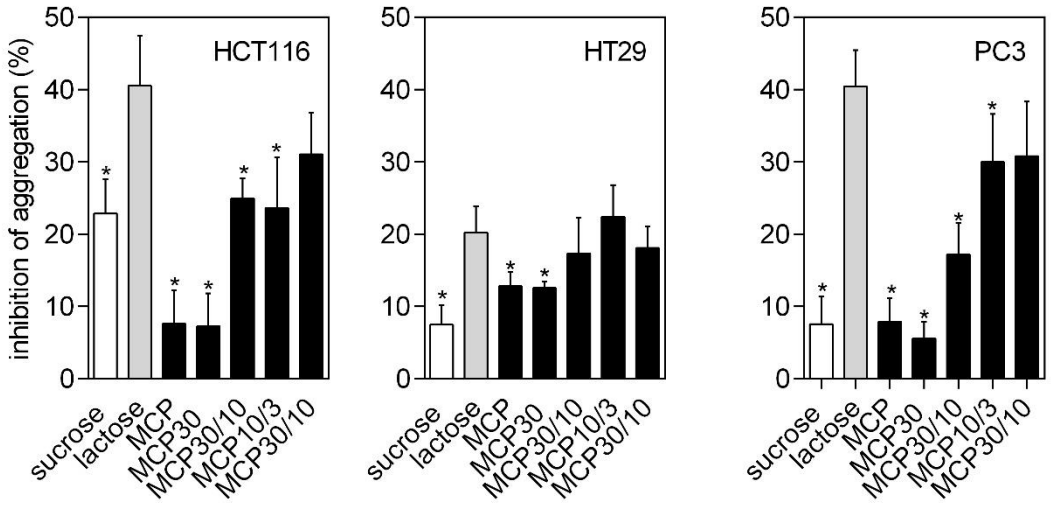

Figure 5. Inhibition of homotypic cell aggregation. Data are shown as mean ± SD and the results were expressed in percentage of cells relative to control (with asialofetuin and no treatment). *$p < 0.05$ vs lactose, according to Dunnett's test.

Cell migration and attachment to the ECM are crucial steps to cancer development and metastasis. Thus, the effects of MCP and MCP fractions on cancer cell migration towards endothelial cells and cell attachment to proteins of the ECM were evaluated by migration assay. MCP3 strongly inhibited cancer cell migration in all three cell lines, but the effects were strongest for HCT116 cells (**Figure 6**). MCP30/10 and MCP10/3 also strongly inhibited migration of HCT116 cells, but MCP and MCP30 did not. The inhibitory effects of MCP3 as well as the absence of effects for both MCP and MCP30 on cancer cell migration were confirmed by the wound healing assay (**Supplemental Figure S5**).

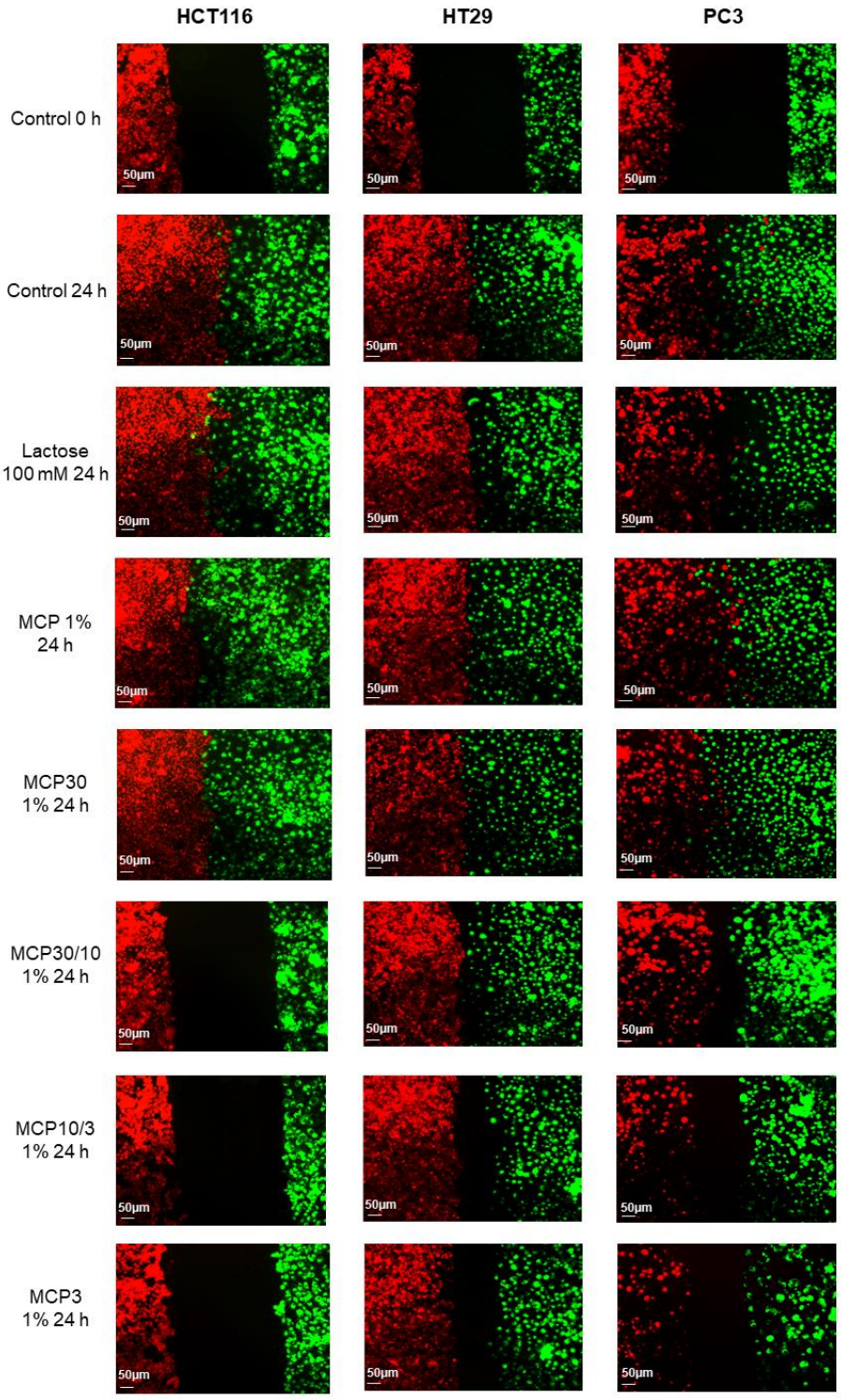

Figure 6. Migration assay using endothelial cells (BAMEC) dyed with DiO (green) and cancer cells dyed with DiI (red). Lower molecular size fractions from MCP had lessen the interaction between cancer cells and BAMEC. Scale bar: 50 µm.

MCP3 gap closing was 27.5 ± 0.3% compared to 63.5 ± 0.7% for the control for HCT116, 14.5 ± 0.3% compared to 22.6 ± 1.3% for the control for HT29, and 51.6 ± 4.2% compared to 77.4 ± 3.8% for the control (**Supplemental Figure S5**).

The ECM-protein assay evaluated the effects of MCP and MCP fractions on inhibiting the interactions between cancer cells and several target ECM proteins (laminin, collagen IV, and fibronectin). Polysaccharides that are chemically similar to some glycoproteins could interfere with cancer cell adhesion to ECM proteins and the inhibition of galectin-3. ECM proteins, such as laminin, collagen IV, and fibronectin are required for cancer cell growth and invasion as previously shown [32]. As lactose inhibits lectin-dependent interaction between cells and ECM proteins, it was used as a positive control. MCP10/3 and MCP3 reduced HCT116, HT29, and PC3 cell density in laminin-coated plates, reduced HCT116 cell density in collagen IV-coated plates, and also reduced HT29 cell density in fibronectin-coated plates (**Figure 7**). In contrast, MCP30/10 only reduced HT29 and HCT116 cell density in laminin-coated plates, whereas MCP30 had a similar effect to that of lactose only in PC3 cell density in laminin-coated plates. The interference of MCP fractions on the adhesion of cancer cells to ECM proteins may be representative of a positive effect against cancer cell spread and metastasis, opening new avenues for the identification of bioactive carbohydrates derived from fruit.

The effects of MCP and MCP fractions on the protein levels normally associated with cancer cell death, survival, and migration were evaluated to yield clues on the biochemical mechanisms of why cancer cells are affected by these treatments. While pAKT (phosphorylated protein kinase B) is normally related to cell survival [33], higher concentrations cause excessive cell stress leading to necroptosis [34,35]. Increased pERK levels are normally linked to cell migration and survival [36–38], but pERK up-regulation can also induce cell necrosis by necroptosis or autophagy [39]. Protein p21 can cause cell cycle arrest and cell death [40], and PARP has a role in DNA repair and promotion of cell survival [41]. Caspase-3 plays an important role in apoptosis [42], and pJNK can be involved in cancer cell growth, survival, and metastasis [43]. Immuno-gel blot analysis demonstrated that the MCP and MCP fractions differentially regulated the expression of these proteins in cancer cells (**Figure 8; Supplemental Figure S6**). MCP and MCP30 reduced pAKT levels in HCT116, HT29, and PC3 cells; however, only MCP increased pERK1/2 and p21 levels in HCT116 and PC3 cells, respectively. MCP30/10 increased

pAKT and p21 levels in HCT116 and PC3 cells, whereas MCP10/3 increased only p21 levels, but not those of pAKT. The MCP3 fraction had differential effects on protein levels in HCT116, HT29, and PC3 cell lines; this fraction increased p21 levels and induced caspase-3 expression in HCT116 cells, but reduced pERK levels in HT29 cells. MCP3 enhanced p21 expression and reduced pJNK levels in HT29 and PC3 cells, but PARP and Galectin-3 levels did not change throughout the treatments.

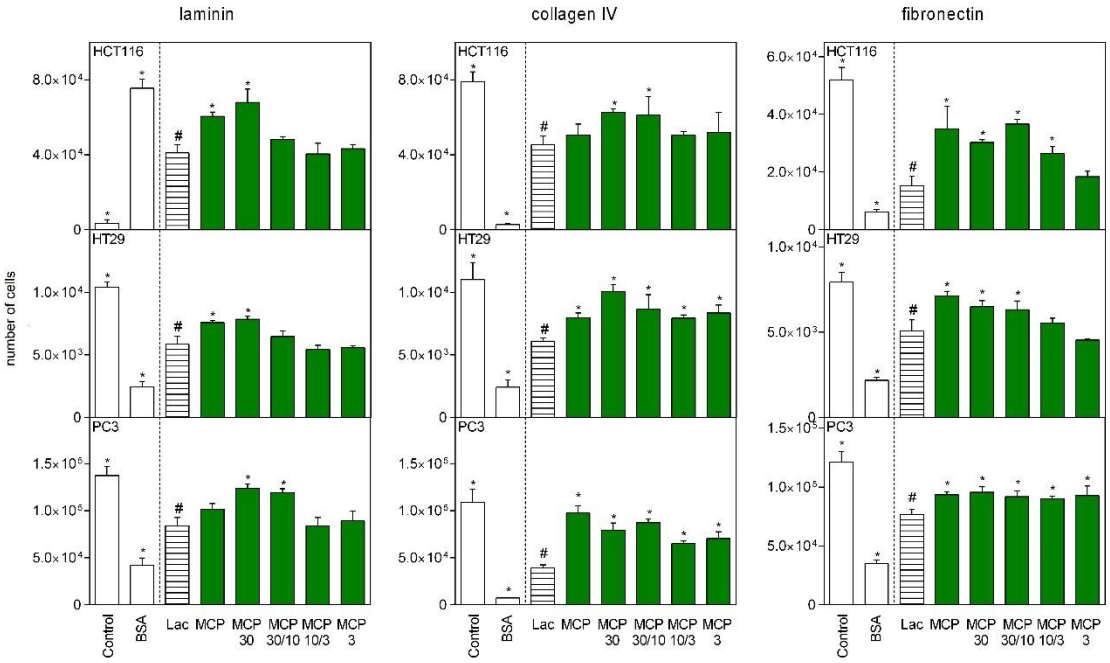

Figure 7. MCP and MCP fractions interaction with extracellular matrix proteins (laminin, collagen IV and fibronectin) and cancer cells lines. Data are shown as mean ± SD. All treatments are significant different from control (Dunnett's test). All samples are compared with lactose (#) by Dunnett's test and significant differences ($p < 0.05$) are marked with an asterisk.

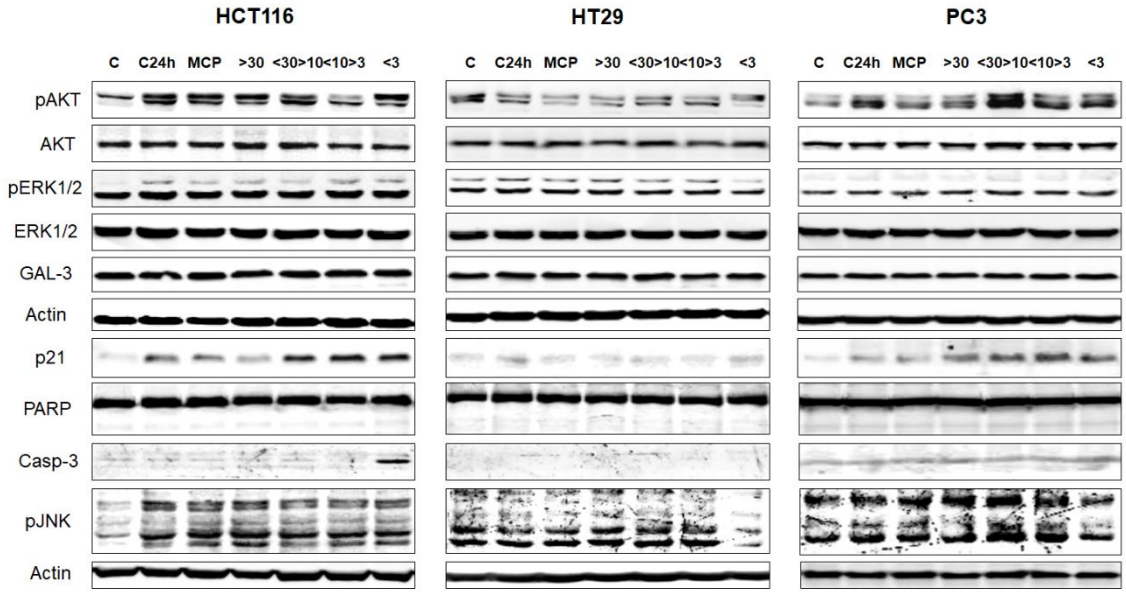

Figure 8. Western blotting analysis. Cell lysates were prepared and processed for immunogel blot assay after 24 h of treatment. After BCA assay, equal amounts of proteins were separated using SDS-PAGE. β-Actin was used as the loading control.

It seems that higher AGI levels and lower RG-I levels are required to activate p21, as MCP30/10, MCP10/3, and MCP3 treatments increased this protein level in HCT116, with an activation of p21 being related to cell cycle arrest that induces cell death [40]. Apoptosis in MCP3 treatment in HCT116 could be triggered by caspase-3 activation, but the higher levels of p21 and the lowest quantity of dead cells when compared to MCP30/10 and MCP10/3 are indicators that other biochemical pathways that lead to cell death might have been activated or repressed. MCP10/3 promoted the reduction of pAKT levels in HCT116, and since increased levels of pAKT are normally related to cell survival [33], this could explain the reduction in cell proliferation and the inhibitory effects on cell migration that were observed. On the other hand, the MCP30/10 induced pAKT expression in PC3 cells could have led to the observed cell proliferation reduction and cell migration inhibition. This could be due to the higher HG fractions in MCP30/10. Since MCP30/10 has the lesser amount of *t*-GalA of all the fractions, it is possible to speculate that HG is important for pAKT expression and/or AKT phosphorylation and could cause an excessive stress to cells leading to necroptosis [34,44]. Our results demonstrate that the smaller MCP fractions (MCP30/10, MCP10/3, and MCP3) were more effective in reducing cancer cell proliferation, migration, and adhesion to ECM proteins. All MCP fractions showed some biological effects in at least one of the three cell lines tested. Thus, the underlying

mechanisms of MCP fractions in cancer cells seem to be both structure- and cell line-dependent. The three cell lines used have different characteristics. HT29 is a colon adenocarcinoma cell line, while HCT116 is a colon carcinoma cell line. HT29 cells are differentiated, while HCT116 cells are poorly differentiated and highly metastatic. And PC3 is a highly metastatic adenocarcinoma cell line [45,46].

Galectin-3 inhibition is dependent on MCP structure rather than molecular size

Galectin-3 is a member of the carbohydrate-binding protein family that exhibits an affinity for β-galactoside sugars in a conserved sequence of the carbohydrate-binding site [27]. The overexpression of galectin-3 might induce cancer cells to become more aggressive by increasing their proliferation and metastasis [47]. Therefore, the interaction of pectin fractions with galectin-3 could prevent this increased activity in cancer cells. Because at least part of the anticancer effects of MCP were related to the inhibition of galectin-3, the hemagglutination assay was performed to evaluate the possible interaction between MCP fractions and galectin-3. High concentrations of CP (negative control) did not inhibit galectin-3-mediated hemagglutination (**Supplemental Figure S7**). In contrast, MCP and MCP30 inhibited galectin-3-mediated hemagglutination at 400 µg/mL. Notably, MCP30/10 did not inhibit galectin-3-mediated hemagglutination even at higher concentrations (500 µg/mL), and MCP10/3 and MCP3 had inhibitory effects at lower concentrations (300 µg/mL). As all fractions possessed high amounts of GalA, the greater activity of the smaller fractions in binding to galectin-3 may explain why the minimum inhibitory concentration was much higher than that of lactose. Gao et al. (2012) fractioned a chemically MCP and demonstrated that neutral fractions showed less galectin-3 binding than did acidic fractions. In our study, thermally MCP fractionated by size showed different galectin-3 binding powers, with the smaller sizes resulting in more inhibition, probably enhancing the observed anticancer activity due to a better penetration in cancer cells because of their smaller molecular sizes.

A concern about thermally modified pectin is the production of cytotoxic molecules and β-elimination with a consequent production of unsaturated sugar residues [49,50]. Using the same HPLC-UV protocol described in Leclere et al. (2016), we did not find any cyclic compounds in our thermally MCP or in the fractionated samples (data not shown). One explanation for not detecting the low molecular size compounds produced by Maillard

reactions, differing from the results of Leclere et al., (2016), is that we precipitated our pectin with ethanol and exhaustively washed the precipitate with 80% ethanol and with acetone. This protocol might have removed any cytotoxic compounds. Moreover, the measurement of UV absorbance (from 210 nm to 260 nm) did not reveal any conjugated dienes produced by β-elimination, possibly because the pH had not been adjusted to 7.0 prior to the heat treatment. Another consequence of β-elimination would be a reduced esterification of the HG backbone, which was not observed in our samples despite the smaller one (with low quantity also). Therefore, the effects observed in our study did not seem to be related to the cytotoxic molecules reported elsewhere [49].

Conclusions

This study demonstrates that treatment with MCP fractions that are fractionated by molecular size results in diverse effects on cancer cell proliferation, migration, and aggregation. These effects were size-, structure-, and cell line-dependent. Beside the smaller sizes, the enrichment of AGI in MCP10/3 and MCP3 with fewer branched structures (RG-I and AGI) and more de-esterified HG oligomers enhances anticancer effects by inhibiting cancer cell migration, aggregation, and proliferation. Furthermore, MCP fractions differentially interact with ECM proteins and galectin-3. Thus, MCP fractionation is an important tool to define possible structure-function relationships. Furthermore, we predict that MCP fractionation will be useful in the development of functional MCP-derived products and food supplements.

References

[1] A.R. Vieira, L. Abar, D.S.M. Chan, S. Vingeliene, E. Polemiti, C. Stevens, D. Greenwood, T. Norat, Foods and beverages and colorectal cancer risk: A systematic review and meta-analysis of cohort studies, an update of the evidence of the WCRF-AICR Continuous Update Project, Ann. Oncol. 28 (2017) 1788–1802. doi:10.1093/annonc/mdx171.

[2] S.J.D. O'Keefe, Diet, microorganisms and their metabolites, and colon cancer, Nat. Rev. Gastroenterol. Hepatol. 13 (2016) 691–706. doi:10.1038/nrgastro.2016.165.

[3] V. Tremaroli, F. Bäckhed, Functional interactions between the gut microbiota and host metabolism, Nature. 489 (2012) 242–9. doi:10.1038/nature11552.

[4] P. Louis, G.L. Hold, H.J. Flint, The gut microbiota, bacterial metabolites and colorectal cancer, Nat. Rev. Microbiol. 12 (2014) 661–672. doi:10.1038/nrmicro3344.

[5] D. Mohnen, Pectin structure and biosynthesis, Curr. Opin. Plant Biol. 11 (2008) 266–277. doi:10.1016/j.pbi.2008.03.006.

[6] E.G. Maxwell, N.J. Belshaw, K.W. Waldron, V.J. Morris, Pectin – An emerging new bioactive food polysaccharide, Trends Food Sci. Technol. 24 (2012) 64–73. doi:10.1016/j.tifs.2011.11.002.

[7] F. Naqash, F.A. Masoodi, S. Ahmad Rather, S.M. Wani, A. Gani, Emerging concepts in the nutraceutical and functional properties of pectin - a review., Carbohydr. Polym. 168 (2017) 227–239. doi:10.1016/j.carbpol.2017.03.058.

[8] C.L. Jackson, T.M. Dreaden, K. Theobald, N.M. Tran, T.L. Beal, M. Eid, M.Y. Gao, R.B. Shirley, T. Stoffel, M.V. Kumar, D. Mohnen, L.K. Theobald, N.M. Tran, T.L. Beal, M. Eid, M.Y. Gao, R.B. Shirley, M.T. Stoffel, M.V. Kumar, D. Mohnen, K. Theobald, T. Stoffel, Pectin induces apoptosis in human prostate cancer cells: correlation of apoptotic function with pectin structure, Glycobiology. 17 (2007) 805–19. doi:10.1093/glycob/cwm054.

[9] L. Leclere, P. Van Cutsem, C. Michiels, Anti-cancer activities of pH- or heat-modified pectin, Front. Pharmacol. 4 (2013) 128. doi:10.3389/fphar.2013.00128.

[10] L. Leclere, M. Fransolet, F. Cote, P. Cambier, T. Arnould, P. Van Cutsem, C. Michiels, Heat-Modified Citrus Pectin Induces Apoptosis-Like Cell Death and Autophagy in HepG2 and A549 Cancer Cells, PLoS One. 10 (2015) e0115831. doi:10.1371/journal.pone.0115831.

[11] M. Hao, X. Yuan, H. Cheng, H. Xue, T. Zhang, Y. Zhou, G. Tai, Comparative

studies on the anti-tumor activities of high temperature- and pH-modified citrus pectins., Food Funct. 4 (2013) 960–71. doi:10.1039/c3fo30350k.

[12] D. Platt, A. Raz, Modulation of the lung colonization of b16-f1 melanoma cells by citrus pectin, J. Natl. Cancer Inst. 84 (1992) 438–442.

[13] C.L. Jackson, T.M. Dreaden, L.K. Theobald, N.M. Tran, T.L. Beal, M. Eid, M.Y. Gao, R.B. Shirley, M.T. Stoffel, M.V. Kumar, D. Mohnen, Pectin induces apoptosis in human prostate cancer cells: correlation of apoptotic function with pectin structure., Glycobiology. 17 (2007) 805–19. doi:10.1093/glycob/cwm054.

[14] V.J. Morris, N.J. Belshaw, K.W. Waldron, E.G. Maxwell, The bioactivity of modified pectin fragments, Bioact. Carbohydrates Diet. Fibre. 1 (2013) 21–37. doi:10.1016/j.bcdf.2013.02.001.

[15] V. V. Glinsky, A. Raz, Modified citrus pectin anti-metastatic properties: one bullet, multiple targets, Carbohydr. Res. 344 (2009) 1788–1791. doi:10.1016/j.carres.2008.08.038.

[16] N.C. Carpita, M.C. McCann, Some new methods to study plant polyuronic acids and their esters, in: R. Townsend, A. Hotchkiss (Eds.), Prog. Glycobiol., New York, NY: Marcel Dekker., 1996: pp. 595–661.

[17] J.B. Kim, N.C. Carpita, Changes in Esterification of the Uronic Acid Groups of Cell Wall Polysaccharides during Elongation of Maize Coleoptiles, Plant Physiol. 98 (1992) 646–653. doi:10.1104/pp.98.2.646.

[18] D.M. Gibeaut, N.C. Carpita, Clean-up procedure for partially methylated alditol acetate derivatives of polysaccharides, J. Chromatogr. 587 (1991) 284–287. doi:0021-9673/91.

[19] G.D. Manrique, F.M. Lajolo, FT-IR spectroscopy as a tool for measuring degree of methyl esterification in pectins isolated from ripening papaya fruit, Postharvest Biol. Technol. 25 (2002) 99–107. doi:10.1016/S0925-5214(01)00160-0.

[20] P. Nangia-Makker, B. Vitaly, R. Avraham, Galectin-3-Binding and Metastasis, Methods Mol. Biol. 878 (2012) 241–250. doi:10.1007/978-1-61779-854-2.

[21] G. Moreno-Bueno, H. Peinado, P. Molina, D. Olmeda, E. Cubillo, V. Santos, J. Palacios, F. Portillo, A. Cano, The morphological and molecular features of the epithelial-to-mesenchymal transition, Nat. Protoc. 4 (2009) 1591–1613. doi:10.1038/nprot.2009.152.

[22] T.P. Nowak, P.L. Haywood, S.H. Barondes, Developmentally regulated lectin in embryonic chick muscle and a myogenic cell line, Biochem. Biophys. Res.

Commun. 68 (1976) 650–657.

[23] J. Ochieng, D. Platt, L. Tait, V. Hogan, T. Raz, P. Carmi, a Raz, Structure-function relationship of a recombinant human galactoside-binding protein., Biochemistry. 32 (1993) 4455–60. http://www.ncbi.nlm.nih.gov/pubmed/8476870.

[24] F. a Pettolino, C. Walsh, G.B. Fincher, A. Bacic, Determining the polysaccharide composition of plant cell walls, Nat. Protoc. 7 (2012) 1590–607. doi:10.1038/nprot.2012.081.

[25] C.H. Chen, M.T. Sheu, T.F. Chen, Y.C. Wang, W.C. Hou, D.Z. Liu, T.C. Chung, Y.C. Liang, Suppression of endotoxin-induced proinflammatory responses by citrus pectin through blocking LPS signaling pathways, Biochem. Pharmacol. 72 (2006) 1001–1009. doi:10.1016/j.bcp.2006.07.001.

[26] E.G. Maxwell, I.J. Colquhoun, H.K. Chau, A.T. Hotchkiss, K.W. Waldron, V.J. Morris, N.J. Belshaw, Modified sugar beet pectin induces apoptosis of colon cancer cells via an interaction with the neutral sugar side-chains, Carbohydr. Polym. 136 (2016) 923–929. doi:10.1016/j.carbpol.2015.09.063.

[27] S.H. Barondes, D.N.W. Cooper, M.A. Gitt, H. Leffler, Galectins: structure and function of a large family of animal lectins, J. Biol. Chem. 269 (1994) 20807–20810. doi:10.1016/j.celrep.2015.02.012.

[28] H. Inohara, A. Raz, Functional Evidence that Cell Surface Galectin-3 Mediates Homotypic Cell Adhesion, Cancer Res. 55 (1995) 3267–3271.

[29] P. Mina-Osorio, I. Soto-Cruz, E. Ortega, A role for galectin-3 in CD13-mediated homotypic aggregation of monocytes, Biochem. Biophys. Res. Commun. 353 (2007) 605–610. doi:10.1016/j.bbrc.2006.12.081.

[30] Y. Zhang, H. Lu, P. Dazin, Y. Kapila, Squamous cell carcinoma cell aggregates escape suspension-induced, p53-mediated anoikis: Fibronectin and integrin αv mediate survival signals through focal adhesion kinase, J. Biol. Chem. 279 (2004) 48342–48349. doi:10.1074/jbc.M407953200.

[31] X. Zhang, L.H. Xu, Q. Yu, Cell aggregation induces phosphorylation of PECAM-1 and Pyk2 and promotes tumor cell anchorage-independent growth, Mol. Cancer. 9 (2010) 1–11. doi:10.1186/1476-4598-9-7.

[32] M.W. Pickup, J.K. Mouw, V.M. Weaver, The extracellular matrix modulates the hallmarks of cancer, EMBO Rep. 15 (2014) 1243–1253. doi:10.15252/embr.201439246.

[33] A. Brunet, A. Bonni, M.J. Zigmond, M.Z. Lin, P. Juo, L.S. Hu, M.J. Anderson,

K.C. Arden, J. Blenis, M.E. Greenberg, Akt promotes cell survival by phosphorylating and inhibiting a forkhead transcription factor, Cell. 96 (1999) 857–868. doi:10.1016/S0092-8674(00)80595-4.

[34] Y. Zhao, X. Hu, Y. Liu, S. Dong, Z. Wen, W. He, S. Zhang, Q. Huang, ROS signaling under metabolic stress: cross-talk between AMPK and AKT pathway, Mol. Cancer. 16 (2017) 79. doi:10.1186/s12943-017-0648-1.

[35] C.L. Buchheit, R.R. Rayavarapu, Z.T. Schafer, The regulation of cancer cell death and metabolism by extracellular matrix attachment, Semin. Dev.Biol. 23 (2012) 402–411. doi:10.1016/j.semcdb.2012.04.007.

[36] S. Han, F.R. Khuri, J. Roman, Fibronectin stimulates non-small cell lung carcinoma cell growth through activation of Akt/mammalian target of rapamycin/S6 kinase and inactivation of LKB1/AMP-activated protein kinase signal pathways, Cancer Res. 66 (2006) 315–323. doi:10.1158/0008-5472.CAN-05-2367.

[37] G. Xue, B.A. Hemmings, PKB/akt-dependent regulation of cell motility, J. Natl. Cancer Inst. 105 (2013) 393–404. doi:10.1093/jnci/djs648.

[38] S.K. More, S. V. Chiplunkar, R.D. Kalraiya, Galectin-3-induced cell spreading and motility relies on distinct signaling mechanisms compared to fibronectin, Mol. Cell. Biochem. 416 (2016) 179–191. doi:10.1007/s11010-016-2706-1.

[39] W. He, Q. Wang, B. Srinivasan, J. Xu, M.T. Padilla, Z. Li, X. Wang, Y. Liu, X. Gou, H.-M. Shen, C. Xing, Y. Lin, A JNK-mediated autophagy pathway that triggers c-IAP degradation and necroptosis for anticancer chemotherapy, Oncogene. 33 (2013) 3004–3013. http://www.ncbi.nlm.nih.gov/pubmed/23831571.

[40] I. Masgras, S. Carrera, P.J. De Verdier, P. Brennan, A. Majid, W. Makhtar, E. Tulchinsky, G.D.D. Jones, I.B. Roninson, S. Macip, Reactive oxygen species and mitochondrial sensitivity to oxidative stress determine induction of cancer cell death by p21, J. Biol. Chem. 287 (2012) 9845–9854. doi:10.1074/jbc.M111.250357.

[41] M. D'Arcangelo, Y. Drew, R. Plummer, The role of PARP in DNA repair and its therapeutic exploitation, Br. J. Cancer. 105 (2011) 1114–1122. doi:10.1016/B978-0-12-803582-5.00004-8.

[42] D. Nicholson, Caspase structure, proteolytic substrates and function during apoptotic cell death, Cell Death Differ. 6 (1999) 1028–1042. doi:10.1038/sj.cdd.4400598.

[43] D.N. Dhanasekaran, JNK Signaling Network and Cancer, Genes Cancer. 4 (2013) 332–3. doi:10.1177/1947601913507949.

[44] C.L. Buchheit, R.R. Rayavarapu, Z.T. Schafer, The regulation of cancer cell death and metabolism by extracellular matrix attachment, Semin. Dev.Biol. 23 (2012) 402–411. doi:10.1016/j.semcdb.2012.04.007.

[45] American Type Culture Collection, Colon cancer and normal cell lines, 2013. http://www.atcc.org/~/media/PDFs/Cancer and Normal cell lines tables/Colon cancer and normal cell lines.ashx.

[46] S. Tai, Y. Sun, J.M. Squires, H. Zhang, W.K. Oh, C.Z. Liang, J. Huang, PC3 is a cell line characteristic of prostatic small cell carcinoma, Prostate. 71 (2011) 1668–1679. doi:10.1002/pros.21383.

[47] J. Dumic, S. Dabelic, M. Flögel, Galectin-3: an open-ended story, Biochim. Biophys. Acta. 1760 (2006) 616–35. doi:10.1016/j.bbagen.2005.12.020.

[48] X. Gao, Y. Zhi, T. Zhang, H. Xue, X. Wang, A.D. Foday, G. Tai, Y. Zhou, Analysis of the neutral polysaccharide fraction of MCP and its inhibitory activity on galectin-3, Glycoconj. J. 29 (2012) 159–165. doi:10.1007/s10719-012-9382-5.

[49] L. Leclere, M. Fransolet, P. Cambier, S. El Bkassiny, A. Tikad, M. Dieu, S.P. Vincent, P. Van Cutsem, C. Michiels, Identification of a cytotoxic molecule in heat-modified citrus pectin, Carbohydr. Polym. 137 (2016) 39–51. doi:10.1016/j.carbpol.2015.10.055.

[50] W. Zhang, P. Xu, H. Zhang, Pectin in cancer therapy: A review, Trends Food Sci. Technol. 44 (2015) 258–271. doi:10.1016/j.tifs.2015.04.001.

Supplementary files

Table S1. MCP and MCP fractions linkage analysis.

Linkages	Mol %				
	MCP	**MCP30**	**MCP30/10**	**MCP10/3**	**MCP3**
t-Rha	0.1 (0.1)	0.1 (0.2)	0.2 (0.2)	0.0 (0.0)	0.0 (0.0)
2-Rha	2.1 (2.1)	2.3 (0.3)	1.7 (0.2)	1.7 (0.1)	1.4 (0.1)
2,4-Rha	0.5 (0.2)	0.6 (0.3)	0.4 (0.2)	0.0 (0.1)	0.1 (0.1)
t-Fuc	0.0 (0.0)	0.0 (0.0)	0.0 (0.0)	0.0 (0.0)	0.0 (0.0)
2,4-Fuc	0.0 (0.0)	0.0 (0.0)	0.0 (0.0)	0.0 (0.0)	0.0 (0.0)
t-Ara*f*	0.4 (0.3)	0.5 (0.3)	0.2 (0.1)	0.2 (0.3)	0.2 (0.1)
t-Ara*p*	0.2 (0.2)	0.2 (0.2)	0.2 (0.1)	0.2 (0.3)	0.2 (0.1)
2-Ara*f*	0.0 (0.0)	0.0 (0.0)	0.0 (0.0)	0.0 (0.0)	0.0 (0.1)
2,5-Ara*f*	0.0 (0.0)	0.0 (0.0)	0.0 (0.0)	0.0 (0.0)	0.0 (0.0)
3-Ara*f*	0.2 (0.2)	0.2 (0.2)	0.1 (0.0)	0.1 (0.2)	0.0 (0.1)
3,5-Ara*f*	0.0 (0.0)	0.0 (0.0)	0.0 (0.0)	0.0 (0.0)	0.0 (0.0)
5-Ara*f*	0.5 (0.4)	0.6 (0.6)	0.2 (0.1)	0.0 (0.1)	0.0 (0.1)
Ara(OAc)5	0.7 (0.4)	0.9 (0.5)	0.3 (0.1)	0.4 (0.2)	0.3 (0.1)
t-Xyl	0.3 (0.3)	0.4 (0.3)	0.1 (0.1)	0.0 (0.0)	0.1 (0.1)
2-Xyl	0.0 (0.0)	0.0 (0.0)	0.0 (0.0)	0.1 (0.0)	0.0 (0.0)
2,4-Xyl	0.0 (0.0)	0.0 (0.0)	0.0 (0.0)	0.0 (0.0)	0.0 (0.0)
3,4-Xyl	0.0 (0.1)	0.0 (0.1)	0.0 (0.0)	0.1 (0.1)	0.0 (0.0)
4-Xyl	0.0 (0.2)	0.3 (0.2)	0.1 (0.0)	0.3 (0.2)	0.2 (0.1)
Xyl(OAc)5	0.6 (0.5)	0.8 (0.7)	0.2 (0.1)	0.1 (0.3)	0.2 (0.1)
t-Man	0.0 (0.0)	0.0 (0.0)	0.0 (0.0)	0.0 (0.0)	0.0 (0.0)
4-Man	0.1 (0.1)	0.1 (0.1)	0.0 (0.0)	0.2 (0.2)	0.3 (0.2)
4,6-Man	0.0 (0.0)	0.0 (0.0)	0.0 (0.0)	0.0 (0.0)	0.0 (0.0)
Man(OAc)6	0.8 (0.1)	0.8 (0.1)	0.5 (0.0)	1.1 (0.2)	0.9 (0.2)
t-Gal	1.2 (0.7)	1.3 (0.7)	0.8 (0.6)	1.0 (0.2)	1.0 (1.0)
2-Gal	0.0 (0.0)	0.0 (0.0)	0.0 (0.0)	0.0 (0.0)	0.0 (0.1)
2,4-Gal	0.4 (0.5)	0.2 (0.2)	0.3 (0.3)	2.2 (3.0)	0.5 (0.7)
2,4,6-Gal	0.6 (0.8)	0.6 (0.8)	0.6 (0.9)	0.8 (0.8)	0.2 (0.3)
3-Gal	0.1 (0.1)	0.2 (0.2)	0.2 (0.2)	0.0 (0.0)	0.0 (0.0)
3,4-Gal	0.4 (0.3)	0.1 (0.1)	0.2 (0.1)	1.7 (1.4)	0.9 (1.0)
3,6-Gal	0.9 (0.7)	1.1 (0.9)	0.8 (0.6)	0.0 (0.0)	0.3 (0.5)
4-Gal	3.3 (1.9)	3.2 (1.8)	4.0 (2.8)	4.6 (1.9)	1.0 (1.1)
4,6-Gal	0.9 (0.5)	0.7 (0.1)	0.8 (0.4)	3.3 (3.3)	0.2 (0.4)
6-Gal	1.6 (0.6)	1.6 (0.4)	1.4 (0.8)	1.9 (1.1)	1.3 (0.8)
Gal(OAc)6	1.6 (1.2)	1.3 (1.1)	1.4 (1.1)	4.1 (1.8)	1.6 (1.0)
t-GalA	6.0 (1.9)	5.4 (1.7)	4.0 (2.2)	7.5 (1.0)	14.1 (4.2)
2,4-GalA	3.9 (4.5)	3.7 (4.4)	5.8 (6.7)	3.0 (2.3)	3.5 (4.3)
3,4-GalA	0.2 (0.1)	0.1 (0.1)	0.2 (0.1)	0.4 (0.4)	0.4 (0.4)
4-GalA	63.2 (5.7)	63.2 (5.2)	66.6 (9.0)	58.2 (4.8)	63.4 (4.4)
4,6-GalA	6.2 (4.4)	6.0 (4.7)	7.4 (3.6)	6.1 (3.4)	5.9 (4.4)
t-Glc	0.1 (0.1)	0.1 (0.1)	0.1 (0.2)	0.1 (0.0)	0.1 (0.0)
2-Glc	0.0 (0.0)	0.0 (0.0)	0.0 (0.0)	0.0 (0.0)	0.0 (0.0)
3-Glc	0.0 (0.0)	0.0 (0.0)	0.0 (0.0)	0.0 (0.0)	0.1 (0.1)

3,4-Glc	0.5 (0.2)	0.5 (0.3)	0.5 (0.1)	0.2 (0.1)	0.3 (0.2)
Linkages	**Mol %**				
	MCP	**MCP30**	**MCP30/10**	**MCP10/3**	**MCP3**
4-Glc	0.5 (0.3)	0.6 (0.4)	0.5 (0.3)	0.3 (0.2)	0.3 (0.1)
4,6-Glc	0.0 (0.0)	0.0 (0.0)	0.0 (0.0)	0.0 (0.1)	0.1 (0.1)
Glc(OAc)6	0.3 (0.1)	0.3 (0.1)	0.3 (0.1)	0.1 (0.1)	0.2 (0.0)
t-GlcA	2.8 (0.1)	2.7 (1.5)	2.5 (0.0)	3.6 (0.0)	3.2 (0.0)

Table S2. Monosaccharides and linkage analysis ratios.

	Ratio of monosaccharides			Ratio of linkage analysis
	GalA:Rha	Gal:Rha	Ara:Rha	Total GalA: *t*-GalA
MCP	28.9	4.1	0.7	12.2
MCP30	25.3	3.4	0.8	13.4
MCP30/10	35.4	4.6	0.4	20.2
MCP10/3	42.0	11.6	0.4	9.0
MCP3	59.4	3.5	0.4	5.2

Table S3. Percentage of cells lost of viability (results from figure 2)

		Cells lost of viability (%)			
	Treatment concentration	**24 h**	**48 h**	**72 h**	**96 h**
HCT116 MCP	0.2%	20.3 (6.8)*	11.8 (1.5)*	6.5 (4.3)	16.3 (4.6)*
	0.5%	19.5 (4.3)*	30.8 (3.6)*	33.3 (6.8)*	33.3 (7.2)*
	1.0%	25.8 (3.8)*	34.5 (6.5)*	46.3 (3.0)*	50.5 (2.5)*
HCT116 MCP30	0.2%	2.3 (10.8)	12.5 (11.5)	7.5 (10.5)	2.8 (6.4)
	0.5%	17.3 (4.3)*	14.0 (8.7)	20.5 (11.6)*	32.5 (5.0)*
	1.0%	13.3 (7.8)	22.5 (4.3)*	33.8 (7.8)*	38.0 (7.2)*
HCT116 MCP30/10	0.2%	12.0 (8.9)*	21.0 (0.7)*	31.8 (10.1)*	24.5 (9.3)*
	0.5%	18.3 (3.6)*	26.3 (2.2)*	32.8 (5.0)*	35.8 (8.6)*
	1.0%	28.5 (3.2)*	44.8 (3.1)*	41.0 (8.1)*	43.8 (7.1)*
HCT116 MCP10/3	0.2%	16.5 (8.5)*	21.0 (4.1)*	25.5 (3.6)*	26.8 (2.5)*
	0.5%	11.8 (8.9)	23.5 (5.9)*	37.8 (7.8)*	40.8 (5.3)*
	1.0%	26.0 (1.9)*	47.3 (4.0)*	56.8 (9.3)*	62.8 (4.6)*
HCT116 MCP3	0.2%	19.8 (4.9)*	21.0 (4.4)*	26.8 (4.2)*	29.0 (6.0)*
	0.5%	10.0 (5.1)*	24.8 (3.3)*	27.0 (4.8)*	41.3 (4.3)*
	1.0%	24.8 (3.0)*	43.8 (5.5)*	47.3 (5.2)*	51.3 (4.7)*
HT29 MCP	0.2%	14.3 (1.9)*	15.5 (8.6)*	13.3 (3.5)*	5.5 (7.2)
	0.5%	5.8 (1.5)*	13.3 (4.4)*	21.8 (6.7)*	24.5 (7.1)*
	1.0%	9.8 (3.6)*	11.0 (3.5)	23.5 (6.2)*	28.5 (3.2)*
HT29 MCP30	0.2%	12.3 (5.7)*	5.8 (3.8)	10.5 (2.7)*	8.8 (5.7)*
	0.5%	11.8 (2.9)*	14.8 (4.0)*	17.5 (5.5)*	21.0 (3.2)*
	1.0%	14.8 (2.9)*	17.5 (3.9)*	20.3 (5.3)*	24.0 (3.2)*
HT29 MCP30/10	0.2%	16.3 (5.7)*	13.3 (3.8)*	19.8 (3.0)*	25.5 (4.2)*
	0.5%	15.8 (2.9)*	21.5 (1.1)*	24.3 (4.8)*	25.0 (3.2)*
	1.0%	13.8 (3.3)*	21.5 (5.1)*	25.3 (4.1)*	30.0 (4.9)*
HT29 MCP10/3	0.2%	11.8 (6.2)*	26.8 (6.3)*	19.3 (7.9)*	32.5 (9.9)*
	0.5%	9.3 (6.1)	23.8 (6.4)*	32.5 (5.7)*	44.3 (7.9)*
	1.0%	15.0 (4.1)*	30.5 (5.6)*	46.5 (4.7)*	51.5 (6.9)*
HT29 MCP3	0.2%	8.8 (5.6)	14.8 (6.8)*	25.5 (6.9)*	29.0 (1.9)*
	0.5%	10.5 (5.0)	30.0 (5.2)*	24.8 (8.0)*	39.8 (2.6)*
	1.0%	12.0 (7.1)*	22.3 (9.1)*	35.0 (2.7)*	43.5 (8.6)*
PC3 MCP	0.2%	18.5 (4.7)*	13.3 (3.3)*	8.5 (4.0)*	13.0 (4.6)*
	0.5%	15.0 (2.7)*	25.0 (3.5)*	29.3 (3.7)*	30.3 (4.7)*
	1.0%	20.5 (3.2)*	26.3 (5.1)*	38.5 (1.1)*	43.3 (1.3)*
PC3 MCP30	0.2%	5.3 (6.1)	10.0 (6.5)*	8.8 (6.3)	4.8 (3.9)
	0.5%	15.5 (3.8)*	14.3 (5.0)*	19.5 (6.7)*	28.8 (4.0)*
	1.0%	13.58 (5.0)*	21.0 (3.7)*	29.5 (6.4)*	33.3 (5.0)*
PC3 MCP30/10	0.2%	13.5 (5.7)*	18.0 (1.6)*	27.8 (5.8)*	24.8 (5.4)*
	0.5%	17.5 (2.5)*	24.8 (1.8)*	30.3 (1.9)*	32.0 (5.2)*
	1.0%	23.8 (1.9)*	37.0 (3.1)*	35.5 (6.4)*	39.0 (5.5)*
PC3 MCP10/3	0.2%	15.0 (4.1)*	21.0 (3.9)*	19.5 (4.5)*	26.0 (2.4)*
	0.5%	11.0 (4.8)*	21.3 (3.7)*	34.5 (7.6)*	40.3 (5.5)*
	1.0%	9.0 (2.1)*	35.8 (3.6)*	49.8 (7.3)*	55.0 (3.3)*
PC3 MCP3	0.2%	16.0 (4.1)*	17.3 (4.7)*	24.8 (4.7)*	27.5 (3.9)*
	0.5%	10.0 (4.1)*	22.3 (3.3)*	22.0 (4.7)*	37.5 (3.2)*
	1.0%	7.8 (5.1)	26.5 (3.4)*	38.5 (2.9)*	27.3 (3.8)*

Each MCP fraction was compared with the control. *$p < 0.05$ vs control, according to Dunnett's test.

A

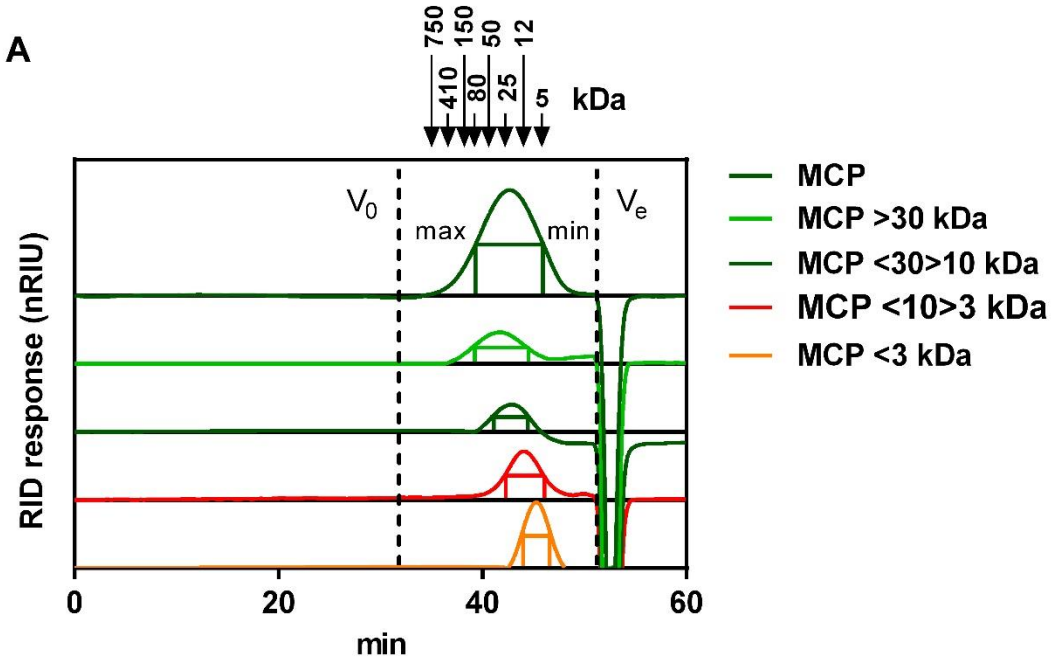

B

Maximum and minimum at half height (kDa)		
	Max	**Min**
MCP	101.9 (6.1)	5 (0.4)
MCP 30	105.1 (4.1)	9.3 (0.7)
MCP 30-10	48.5 (4.7)	8.6 (0.9)
MCP 10-3	25.3 (2.0)	4.1 (0.3)
MCP 3	11.8 (0.5)	3.8 (0.4)

Figure S1. Polysaccharides molecular size profile. A) HPSEC-RID elution profile of MCP and MCP fractions. Black circles above the figure are dextran standards: 1 (750 kDa), 2 (410 kDa), 3 (150 kDa), 4 (80 kDa), 5 (50 kDa), 6 (25 kDa), 7 (12 kDa) and 8 (5 kDa). MCP: modified citrus pectin. Vo: void volume (blue dextran elution time); Ve: elution volume (glucose elution time). Min and max at half height represented by the vertical line in the peak. B) The maximun and minimun at half height molecular size of MCP and MCP fractions. These results are expressed in average and standard deviation.

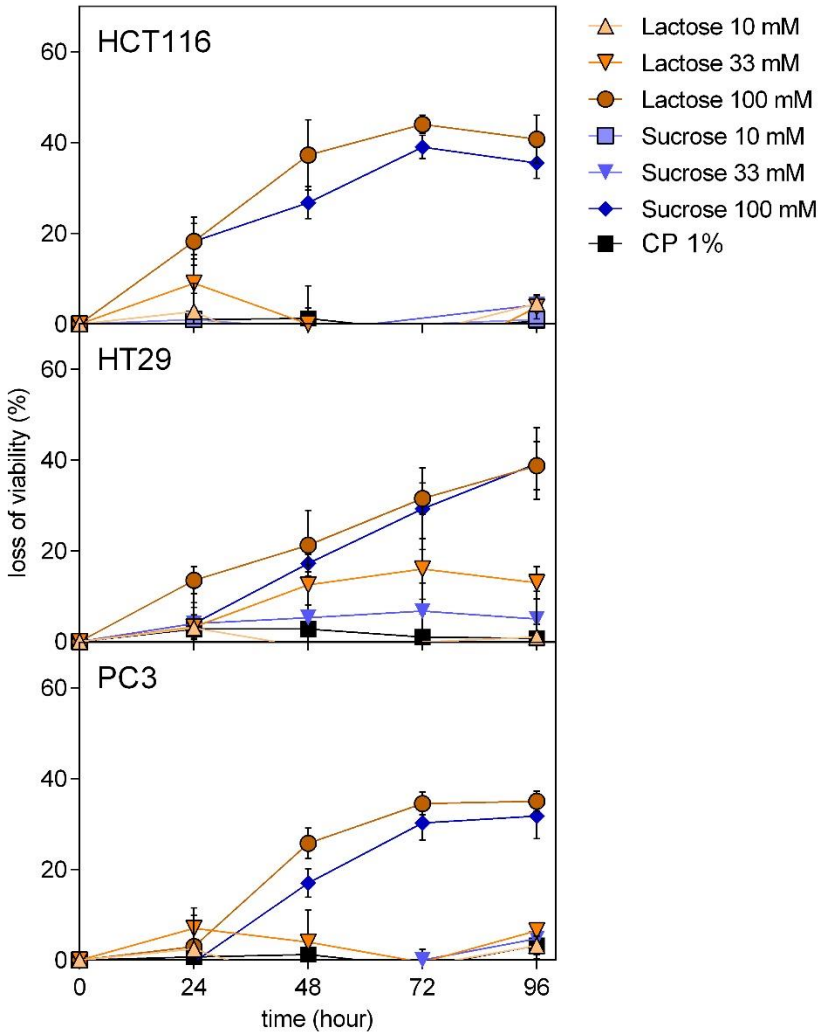

Figure S2. Lactose, sucrose and Citrus Pectin effects on viability cell loss measured by MTT. The loss of viability was calculated based on control (without treatment) as 100%.

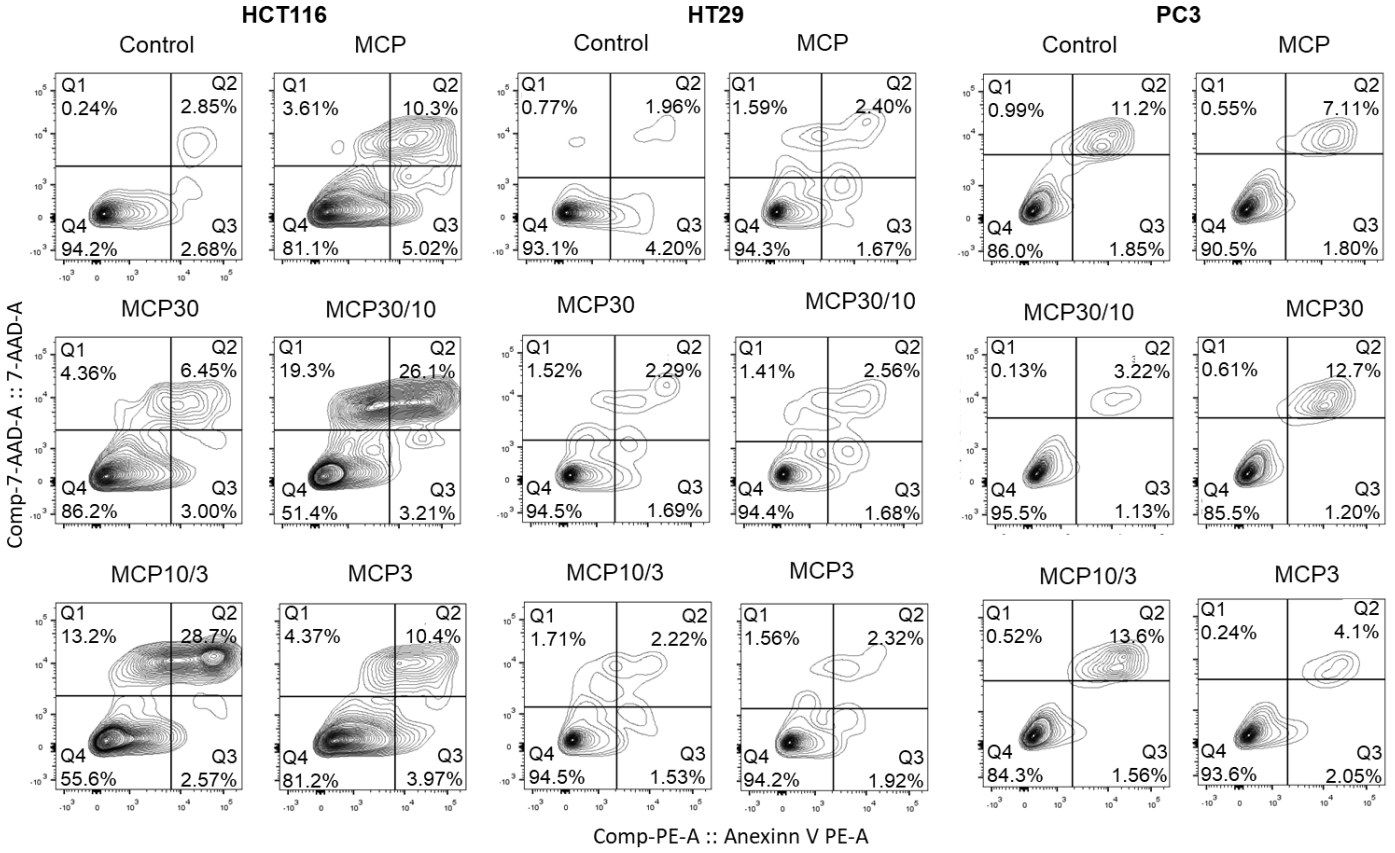

Figure S3. Effects of MCP and MCP fractions in HCT116, HT29 and PC3 apoptosis by flow cytometry. Q1: necrosis quadrant; Q2: necroptosis quadrant; Q3: apoptosis quadrant; Q4: viable cells quadrant. The most significant differences in graphics are shown in the figure (HCT116 and PC3 cells treatment).

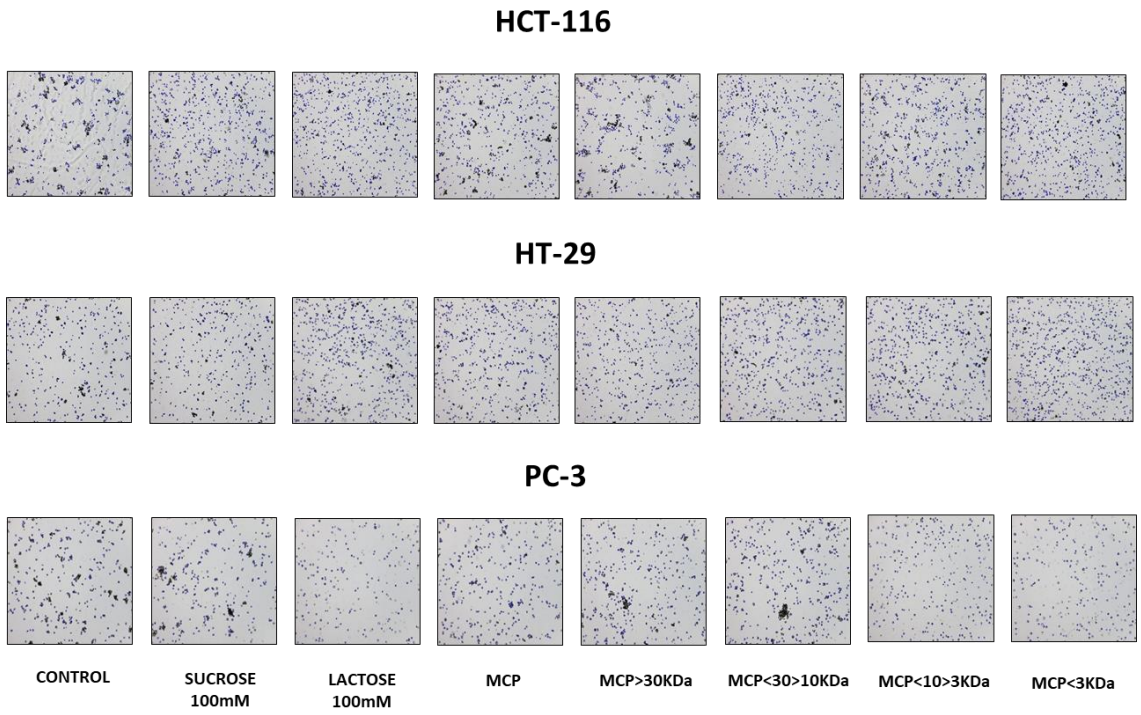

Figure S4. Homotypic aggregation. Cells were counted in an automatic cell counter and the blue circles were automatic generated by the machine software and is related to single or double cells.

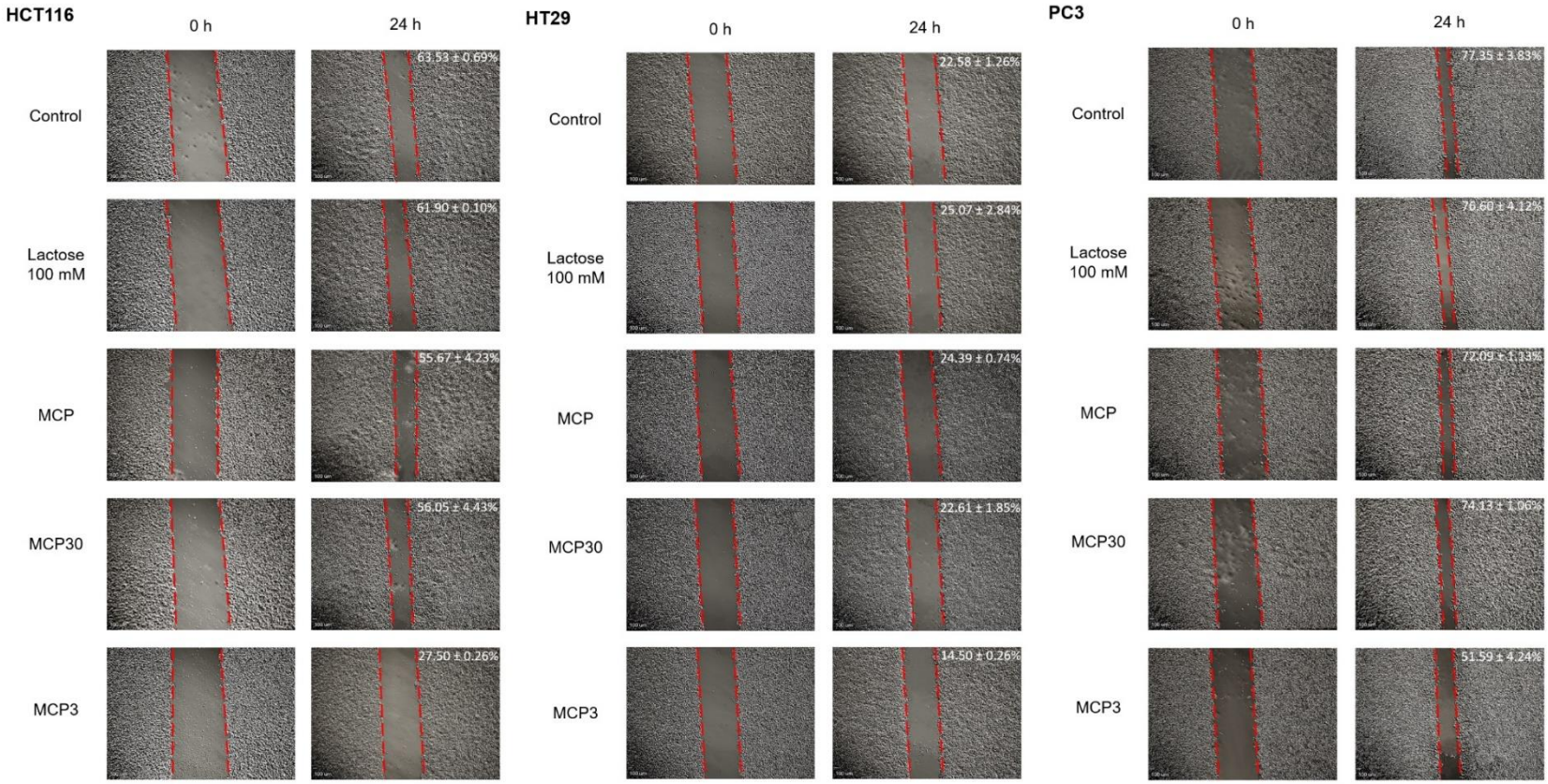

Figure S5. Cell migration by wound healing assay after 24 h of MCP and MCP fractions treatment. The results showed in white at the upper-right of each figure are expressed in percentage of cells that invaded the gap compared with control. Data were shown as mean ± SD (*n*=4).

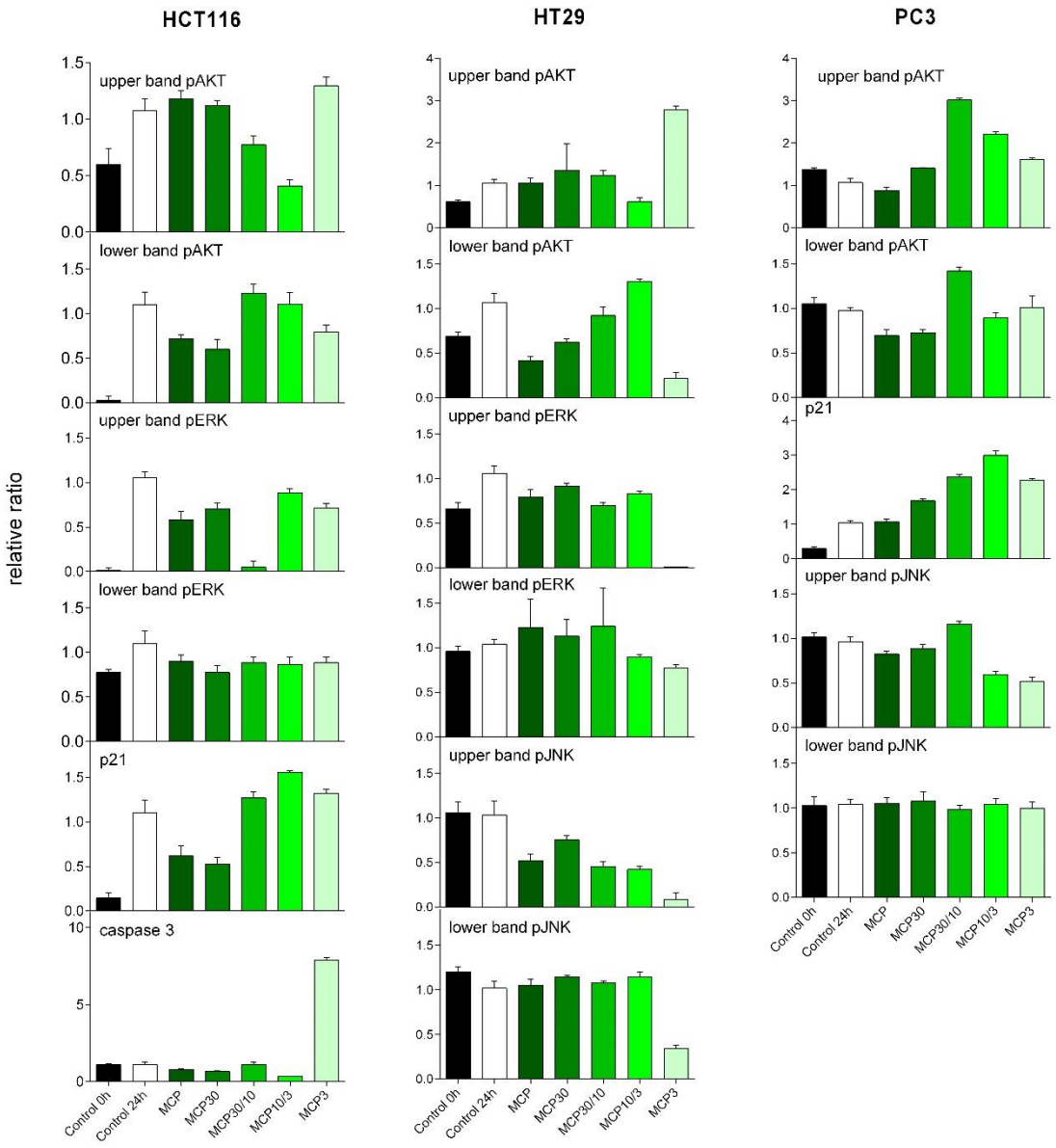

Figure S6. Relative density of bands from western blotting experiments. Relative ratio was calculated of target protein over β-actin. Band intensities were separated in upper and lower bands for pAKT, pERK1/2 and pJNK from two independent experiments.

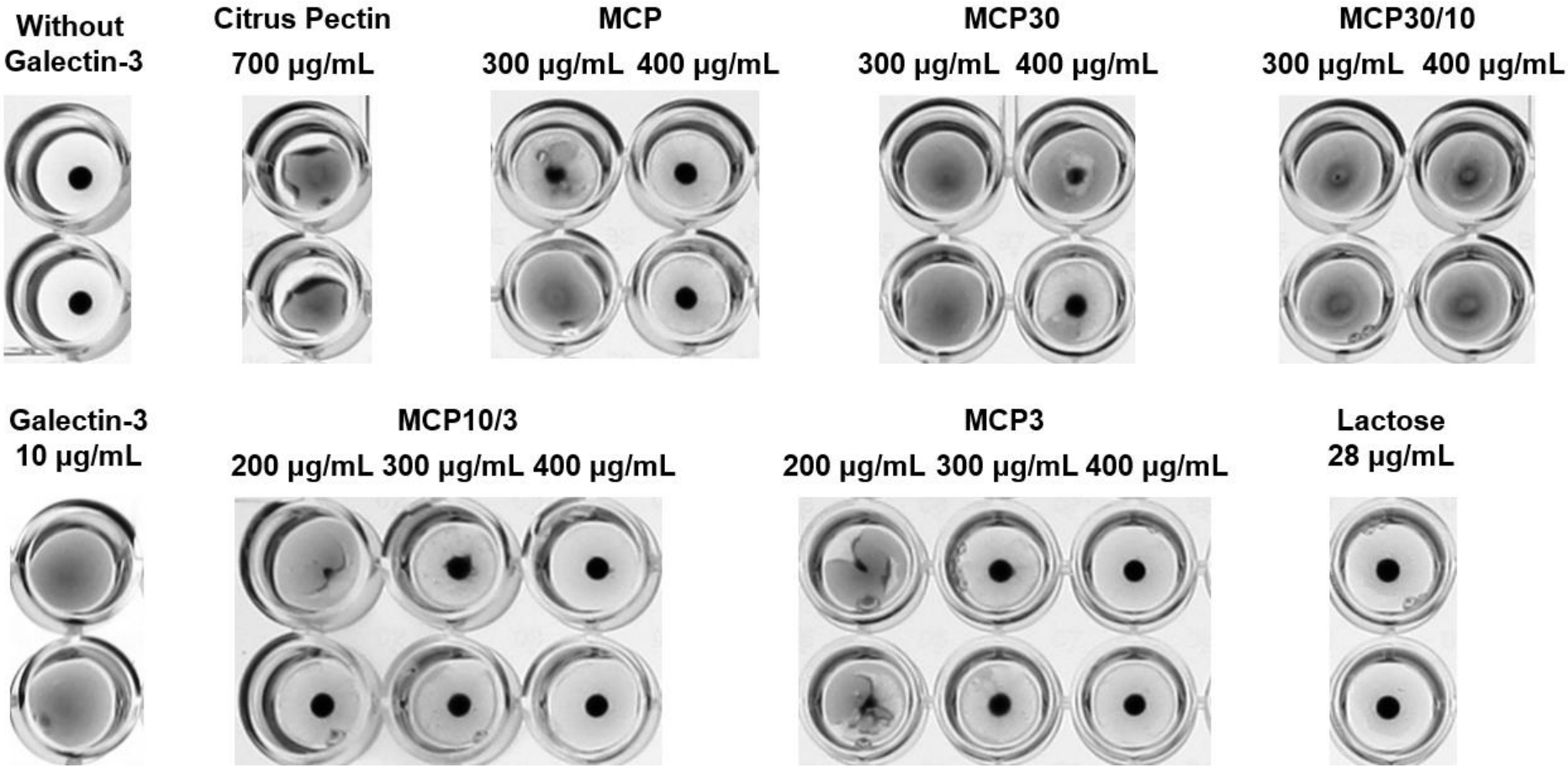

Figure S7. Inhibition of hemagglutination assay. Samples from MCP and MCP fractions were evaluated using different concentrations and compared to negative control (without galectin-3), to positive control (with galectin-3), to citrus pectin and to a hemagglutination inhibition control (lactose tittered to 28µg/mL)

Chapter 4

Part II: Ripening-induced chemical modifications of papaya pectin inhibit cancer cell proliferation

Samira Bernardino Ramos do Prado[1], Gabrielle Fernandez Ferreira[1], Yosuke Harazono[2,3], Tânia Misuzu Shiga[1], Avraham Raz[2], Nicholas C. Carpita[4], João Paulo Fabi[1,5,6]*

[1]Department of Food Science and Experimental Nutrition, School of Pharmaceutical Sciences, University of São Paulo, São Paulo, SP, Brazil
[2]Departments of Oncology and Pathology, School of Medicine, Wayne State University, and Karmanos Cancer Institute, Detroit, MI, USA.
[3]Department of Maxillofacial Surgery, Tokyo Medical and Dental University, Bunkyo-ku, Tokyo 113–8510, Japan.
[4]Department of Botany & Plant Pathology, Purdue University, West Lafayette, IN, USA.
[5]Food and Nutrition Research Center (NAPAN), University of São Paulo, São Paulo, SP, Brazil.
[6]Food Research Center (FoRC), CEPID-FAPESP (Research, Innovation and Dissemination Centers, São Paulo Research Foundation), São Paulo, SP, Brazil.

Scientific Reports, v. 7, p. 16564, 2017.

Abstract

Papaya (*Carica papaya* L.) is a fleshy fruit with a rapid pulp softening during ripening. Ripening events are accompanied by gradual depolymerization of pectic polysaccharides, including homogalacturonans, rhamnogalacturonans, arabinogalactans, and their modified forms. During intermediate phases of papaya ripening, partial depolymerization of pectin to small size with decreased branching had enhanced pectin anti-cancer properties. These properties were lost with continued decomposition at later phases of ripening. Pectin extracted from intermediate phases of papaya ripening markedly decreased cell viability, induced necroptosis, and delayed culture wound closing in three types of immortalized cancer cell lines. The possible explanation for these observations is that papaya pectins extracted from the third day after harvesting have disrupted interaction between cancer cells and the extracellular matrix proteins, enhancing cell detachment and promoting apoptosis/necroptosis. The anticancer activity of papaya pectin is dependent on the presence and the branch of arabinogalactan type II (AGII) structure. These are first reports of AGII in papaya pulp and the first reports of an *in vitro* biological activity of papaya pectins that were modified by natural action of ripening-induced pectinolytic enzymes. Identification of the specific pectin branching structures presents a biological route to enhancing anti-cancer properties in papaya and other climacteric fruits.

Key-words: colorectal cancer, dietary fiber, fruit, necroptosis, polysaccharides.

Abbreviations: AFM, Atomic force microscopy; AGII, type II arabinogalactans; Ara, arabinose; ATR, attenuated total reflectance; BAMEC, bovine adrenal medullary endothelial cells; BSA, bovine serum albumin; DMEM, Dulbecco's modified Eagle's medium; DTGS, deuterated triglycine sulfate; ECM, extracellular matrix; EGFR, epidermal growth factor receptor; f, furanose; FBS, fetal bovine serum; FTIR, Fourier Transform-Infrared; Fuc, fucose; Gal, galactose; GalA, galacturonic acid; Glc, glucose; GlcA, glucuronic acid; HG, homogalacturonan; LDH, lactate dehydrogenase; Man, mannose; p, pyranose; PGA, polygalacturonic acid; PME, pectinesterases; PP, papaya pectin; RG-I, rhamnogalacturonan type I; RG-I, rhamnogalacturonan type I; RG-II, rhamnogalacturonan type II; Rha, rhamnose ; ROS, reactive oxygen species; SD, standard deviation; t, terminal; TCW, total cell wall fraction; WSF, water-soluble fraction; Xyl, xylose.

Introduction

Dietary fiber are generally considered carbohydrates that are incompletely processed by human digestive enzymes [1], but can provide health benefits [2], such as lowering the risk of colorectal cancer development [3]. Fruits and vegetables are rich in pectin, a soluble dietary fiber found in plant cell walls [4]. Pectin is a complex structure comprising two principal polymers of homogalacturonan (HG) and rhamnogalacturonan type I (RG-I), but each can be modified through side-croup addition to add functional complexity. HGs are linear homopolymers composed of *1,4*-α-D-galacturonic acid (GalA) residues in which some carboxyl groups are esterified with methyl and acetyl groups. Addition of xylose (Xyl) residues forms xylogalacturonan, and addition of four highly conserved oligomers of 21 different sugar residues forms the boron-crosslinking rhamnogalacturonan type II (RG-II). RG-Is are defined by a backbone of 4-α-D-GalA-1-2-α-L-Rha-1 repeating units, with highly branched side-chains of arabinans, galactans and arabinogalactans attached to the Rha residues [5].

Many types of pectin, especially the modified ones, have been associated with anti-cancer activity in both *in vitro* and *in vivo* studies, such as the reduction of cell proliferation, migration, adhesion, and the induction of apoptosis [6–10]. These anti-cancer activities were shown for modified pectins of citrus [11–14], apple [15,16], sugar beet [6]. and ginseng [8]. The biological effects of modified pectin have been associated, at least partially, with the inhibition of galectin-3 function, a multifaceted and pro-metastatic protein whose expression is up-regulated in many cancers [14,17–19]. Pectin modification decreases the overall molecular weight, thereby releasing fragments of RG-I that can bind to galectin-3 [20]. HG and RG-I fragments are known to induce cancer cell detachment [7,9], but lack of structural-functional relationships makes determination of specific anti-cancer activities difficult. Moreover, pectin from different sources can vary widely in size, composition and branching pattern [21], and consequently, tracing anti-cancer properties to specific carbohydrate structures and interactions is still poorly understood. To our knowledge, there are no reports that have investigated the association between the alterations of pectin structure by endogenous action of pectolytic enzymes and the anti-cancer activities.

Climacteric fleshy fruits shows substantial changes in the pulp cell wall polysaccharides as they ripen [22]. Thus, physiological modification of cell wall during ripening could be an alternative to pectin modification as several cell wall degrading enzymes are coordinately expressed throughout ripening [23]. Papaya is a climacteric fleshy fruit with a fast ripening and a massive solubilization of galacturonan chains arose from extensive action of pectinolytic enzymes during ripening [24–26]. Thus, increased action of cell wall degrading enzymes during ripening of papaya and consequent decrease of pectin molecular weight [27] might naturally modify pectin structures possibly increasing pectin's anti-cancer activity. As such, the present study aimed to characterize and to evaluate pectin isolated from papaya fruits harvested at different ripening stages to investigate the relationship between changes in pectin's structure and their anti-proliferative activity on three cancer cell lines.

Materials and methods

Antibodies, Chemicals, and Reagents

Heat-inactivated fetal bovine serum (FBS), trypsin/EDTA and Dulbecco's modified Eagle's medium (DMEM) containing penicillin (100 UI/mL) and streptomycin (100 μg/mL) were from Gibco (Grand Island, NY) or Cultilab (Campinas, SP). Unless stated otherwise, other reagents and chemicals used were from Sigma-Aldrich (St. Louis, MO). P-Akt (sc-7985-R), p-Erk (sc-7383) and Erk 1/2 (sc-135900) were purchased from Santa Cruz Biotechnology (Santa Cruz, CA). Akt (#9272), p21 (2946S), PARP (#9542), cleaved caspase-3 (#9661) antibodies were purchased from Cell Signaling Technology (Beverly, MA). Monoclonal rat anti-Gal-3 antibody was isolated from the supernatant of hybridoma (catalog number: TIB- 166, American Type Culture Collection; Manassas, VA). Mouse anti-β-actin was purchased from Sigma-Aldrich.

Plant material

Papaya fruits (*Carica papaya* L. cv. 'Golden') were acquired from a producer in Linhares City, Espírito Santo, Brazil (19°21'33.9"S 40°08'15.6"W). The fruits were harvested at color break to one-fourth yellow and stored at ambient temperature during ripening. Respiration, ethylene production and pulp firmness were measured daily from, at

least, six fruits [25]. Fruit pulps were cut in small pieces, frozen in liquid nitrogen, pooled and stored (-80 ºC) at each day for further analysis [25]. For the following analysis, it was used different phases of ripening, separated by one to four days after harvesting from two independent ripening curves (biological duplicate) as previously stated [25].

Extraction of water-soluble fraction

The frozen papaya pulp was grounded to fine powder in N_2 and extracted three times (or until samples were colorless) with chloroform:methanol (1:1; v/v) for enzyme inactivation and protein/pigment removal. Residues were washed with three volumes of 80% boiling ethanol for monosaccharide removal and were also washed with three volumes of acetone for drying purposes. Finally, residues from triplicate extractions were dried and weighed, resulting in a total cell wall fraction (TCW). Extraction yields were achieved using the total pulp values used in experiments. Then, each TCW sample was extracted three times with deionized water under constant magnetic stirring for 20 min at 25 °C and centrifuged (10,000 x *g*, 20 min, 25 °C). The supernatant (water-soluble fraction-WSF) was lyophilized and weighed for extraction yields calculation related to TCW quantity. Qualitative analysis for starch, proteins and phenolic compounds were performed in order to test the purity of WSF fractions. The water-soluble papaya pectin (PP) was extracted from different ripening stages of papaya fruit, one to four days after harvest (named 1PP, 2PP, 3PP and 4PP, respectively).

Cell culture and treatments

Colon cancer cells line HCT116 and HT29 and prostate cancer cell line PC3 were purchased from American Type Culture Collection guidelines (ATCC) or Rio de Janeiro Cell Bank (BCRJ, Rio de Janeiro, RJ). Cell lines were cultured in Dulbecco's modified Eagle's medium (DMEM) containing penicillin (100 µL/mL) and streptomycin (100 µg/mL) with 10% fetal bovine serum and cells were maintained at 37 °C in a humidified atmosphere of 95% air and 5% CO_2. The ATCC for the maintenance of cells were followed. Cells were dissociated from growth dishes by using trypsin/EDTA when reached a confluence of 70–90%. For treatment, 0.22 µm filtered WSF (0, 0.013, 0.025, 0.05 or 0.2%), lactose (33 or 100 mM) or Triton-X (0.2%) was added to the medium at those final concentrations.

MTT assay

Cells were plated on a 96-well cell culture plates at a density of 1 x 10^4 cells/well (200 µL) overnight. For MTT assay cells were incubated with the culture medium (control) or papaya WSF (0.013, 1.025, 0.05 or 0.2%) for 24, 48 and 72 h. After incubation, MTT (0.5 mg/mL) was added for 3 h. Supernatants were removed and the formazan crystals were solubilized with DMSO. Absorbance at 490 nm was measured in a microplate reader (Bio-Rad, Hercules, CA). Cells viability at each incubation time was expressed in relation to the untreated cells (control).

LDH assay

The lactate dehydrogenase (LDH) was evaluated using the Cytotoxicity Detection Kit (Roche Diagnostics, Mannheim, Germany) following the manufacturer's instructions. Briefly, cells were plated overnight as described for viability assays and incubated with the culture medium (control) or polysaccharides. After incubation, supernatants (100 µL) were transferred to 96-well cell culture plates, mixed with the Substrate solution and incubated at 25 °C for 30 min protected from light. Finally, the stop solution was added and the absorbance at 490 nm was measured in a microplate reader (Bio-Rad). The cytotoxicity (%) was expressed as the amount of LDH released by cells in relation to cells treated with a Lysis solution. Only samples from 3PP and 4PP were analyzed because of the prominent difference in the initial cell proliferation assays.

Homotypic aggregation assay

The assay was performed as described by Nangia-Makker, Balan and Raz (2012)[28]. Cells were detached from monolayer with 0.02% EDTA in calcium-Magnesium free PBS (CMF-PBS) and suspended at 1 x 10^6 cells per mL in CMF-PBS with or without 20 g/mL asialofetuin. Samples were placed in 0.5 mL aliquots into siliconized glass tubes and agitated at 80 *g* for 60 min at 37 °C. The aggregation was terminated by fixing the cells with 1% formaldehyde in CMF-PBS. Single cells were counted in a TC10™ Automated Cell Counter (Bio-Rad) and the percentage of aggregation inhibition was calculated as suggested by the above-referred article.

Migration assay

Migration assay was performed as described by Nangia-Makker, Balan and Raz (2012) [28]. Briefly, bovine adrenal medullary endothelial cells (BAMEC) or HCT116, HT29 and PC3 cells (2.4×10^4) were seeded in each chamber of the cell culture insert (Ibidi GmbH). BAMEC were maintained in Earle's Minimal Essential Medium (EMEM - Invitrogen, Carlsbad, CA) containing 10% heat-inactivated FBS, 2 mM glutamine and antibiotics. Cells were prelabeled with DiO (green) or DiI (red) (Invitrogen, Carlsbad, CA). After 12 h, the cell culture insert was removed, cells were washed with PBS and EMEM medium without FBS and with the respective components was loaded and the cell migration of the co-cultures towards each other was observed after 24 h under fluorescent microscope and compared to a previous 0 h observation to analyze migration. Photos were taken using a Zeiss Confocal Laser Microscope LSM 510 META NLO (The Wayne State University Microscopy and Imaging Core Facility). Only samples from 3PP and 4PP were analyzed because of the prominent difference in the initial cell proliferation assays.

Wound healing assay

Wound healing assay was performed as described by Moreno-Bueno et al. (2009). Cancer cells were plated (2×10^5) in 35-mm cell culture dishes in 1.5 mL growth medium without FBS. Cells were incubated in a humidified incubator at 37 °C, 5% CO_2 until reached 85% confluence. A wound was made by scratching the monolayer culture using a sterile 200 µL micropipette tip. Afterwards, cells were washed with PBS to remove floating cells and 1.5 mL of culture medium was added with or without pectin treatments. Only samples from 3PP and 4PP were analyzed because of the prominent difference in the initial cell proliferation assays.

Extracellular matrix proteins

Extracellular matrix proteins interactions were performed according to Nangia-Makker, Balan and Raz (2012) [28]. Firstly, a 96-well microtiter cell culture plates were coated with serially diluted (0 to 10 µg) EHS laminin, collagen type IV, or fibronectin. Plates were incubated for 1 h at 37 °C to dry the extracellular matrix (ECM) protein. The non-specific sites were blocked in the wells by incubating with sterile 1% BSA in PBS for

1 h at 37 °C. Wells were washed with sterile PBS three times to remove extra proteins. Cells were detached from the plate using 0.02% EDTA. Viable cells were counted using trypan blue and seeded at 4 x 10^4 cells per well. Cells were allowed to adhere to the plates for 16 h. Non-adherent cells were washed off with medium three times. To count the number of cells attached to the ECM proteins was added 200 mL of the medium and a 1:10 dilution of Alamar blue was added. The live cells created a reducing environment, which changed the color of dye from blue to pink. Cells were incubated for 3 h at room temperature and read absorbance at 570 nm and with a fluorescence excitation at 570 nm, fluorescence emission was read at 585 nm. After achieving the best ECM quantity for each well (1 µg for laminin, 0.5 µg for collagen IV and 2.5 µg for fibronectin), the same experiment described above was done but using the different cells treatment (100 mM lactose and 0.2% papaya pectin – 24 h) with no coated proteins as positive control and 0.1% BSA-coated wells as negative control.

Apoptosis assay

Cells were plated on a 24-well cell culture plates at a density of 2 x 10^5 cells/well (1 mL) overnight. Then, cells were incubated with the culture medium (control), WSF (3PP and 4PP; 0.2%) or lactose (100 mM) for 24 h. Apoptosis was evaluated using PE Annexin V Apoptosis Detection Kit I (BD Biosciences, San Diego, CA) according to the manufacturer's instructions. Briefly, cells were washed twice with cold PBS with 2% BSA and then ressuspended in 1x Binding Buffer at a concentration of 1 x 10^6 cells / mL. A solution of 1 x 10^5 cells (100 µL) was transferred to a 5 mL culture tube. FITC Annexin V (5 µL) and 7AAD (5 µL) were added in the tube, gently vortex and incubated for 15 min at RT (25°C) in the dark. Finally, 400 µl of 1x Binding Buffer were added to each tube and analyzed by flow cytometry within 1 h using a FACSVerse flow cytometer (BD Biosciences, San Diego, CA). Controls of unstained cells and staining only with FITC Annexin V or 7AAD were used. Data analysis was performed with FlowJo software (Tree Star, Ashland, OH). Only samples from 3PP and 4PP were analyzed because of the prominent difference in the initial cell proliferation assays.

Western blotting assay

Cells were plated on a 6-well cell culture plates at a density of 5 x 10^5 cells/well (2 mL) overnight. Then, medium was changed and new medium with lactose (100 mM), 3PP (0.2%), 4PP (0.2%) or without any source of carbohydrate were added and left at incubation for 24 h. The medium was discarded and cells were washed with PBS twice (0 and 24 h of treatment). Cells were lysed in RIPA buffer (50 mM Tris-HCl pH 7.4, 1% NP-40, 0.5% Na-deoxycholate, 0.1% SDS, 150 mM NaCl, 2 mM EDTA, 50 mM NaF and 0.2 mM Na_3VO_4) containing protease and phosphate inhibitors (Roche Applied Science, Nutley, NJ). BCA protein assay (Pierce Biotechnology, Rockford, IL) was performed to determine equal amounts of proteins for 8% or 10% SDS-polyacrylamide gel electrophoresis (PAGE) and transferred to polyvinylidene fluoride membranes (Millipore, Bedford, MA). Membranes were blocked in 0.1% casein/Tris buffered saline (TBS) for 1 h, incubated with appropriate primary antibodies for overnight at 4°C, and after, incubated with secondary antibodies conjugated with IRDye 800 (Rockland Immunochemicals, Gilbertsville, PA) or Alexa Fluor 680 (Invitrogen, Carlsbad, CA) for 1 h at room temperature. Membranes were washed three times with TBS including 0.1% Tween20 at 5 min intervals, and were visualized using an Odyssey Infrared Imaging System. Each experiment was repeated at least, twice. Only samples from 3PP and 4PP were analyzed because of the prominent difference in the initial cell proliferation assays.

Measurement of reactive oxygen species (ROS)

ROS production was evaluated similar to that described by the DCFDA Cellular ROS Detection Assay Kit (Abcam, Cambridge, UK), using 2',7'-dichlorodihydrofluorescein diacetate (DCFDA) as a fluorescent probe. Cells were plated in a density of 3.0 x 10^4 cells/well in a 96-well clear-bottom black plate. After treatments time (4 h and 24 h) cells were incubated with DCFDA (25 µM in PBS) in darkness for 45 min at 37 °C. After incubation, cells were washed and the fluorescence was measured (excitation/emission = 485/535 nm) using a Biotek Synergy H1 Hybrid Reader (Biotek, Winooski, USA). At the same time cell viability for the same treatments were done by MTT. The fluorescence intensity was calculated in relation to the correspondent cell viability after treatments.

Water-soluble fraction characterization

Monosaccharide analysis

Samples of WSF from papaya were carboxyl-reduced with $NaBD_4$ after activation with carbodiimide, as described by Kim and Carpita (1992) [29] and modified by Carpita and McCann (1996) [30]. The sugar alditol acetates were prepared according to Gibeaut and Carpita (1991) [74]. Derivatives were separated by gas-liquid chromatography (GLC) on a 0.25-mm x 30-m column (SP-2330, Supelco, Bellefonte, PA). Temperature was held at 80 ºC during injection, then ramped to 170 ºC at 25 ºC·min^{-1}, and then to 240 ºC at 5 ºC·min^{-1}, with a 10 min hold at the upper temperature. Helium flow was 1 mL min^{-1} with splitless injection. The electron impact mass spectrometry (EIMS) was performed with a Hewlett-Packard MSD at 70 eV with the temperature source at 250 ºC. The proportion of 6,6-dideuteriogalactosyl was calculated using pairs of diagnostic fragments (*m/z* 187/189, 217/219 and 289/291) according to Kim and Carpita (1992) [29].

Linkage analysis

For linkage analysis 1 mg of WSF was per-*O*-methylated according to Gibeaut and Carpita (1991) [31]. The partially methylated alditol acetates were separated on the same column as the alditol acetates. After a hold of 1 min at 80 ºC during injection, the derivatives were separated in a temperature program of 160 ºC to 210 ºC at 2 ºC·min^{-1}, then to 240 ºC at 5 ºC·min^{-1}, with a pause of 5 min at the upper temperature. All derivative structures were confirmed by electron-impact mass spectrometry [32].

Homogeneity and molecular weight

Molecular mass distribution of the papaya WSF was analyzed by high performance size exclusion chromatography coupled to a refractive index detector (HPSEC-RID) using a 1250 Infinity system (Agilent, Santa Clara, CA). Samples were diluted with water (1 mg/mL), injected (25 µL) and separation was conducted through four PL aquagel-OH MIXED-M (300 x 7.5 mm, 8 µm) columns in tandem (Agilent, Santa Clara, CA). The eluent was 0.2 M $NaNO_3$ at 35 °C with a flow of 0.6 mL·min^{-1}. Molecular weights were

estimated using dextran T-series (5, 25, 50, 80, 150 and 410 kDa; Fluka^{TM}) as external standards.

Determination of Degree of O-Methyl Esterification

Lyophilized samples were used to determine the degree of *O*-methyl esterification using a Bruker Alpha Fourier Transform-Infrared (FTIR) spectrometer (Bruker Optic GmbH, Ettlingen, Germany), equipped with deuterated triglycine sulfate (DTGS) detector and a single bounce attenuated total reflectance (ATR) accessory (diamond crystal). FTIR–ATR spectra were obtained with 4 cm^{-1} resolution and a total of 50 scans were co-added. The spectra were analyzed with the GRAMS/AI (v. 9.1) package (Thermo Scientific). Methyl esterified and free uronic acids correspond to the band areas at 1749 cm^{-1} and 1630 cm^{-1}, respectively. Pectins of known degrees of *O*-methyl esterification (Sigma) were analyzed and a standard curve was constructed according to Manrique and Lajolo (2002)[76] to determine the degree of *O*-methyl esterification of papaya pectin.

Atomic force microscopy (AFM)

Aqueous samples (5 µL of concentration 2.5 µL/mL) were sonicated, drop deposited on freshly cleaved mica and dried over in vacuum at 30 ºC for 20 min. The samples were maintained in desiccator until analysis. Topography images were obtained in a NX-10 Atomic Force Microscope (Park Systems, Suwon, South Korea) in an acrylic glove box with controlled temperature (around 22 °C) and humidity (around 3%). AFM imaging was acquired at tapping mode using a NCHR probe (NanoWorld) with a spring constant of 42 N/m and 320 kHz resonance frequency. The imaging was obtained with a scan speed of 0.5 Hz with a scanning resolution of 512 x 512 points. For each sample, at least 10 images were collected. Image measurements and automatic processing (plane subtraction and rows alignment) were performed using Gwyddion 2.47 software (http://gwyddion.net/).

Oligosaccharides qualitative analysis

Papaya pectin solutions (1 mg/mL) were analyzed using a PA1 pellicular anion-exchange analytical (Dionex, 250 × 4 mm) column with its respective guard column in a ICS5000+ HPAEC-PAD System (Thermo-Dionex) with a gold working electrode and an

Ag/AgCl reference electrode and an AS-AP autosampler to detect cell wall polysaccharides oligomers. NaOH 100 mM was used as eluent, with a 50 mM NaOAc gradient from 50 to 600 mM starting at 5 min and ending at 25 min. Column temperature was set in 30 °C and a cleaning step of 10 min of NaOH 50 mM containing 600 mM of NaOAc was added.

Statistics

The results were expressed as the mean ± standard deviation (SD). Data were analyzed using GraphPad Prism version 6.0 software (GraphPad Software, San Diego, CA using one-way ANOVA with Tukey's (to assess differences between all groups) or Dunnett's (to assess differences between the control and two or more groups) post hoc tests. Values of $P < 0.05$ were considered as statistically significant.

Results

Papaya pectin from different ripening stages induces death of cancer cells at different levels

The three cell lines used in this work showed different responses to papaya pectin treatment based on their different types of mutations and different grades of aggressiveness. HCT116 is $KRAS^{G13D}$, HT29 is $BRAF^{V600E}$ and PC3 is *KRAS* and *BRAF* wild type and possess a mutation on p53, though [33,34]. HCT116 has an undifferentiated phenotype with a high metastatic potential and an unstable adherent junctions [35]. In turn, HT29 is differentiated with less aggressive behavior [36]. PC3 cells represent very aggressive forms of prostatic adenocarcinoma [37].

The 1PP, 2PP, 3PP and 4PP were screened for viability of HCT116, HT29 and PC3 cancer cells lines (**Figure 1**). 3PP and 4PP induced very distinct effects in cells viability after 24 h of treatment (**Figure 2**). 3PP (0.20%) induced the highest decrease on cells viability, significantly higher when compared to 4PP (0.20%; **Figure 2A)**. 3PP was cytotoxic for all cells whereas 4PP was not (**Figure 2B**). Because of these striking results with age-dependent changes on the biological effects of pectin, subsequent experiments on cancer cells were done with the 3PP and 4PP at 0.20%.

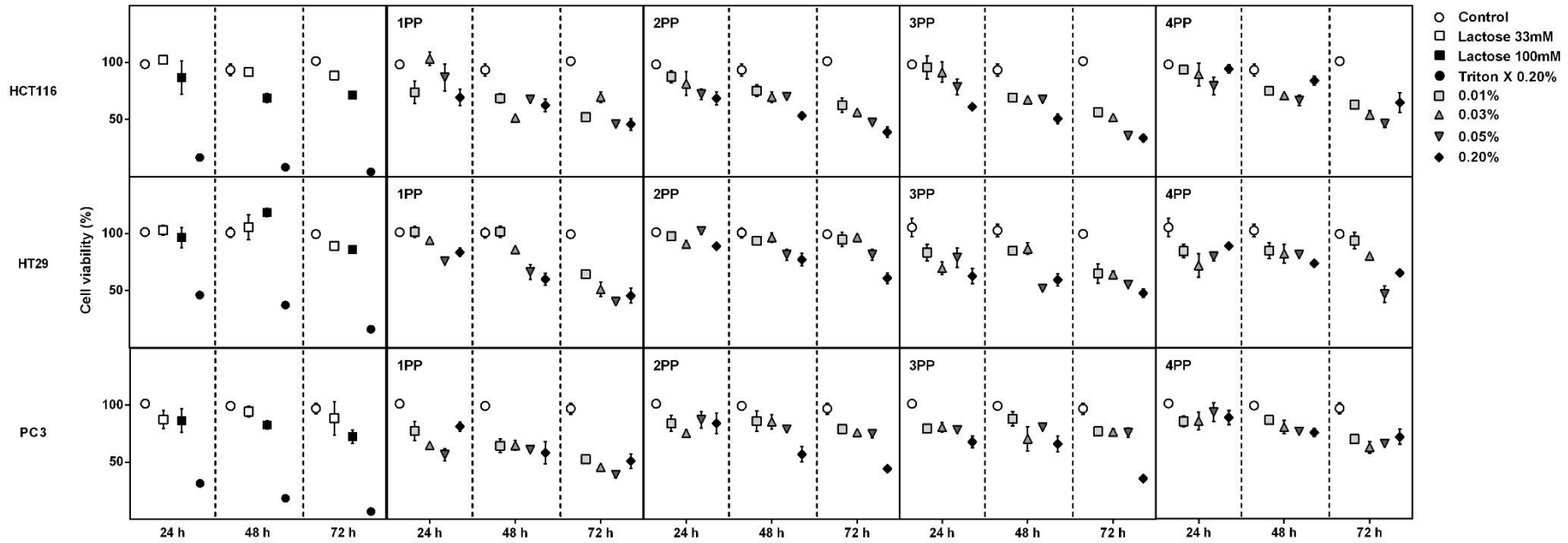

Figure 1. Effects on cell viability of papaya pectin treatment in HCT116, HT29 and PC3. Cells were treated with papaya pectin at different dosages. Papaya pectin decreased HCT116, HT29 and PC3 viability at different levels. The results were expressed in percentage of cell viability in comparison with control (no treatment) of which time. Data were shown as mean ± SD. *P < 0.05 vs control, according to Dunnetts's test. The results were from three independent WSF samples (each one performed in technical triplicate) from the biological duplicate (n = 6). PP: papaya pectin (water-soluble fraction).

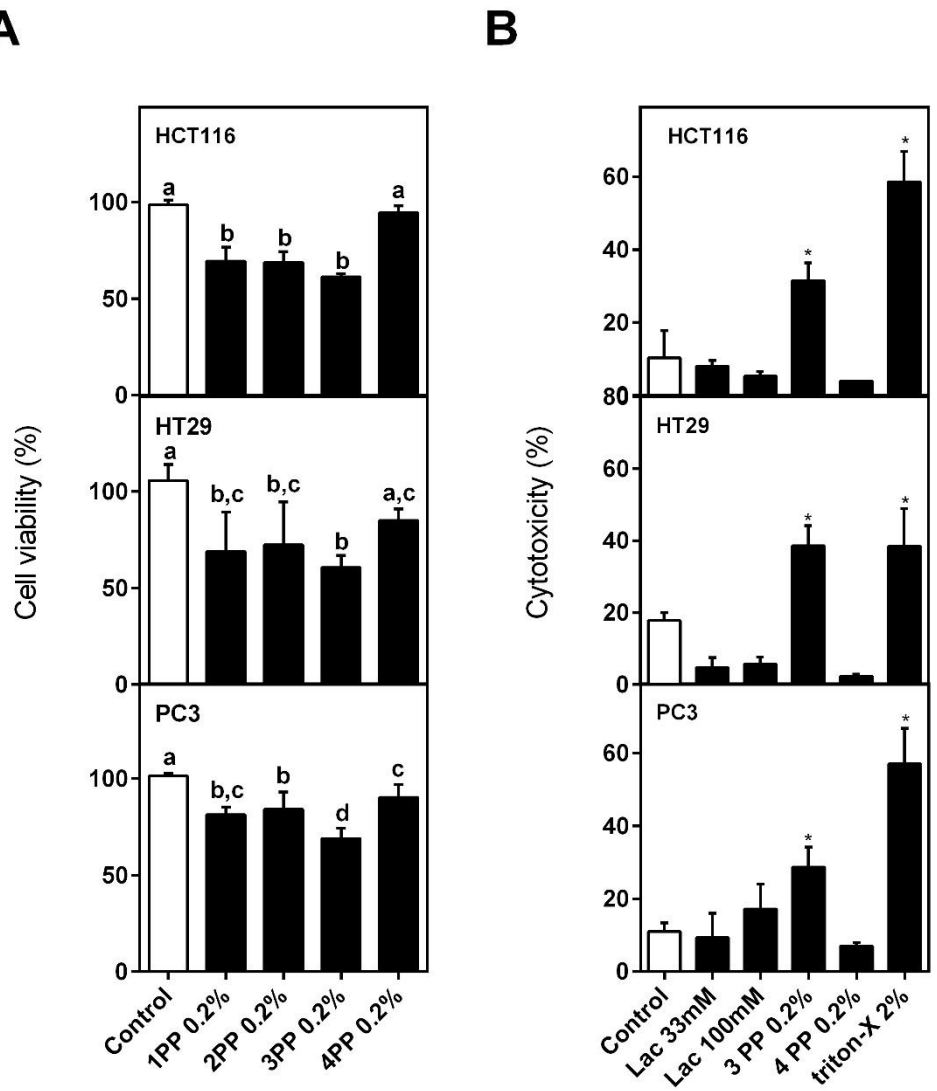

Figure 2. Effects on cell viability and cytotoxicity. A) Effects on cell viability of the higher concentration of papaya pectin t24 h. 3PP strongly reduced cell viability and 3PP and 4PP showed the most distinct results. Data were shown as mean ± SD. Tukey's test (*P < 0.05) was performed. Different letters represent significant differences between the treatments (as previously explained in Figure 1). B) Cytotoxicity by LDH assay after 24 h of incubation. 3PP and not 4PP induced cell cytotoxicity. The results were expressed in percentage of cell viability in comparison with control (no treatment) of each time. Results were represented as mean ± SD (as previously explained in Figure 1). *P < 0.05 vs control, according Dunnetts's test. PP: papaya pectin (water-soluble fraction).

3PP inhibits cancer cells aggregation and migration

Beta-D-lactose (in 100mM concentration) is widely used as a non-cytotoxic cell aggregation inhibitor or apoptosis-inducing in the cancer cells in these experiments (**Figure 2B**; **Supplementary Figure S3**) [38,39]. 3PP and β-D-lactose (100mM) inhibited the homotypic aggregation for all cell lines with HCT116 and PC3 cells showing the highest inhibition rates (**Figure 3A, Supplementary Figure S1**), indicating a possible interaction between 3PP sample with cancer cells. PC3 cells showed lower rates of aggregation after 3PP treatment rather than β-D-lactose and the inhibition of cell aggregation by 3PP treatment was higher than 4PP for all evaluated cell lines. Moreover, cancer cells were assessed for inhibition of migration after papaya pectin treatments. Because growth and spread of cancer cells is dependent on the interaction between cancer cells and endothelial cells [40,41] it was tested the interaction of endothelial cells BAMEC (bovine adrenal medullary endothelial cells) with cancer cells, as well as the interaction between cancer cells in the wound-healing experiments (**Figure 3B, C, Supplementary Figure S2**). Compared with the control (no treatment), 3PP treatments showed the slowest cell migration for endothelial cells and slower gap closing in wound healing assay after 24 h. 4PP treatment had only slowed cancer cell migration in direction of BAMEC for HCT116 cell treatments and had significantly diminished gap closing for PC3 cells, but with slower rates than for 3PP.

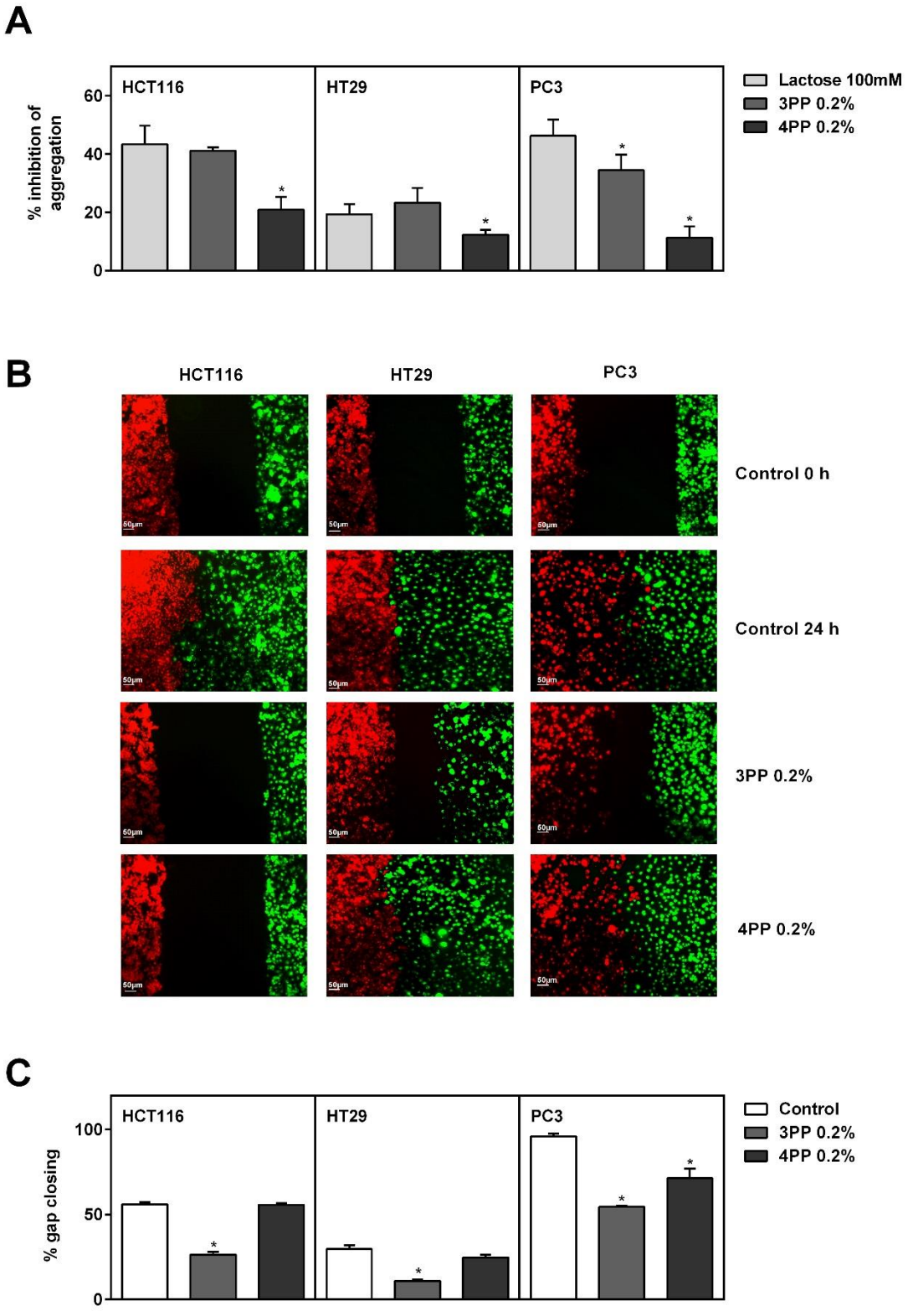

Figure 3. Homotypic aggregation and migration assays (wound healing and endothelial vs cancer cells). A) Inhibition of homotypic cell aggregation using asialofetuin treated with lactose or papaya pectin at 0.2%. 3PP strongly inhibited cancer cells

aggregation. The results were expressed in percentage of cells in relation to control (with asialofetuin and no treatment). Data were shown as mean ± SD from two independent WSF samples, each one performed in technical duplicate, from the biological duplicate (n = 4). *P < 0.05 vs lactose, according to Dunnetts's test. Images of homotypic aggregation test were in supplementary figure S1. B) Endothelial cells (BAMEC) dyed with DiO (green) and cancer cells dyed with DiI (red). 3PP diminish the interaction between cancer cells and BAMEC. Scale bar: 50 μm. Representative image of, at least, two experiments from the biological samples. C) Quantification of gap closing after 24 h. 3PP slowest gap closing compared with control and with 4PP. The results were expressed in percentage of cells that invaded the gap compared with control. Data were shown as mean ± SD (as previously explained in Figure 3A). *P < 0.0001 vs control (without treatment), according to Dunnetts's test. Images of wound healing were in supplementary figure S2. PP: papaya pectin (water-soluble fraction).

Papaya pectin affects interaction between cancer cells and extracellular matrix proteins

An evaluation of interactions of cancer cell lines with ECM proteins laminin, collagen IV and fibronectin was performed to evaluate if papaya pectin were disturbing cancer cells attachment. In this assay, the numbers of cells that could bind to the ECM proteins pre-coated on cell culture plates and cells viability were assayed. Untreated cells were the control (100% viability/attachment), and cells poured in BSA-coated wells were the negative control of interaction (without proteins of ECM). All treatments lowered cell interactions with ECM proteins significantly from untreated control cells, indicating that papaya pectin affected interactions between cancer cells and ECM proteins (**Figure 4**). As lactose is known to interact with galectins to inhibit binding of ECM proteins to cancer cells, data from papaya samples were statistically compared with β-D-lactose treatment. Behaviors of HCT116 cells with 3PP were equal to those treated with lactose treatment for attachment of viable cells to all ECM proteins tested, except for fibronectin in HT29 cells and collagen IV in PC3 cells, where affects were lower than with lactose. 4PP treatments yielded equal or significantly higher attachment than did lactose, indicating they were less effective in inhibiting interactions of cancer cells and ECM proteins. Notably, the lowest attachment values from the interaction between fibronectin and HCT116 and HT29 cells, and between collagen IV and PC3 cells, predict interference of papaya pectins extracted

from the third day after harvesting (3PP) on binding of ECM proteins to cancer cells, possibly resulting in cell detachment and cell death during growth.

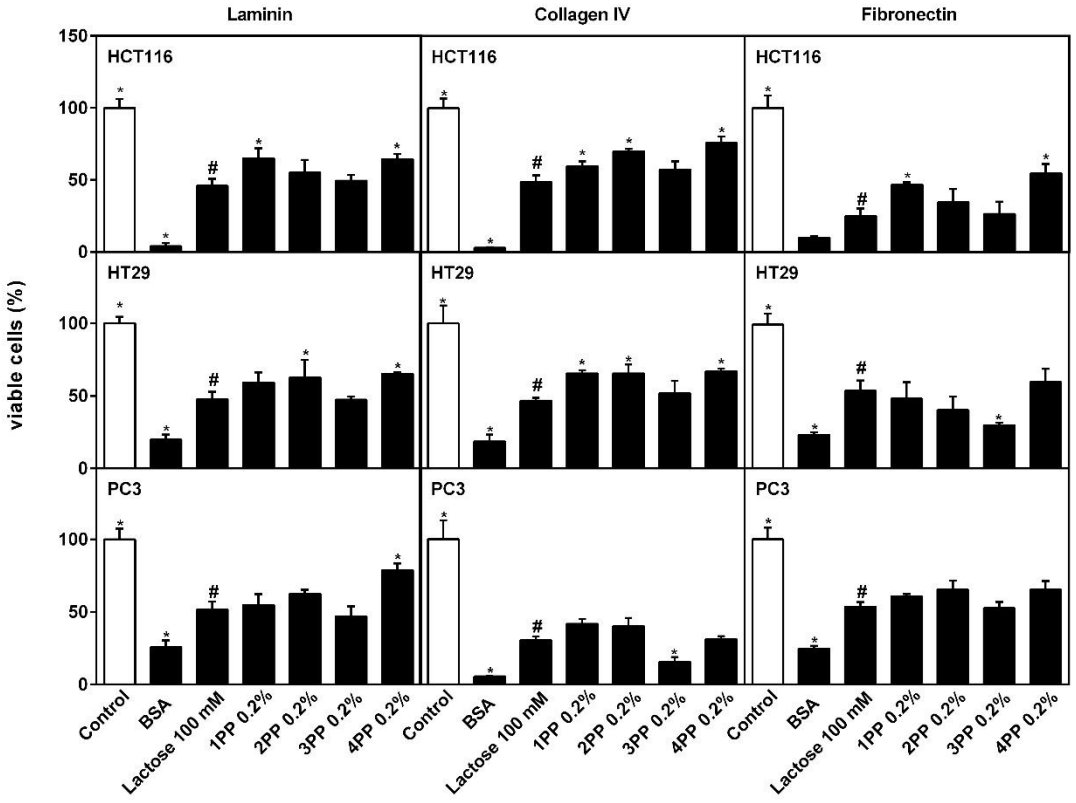

Figure 4. Extracellular matrix proteins (laminin, collagen IV and fibronectin) interactions with cancer cells lines with ou without papaya pectin treatment. Papaya pectin affects interaction between cancer cell and proteins from ECM. The results were expressed in percentage of cells in comparison with control. Data were shown as mean ± SD from two independent WSF samples, each one performed in technical quadruplicate, from the biological duplicate ($n = 4$). All treatments were significant different from control (Dunnetts's test). All samples were compared with lactose (#) by Dunnetts's test and significant differences ($P < 0.05$) are marked with an asterisk. PP: papaya pectin (water-soluble fraction).

‘3PP’ induces late apoptosis/necroptosis on cancer cells

To explore by which mechanisms papaya pectin induced cancer cells death, a flow cytometry analysis was performed in order to verify cell viability and the induction of cell apoptosis, late apoptosis/necroptosis and necrosis through PE Annexin V and/or 7-AAD staining and results were compared to the Western Blotting analysis. 3PP showed higher amounts of late apoptosis/necroptosis events (**Figure 5**). In addition, the decrease on cell viability was stronger on HCT116 and HT29 cells. In contrast, 4PP and lactose had no effects when compared to control (**Figure 5, Supplementary Figure S3**). Differential protein blotting indicated that the anti-cancer mechanism of papaya pectin varied among different cell lines (**Figure 6**). The induced apoptosis after 3PP treatment in HCT116 could be related with caspase 3 pathways activation, despite the fact that 4PP treatment also induced caspase 3 and did not show significant apoptosis. The 3PP treatment increased phosphorylated Akt (pAkt) and phosphorylated Erk1/2 (pErk1/2) protein levels in HCT116 cell line, whereas the opposite effects were observed in HT29 cells. Increased expression of pAkt and cell death for HCT116 cells after 3PP treatment might be related to rapid reactive oxygen species (ROS) accumulation [42]. After 4 h and 24 h of treatment, ROS accumulation was significantly higher in 3PP (**Supplementary Figure S4**). 3PP, and to a lesser extent 4PP, decreased pAkt and increased p21 expression in PC3 cells. Intracellular quantities of galectin-3 were not affected by treatments. Action of papaya polysaccharides on extracellular area likely do not influence endogenous galectin-3 expression in a short period of time (24 h treatment).

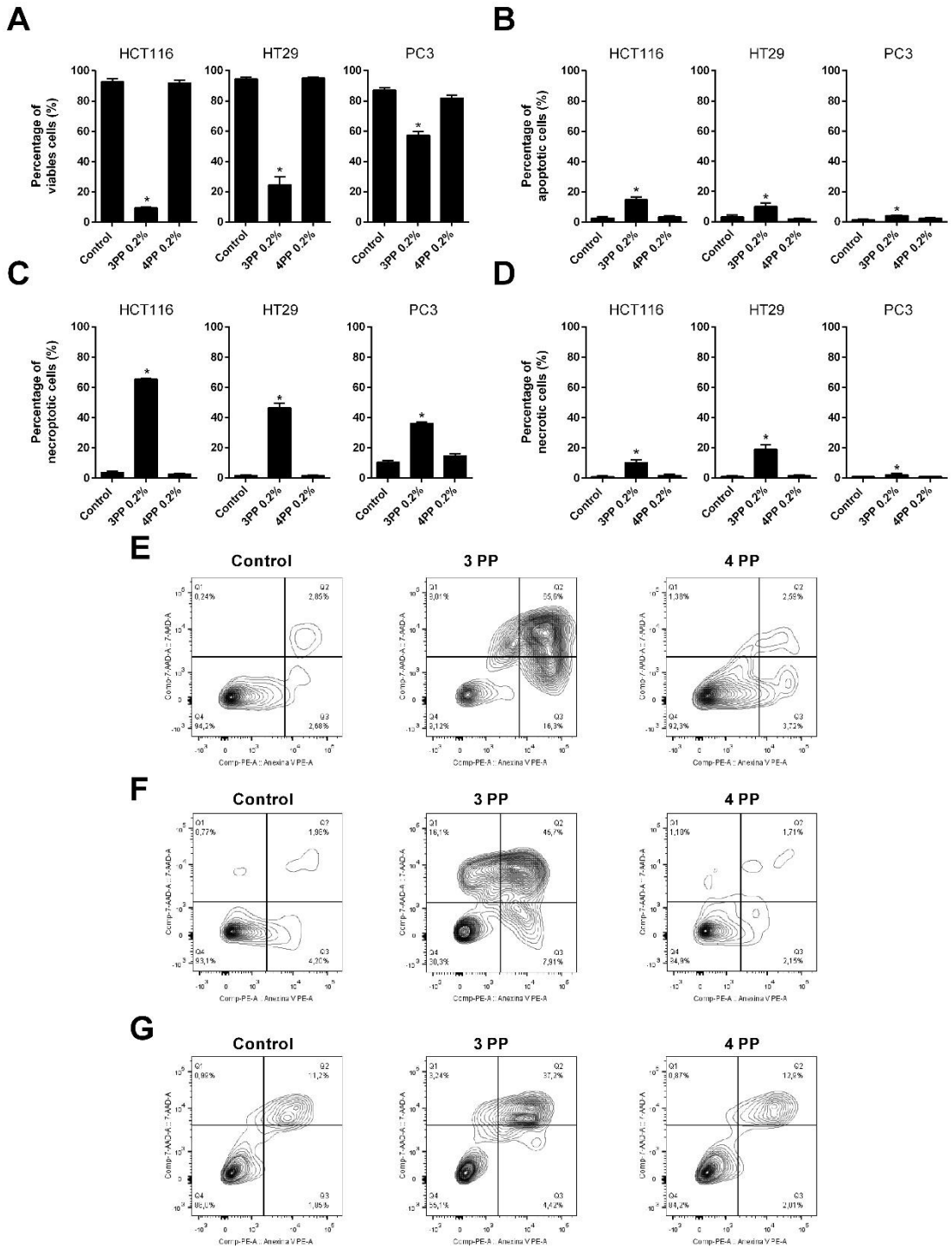

Figure 5. Effects of papaya pectin in HCT116, HT29 and PC3 apoptosis by flow cytometry. Cancer cells had induced late apoptosis/necroptosis with 3PP. Cells were treated with 0.20% of 3 PP and 4 PP pectin for 24 h. A) Percentage of viable cells. B)

Percentage of apoptotic cells. C) Percentage of necroptotic cells. D) Percentage of necrotic cells. E) Flow cytometry plots of HCT116. F) Flow cytometry plots of HT29. G) Flow cytometry plots of PC3. The results were expressed in percentage of cells in comparison with control (no treatment). Results were represented as mean ± SD of two independent WSF samples, each one performed in technical triplicate, from the biological duplicate (*n* = 4). *P < 0.05 vs control, according to Dunnetts's test. PP: papaya pectin (water-soluble fraction).

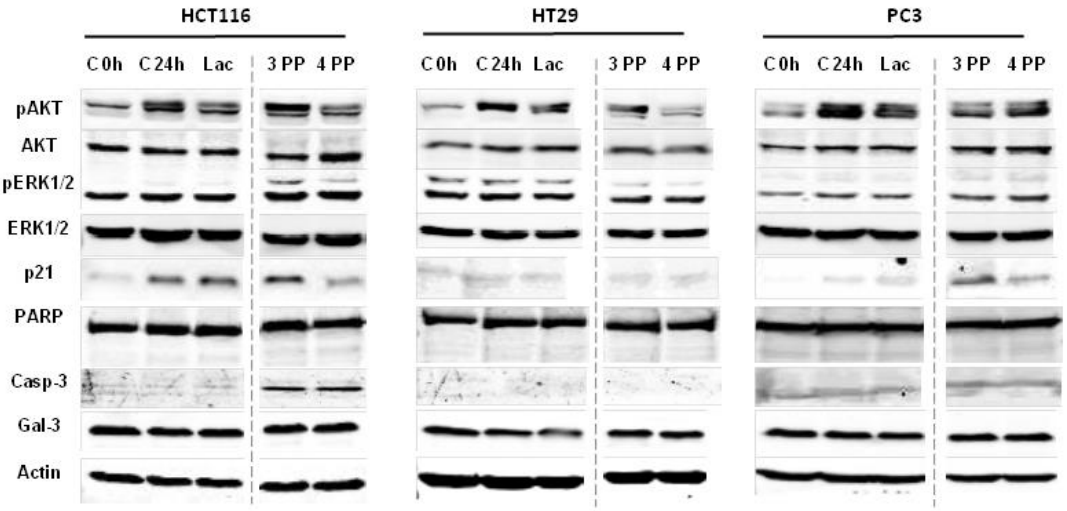

Figure 6. Western blot analysis. Mechanisms of papaya pectin vary among different cell line. Cell lysates were prepared and processed for western blot assay after 24 hours of treatments. After BCA assay, equal amounts of proteins were separated using SDS-PAGE. β-actin was used as the loading control. PP: papaya pectin (water-soluble fraction).

Papaya pectin characterization

The extraction yields and water-soluble papaya pectic polysaccharides structures were evaluated during the four phases of ripening. Total cell wall yields (TCW) were unchanged throughout ripening. Soluble pectins extracted from different ripening stages increased sequentially from 4.1 ± 1.7% of TCW at phase 1, 12.3 ± 3,3% at phase 2, 25.1 ± 3,7% at phase 3 and 28.7 ± 1.9% at phase 4. Molecular weight distributions analyzed by HPSEC-RID showed that polysaccharides from 1PP and 2PP had similar profiles, but with higher molecular weights, 888 ± 56kDa and 298 ± 10kDa, respectively, compared to 102 ± 5kDa and 96 ± 2kDa for 3PP and 4PP (**Figure 7A** and **B**). Papaya pectin comprised mostly

GalA, Gal, Rha and Ara, demonstrating those fractions were mainly formed by pectin (**Figure 7C**). The amounts of GalA and Rha in the solubilized fractions increased throughout ripening, while amounts of Gal and Ara decreased. The degree of esterification has also increased during the course of ripening (**Figure 7D**), demonstrating that pectinesterases (PME) are not actively de-methylating pectins after fruit harvesting, corroborating what it has already been proposed elsewhere [25]. This increase in methylation could be explained by the enrichment of pectins in water soluble fraction after being solubilized from insoluble fractions after massive action of polygalacturonases as it had already been stated[25,26]. Linkage analysis (**Figure 7E; Table S1**) revealed a high proportion of *4*-GalA indicating higher presence of HG with reasonable amounts of *2,4*-, *3,4*-, *4,6*-GalA and *2*-, *2,4*-Rha linkages that are related to the RG-I presence and *3,4*-GalA indicating the presence of xylogalacturonan[43]. RG-I galactans side-chains were found by the identification of *4*-, *3,4*- and *4,6*-Gal linkages. Type II arabinogalactans (AGII) appear to be the predominantly ramification of RG-I in papaya pulp pectin structures. AGII structures consist in backbones of *1,3*- β-D-and *1,6*-β-D-galactan chains with *3,6*-Gal branch points and substituted with mostly *t*-Ara*f* at *O*-6 and *O*-3 position of the available Gal residues [44]. To estimate the variation ratios of HG and RG-I regions during ripening, data from monosaccharide composition and linkage analyses were summed and compared as GalA:Rha ratio for proportions of HG and RG-I, and Gal:Rha and Ara:Rha ratios for proportions of neutral sugars side chains attached to RG-I (**Table I**). The decrease in the ratio of GalA:Rha during ripening indicated an increment of RG-I papaya pectin from ripen fruits. In contrast, Gal:Rha and Ara:Rha decreased during ripening, and this decrease was accompanied by a decrease in proportions of *4*-Gal and *3,4*-Gal, indicating loss of galactan and type I arabinogalactan side-chains of RG-I. Persistence of *t*-Ara*f* and 5-Ara*f* during ripening demonstrated selective arabinogalactan/arabinan depolymerization by an arabinofuranosidase. The highest amounts of *2*- and *2,4*-Rha in the soluble fractions of 3PP and 4PP, and increased ratios of *2,4*-Rha:*2*-Rha during ripening indicated that the RG-I backbone was depolymerized and solubilized to a greater extent than was HG [26]. Ratios of *3*-, *6*-, and *3,6*-Gal:*t*-Gal were lowest in 3PP and 4PP, indicating smaller sizes of AGII. The lowest ratio of *4*-, *2,4*, and *3,4*-GalA:*t*-GalA in 3PP demonstrated that HG backbone was shortest in 3PP than in 4PP.

Because size distributions and branching patterns varied widely among 1PP and 3PP, we investigated their ultrastructural features through atomic force microscopy in order

to compared unripe and ripe fruits with or without biological activity. Side chains were not easily visualized even at higher magnification (1 μm × 1 μm), probably because of the relatively high predominance of HG on papaya pectin (**Figure 8**)**.** 1PP was characterized by linear chains and micellar aggregates **(Figure 8A)**, and 3PP showed a decrease in chain length and micellar aggregates **(Figure 8B)**. The height profile was similar in both samples, but the higher weight of profile 3 in 1PP sample indicates larger micellar aggregates. Length histogram clearly shows higher frequency of smaller lengths around 50 nm in 3PP.

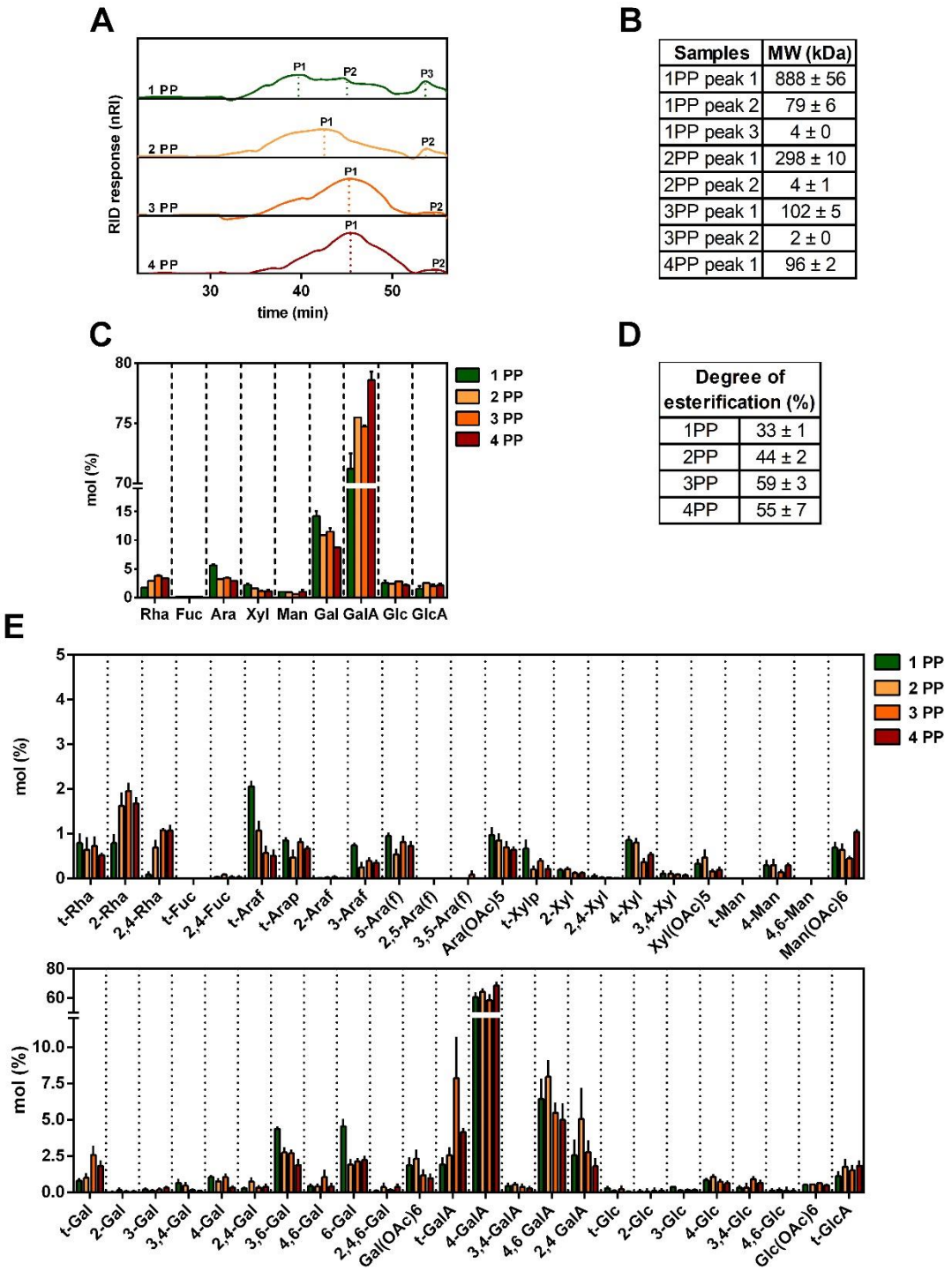

Samples	MW (kDa)
1PP peak 1	888 ± 56
1PP peak 2	79 ± 6
1PP peak 3	4 ± 0
2PP peak 1	298 ± 10
2PP peak 2	4 ± 1
3PP peak 1	102 ± 5
3PP peak 2	2 ± 0
4PP peak 1	96 ± 2

Degree of esterification (%)	
1PP	33 ± 1
2PP	44 ± 2
3PP	59 ± 3
4PP	55 ± 7

Figure 7. Profile and composition of water-soluble fraction isolated from papaya during 4 days after harvesting. A) HPSEC-RID elution profile. 1PP and 2PP had similar profiles and higher molecular weight compared to 3PP and 4PP. B) Molecular weight was estimated using a standard curve of dextran T-series (5, 25, 50, 80, 150 and 410 kDa; technical triplicate, from the biological duplicate). C) Monosaccharides composition.

Papaya pectin is composed mainly by GalA, Gal, Rha and Ara, at different proportions depending on the ripening stage. Results represents mean ± SD (at least seven technical replicates from a pooled WSF triplicate from the biological duplicate; $n \geq 7$). D) Degree of O-Methyl Esterification. Papaya pectin had esterification increased during ripening. Values were calculated using the calibration curve ($R^2 = 0.9798$) and results are expressed in mean ± SD (three technical replicates from a pooled WSF triplicate from the biological duplicate; $n = 3$). E) Water-soluble fraction polysaccharides linkage analysis. Papaya pectin 4-GalA indicates presence of homogalacturonan with reasonable amounts of 2,4-, 4,6-GalA and 2-, 2,4-Rha linkages that are related to type I rhamnogalacturonan. Error bars indicate SDs of the mean (at least seven technical replicates from a pooled WSF triplicate from the biological duplicate). The table of likage results was in Supplementary table 1. Rhamnose (Rha); fucose (Fuc); arabinose (Ara); xylose (Xyl); mannose (Man); galactose (Gal); Galacturonic acid (GalA); glucose (Glc); glucuronic acid (GlcA); terminal (t); pyranose (p); furanose (f). PP: papaya pectin (water-soluble fraction).

Table 1. Monosaccharide and linkages ratios of water-soluble fraction isolated from papaya during 4 days after harvesting.

	Ratio of monosaccharides			Ratio of linkage analysis				
	GalA:Rha	Gal:Rha	Ara:Rha	totalGalA: *t*-GalA	*4-,2,4,3,4*-GalA: *t*-GalA	*3-,3,4-,4-,4,6-,3,6-,6*-Gal: *t*-Gal	*2,4*-Rha: *2*-Rha	*3-,6-, and 3,6-Gal: t-Gal*
1 PP	41.9	8.4	3.3	36.0	33.1	14.0	0.1	11.5
2 PP	26.0	3.8	1.1	30.0	27.2	6.0	0.4	4.8
3 PP	19.7	3.0	0.9	9.0	7.8	3.0	0.6	1.9
4 PP	23.8	2.6	0.9	18.0	17.0	3.0	0.6	2.4

Rhamnose (Rha); fucose (Fuc); arabinose (Ara); xylose (Xyl); mannose (Man); galactose (Gal); Galacturonic acid (GalA); glucose (Glc); glucuronic acid (GlcA); terminal (t); pyranose (p); furanose (f). PP: papaya pectin (water-soluble fraction).

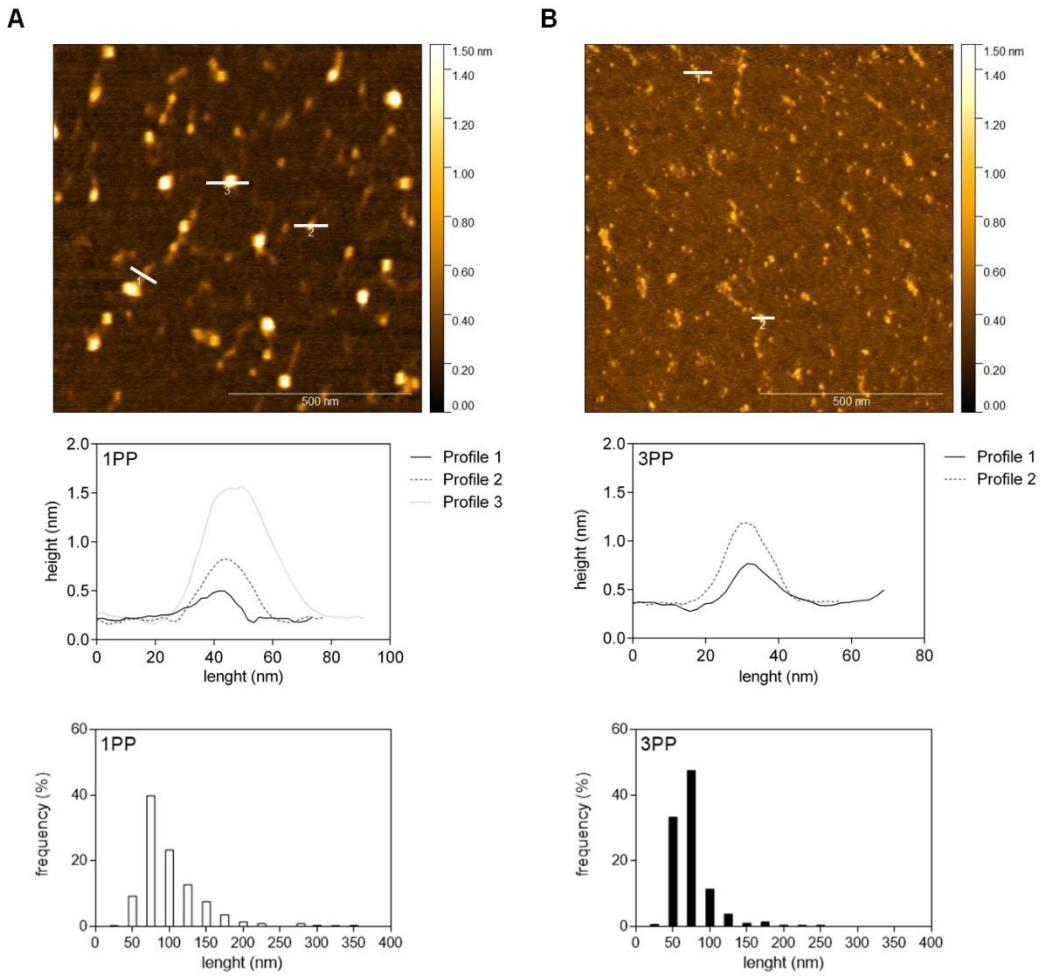

Figure 8. Representative topographical AFM images of papaya water-soluble pectins. A) 1PP sample topography, height profile and length frequency. 1PP had linear chains and micellar aggregates. B) 3PP sample topography, height profile and length frequency. 3PP had both chains length and micellar aggregates decrease. PP: papaya pectin (water-soluble fraction). Representative image of, at least, two experiments from the biological samples.

Discussion

The softening of papaya fruit is a complex process that occurs during fruit ripening, being coordinated by the action of several cell wall degrading enzymes [25]. In a previous study, we identified a mobilization of high molecular weight pectin from less soluble to more soluble fractions during the papaya ripening because of pectin modification by endogenous pectinolytic enzymes [26]. Several studies have attributed anti-cancer activities to pectins which have been thermally, chemically or enzymatically modified

[6,14,16,45–48]. The pectin structure described as responsible for anti-cancer activities are the galactan and arabinan side-chains together with an RG-I/HG backbone [6]. In this regard, papaya pectin previously isolated from different ripening stages seems to have a promising composition concerning the presence of galactans, arabinans, RG-I and HG structures [24,26]. To explore the biological activity of papaya pectin naturally modified by ripening phenomenon, three cancer cell lines were treated with water-soluble papaya pectin extracted from fruits in distinct ripening stages. Initially, papaya pectins were screened for their biological activity on cancer cells. Following this, the mechanisms by which papaya pectins affected the behaviors of cancer cells were explored. Finally, papaya pectins were identified and chemically characterized to pinpoint possible structure-activity relationships.

In a previous work, the key enzymes responsible for physiological degradation of papaya pectins in fruit cell wall were endo-polygalacturonases and exo-galactosidases [25]. Besides, endo-polygalacturonases overexpression during papaya ripening solubilized pectin from the less soluble fractions yielded incremental increases of GalA during ripening [26]. The action of endo-polygalacturonases and exo-galactosidases could explain why *t*-GalA and *t*-Gal linkages increased during ripening. Endo-polygalacturonases would hydrolyze HG in smaller chains, increasing *t*-GalA, while exo-galactosidases could cleave terminal sites of AGII or RG-I thus increasing *t*-Gal and decreasing Gal. Ara also decreased during ripening, while *2*- and *2,4*-Rha and the ratio *2,4*-Rha:*2*-Rha increased, indicating the presence of smaller chains of more highly branched RG-I. This is the first academic report of AGII structures in papaya pulp. Decreased *4*-Gal and *3,4*-Gal indicate less branching with *4*-galactan and type I arabinogalactan side-chains. The increased *2*- and *2,4*-Rha and ratio of *2,4*-Rha:*2*-Rha during ripening has two possible explanations. Firstly, RG-I depolymerization at the unbranched *2*-Rha linkages through the action of rhamnogalacturonan hydrolases or rhamnogalacturonan lyases (RGases) would shorten chains and increase the ratio of branched to unbranched Rha, but these genes/enzymes have never been identified in papayas. Secondly, as previously reported by our group [26], enhanced of solubility of HG and RG polysaccharides during ripening occurs. In addition, the significant increase of GalA may have proportionally reduced the Gal and Ara amounts. Besides, the higher expression of an L-arabinofuranosidase during the early days before harvesting [25] could be responsible for *t*-Araf decreases.

Samples from 1PP had the highest Gal and Ara amounts and the highest proportion of linkages related to AGII. 1PP had also the highest total GalA:*t*-GalA ratios, indicating larger chains of HG and RG-I. The relatively high molecular weight with the lowest yields and difficulty of solubilization of 1PP and 2PP is likely to have interfered with these pectins ability to interact with cancer cells, thus decreasing their biological activity. On the other hand, as described above, the decreased values of total GalA:*t*-GalA ratios in 3PP samples indicated smaller chains with reduced side-chains, thus increasing possible interactions with cancer cells.

Unexpectedly, 4PP had the least anti-cancer activity among all papaya pectins. The reduced anti-cancer activity of 4PP seems to be related to an increment of the total GalA:*t*-GalA ratio as well as the increase of total GalA, indicating higher amounts of longest HG chains when compared to 3PP. The massive endo-polygalacturonase action during fruit ripening can result in the addition of HG in 4PP as endo-polygalacturonases hydrolyze pectins from the less soluble fraction (the ones chelated with calcium with fewer neutral sugar ramifications) to the water-soluble fraction, as previously shown by our group [26]. A qualitative analysis for oligosaccharides was done in order to visualize this massive endoPG activity and the possibility of being some specific oligo that conferred the anti-cancer activity to 3PP. **Figure S6** shows 4PP presented a broader detection of oligosaccharides than other pectin fractions with slightly differences, though. This could endorse the generation of oligosaccharides throughout ripening but this was not responsible for the *in vitro* biological activity observed. Contents of starch, proteins and phenolic compounds in the water-soluble fractions of these papaya pectin fractions were insignificant.

Ultrastructural analysis by AFM confirms that 3PP had smaller backbones when compared to 1PP. The micellar aggregates observed mainly in 1PP are characteristic of polymers complexes held together by intermolecular interactions showing pectin heterogeneity and complexity [49]. In a study with strawberry, pectins treated with endo-polygalacturonases showed a decrease in micellar aggregates length, distribution and branching patterns [50]. Thus, the increase of endo-polygalacturonases action during papaya ripening could be responsible for decreasing the pectin length and the micellar aggregates in 3PP. The branched fractions could not be visualized by AFM, because papaya

pectins were mainly composed by linear GalA (HG) and the length of neutral sugars branch were not long enough to be easily visualized [51].

The majority of colorectal cancer cells (53%) show mutation on KRAS, being characterized by the activation of both mitogen activated protein kinase (MAPK) and phosphoinositide 3-kinase (PI3K) signaling pathways [33]. HCT116 had KRAS mutation and possess high metastatic potential compared with HT29 [35,52]. PC3 cells had p53 mutation that are more common in prostate cancers of higher tumor stage and metastases [53]. Therefore, cell treatments in the present work could simulate a local effect of papaya pectin ingestion (HCT116 and HT29) or a possible systemic effect (PC3), with results being cell-line dependent.

Although 1PP, 2PP and 4PP significantly affected cell proliferation, samples from 3PP have shown the most striking results. Because 3PP and 4PP treatments (0.20%) showed the highest inhibition in the MTT assay, those samples were chosen for further assays. Although size distribution patterns were similar for 3PP and 4PP, deeper structural analysis revealed that 3PP had an addition of smaller HG and higher ramifications proportions. 4PP showed an increase of a larger HG backbone that could explain the weaker results observed in viability assays. Polygalacturonic acid (PGA), an unbranched HG backbone, had no effect on the viability of colon cancer cells [7].

Homotypic aggregation was tested with asialofetuin, a glycoprotein with several branched oligosaccharide side chains with terminal non-reducing galactosyl residues [28]. Asialofetuin binds to the lectins galectin-1 and galectin-3, which are located on the surface of cancer cells, and induces homotypic aggregation by serving as a cross-linking bridge between adjacent cells [12]. All cell lines studied here express galectin-3, which induce cell aggregation by interaction with cancer associated MUC1 (large and heavily glycosylated transmembrane mucin protein) [54]. The homotypic aggregation is associated not only with the tumor formation and anoikis resistance, but also with cancer cells heterotypic adhesion to endothelium stimulating metastasis [55]. β-D-Lactose and 3PP showed the highest inhibition of aggregation, which could be related with galectin interaction. Effects of papaya pectin on cell aggregation were more easily visualized with HCT116 and PC3 cells than with HT29 cells. As mentioned previously, HCT116 and PC3 have higher metastatic

potential that are related with superior ability to form homotypic aggregates when compared with the less aggressive HT29 cells [56].

Compared with 3PP, lactose (100 mM) showed less activity in decreasing viability of cancer cells. Because lactose is a classical galectin-3 inhibitor, other targets of papaya pectin exist in addition to galectin-3. Thus, other potential mechanisms of papaya pectin on cancer cells were also screened. 3PP decreased cancer cell migration (endothelial cells vs cancer cell and wound healing assay) without significantly affecting viability of BAMEC endothelial cells. Curiously, 4PP treatment reduced migration of HCT116 and endothelial cells (BAMEC), but HCT116 cell migrated normally in wound healing experiments. The differences in cell migration could be related to the microenvironment that likely plays a crucial role in tumor growth and metastasis [40,41]. Further study will be necessary to evaluate the effects of papaya pectin on the complex interaction between cancer cells and endothelial cells.

The interaction between cells and the ECM is crucial for cell adhesion and migration. We investigated the cell interaction with three glycosylated proteins that comprise the ECM, laminin, collagen IV and fibronectin. In HCT116 cells, fibronectin seems to plays a major role in cell spreading and migration rather than does laminin and collagen [57]. That HCT116 cells did not adhere to culture plates pre-coated with fibronectin after lactose and 3PP treatments supports this conclusion. This could explain why cells treated with 3PP exhibited decreased cell migration, indicating a 3PP-mediated disruption in the interaction between fibronectin-linked glycans and integrins. In addition, the effect of lactose on HCT116 cells in plates pre-coated with fibronectin could indicate a disruption of fibronectin interaction with galectin-3 that could bias fibronectin function on cell migration. Galectin-3 has been shown to modulate fibronectin tumor cell motility [58]. However, as mentioned above, galectin-3 inhibition might not be the main cause of reduced cell migration after treatment with papaya pectins.

Pectin from the third day after harvesting (3PP) was the most effective treatment to cause cell death, increased expression of pAkt and pErk in HCT116 cells. Higher pAkt and pErk expression is usually related with cell migration and survival [59–61]. PI3K/Akt pathway is likely to be a key mediator of fibronectin-integrin effects on cell proliferation [59], whereas cellular dispersal and motility are known to be mainly regulated by PI3K/Akt

and Erk–MAPK signaling pathways [60,61]. On the other hand, pAkt expression is associated with ROS accumulation [42], and necroptosis can be linked to the metabolic stress caused by partial cell detachment [62], a probable cause that could explain the 3PP-induced cell necroptosis verified in HCT116 cells. The up-regulation of the Erk pathway could also induce cell necrosis by necroptosis or autophagy responses as previously observed in lung cancer cells [63]. Furthermore, HCT116 *KRAS* mutation has been related with inhibition of caspase-3/7 and promotion of cell viability [64]. 3PP and 4PP, but not lactose, had up-regulated cleaved caspase 3 on HCT116 cells, suggesting the induction of apoptosis. Moreover, activation of p21 may have stimulated apoptosis through both p53-dependent and p53-independent mechanisms as it has already been detected under certain cellular stresses [65]. However, because 3PP led to fewer numbers of apoptotic cells than necroptotic cells, the mechanism of why cells have rapidly passed from apoptosis to necroptosis is still elusive but is clearly dependent on papaya pectin structure.

Results from HT29 cells treatment could be explained by other mechanisms. Integrin consists of two subunits (α and β) of proteins tightly associated with each other [66]. The α5β1 integrin is the fibronectin receptor and the interference in the association between subunits decreases protein binding impairing fibronectin-mediated cell adhesion [67]. 3PP reduced HT29 attachment in plates coated with fibronectin, which is highly expressed in HT29 cells and is associated with cancer cell metastasis [68]. In addition, 4PP, and to a lesser extent 3PP, reduced pAkt expression in HT29 cells. Because 3PP had higher inhibitory activity on cell migration than 4PP, pathways other than p-AKT signaling could be involved in reducing HT29 migration and cell death.

3PP treatment reduced PC3 attachment in plates coated with all three ECM proteins with the stronger results on collagen IV interaction. PC3 cell lines express high levels of integrin subunits associated with collagen binding and lower levels of integrin subunits associated with fibronectin binding. This is the main cause for the enhancement of metastasis guided by cell migration [69]. Because 3PP treatment decreased PC3 cell attachment to collagen IV, papaya pectin might disrupt integrin binding to collagen IV. Moreover, 3PP down-regulated pAkt and up-regulated p21 on PC3 cells. For prostate cancer cells, pAkt expression has a pivotal role in cell migration dependent of epidermal growth factor receptor (EGFR) by activating epithelial–mesenchymal transition [70]. Thus, lower levels of pAkt could be associated with reduced PC3 cell migration and increased

cell death. Further, p21 up-regulation in PC3 and in HCT116 cells could be responsible for induction of cell death as it has been observed to glioma and ovarian cancer cells overexpressing p21 [71,72] with a cell-specific sensitivity to oxidative stress, leading to cell death [73].

The variation of biological activities of papaya pectin obtained from different fruit ripening stages is interesting, as the unmodified citrus pectin and unmodified sugar beet pectin have weak activity on decreased viability of cancer cells [6,12]. Decreasing the average molecular weight by high temperature, alteration in pH, or pectinolytic enzymes improve the anti-cancer activities. Low-molecular-weight modified citrus pectins (1% w/v) are associated with the inhibition of gastrointestinal cancer cells growth and metastasis [11]. Sugar beet pectin modified by alkali treatment (0.05% or 0.1%; for 72 h) induced apoptosis in HT29 colon cancer cells via an interaction with the neutral sugar side-chains from the RG-I [6]. A similar pectin structure from ginseng described as a RG-I-rich polysaccharide with (1,4)-β-D-galactan side-chains showed high affinity to galectin-3 revealed by the hemagglutination assay [19]. Although some researchers proposed that pectin anti-cancer activities can be explained by the binding to the carbohydrate recognition domain of extracellular galectin-3 binding [12,74], the precise mechanisms remain unclear. Morris et al. (2011) [75] suggested that pectin with charged GalA residues attached to the RG-I backbone could be responsible for a non-specific binding to galectin-3 through non-specific charge–charge interactions [75]. However, LNCaP prostate cancer cells (a non-expressing galectin-3 cell line) treatment with pectins showed some apoptotic effects which were due to mechanisms not mediated by galectin-3 inhibition [13]. Another study suggests that polysaccharides with content of RG-I and HG variation could inhibit colon cancer cells proliferation by decreasing ICAM1 expression, a protein responsible for cell–cell interaction and cell–ECM interaction independent of galectin-3 expression [7]. In our experiments, none of the papaya pectins inhibited the hemagglutination mediated by recombinant human galectin-3 (even at high concentrations), demonstrating that the biological activity observed herein for papaya pectins is independent of galectin-3 inhibition.

In summary, we show here that papaya pectin compositions and structure are affected by the coordinated action of several pectinolytic enzymes during fruit ripening. Those changes in pectin structures influenced the possible structure-activity relationships

when cancer cell lines were treated with naturally modified papaya pectin. We observed that 3PP has increased the anti-cancer activity when compared to pectin isolated from other ripening stages. These differences could be related, at least in part, because 3PP had smaller HG chains, smaller RG-I side-groups, and AGII associated with RG-I. It was the first time that these pectin structures were isolated and identified in papaya fruit. The inhibitory effects of the smaller neutral chains of RG-I identified in ripe papaya pulp on the interaction of ECM proteins laminin, collagen IV and fibronectin with cancer cells that might be the causal cancer cell death. As different mechanisms of cell death and migration are affected in cancer cells, additional studies regarding the signaling pathways of migration and cell death should be performed. Differences in papaya pectin structures and the different cell types used in these experiments would exhibit the distinct biological effects on cancer cells treatments. The changes in the structure of the papaya pectin driven by natural ripening provide promising clues regarding the structures of bioactive fruit compounds, especially bioactive polysaccharides that are found in fleshy fruit.

References

[1] D. Mudgil, S. Barak, Composition, properties and health benefits of indigestible carbohydrates polymers as dietary fiber: A review., Int. J. Biol. Macromol. 61 (2013) 1–6.

[2] J.W. Anderson, P. Baird, R.H. Davis, S. Ferreri, M. Knudtson, A. Koraym, V. Waters, C.L. Williams, Health benefits of dietary fiber., Nutr. Rev. 67 (2009) 188–205. doi:10.1111/j.1753-4887.2009.00189.x.

[3] J. Tuan, Y.-X. Chen, Dietary and Lifestyle Factors Associated with Colorectal Cancer Risk and Interactions with Microbiota: Fiber, Red or Processed Meat and Alcoholic Drinks, Gastrointest. Tumors. 3 (2015) 17–24. doi:10.1159/000442831.

[4] B.L. Ridley, M.A. O'Neill, D. Mohnen, Pectins: Structure, biosynthesis, and oligogalacturonide-related signaling, Phytochemistry. 57 (2001) 929–967. doi:10.1016/S0031-9422(01)00113-3.

[5] E.G. Maxwell, N.J. Belshaw, K.W. Waldron, V.J. Morris, Pectin – An emerging new bioactive food polysaccharide, Trends Food Sci. Technol. 24 (2012) 64–73. doi:10.1016/j.tifs.2011.11.002.

[6] E.G. Maxwell, I.J. Colquhoun, H.K. Chau, A.T. Hotchkiss, K.W. Waldron, V.J. Morris, N.J. Belshaw, Modified sugar beet pectin induces apoptosis of colon cancer cells via an interaction with the neutral sugar side-chains, Carbohydr. Polym. 136 (2016) 923–929. doi:10.1016/j.carbpol.2015.09.063.

[7] E.G. Maxwell, I.J. Colquhoun, H.K. Chau, A.T. Hotchkiss, K.W. Waldron, V.J. Morris, N.J. Belshaw, Rhamnogalacturonan I containing homogalacturonan inhibits colon cancer cell proliferation by decreasing ICAM1 expression, Carbohydr. Polym. 132 (2015) 546–553. doi:10.1016/j.carbpol.2015.06.082.

[8] X. Gao, Y. Zhi, L. Sun, X. Peng, T. Zhang, H. Xue, G. Tai, Y. Zhou, The inhibitory effects of a rhamnogalacturonan I (RG-I) domain from ginseng pectin on galectin-3 and its structure-activity relationship., J. Biol. Chem. 288 (2013) 33953–65. doi:10.1074/jbc.M113.482315.

[9] Y. Fan, H. Cheng, S. Li, J. Wang, D. Liu, M. Hao, X. Gao, E. Fan, G. Tai, Y. Zhou, Relationship of the inhibition of cell migration with the structure of ginseng pectic polysaccharides, Carbohydr. Polym. 81 (2010) 340–347. doi:10.1016/j.carbpol.2010.02.028.

[10] D. Chauhan, G. Li, K. Podar, T. Hideshima, P. Neri, D. He, N. Mitsiades, P.

Richardson, Y. Chang, J. Schindler, B. Carver, K.C. Anderson, A novel carbohydrate-based therapeutic GCS-100 overcomes bortezomib resistance and enhances dexamethasone-induced apoptosis in multiple myeloma cells., Cancer Res. 65 (2005) 8350–8. doi:10.1158/0008-5472.CAN-05-0163.

[11] S. Wang, P. Li, S.-M. Lu, Z.-Q. Ling, Chemoprevention of Low-Molecular-Weight Citrus Pectin (LCP) in Gastrointestinal Cancer Cells, Int. J. Biol. Sci. 12 (2016) 746–756. doi:10.7150/ijbs.13988.

[12] H. Inohara, A. Raz, Effects of natural complex carbohydrate (citrus pectin) on murine melanoma cell properties related to galectin-3 functions, Glycoconj. J. 11 (1994) 527–32. http://www.ncbi.nlm.nih.gov/pubmed/7696855.

[13] C.L. Jackson, T.M. Dreaden, L.K. Theobald, N.M. Tran, T.L. Beal, M. Eid, M.Y. Gao, R.B. Shirley, M.T. Stoffel, M.V. Kumar, D. Mohnen, Pectin induces apoptosis in human prostate cancer cells: correlation of apoptotic function with pectin structure., Glycobiology. 17 (2007) 805–19. doi:10.1093/glycob/cwm054.

[14] P. Nangia-Makker, V. Hogan, Y. Honjo, S. Baccarini, L. Tait, R. Bresalier, A. Raz, Inhibition of human cancer cell growth and metastasis in nude mice by oral intake of modified citrus pectin., J. Natl. Cancer Inst. 94 (2002) 1854–62. http://www.ncbi.nlm.nih.gov/pubmed/12488479.

[15] Y. Li, Y. Niu, H. Wu, Y. Sun, Q. Li, X. Kong, L. Liu, Q. Mei, Modified apple polysaccharides could induce apoptosis in colorectal cancer cells, J. Food Sci. 75 (2010) H224-9. doi:10.1111/j.1750-3841.2010.01781.x.

[16] Y. Li, L. Liu, Y. Niu, J. Feng, Y. Sun, X. Kong, Y. Chen, X. Chen, H. Gan, S. Cao, Q. Mei, Modified apple polysaccharide prevents against tumorigenesis in a mouse model of colitis-associated colon cancer: role of galectin-3 and apoptosis in cancer prevention., Eur. J. Nutr. 51 (2012) 107–17. doi:10.1007/s00394-011-0194-3.

[17] U. V Sathisha, S. Jayaram, M. a Harish Nayaka, S.M. Dharmesh, Inhibition of galectin-3 mediated cellular interactions by pectic polysaccharides from dietary sources, Glycoconj. J. 24 (2007) 497–507. doi:10.1007/s10719-007-9042-3.

[18] L. Leclere, P. Van Cutsem, C. Michiels, Anti-cancer activities of pH- or heat-modified pectin, Front. Pharmacol. 4 (2013) 128. doi:10.3389/fphar.2013.00128.

[19] T. Zhang, Y. Lan, Y. Zheng, F. Liu, D. Zhao, K.H. Mayo, Y. Zhou, G. Tai, Identification of the bioactive components from pH-modified citrus pectin and their inhibitory effects on galectin-3 function, Food Hydrocoll. 58 (2016) 113–119. doi:10.1016/j.foodhyd.2016.02.020.

[20] V.J. Morris, N.J. Belshaw, K.W. Waldron, E.G. Maxwell, The bioactivity of modified pectin fragments, Bioact. Carbohydrates Diet. Fibre. 1 (2013) 21–37. doi:10.1016/j.bcdf.2013.02.001.

[21] C. Rolin, Commercial pectin preparations, in: G. B. Seymour, J. P. Knox Pectins Their Manip., Oxford: Blackwell Publishing Publishing Ltd., 2002: pp. 222 – 239.

[22] J. Giovannoni, Molecular Biology of Fruit Matturation and Ripening, Annu. Rev. Plant Biol. 52 (2001) 725–749.

[23] D. a Brummell, M.H. Harpster, Cell wall metabolism in fruit softening and quality and its manipulation in transgenic plants., Plant Mol. Biol. 47 (2001) 311–40. http://www.ncbi.nlm.nih.gov/pubmed/11554479.

[24] T.M. Shiga, J.P. Fabi, J.R.O. do Nascimento, C.L.D.O. Petkowicz, L.C. Vriesmann, F.M. Lajolo, B.R. Cordenunsi, Changes in cell wall composition associated to the softening of ripening papaya: evidence of extensive solubilization of large molecular mass galactouronides, J. Agric. Food Chem. 57 (2009) 7064–71. doi:10.1021/jf900073b.

[25] J.P. Fabi, S.G. Broetto, S.L.G.L. Da Silva, S. Zhong, F.M. Lajolo, J.R.O. Nascimento, Analysis of Papaya Cell Wall-Related Genes during Fruit Ripening Indicates a Central Role of Polygalacturonases during Pulp Softening, PLoS One. 9 (2014) e105685. doi:10.1371/journal.pone.0105685.

[26] S.B.R. do Prado, P.R. Melfi, V.C. Castro-Alves, S.G. Broetto, E.S. Araújo, J.R.O. do Nascimento, J.P. Fabi, Physiological Degradation of Pectin in Papaya Cell Walls: Release of Long Chains Galacturonans Derived from Insoluble Fractions during Postharvest Fruit Ripening, Front. Plant Sci. 7 (2016) 1120. doi:10.3389/fpls.2016.01120.

[27] D. a. Brummell, Cell wall disassembly in ripening fruit, Funct. Plant Biol. 33 (2006) 103. doi:10.1071/FP05234.

[28] P. Nangia-Makker, B. Vitaly, R. Avraham, Galectin-3-Binding and Metastasis, Methods Mol. Biol. 878 (2012) 241–250. doi:10.1007/978-1-61779-854-2.

[29] J.B. Kim, N.C. Carpita, Changes in Esterification of the Uronic Acid Groups of Cell Wall Polysaccharides during Elongation of Maize Coleoptiles, Plant Physiol. 98 (1992) 646–653. doi:10.1104/pp.98.2.646.

[30] N.C. Carpita, M.C. McCann, Some new methods to study plant polyuronic acids and their esters, in: R. Townsend, A. Hotchkiss (Eds.), Prog. Glycobiol., New York, NY: Marcel Dekker., 1996: pp. 595–661.

[31] D.M. Gibeaut, N.C. Carpita, Clean-up procedure for partially methylated alditol acetate derivatives of polysaccharides, J. Chromatogr. 587 (1991) 284–287. doi:0021-9673/91.

[32] N.C. Carpita, E.M. Shea, Linkage structure of carbohydrates by gas chromatography–mass spectrometry (CG–MS) of partially methylated alditol acetates, in: Anal. Carbohydrates by GLC MS, Boca Raton, FL: CRC Press, 1989: pp. 157–216.

[33] H. Tabusa, T. Brooks, A.J. Massey, Knockdown of PAK4 or PAK1 Inhibits the Proliferation of Mutant KRAS Colon Cancer Cells Independently of RAF / MEK / ERK and PI3K / AKT Signaling, Mol. Cancer Res. 11 (2013) 109–121. doi:10.1158/1541-7786.MCR-12-0466.

[34] M. He, P.S. Rennie, V. Dragowska, C.C. Nelson, W. Jia, A mutant P53 can activate apoptosis through a mechanism distinct from those induced by wild type P53, FEBS Lett. 517 (2002) 151–154. doi:10.1016/S0014-5793(02)02609-1.

[35] J.C.M. de Freitas, B.D.R.D.A. Silva, W.F. De Souza, W.M. De Araújo, E.S.F.W. Abdelhay, J.A. Morgado-Díaz, Inhibition of N-linked glycosylation by tunicamycin induces E-cadherin-mediated cell-cell adhesion and inhibits cell proliferation in undifferentiated human colon cancer cells, Cancer Chemother. Pharmacol. 68 (2011) 227–238. doi:10.1007/s00280-010-1477-8.

[36] J. Christensen, S. El-Gebali, M. Natoli, T. Sengstag, M. Delorenzi, S. Bentz, H. Bouzourene, M. Rumbo, A. Felsani, S. Siissalo, J. Hirvonen, M.R. Vila, P. Saletti, M. Aguet, P. Anderle, Defining new criteria for selection of cell-based intestinal models using publicly available databases, BMC Genomics. 13 (2012) 274. doi:10.1186/1471-2164-13-274.

[37] S. Tai, Y. Sun, J.M. Squires, H. Zhang, W.K. Oh, C.Z. Liang, J. Huang, PC3 is a cell line characteristic of prostatic small cell carcinoma, Prostate. 71 (2011) 1668–1679. doi:10.1002/pros.21383.

[38] H. Inohara, A. Raz, Functional Evidence that Cell Surface Galectin-3 Mediates Homotypic Cell Adhesion, Cancer Res. 55 (1995) 3267–3271.

[39] P. Mina-Osorio, I. Soto-Cruz, E. Ortega, A role for galectin-3 in CD13-mediated homotypic aggregation of monocytes, Biochem. Biophys. Res. Commun. 353 (2007) 605–610. doi:10.1016/j.bbrc.2006.12.081.

[40] H. Cheng, Y. Chen, J. Wong, C. Weng, H. Chen, S. Yu, H. Chen, A. Yuan, J.J.W. Chen, Cancer cells increase endothelial cell tube formation and survival by

activating the PI3K/Akt signalling pathway, J. Exp. Clin. Cancer Res. 36 (2017) 1–13. doi:10.1186/s13046-017-0495-3.

[41] N. Reymond, B. Borda, A.J. Ridley, Crossing the endothelial barrier during metastasis, Nat. Rev. Cancer. 13 (2013) 858–870. doi:10.1038/nrc3628.

[42] Y. Zhao, X. Hu, Y. Liu, S. Dong, Z. Wen, W. He, S. Zhang, Q. Huang, ROS signaling under metabolic stress: cross-talk between AMPK and AKT pathway, Mol. Cancer. 16 (2017) 79. doi:10.1186/s12943-017-0648-1.

[43] M.J. Peña, N.C. Carpita, Loss of highly branched arabinans and debranching of rhamnogalacturonan I accompany loss of firm texture and cell separation during prolonged storage of apple., Plant Physiol. 135 (2004) 1305–13. doi:10.1104/pp.104.043679.

[44] T.M. Shiga, F.H.G. Peroni-Okita, N.C. Carpita, F.M. Lajolo, B.R. Cordenunsi, Polysaccharide composition of raw and cooked chayote (Sechium edule Sw.) fruits and tuberous roots, Carbohydr. Polym. 130 (2015) 155–165. doi:10.1016/j.carbpol.2015.04.055.

[45] H.-Y. Liu, Inhibitory effect of modified citrus pectin on liver metastases in a mouse colon cancer model, World J. Gastroenterol. 14 (2008) 7386. doi:10.3748/wjg.14.7386.

[46] G. Hossein, M. Keshavarz, S. Ahmadi, N. Naderi, Synergistic effects of PectaSol-C modified citrus pectin an inhibitor of Galectin-3 and paclitaxel on apoptosis of human SKOV-3 ovarian cancer cells., Asian Pac. J. Cancer Prev. 14 (2013) 7561–8. http://www.ncbi.nlm.nih.gov/pubmed/24460334.

[47] M. Hao, X. Yuan, H. Cheng, H. Xue, T. Zhang, Y. Zhou, G. Tai, Comparative studies on the anti-tumor activities of high temperature- and pH-modified citrus pectins., Food Funct. 4 (2013) 960–71. doi:10.1039/c3fo30350k.

[48] L. Leclere, M. Fransolet, F. Cote, P. Cambier, T. Arnould, P. Van Cutsem, C. Michiels, Heat-Modified Citrus Pectin Induces Apoptosis-Like Cell Death and Autophagy in HepG2 and A549 Cancer Cells, PLoS One. 10 (2015) e0115831. doi:10.1371/journal.pone.0115831.

[49] S. Posé, A.R. Kirby, J.A. Mercado, V.J. Morris, M.A. Quesada, Structural characterization of cell wall pectin fractions in ripe strawberry fruits using AFM, Carbohydr. Polym. 88 (2012) 882–890. doi:10.1016/j.carbpol.2012.01.029.

[50] C. Paniagua, A.R. Kirby, A.P. Gunning, V.J. Morris, A.J. Matas, M.A. Quesada, J.A. Mercado, Unravelling the nanostructure of strawberry fruit pectins by atomic

force microscopy, Food Chem. 224 (2017) 270–279. doi:10.1016/j.foodchem.2016.12.049.

[51] A.N. Round, N.M. Rigby, A.J. MacDougall, V.J. Morris, A new view of pectin structure revealed by acid hydrolysis and atomic force microscopy, Carbohydr. Res. 345 (2010) 487–497. doi:10.1016/j.carres.2009.12.019.

[52] J. Christensen, S. El-Gebali, M. Natoli, T. Sengstag, M. Delorenzi, S. Bentz, H. Bouzourene, M. Rumbo, A. Felsani, S. Siissalo, J. Hirvonen, M.R. Vila, P. Saletti, M. Aguet, P. Anderle, Defining new criteria for selection of cell-based intestinal models using publicly available databases, BMC Genomics. 13 (2012) 274. doi:10.1186/1471-2164-13-274.

[53] J.T. Dong, Prevalent mutations in prostate cancer, J. Cell. Biochem. 97 (2006) 433–447. doi:10.1002/jcb.20696.

[54] J. Taylor-Papadimitriou, J. Burchell, D.W. Miles, M. Dalziel, MUC1 and cancer, Biochim. Biophys. Acta - Mol. Basis Dis. 1455 (1999) 301–313. doi:10.1016/S0925-4439(99)00055-1.

[55] Q. Zhao, M. Barclay, J. Hilkens, X. Guo, H. Barrow, J.M. Rhodes, L.-G. Yu, Interaction between circulating galectin-3 and cancer-associated MUC1 enhances tumour cell homotypic aggregation and prevents anoikis., Mol. Cancer. 9 (2010) 154. doi:10.1186/1476-4598-9-154.

[56] V. V. Glinsky, G. V. Glinsky, O. V. Glinskii, V.H. Huxley, J.R. Turk, V. V. Mossine, S.L. Deutscher, K.J. Pienta, T.P. Quinn, Intravascular metastatic cancer cell homotypic aggregation at the sites of primary attachment to the endothelium, Cancer Res. 63 (2003) 3805–3811.

[57] M.J. Kwon, Y. Kim, Y. Choi, S.H. Kim, S. Park, I. Han, D.H. Kang, E.S. Oh, The extracellular domain of syndecan-2 regulates the interaction of HCT116 human colon carcinoma cells with fibronectin, Biochem. Biophys. Res. Commun. 431 (2013) 415–420. doi:10.1016/j.bbrc.2012.12.155.

[58] A. Lagana, J.G. Goetz, P. Cheung, A. Raz, J.W. Dennis, I.R. Nabi, Galectin binding to Mgat5-modified N-glycans regulates fibronectin matrix remodeling in tumor cells., Mol. Cell. Biol. 26 (2006) 3181–93. doi:10.1128/MCB.26.8.3181-3193.2006.

[59] S. Han, F.R. Khuri, J. Roman, Fibronectin stimulates non-small cell lung carcinoma cell growth through activation of Akt/mammalian target of rapamycin/S6 kinase and inactivation of LKB1/AMP-activated protein kinase

signal pathways, Cancer Res. 66 (2006) 315–323. doi:10.1158/0008-5472.CAN-05-2367.

[60] S.K. More, S. V. Chiplunkar, R.D. Kalraiya, Galectin-3-induced cell spreading and motility relies on distinct signaling mechanisms compared to fibronectin, Mol. Cell. Biochem. 416 (2016) 179–191. doi:10.1007/s11010-016-2706-1.

[61] G. Xue, B.A. Hemmings, PKB/akt-dependent regulation of cell motility, J. Natl. Cancer Inst. 105 (2013) 393–404. doi:10.1093/jnci/djs648.

[62] C.L. Buchheit, R.R. Rayavarapu, Z.T. Schafer, The regulation of cancer cell death and metabolism by extracellular matrix attachment, Semin. Dev.Biol. 23 (2012) 402–411. doi:10.1016/j.semcdb.2012.04.007.

[63] W. He, Q. Wang, B. Srinivasan, J. Xu, T. Mabel, Z. Li, X. Wang, Y. Liu, X. Gou, H. Shen, C. Xing, Y. Lin, L.C. Program, T. First, A. Hospital, T. Medicine, A JNK-mediated autophagy pathway that triggers c-IAP degradation and necroptosis for anticancer chemotherapy, Oncogene. 33 (2014) 612–626. doi:10.1038/onc.2013.256.A.

[64] J.A. Mason, C.A. Davison-Versagli, A.K. Leliaert, D.J. Pape, C. McCallister, J. Zuo, S.M. Durbin, C.L. Buchheit, S. Zhang, Z.T. Schafer, Oncogenic Ras differentially regulates metabolism and anoikis in extracellular matrix-detached cells, Cell Death Differ. 23 (2016) 1–12. doi:10.1038/cdd.2016.15.

[65] T. Abbas, A. Dutta, p21 in cancer: intricate networks and multiple activities, Nat. Rev. Cancer. 9 (2009) 400–414. doi:10.1038/nrc2657.p21.

[66] E.Y.L. Kim, C. Gronewold, A. Chatterjee, C.W. Von Der Lieth, C. Kliem, B. Schmauser, M. Wiessler, E. Frei, Oligosaccharide mimics containing galactose and fucose specifically label tumour cell surfaces and inhibit cell adhesion to fibronectin, ChemBioChem. 6 (2005) 422–431. doi:10.1002/cbic.200400092.

[67] M. Zheng, H. Fang, S.I. Hakomori, Functional role of N-glycosylation in α5β1 integrin receptor, J. Biol. Chem. 269 (1994) 12325–12331.

[68] W. Yi, E. Xiao, R. Ding, P. Luo, Y. Yang, High expression of fibronectin is associated with poor prognosis, cell proliferation and malignancy via the NF-B/p53-apoptosis signaling pathway in colorectal cancer, Oncol. Rep. 36 (2016) 3145–3153. doi:10.3892/or.2016.5177.

[69] R.D. Loberg, K. Tantivejkul, M. Craig, C.K. Neeley, K.J. Pienta, PAR1-mediated RhoA activation facilitates CCL2-induced chemotaxis in PC-3 cells, J. Cell. Biochem. 101 (2007) 1292–1300. doi:10.1002/jcb.21252.

[70] Y. Gan, C. Shi, L. Inge, M. Hibner, J. Balducci, Y. Huang, Differential roles of ERK and Akt pathways in regulation of EGFR-mediated signaling and motility in prostate cancer cells., Oncogene. 29 (2010) 4947–4958. doi:10.1038/onc.2010.240.

[71] S. Kondo, B.P. Barna, Y. Kondo, Y. Tanaka, G. Casey, J. Liu, T. Morimura, R. Kaakaji, J.W. Peterson, B. Werbel, G.H. Barnett, WAF1/CIP1 increases the susceptibility of p53 non-functional malignant glioma cells to cisplatin-induced apoptosis, Oncogene. 13 (1996) 1279–1285.

[72] H. Lincet, L. Poulain, J.S. Remy, E. Deslandes, F. Duigou, Cytotoxic Effect of Cisplatin in Human Ovarian Carcinoma Cells, Cancer Lett. 161 (2000) 17–26.

[73] I. Masgras, S. Carrera, P.J. De Verdier, P. Brennan, A. Majid, W. Makhtar, E. Tulchinsky, G.D.D. Jones, I.B. Roninson, S. Macip, Reactive oxygen species and mitochondrial sensitivity to oxidative stress determine induction of cancer cell death by p21, J. Biol. Chem. 287 (2012) 9845–9854. doi:10.1074/jbc.M111.250357.

[74] V. V. Glinsky, A. Raz, Modified citrus pectin anti-metastatic properties: one bullet, multiple targets, Carbohydr. Res. 344 (2009) 1788–1791. doi:10.1016/j.carres.2008.08.038.

[75] V.J. Morris, A. Gromer, A.R. Kirby, R.J.M. Bongaerts, A. Patrick Gunning, Using AFM and force spectroscopy to determine pectin structure and (bio) functionality, Food Hydrocoll. 25 (2011) 230–237. doi:10.1016/j.foodhyd.2009.11.015.

Supplementary files

Table S1. Papaya water-soluble polysaccharides linkage analysis.

Monomer	1PP	2PP	3PP	4PP
	Mol (%)			
t-Rha	0.8 ± 0.2	0.6 ± 0.3	0.7 ± 0.2	0.5 ± 0.1
2-Rha	0.8 ± 0.2	1.6 ± 0.3	2.0 ± 0.2	1.7 ± 0.1
2,4-Rha	0.1 ± 0.1	0.7 ± 0.2	1.1 ± 0.1	1.1 ± 0.1
t-Fuc	0.0 ± 0.0	0.0 ± 0.0	0.0 ± 0.0	0.0 ± 0.0
2,4-Fuc	0.1 ± 0.1	0.1 ± 0.1	0.1 ± 0.1	0.1 ± 0.1
t-Araf	2.1 ± 0.1	1.1 ± 0.2	0.6 ± 0.1	0.5 ± 0.1
t-Arap	0.9 ± 0.1	0.5 ± 0.2	0.8 ± 0.1	0.7 ± 0.1
2-Araf	0.1 ± 0.0	0.1 ± 0.1	0.1 ± 0.1	0.1 ± 0.0
3-Araf	0.7 ± 0.1	0.3 ± 0.1	0.4 ± 0.1	0.4 ± 0.1
5-Ara(f)	1.0 ± 0.1	0.5 ± 0.1	0.8 ± 0.1	0.7 ± 0.1
2,5-Ara(f)	0.0 ± 0.0	0.0 ± 0.0	0.0 ± 0.0	0.0 ± 0.0
3,5-Ara(f)	0.0 ± 0.0	0.0 ± 0.0	0.1 ± 0.1	0.0 ± 0.0
Ara(OAc)5	1.0 ± 0.2	0.9 ± 0.1	0.7 ± 0.1	0.6 ± 0.1
t-Xylp	0.7 ± 0.2	0.2 ± 0.1	0.4 ± 0.1	0.2 ± 0.1
2-Xyl	0.2 ± 0.1	0.2 ± 0.1	0.1 ± 0.1	0.1 ± 0.1
2,4-Xyl	0.1 ± 0.1	0.1 ± 0.1	0.1 ± 0.0	0.1 ± 0.0
4-Xyl	0.9 ± 0.1	0.8 ± 0.1	0.4 ± 0.1	0.5 ± 0.1
3,4-Xyl	0.1 ± 0.1	0.1 ± 0.1	0.1 ± 0.1	0.1 ± 0.1
Xyl(OAc)5	0.3 ± 0.1	0.5 ± 0.2	0.2 ± 0.1	0.2 ± 0.1
t-Man	0.0 ± 0.0	0.0 ± 0.0	0.0 ± 0.0	0.0 ± 0.0
4-Man	0.3 ± 0.1	0.3 ± 0.1	0.1 ± 0.1	0.3 ± 0.1
4,6-Man	0.0 ± 0.0	0.0 ± 0.0	0.0 ± 0.0	0.0 ± 0.0
Man(OAc)6	0.7 ± 0.1	0.7 ± 0.1	0.5 ± 0.1	1.0 ± 0.1
t-Gal	0.8 ± 0.1	1.0 ± 0.3	2.6 ± 0.6	1.8 ± 0.3
2-Gal	0.1 ± 0.1	0.2 ± 0.1	0.1 ± 0.1	0.1 ± 0.1
3-Gal	0.2 ± 0.1	0.1 ± 0.1	0.2 ± 0.1	0.3 ± 0.1
3,4-Gal	0.6 ± 0.2	0.5 ± 0.2	0.2 ± 0.1	0.1 ± 0.1
4-Gal	1.0 ± 0.1	0.8 ± 0.2	1.1 ± 0.2	0.3 ± 0.1
2,4-Gal	0.3 ± 0.1	0.8 ± 0.2	0.3 ± 0.1	0.4 ± 0.2
3,6-Gal	4.4 ± 0.1	2.7 ± 0.3	2.7 ± 0.2	1.9 ± 0.3
4,6-Gal	0.4 ± 0.1	0.4 ± 0.1	1.1 ± 0.4	0.4 ± 0.2
6-Gal	4.6 ± 0.4	1.9 ± 0.3	2.1 ± 0.2	2.2 ± 0.2
2,4,6-Gal	0.1 ± 0.1	0.4 ± 0.3	0.2 ± 0.1	0.4 ± 0.2
Gal(OAc)6	1.2 ± 0.5	2.3 ± 0.6	1.2 ± 0.3	1.0 ± 0.2
t-GalA	1.9 ± 0.4	2.6 ± 0.5	7.9 ± 2.8	4.2 ± 0.2
4-GalA	60.7 ± 2.4	64.3 ± 2.1	58.5 ± 3.5	68.5 ± 2.0
3,4-GalA	0.4 ± 0.2	0.5 ± 0.1	0.4 ± 0.2	0.3 ± 0.1
4,6 GalA	6.4 ± 1.3	8.0 ± 1.1	5.5 ± 0.6	5.0 ± 1.1
2,4 GalA	2.6 ± 1.1	5.1 ± 2.1	2.8 ± 0.7	1.8 ± 0.5
t-Glc	0.3 ± 0.1	0.1 ± 0.1	0.2 ± 0.2	0.1 ± 0.1
2-Glc	0.1 ± 0.1	0.1 ± 0.2	0.1 ± 0.2	0.1 ± 0.1
3-Glc	0.4 ± 0.1	0.1 ± 0.1	0.2 ± 0.1	0.2 ± 0.1
4-Glc	0.8 ± 0.1	1.1 ± 0.1	0.7 ± 0.1	0.6 ±0.1
3,4-Glc	0.3 ± 0.1	0.3 ± 0.3	0.9 ± 0.2	0.7 ± 0.1
4,6-Glc	0.1 ± 0.1	0.8 ± 0.1	0.1 ± 0.2	0.1 ± 0.1
Glc(OAc)6	0.5 ± 0.1	0.5 ± 0.1	0.6 ± 0.1	0.5 ± 0.1
t-GlcA	1.1 ± 0.3	1.8 ± 0.5	1.5 ± 0.3	1.8 ± 0.3

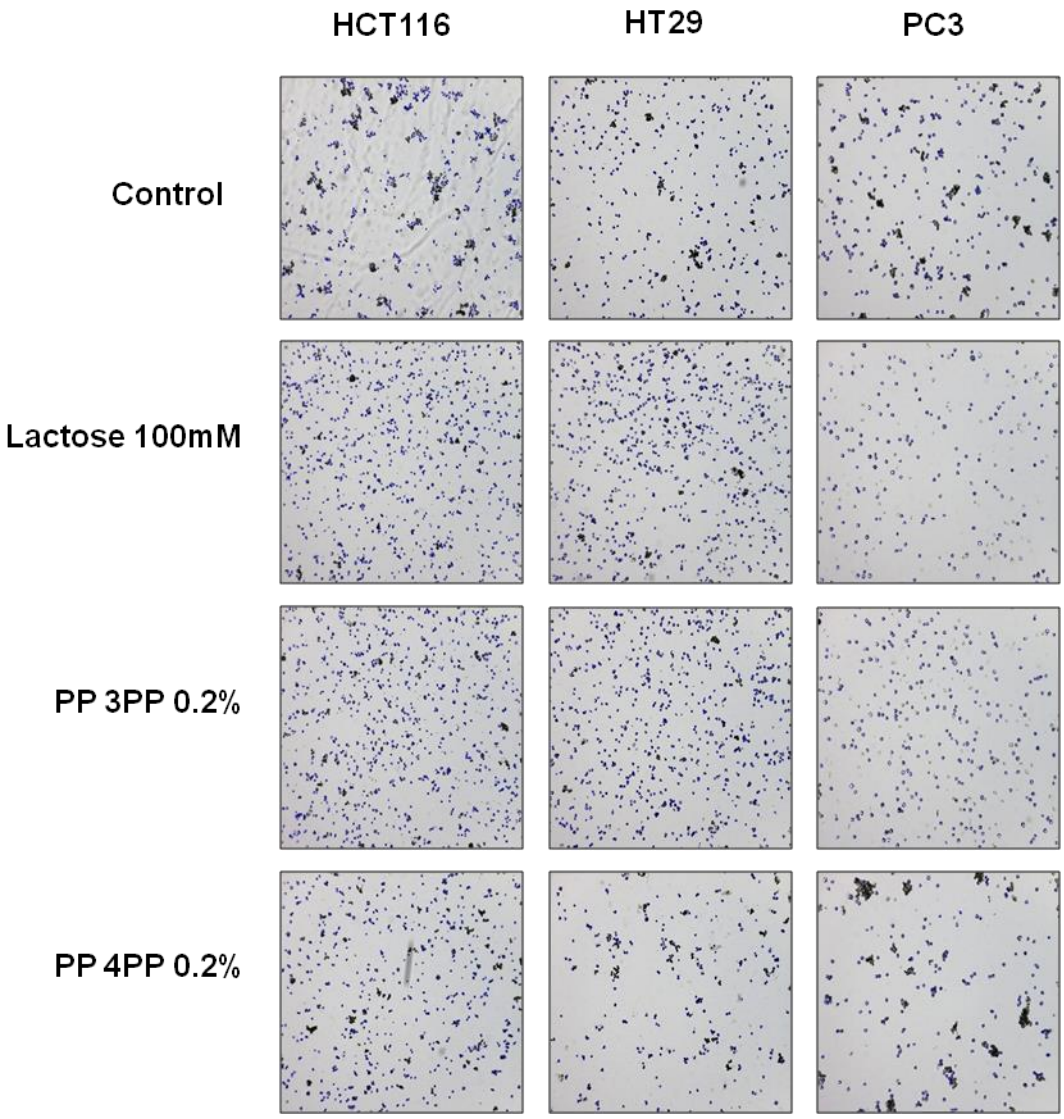

Figure S1. Homotypic aggregation. Cells were counted in an automatic cell counter and the blue circles were automatic generated by the machine software and is related to single or double cells.

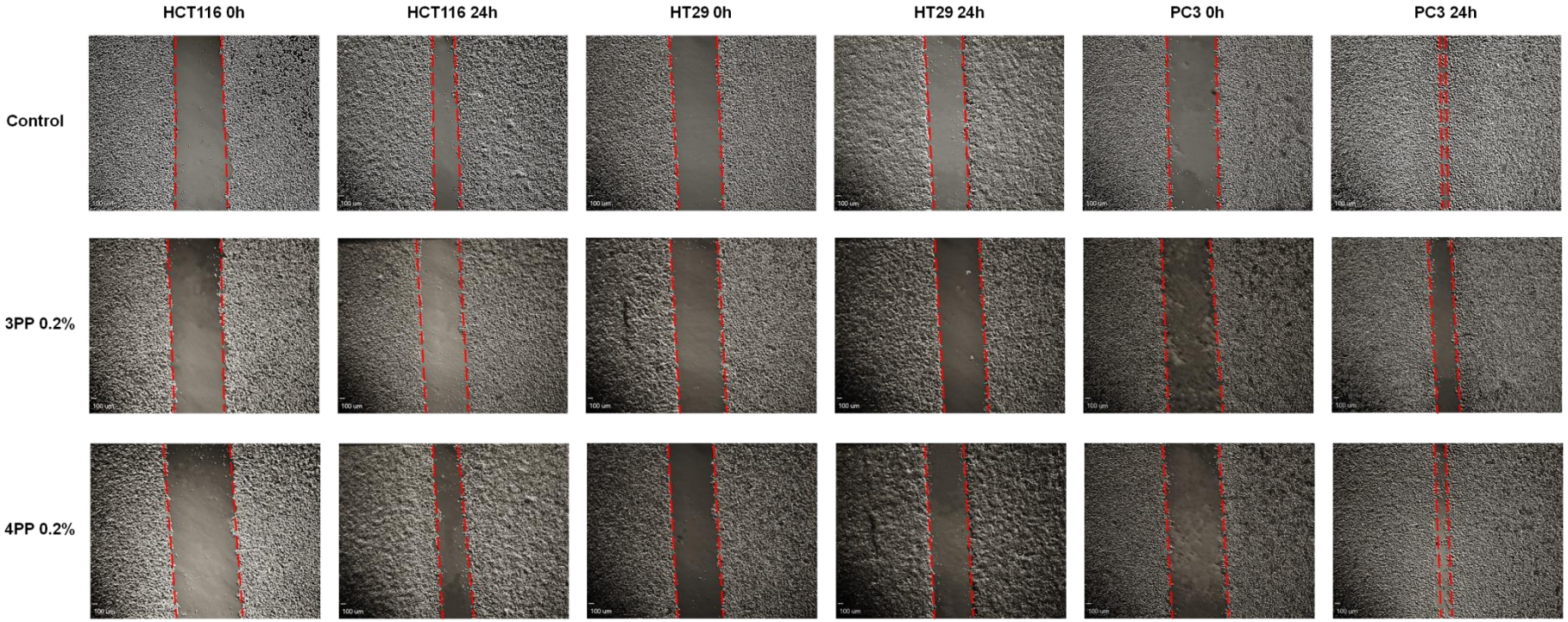

Figure S2. Migration assay based on wound healing assay. Photographs of cancer cell cultures in 0 h (after scratching) and after 24 h of treatment or not (control) indicating the wound cloasure. Scale bar: 100 µm.

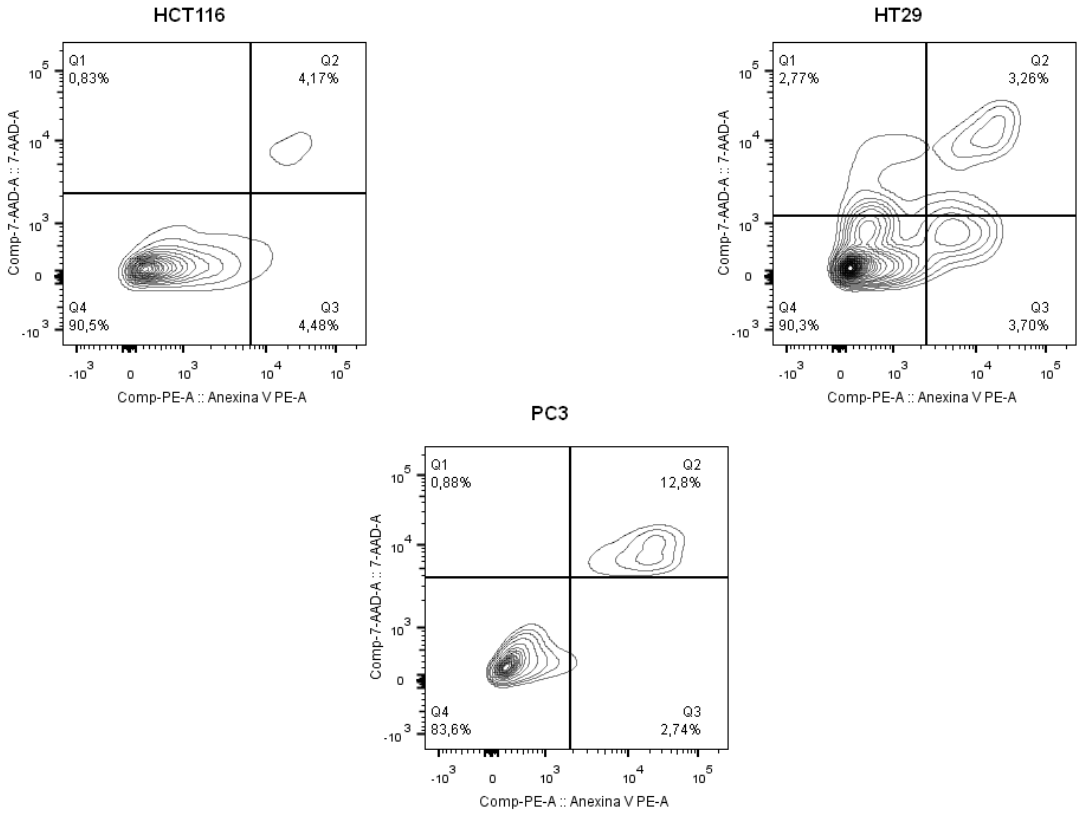

Figure S3. Effects of lactose in HCT116, HT29 and PC3 apoptosis by flow cytometry. Lactose did not induce cell death. Cells were treated with 100 mM of lactose for 24 h.

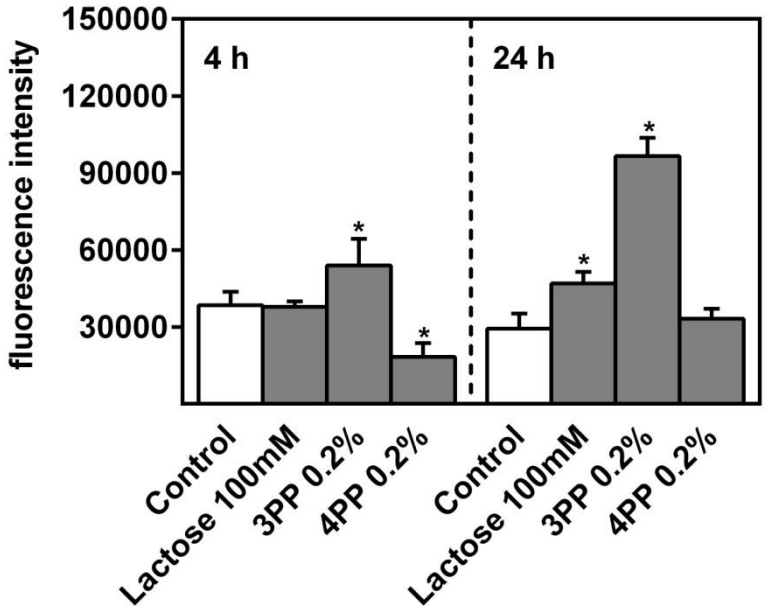

Figure S4. ROS detection on HCT116 cells measured by DCFDA. 3PP and not 4PP induced ROS accumulation. Cells were treated and after 4 h or 24 h cells were incubated with DCFDA for 45 min. Data was expressed as mean ± SD of fluorescence ratios for two independent experiments. **P* < 0.05 vs control, according to Dunnetts's test. PP: papaya pectin (water-soluble fraction).

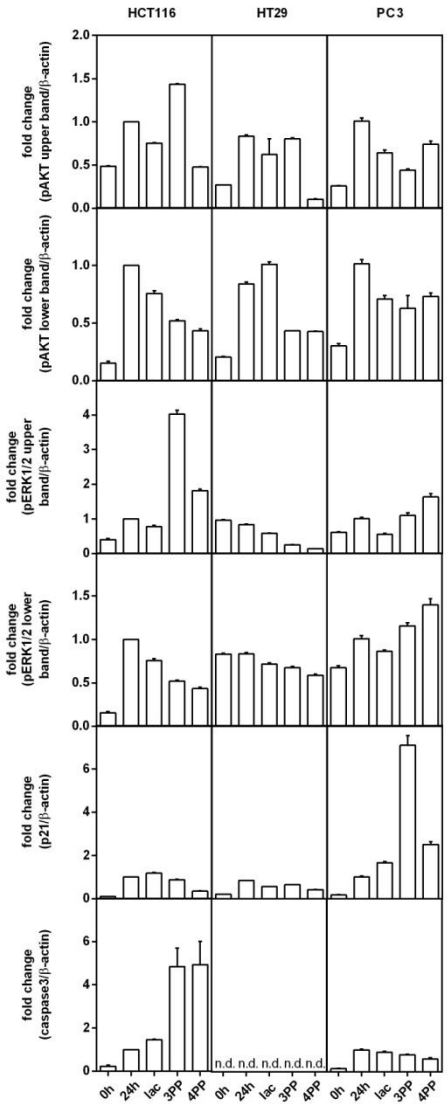

Figure S5. Relative density of western blot. PP: papaya pectin (water-soluble fraction).

Chapter 5

Ripening processes in papaya creates unique pectin structures with differential signaling effects on pattern recognition receptors

Samira Bernardino Ramos do Prado[1,2], Martin Beukema[3], Eva Jermendi[4], Henk Schols[4], Paul de Vos[3], João Paulo Fabi[1,2]

[1]Department of Food Science and Experimental Nutrition, School of Pharmaceutical Sciences, University of São Paulo, São Paulo, SP, Brazil
[2]Food Research Center (FoRC), CEPID-FAPESP (Research, Innovation and Dissemination Centers, São Paulo Research Foundation), São Paulo, SP, Brazil
[3]Immunoendocrinology, Division of Medical Biology, Department of Pathology and Medical Biology, University of Groningen, University Medical Center Groningen, Groningen, Netherlands
[4]Laboratory of Food Chemistry, Wageningen University, Wageningen, Netherlands

Abstract

Dietary fiber consumption is known to exert healthy benefits and more recently was associated to be able to interact with pattern recognition receptors (PRR). The interaction with these receptors, like toll-like receptors (TLR) and nucleotide binding oligomerization domain (NOD)-like receptors can modulate immune responses. The papayas pectin extracted from unripe and ripe fruits exerts structural-dependent effects on cancel cell lines, and the aim of this work was evaluating whether the unripe and ripe papayas pectin also has different interactions with PRR. The pectin from ripe papayas activate TLR and in a less extension NOD receptors. The pectins from unripe papayas also activated some TLR but not for TLR3 and TLR9. The pectin from unripe papayas not activated TLR3 and TLR9 and also block the agonist activation. The main difference in the pectin structure is higher esterification and smaller chains of pectin from ripe papayas. Therefore, the distinct biological effects using papayas pectin can be due to the different PRR interaction.

Keywords: pectin; papaya; pattern recognition pattern; toll-like receptors.

Abbreviations: AFM, atomic force microscopy; Ara, arabinose; ATR, attenuated total reflectance; DAH, days after harvest; DM, degree of methyl-esterification; FTIR, fourier transform infrared; Fuc, fucose; Gal, galactose; GalA, Galacturonic acid; Glc, glucose; GlcA, glucuronic acid; HG, homogalacturonan; I-WSF, intermediate ripening time point - papaya from 3rd day after harvest - water-soluble fraction; LPS, lipopolysaccharides; Man, mannose; Mw, molecular weight; NOD, nucleotide-binding oligomerization domain; PRR, pattern recognition receptors; R-1-WSF, ripe - papaya from 4th day after harvest - water-soluble fraction; R-2-WSF, ripe - papaya from 5th day after harvest - water-soluble fraction; RG-I, type I rhamnogalacturonans; Rha, rhamnose; SD, standard deviation; SEAP, soluble embryonic alkaline phosphatase; TLR, toll-like receptors; Un-1-WSF, unripe - papaya from 1st day after harvest - water-soluble fraction; Un-2-WSF, unripe - papaya from 2nd day after harvest - water-soluble fraction; V_e, elution volume; V_o, void volume ; WSF, water-soluble fraction; Xyl, xylose; DF, dietary fiber.

Introduction

Dietary fiber (DF) commonly represents a wide variety of polysaccharides originating from fruits, vegetables, whole grains and legumes. Consumption of DF has been shown to influence the consumers health status including its immune response. This can be accomplished by direct effects of DF on consumer's immunity or by beneficial effects on gut microbiota that ferment DF into short chain fatty acids that may influence immune regulation[1]. DF also induces a slower, desired gastric emptying [2], improves physical bowel function [3], and can interact directly with intestinal cells and/or the cells from the mucosal immune [4–6].

The direct interaction of DF with the intestinal cells can be throughout Pattern Recognition Receptors (PRR) [7]. The PRR are germline-encoded sensors expressed in intestine epithelial cells and gut immune cells, being the key receptors responsible for the recognition of exogenous molecules by the host [6,7]. Toll-like receptors (TLR) is a family of PRR and play a central role in the activation of innate immunity [8] and have been shown to be involved in DF induced immune signaling. The immune response mediated by TLR activation requires the recruitment of MyD88 adaptor protein and the translocation of NF-κB to the nucleus [8], unless TLR3 that NF-κB is activated mediated TIR domain-containing adapter inducing IFN- β (TRIF) [9]. The interaction between a wide variety of DF-polysaccharides and TLR has been extensively studied and is extremely complex, some DF activates TLR to different extends [10] while other DF such as pectins may block TLR signaling and attenuate intestinal inflammation [11]. Nucleotide-binding oligomerization domain (NOD) have also been shown to be influenced by DF such as β2→1-fructans. NOD are proteins responsible for the recognition of intracellular bacteria [8]. Through this signaling via PRRs DF have been shown to mediate several host effects such as reducing intestinal permeability and thereby supporting gut barrier function [10,12], supporting immune responses against pathogens [13], and reducing intestinal inflammation [11].

The DF isolated from fleshy fruit is mainly formed by cell wall-derived polysaccharides: cellulose, hemicelluloses and pectin [14] with the most water-soluble fraction being composed of pectin. Papaya (*Carica papaya* L.) is a climacteric fruit which ripens fast resulting in fruit softening [15]. The ripening-induced expression of cell wall-degrading enzymes is responsible for cell wall disassembling with concomitant changes in papaya DF structures, e.g. through the generation of water-soluble pectins during ripening

[16]. The papaya water-soluble fraction (WSF) isolated from pulp is mainly composed of pectin (~95%) with different structural features depending of the papaya ripening stage [17]. These different pectin structures might have different host effects by differential modulation of PRR signaling [10,11].

Here we studied PRR signaling of water-soluble fractions of pectins isolated from papaya fruit at different stages of ripening. We focused on attenuation and activating activity of the pectins of TLR and NOD receptors as these have been shown to be the predominant PRRs involved in pectin signaling.

Methods

Plant material

Papayas (*C. papaya* L. cv. 'Golden') were acquired from a producer in Aracruz (Espírito Santo, Brazil) in biological duplicate (2015 and 2016 harvest). The fruit characterization to assure the unripe and ripe classifications was done daily by analyzing fruit respiration (CO_2), ethylene production and pulp firmness [15]**.** The fruits were harvested at color break to one-fourth yellow and stored at ambient temperature until ripe. Five time points were chosen to represent the unripe, intermediate and ripe time points of ripening (1 to 5 five days after harvest - DAH). The total of 6 fruits of each DAH (from two biological replicates) were sliced in small pieces, frozen on N_2 and stored in -80 ºC until the following analysis.

Water-soluble fraction (WSF) extraction

The frozen and sliced papaya were grounded in N_2 and total cell wall was isolated as stated before [16]. From the total cell wall preparation, the WSF was extracted. Briefly, the total cell wall was treated with deionized water under constant magnetic stirring for 20 min at 25 °C and centrifuged (10,000 × g, 20 min, 25 °C) and this step was repeated three times. The WSF were passed through a column with polymyxin B-Agarose to ensure samples were not contaminated with lipopolysaccharides (LPS) as following manufacturer's instructions (Polymyxin B – agarose, Sigma P1411). The LPS-free supernatant (WSF) was lyophilized. Samples were tested for ash content, starch content (Lugol test, and if positive the AA/AMG technique), protein content (microKjeldahl following the AOAC 960.52 method and/or BCA method using Pierce BCA Protein Assay Kit - Thermo Scientific, Waltham, MA, USA) and tested for phenolic compounds (Folin-Ciocalteu test and the SPE-

HPLC-DAD technique if Folin is positive) [18]. The tests all resulted in negligible values, confirming the purity of polysaccharides from more than 99%. WSF samples obtained from the fruits at the first and second DAH correspond to fibers extracted from unripe fruits and the samples were named Un-1-WSF and Un-2-WSF, respectively. WSF sample obtained by the fruits from the third DAH correspond to fibers extracted from the intermediate point fruits and was named I-WSF. WSF samples obtained by the fruits from the fourth and fifth DAH correspond to fibers extracted from the ripe fruits and were named R-1-WSF and R-2-WSF.

Molecular weight distribution

The WSF (3 mg/mL) from different ripening points were analyzed by high-performance size-exclusion chromatography coupled with a refractive index detector (HPSEC-RID) using a 1250 Infinity system (Agilent, Santa Clara, CA). The system was equipped with four PL aquagel-OH columns (60, 50, 40, and 30; 429 300 × 7.5 mm) connected in series. The eluent used was 0.2 M $NaNO_3$/0.02% NaN_3 (0.6 mL/min). The RID temperature was set at 30 °C. Average molecular weight (Mw) was calculated using a standard curve of dextrans (MW 5–1,800 kDa; Sigma-Aldrich (St. Louis, MO, USA)). The void volume (V_o) was the elution time of the heavier molecule (blue dextran; ~1800 kDa), and the elution volume (V_e) was the release time of glucose.

Monosaccharide analysis

High-performance anion-exchange chromatography coupled to a pulsed amperometric detector (HPAEC-PAD) was used for monosaccharide composition analysis [19,20]. Samples (1 mg/mL) were hydrolyzed with 2 M trifluoroacetic acid at 120 °C for 90 min. After the samples were cooled down to room temperature, *t*-butyl alcohol was added, and the mixture was evaporated under N_2 flow. The dried samples were solubilized in water and filtered (0.45 µm) and analyzed in a DX 500 system (Dionex, Sunnyvalle, CA, USA) equipped with a CarboPac PA10 column (250 × 4 mm). Neutral sugars analysis was performed in water (1 mL/min; 40 min). A postcolumn adjustment with 300 mM NaOH was used for detection. Uronic acids analysis was performed in 150 mM NaOH (1 mL/min; 30 min) with a 0–220 nM sodium acetate gradient and postcolumn adjustment with 150 mM. Neutral sugars (arabinose, fucose, galactose, glucose, mannose, rhamnose, and xylose) and uronic acids (galacturonic acid and glucuronic acid) were used as standards.

Determination of degree of methyl-esterification (DM)

The WSF samples (5 mg) was weighed in head-space vials in triplicate. WSF were saponified in duplicate using 1 mL of 0.1M NaOH for 24 h (1 h at 4 °C, followed by 23 h at room temperature). To the WSF blank, 1 mL of water was added. The head-space vials were immediately sealed with a Teflon lined rubber septum. To determine the degree of methyl-esterification (DM) a GC method was used as previously described [21].

Gas chromatography was run on a HS-GC equipped with a flame ionization detector and an automatic injection system. For GC, a Trace GC system (Thermo Scientific, Waltham, MA, USA) equipped with a DB-WAX 30 m × 0.25 mm × 0.25 µm was used. The conditions were as following: helium as carrier gas with a flow rate of 20 mL/min. Column temperature was set at 40 °C for 1,25 min and then programmed to 160 °C at a rate of 20 °C/min. The injector was set at 200 °C and the detector performed at 225 °C. Samples were heated at 50 °C for 10 min in the head-space sampler prior to spitless injection. Two mL of the head-space volatiles was automatically injected in 10 s on the column.

Atomic force microscopy (AFM)

Un-1-WSF and R-2-WSF were diluted in water and sonicated (2.5 µg/mL). The samples were dropped onto freshly cleaved mica, dried in a vacuum at 30 °C for 20 min and maintained in a desiccator until the analysis. An NX-10 Atomic Force Microscope (Park Systems, Suwon, South Korea) in an acrylic glove box was used to obtain the topography images with controlled temperature (~22 °C) and humidity (~3%). AFM images were acquired on tapping mode using an NCHR probe (NanoWorld) with a spring constant of 42 N/m and 320 kHz resonance frequency. The scan speed and scanning resolution were 0.5 Hz and 512 × 512 points, respectively. At least ten images were collected for each sample. Gwyddion 2.47 software (http:// gwyddion.net/) was used to get the images.

Fourier transform infrared (FTIR) attenuated total reflectance (ATR)

The Fourier Transform Infrared (FTIR) spectroscopy was used as a tool to characterize the polysaccharides [22,23]. The Alpha FTIR spectrometer (Bruker Optic, Ettlingen, Germany) equipped with a deuterated triglycine sulfate detector and a single bounce attenuated total reflectance (ATR) accessory (diamond crystal) was used. FTIR–ATR spectra of samples were obtained with a resolution of 4 cm^{-1} and 50 scans.

Reporter cell lines

THP-1 human acute monocytic leukemia reporter and HEK-Blue™ TLR cells were used in the assays (InvivoGen, Toulouse, France). THP-1 MD2-CD14 and THP-1 DefMyD endogenously expresses all human pattern recognition receptors, including all TLRs and express the soluble embryonic alkaline phosphatase (SEAP) gene coupled to the NF-kB/AP-1 promoter. THP-1 MD2-CD14 overexpress CD14 which increases the response to the majority of TLR ligands. THP-1 DefMyD cells are deficient in MyD88 activity turning unable to activate TLR ligands. We used human Embryonic Kidney (HEK 293) blue reporter cell lines with different inserted construct for TLR2, TLR3, TLR4, TLR5, TLR9, NOD1, or NOD2 with all cell lines inserted with the construction for SEAP expression (InvivoGen, Toulouse, France). The activation of TLR and consecutively NF-κB activation will express SEAP. The SEAP is quantified using Quanti-Blue (InvivoGen, Toulouse, France). Specific agonists were used as positive controls for each TLR activation (**Supplementary Table 1**).

THP-1 cell lines were cultured in RPMI1640 culture media (Lonza, Basel, Switzerland) with 10% heat inactivated fetal bovine serum (FBS), L-glutamine (2 mM), HEPES (10 mM), D-glucose (4,5 g/L), sodium pyruvate (10 mM), normocin (100 µg/ml), penicillin/streptomycin (50 µg/mL) and $NaHCO_3$ (1,5 g/L).

HEK cells were cultured in DMEM culture media (Lonza, Basel, Switzerland) with 10% heat inactivated FBS, L-glutamine (2 mM), D-glucose (4,5 g/L), normocin (100 µg/ml) and penicillin/streptomycin (50 µg/mL).

The culture medium of each cell line was supplemented with the selected antibiotic of each cell line (**Supplementary Table 1)**. The WSF were solubilized in DMEM or RPMI1640 at 2 mg/mL, 1 mg/mL and 0.5 mg/mL and cells were treated with these solutions. For the TLR inhibiting/blockage by the polysaccharides, the HEK cells were treated with WSF for 1 h and then, with the specific agonists of each TLR.

After 24 h incubation of cells with the WSF or the other treatments, 20 µL of the cells suspension was added in a new 96-well plate with 180 µL of QuantiBlue solution. After 1 hour of incubation, the plate was read at 650nm in an ELISA plate reader Versa Max (Molecular Devices, Sunnyvale, California, USA).

Statistics

The results were expressed as the mean ± standard deviation (SD). Parametric distribution of data was tested using Shapiro-Wilk normality test. Data were analyzed using GraphPad Prism 6.0 software (GraphPad Software, San Diego, CA). One-way ANOVA with Tukey's (to assess differences between all groups) or Dunnett's (to assess differences between the control and two or more groups) were used as post hoc tests. Significance was set at $p < 0.001$***, $p < 0.01$** and $p < 0.05$*.

Results

Water-soluble fraction characterization

The WSF samples were obtained from papayas from the first to the fifth days after harvest and the following yield of each fraction is depicted (Un-1-WSF – 1st day after harvest: 0,38 ± 0,02 mg/100g Fresh Weight, Un-2-WSF – 2nd day after harvest: 0,51 ± 0,04 mg/100g FW, I-WSF – 3rd day after harvest: 0,56 ± 0,05 mg/100g FW, R-1-WSF – 4th day after harvest: 0,87 ± 0,05 mg/100g FW, and R-2-WSF – 5th day after harvest: 0,91 ± 0,02 mg/100g FW). The WSF extraction yield increased during papaya ripening as expected [24]. Ash, starch, proteins and phenolic compounds contents were insignificant in the WSF fractions, demonstrating the polysaccharide fractions were highly-purified ones.

Overall, homogeneity and Mw were heterogeneous and with a broad Mw distribution with two distinct populations with the WSF obtained from unripe papayas (Un-1-WSF and Un-2-WSF) having the higher Mw (**Figure 1A, 1B**). The Un-1-WSF and Un-2-WSF were similar between them but different from R-1-WSF and R-2-WSF, these two-last showing lower Mw with similar Mw distribution. The I-WSF possess an intermediary Mw profile compared to other fractions. These statements regarding Mw show that the papaya ripening process hydrolyze pectin while decreasing WSF Mw which will lead to plant cell wall disassembling. The changes in Mw can also be visualized by AFM (**Figure 1C**). In the **Figure 1C** the white arrows represent the linear structure of Un-1-WSF, the black arrows the aggregates with an oval shape and the grey arrow represents the smaller structures of the R-2-WSF. The monosaccharide composition analyses demonstrated that the WSF were mainly composed of galacturonic acid (GalA), a main characteristic of HG portion from pectin structure. The predominant changes during ripening were the enhancement of galacturonic acid (GalA) abundance, while galactose (Gal) and glucose (Glc) were reduced during ripening (**Figure 2**). However, higher amount of Rha was

observed during ripening. When some sugar ratios were compared, a profound difference in the GalA:Rha ratio was observed which was lower in ripe papaya (Table 1) due to high amounts of both GalA and Rha. Gal:Rha and Ara:Rha ratios were also decreased during ripening, which could mean the loss of galactans and arabinogalactans side-chains of RG-I. Taken together this results with our previous study in which papaya WSF was characterized within different timepoints of ripening [17], we suggest that it is occurring an increment of RG-I in WSF from ripe papayas during ripening. Besides that, Ara and Gal decreased during ripening while Rha increased, suggesting the presence of smaller chains of more highly branched RG-I, which is also in accordance with previous study [17], we suggest that is occurring an increment of RG-I in WSF from ripe papayas. Besides that, Ara and Gal decreased during ripening while Rha increased, suggest the presence of smaller chains of more highly branched RG-I, which is also in accordance with previous study [17]. These changes in the WSF profile indicate higher neutral sugars ramifications but with shorter neutral sugar chains in the ripe papaya pectin. The DM was measured in one unripe sample and in two ripe samples. The WSF from unripe (Un-2-WSF) had a DM of 15% and in the ripe samples (R-1-WSF and R-2-WSF) the DM was higher than 40%, demonstrating a proportional increment of methyl-ester groups during ripening due to increase in the WSF yield (**Table 1**). The WSF yield increases during papaya ripening which could indicate an increment of highly esterified pectin. FT-IR spectroscopy was used to characterize the polysaccharide fractions. The frequency band from 1800 to 800 cm^{-1} was selected as the most representative for pectin characterization (**Figure 3**). The pectin structure is assigned by bands in 1740 cm^{-1} (C═O stretching) and 1600-1630 cm^{-1} (COO^- antisymmetric stretching) [22]. The differences in these two bands along the papaya ripening represents the changes in the methyl esterification profile. The 1440 cm^{-1} band represents pectin asymmetric stretching modes vibration of methyl esters [25], 1410 cm^{-1} band the pectin COO^- symmetric stretching [22] and 1235 cm^{-1} band the bending of O─H groups in pyranose ring of pectin [25]. All these bands 1440 cm^{-1}, 1410 cm^{-1}, 1235 cm^{-1} and 832 cm^{-1} (pectin ring vibration [22]) increases as the fruit ripens, demonstrating a possible alteration in ripe pectin structure, with more proportionally galacturonic acid (methyl or not esterified) as it was confirmed by the sugar composition analysis (w/w %, **Figure 2** and **Table 1**).

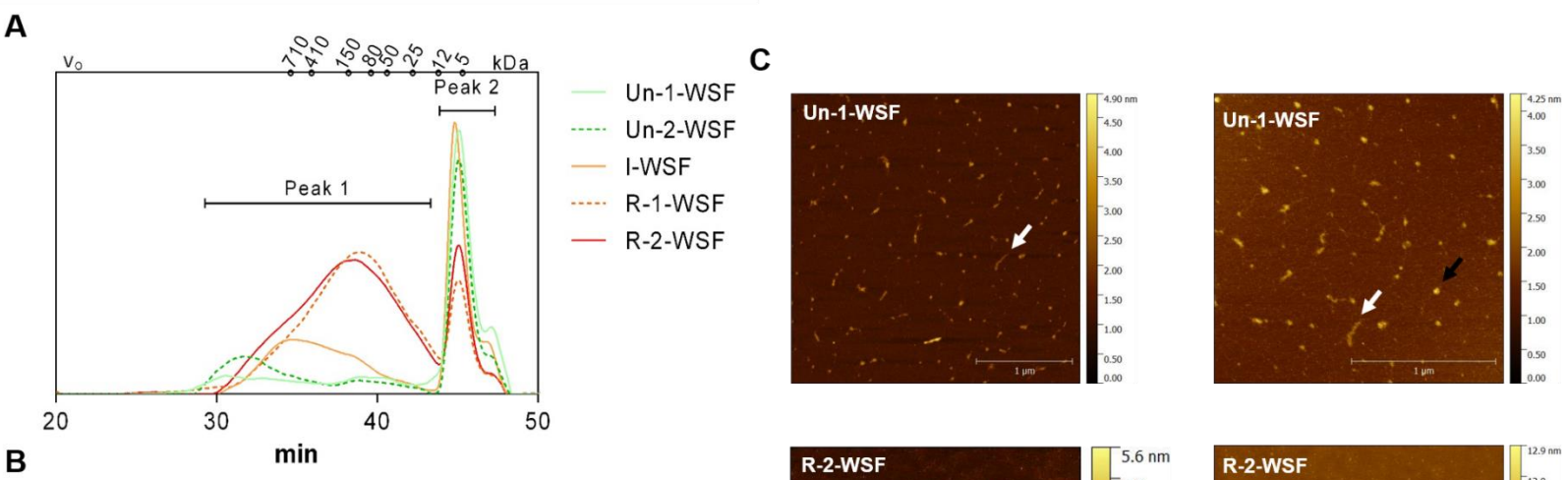

B

Samples	Molecular weight	
	Mean	sd
Un-1-WSF Peak 1	587	47
Un-1-WSF Peak 2	11	3
Un-2-WSF Peak 1	611	17
Un-2-WSF Peak 2	11	4
I-WSF Peak 1	143	9
I-WSF Peak 2	11	2
R-1-WSF Peak 1	71	17
R-1-WSF Peak 2	11	3
R-2-WSF Peak 1	73	19
R-2-WSF Peak 2	11	1

Figure 1. HPSEC-RID elution profile, molecular weight and AFM images. A) HPSEC elution profile. B) Molecular weight. Values represented by technical triplicate from the biological duplicate. C) Representative topographical AFM images of Un-1-WSF and R-2-WSF. White arrow indicates linear structures, black arrow aggregates and grey arrow the smaller structure from the R-2-WSF. Un-1-WSF: unripe - papaya from 1st day after harvest - water-soluble fraction; Un-2-WSF: unripe - papaya from 2nd day after harvest - water-soluble fraction; I-WSF: intermediate ripening time point - papaya from 3rd day after harvest - water-soluble fraction; R-1-WSF: ripe - papaya from 4th day after harvest - water-soluble fraction; R-2-WSF: ripe - papaya from 5th day after harvest - water-soluble fraction.

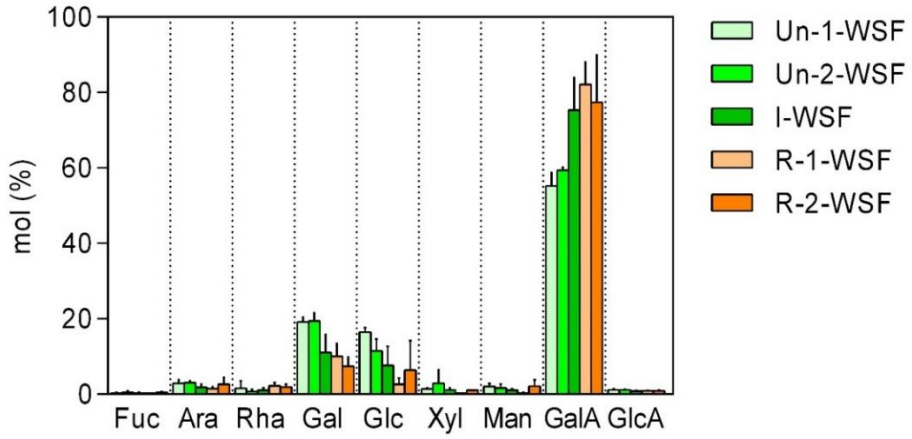

Figure 2. Monosaccharide analysis from papaya water-soluble fractions. WSF: water-soluble fractions. The numbers represent the papaya day (s) after harvested. Un-1-WSF: unripe - papaya from 1st day after harvest - water-soluble fraction; Un-2-WSF: unripe - papaya from 2nd day after harvest - water-soluble fraction; I-WSF: intermediate ripening time point - papaya from 3rd day after harvest - water-soluble fraction; R-1-WSF: ripe - papaya from 4th day after harvest - water-soluble fraction; R-2-WSF: ripe - papaya from 5th day after harvest - water-soluble fraction; Rha: rhamnose; Fuc: fucose; Ara: arabinose; Xyl: xylose; Man: mannose; Gal: galactose; GalA: Galacturonic acid; Glc: glucose; GlcA: glucuronic acid. Values represented by technical triplicate from the biological duplicate.

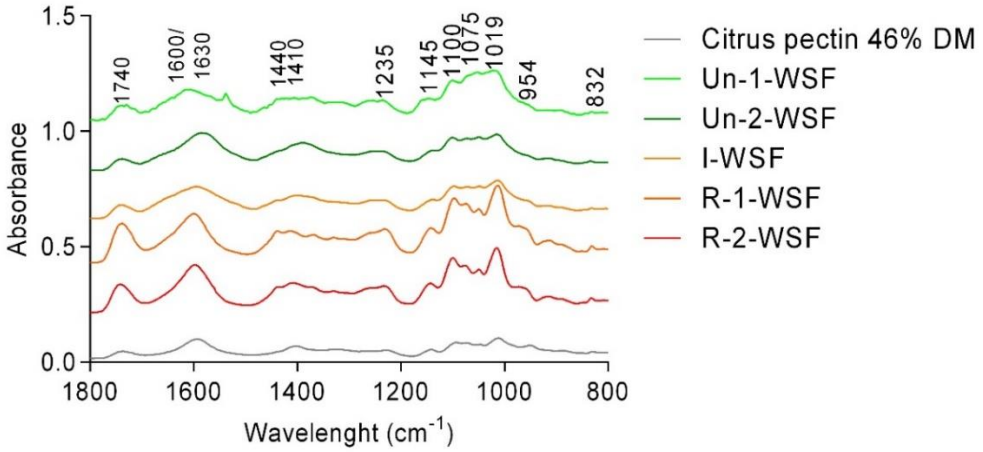

Figure 3. FT-IR spectra of citrus pectin DM 46% and papayas water-soluble fraction (WSF). Un-1-WSF: unripe - papaya from 1st day after harvest - water-soluble fraction; Un-2-WSF: unripe - papaya from 2nd day after harvest - water-soluble fraction; I-WSF: intermediate ripening time point - papaya from 3rd day after harvest - water-soluble fraction; R-1-WSF: ripe - papaya from 4th day after harvest - water-soluble fraction; R-2-WSF: ripe - papaya from 5th day after harvest - water-soluble fraction.

Table 1. Monosaccharide ratios, degree of methyl esterification and monosaccharide composition (w/w %) from papaya water-soluble fractions.

Samples	GalA: Rha	Gal: Rha	Ara: Rha	DM (%)	Fuc	Ara	Rha	Gal	Glc	Xyl	Man	GalA	GlcA
Un-1-WSF	30.3	11.3	2	NE	0.32 ± 0.25	3.64 ± 1.49	1.66 ± 2.04	19.62 ± 1.19	17.00 ± 2.36	1.72 ± 0.65	2.00 ± 0.63	52.95 ± 7.15	1.14 ± 0.21
Un-2-WSF	67.8	23.9	4.5	15.4	0.56 ± 0.53	3.78 ± 0.43	0.87 ± 0.66	20.22 ± 3.31	12.15 ± 4.38	3.31 ± 3.82	1.69 ± 1.13	57.36 ± 6.10	1.05 ± 0.10
I-WSF	60.6	9.6	1.8	NE	0.16 ± 0.1	2.16 ± 1.24	1.21 ± 0.81	11.18 ± 5.80	6.23 ± 3.92	1.47 ± 0.61	1.08 ± 0.30	76.75 ± 16.48	0.81 ± 0.23
R-1-WSF	31.4	4.1	0.7	41.4	0.20 ± 0.08	2.15 ± 0.73	3.02 ± 1.25	12.58 ± 3.28	3.60 ± 1.70	0.38 ± 0.03	0.31 ± 0.23	77.79 ± 6.20	0.87 ± 0.12
R-2-WSF	35.2	3.6	1.5	45.3	0.25 ± 0.31	5.18 ± 3.23	3.8 ± 0.73	12.48 ± 4.87	1.22 ± 0.36	1.86 ± 1.63	0.81 ± 0.40	85.00 ± 2.60	0.83 ± 0.07

NE: not evaluated.
Un-1-WSF: unripe - papaya from 1st day after harvest - water-soluble fraction; Un-2-WSF: unripe - papaya from 2nd day after harvest - water-soluble fraction; I-WSF: intermediate ripening time point - papaya from 3rd day after harvest - water-soluble fraction; R-1-WSF: ripe - papaya from 4th day after harvest - water-soluble fraction; R-2-WSF: ripe - papaya from 5th day after harvest - water-soluble fraction. Rha: rhamnose; Fuc: fucose; Ara: arabinose; Xyl: xylose; Man: mannose; Gal: galactose; GalA: Galacturonic acid; Glc: glucose; GlcA: glucuronic acid. Values represented by technical triplicate from the biological duplicate.

TLR and NOD signaling of pectin fractions

THP1 MD2-CD14 is a reporter cell line carrying all TLRs coupled to a SEAP reporter gene. Comparison of signaling in this reporter cell with that of a THP-1 cells line with a truncated defective Myd88 (THP1 defMyD88) gene reveals whether a pectin induced SEAP activation is TLR dependent. All papaya WSF significantly increased NF-kB production in THP1 MD2-CD14 when compared with the negative control ($p < 0.0001$; **Figure 4**) while signaling in THP1 defMyD88 was virtually absent. Only in the highest concentration, papaya fractions were able to induce a slight increase in NF-kB production in THP1 defMyD88 reporter cells (p values ranging from 0.05 to 0.0001, **Figure 4**). As this could indicate a concentration dependent activation of other pattern recognition receptors, such as NOD, we decided to also test WSF papaya fractions on NOD signaling in HEK NOD 1 and HEK NOD 2 reporter cells. As shown in **Figure 5**, WSF from ripe papayas induced NOD1 and NOD2 activation in a concentration dependent manner. The pectin from ripe papaya was more profoundly activating NOD2 than NOD1 ($p < 0.05$).

As pectin fractions predominantly activated TLRs in THP1 MD2-CD14 we next determined which specific TLRs are inhibited and/or activated. To this end reporter cell lines expressing either TLR2, TLR3, TLR4, TLR5 or TLR9 were applied (**Figure 6**). We separately studied activating and inhibiting effects of the pectin fractions as following.

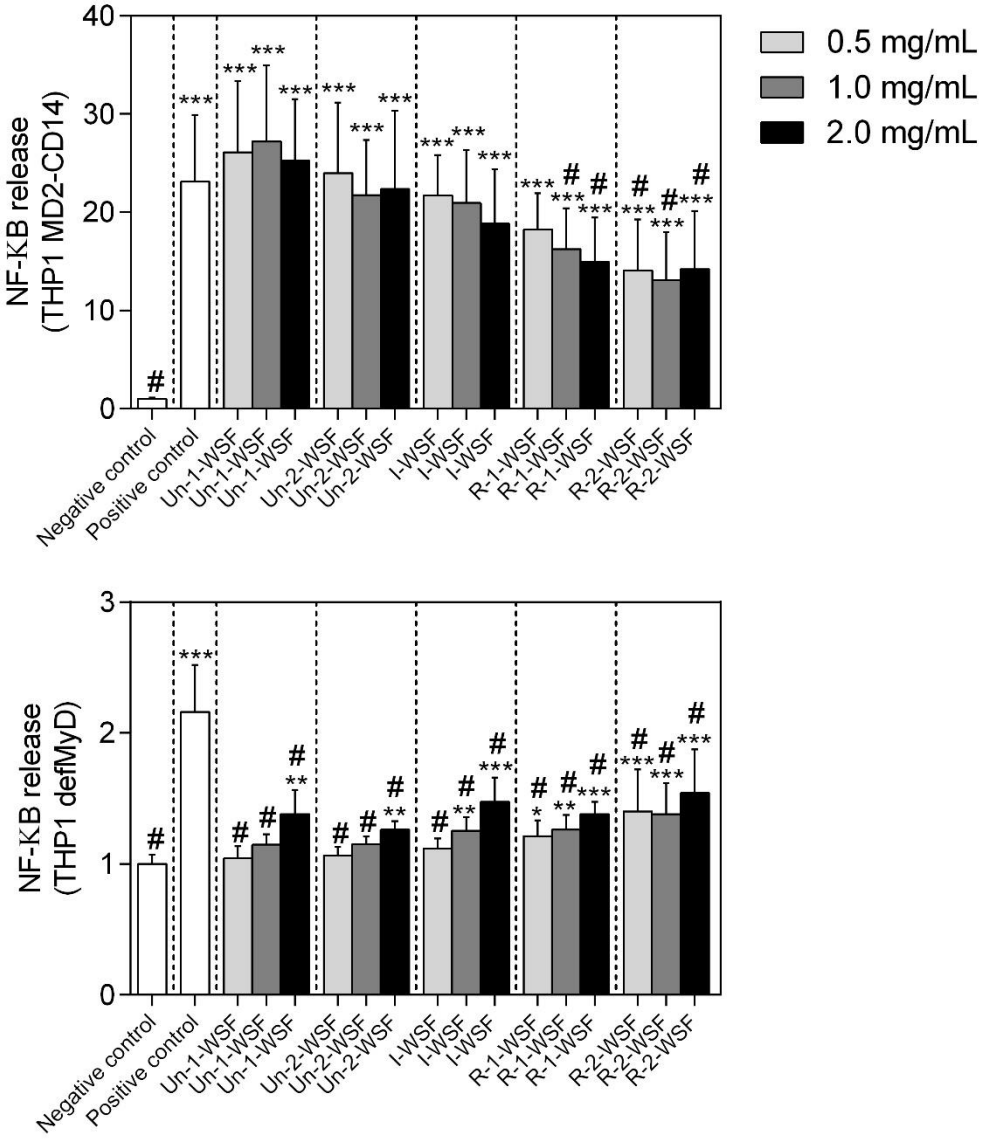

Figure 4. THP1 MD2 CD14 and THP1 defMyD88 reporter cells NF-kB/AP-1 activation after papaya pectin treatments. Un-1-WSF: unripe - papaya from 1st day after harvest - water-soluble fraction; Un-2-WSF: unripe - papaya from 2nd day after harvest - water-soluble fraction; I-WSF: intermediate ripening time point - papaya from 3rd day after harvest - water-soluble fraction; R-1-WSF: ripe - papaya from 4th day after harvest - water-soluble fraction; R-2-WSF: ripe - papaya from 5th day after harvest - water-soluble fraction. According Dunnett's *** p value < 0.0001, ** p value < 0.001, * p value < 0.05 when compared with negative control and # means significantly difference when compared with the positive control.

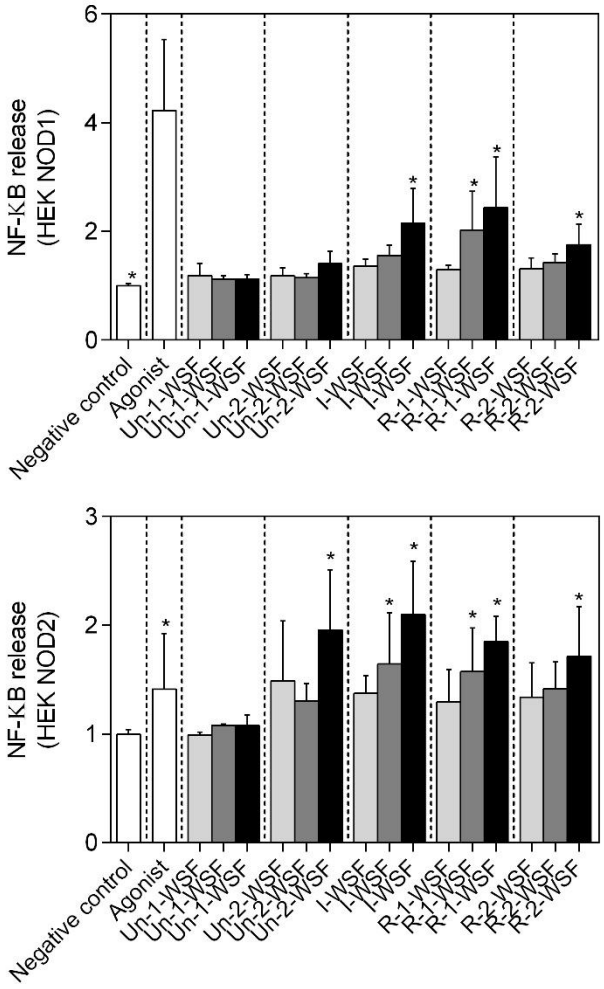

Figure 5. NOD1 and NOD2 reporter cells NF-kB/AP-1 activation after papaya pectin treatments. Un-1-WSF: unripe - papaya from 1st day after harvest - water-soluble fraction; Un-2-WSF: unripe - papaya from 2nd day after harvest - water-soluble fraction; I-WSF: intermediate ripening time point - papaya from 3rd day after harvest - water-soluble fraction; R-1-WSF: ripe - papaya from 4th day after harvest - water-soluble fraction; R-2-WSF: ripe - papaya from 5th day after harvest - water-soluble fraction. According Dunnett's * p value < 0.05 when compared with negative control.

Activating effects

HEK TLR2 cell lines expresses TLR2, TLR1 and TLR6 since signaling of TLR2 activation is dependent of TLR2/TLR6 and TLR1/TLR2 interaction. Activation and/or dimerization of TLR2, TLR2/1 and TLR2/6 was confirmed by stimulation with the specific agonists HKLM, Pam3CSK4 and FSL-1, respectively. We found that all pectins mainly

activated TLR2 and TLR4 ($p < 0.001$). I-WSF, R-1-WSF and R-2-WSF activated TLR3 and TLR5 ($p < 0.001$) and pectin from unripe papayas (Un-1-WSF and Un-2-WSF) did not activate these receptors. I-WSF, R-1-WSF and R-2-WSF significantly activate TLR9 ($p < 0.001$), and only the highest concentration of pectins extracted from unripe papayas (Un-1-WSF and Un-2-WSF) increased TLR9 activation after cell treatment ($p < 0.01$). The unripe fractions Un-1-WSF and Un-2-WSF were not able to activate all TLRs while I-WSF, R-1-WSF and R-2-WSF were able to activate all TLRs. The Un-2-WSF activated TLR 9 in the highest concentration.

Inhibiting effects

As pectins have been reported to have inhibiting effects on TLR signaling in addition to stimulating effects, we also study the possible inhibition. To this end, reporter cells were first treated with papaya WSF for 1 h and then treated with the specific agonists (**Figure 7**). Results for TLR2 (using Pam3CSK4 agonist) and TLR4 were the same as the treatment with only papaya pectin, showing all pectin samples might have in fact activated the receptors. WSF extracted from unripe papaya (Un-1-WSF and Un-1-WSF) inhibited the release of NF-kB after TLR3 induction by the specific agonist, demonstrating a possible irreversible ligation and inhibition of long chain papaya pectin and TLR3. It was observed that the pectin extracted from unripe papaya, both time points (Un-1-WSF and Un-1-WSF), were not able to inhibit the NF-kB release after TLR5 activation by specific agonists, suggesting that those pectins do not interact with TLR5. Only the pectin from the unripe papayas (Un-1-WSF) was able to inhibit TLR9, suggesting this long chain pectin could irreversible interact with TLR9. Another possibility would be a concentration effect, as in unripe WSF has high Mw molecules and in ripe WSF less as it can be seen in HPSEC profile in earlier elution time (31-32 min).

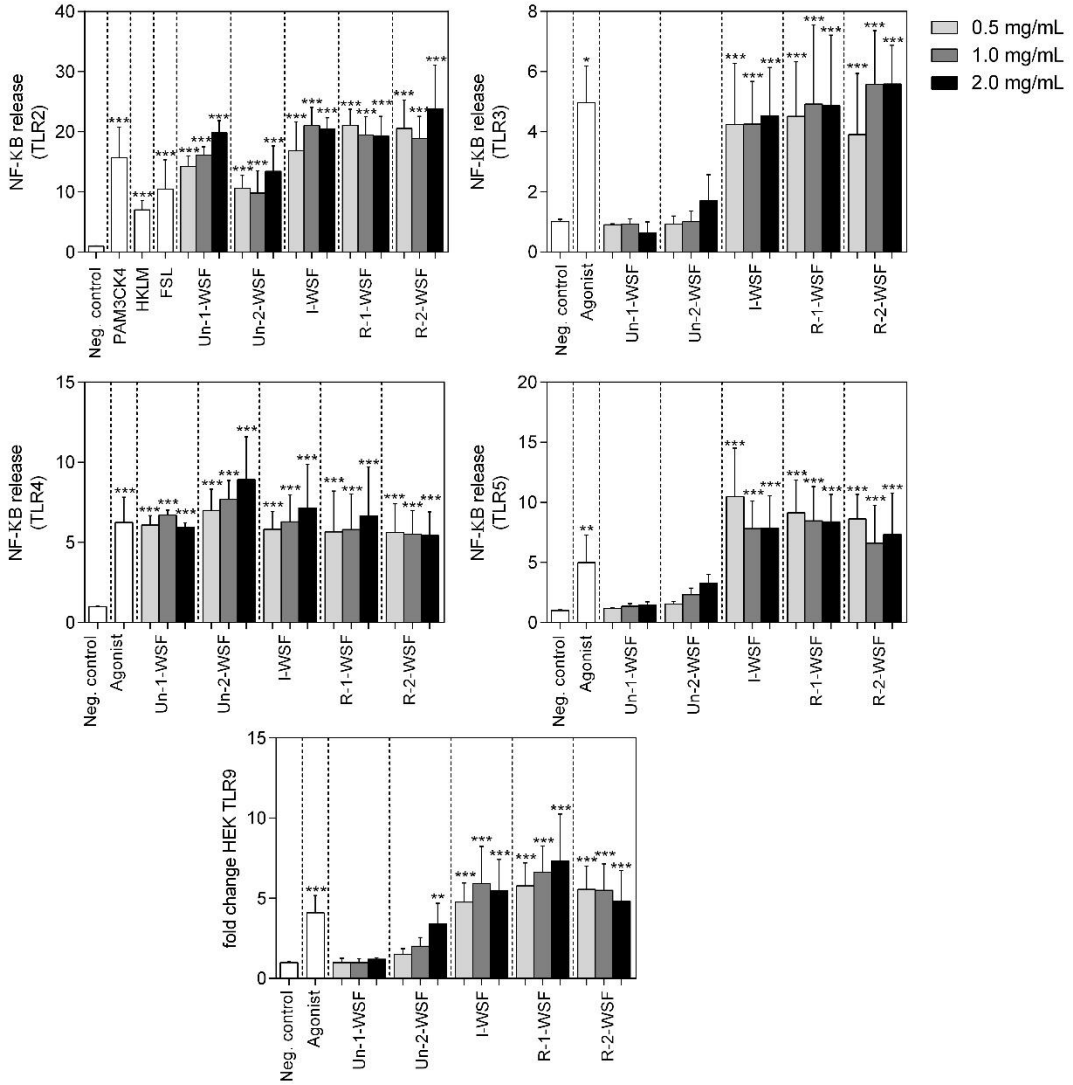

Figure 6. Activation of TLR2, TLR3, TLR4, TLR5 and TLR9 by different papaya pectins. Un-1-WSF: unripe - papaya from 1st day after harvest - water-soluble fraction; Un-2-WSF: unripe - papaya from 2nd day after harvest - water-soluble fraction; I-WSF: intermediate ripening time point - papaya from 3rd day after harvest - water-soluble fraction; R-1-WSF: ripe - papaya from 4th day after harvest - water-soluble fraction; R-2-WSF: ripe - papaya from 5th day after harvest - water-soluble fraction. According Dunnett's test *** p value < 0.0001 and ** p value < 0.001 when compared with negative control.

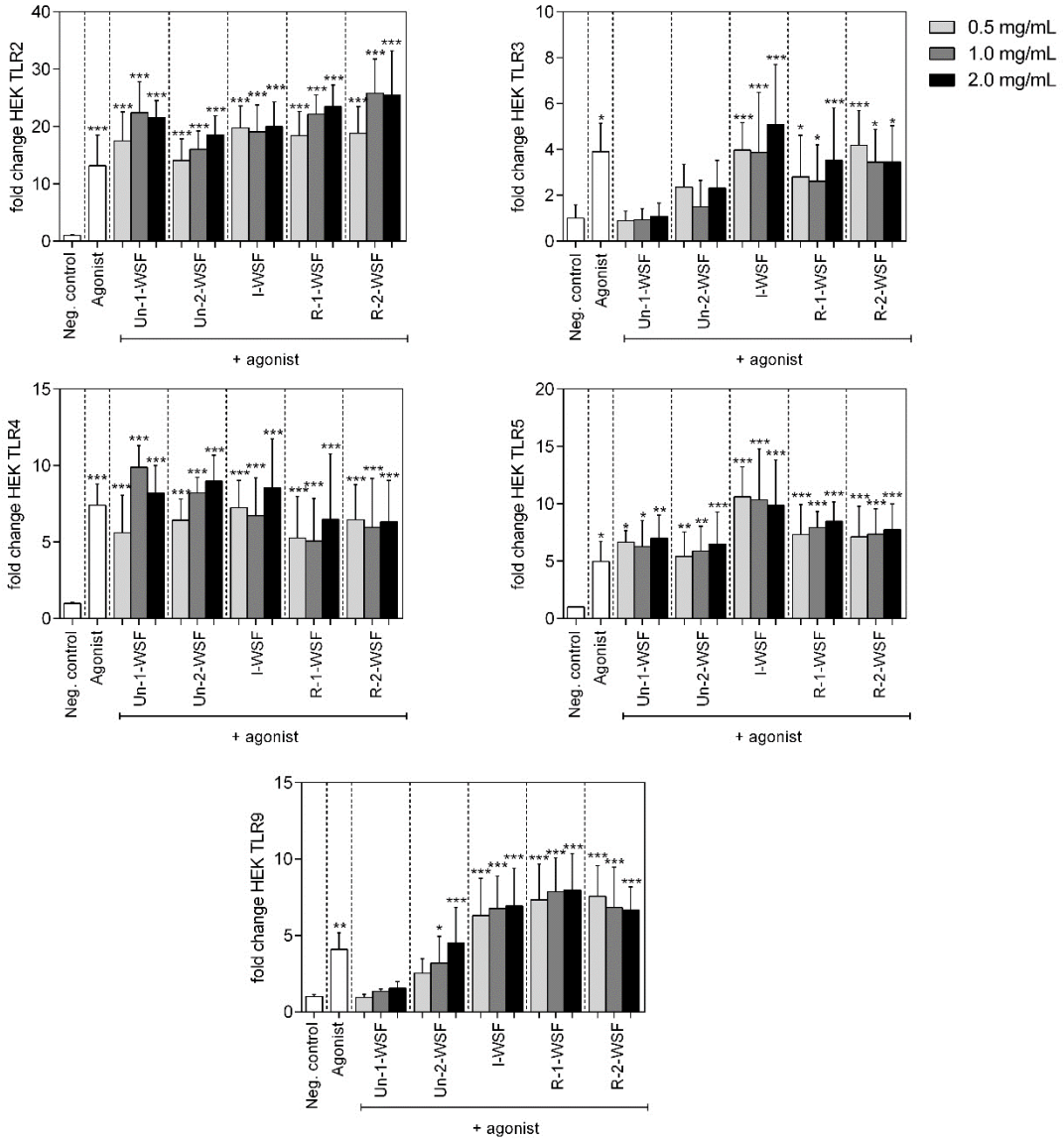

Figure 7. Inhibition of TLR2, TLR3, TLR4, TLR5 and TLR9 by papaya pectin. A agonist of the TLR was applied together with the pectin fraction isolated form papaya Un-1-WSF: unripe - papaya from 1st day after harvest - water-soluble fraction; Un-2-WSF: unripe - papaya from 2nd day after harvest - water-soluble fraction; I-WSF: intermediate ripening time point - papaya from 3rd day after harvest - water-soluble fraction; R-1-WSF: ripe - papaya from 4th day after harvest - water-soluble fraction; R-2-WSF: ripe - papaya from 5th day after harvest - water-soluble fraction. According Dunnett's test *** p value < 0.0001 and ** p value < 0.001 when compared with negative control.

Discussion

Papaya ripening in an enzymatic biochemical driven process that occurs in a short period of time (4-5 days) involving macromolecule mobilization and formation of new unique pectin molecules. Just in three days after harvesting the fruit pulp is completely soft and new pectin molecules are formed due to pectinase time- and ethylene-dependent action [15]. The over-expression of cell wall degrading enzymes, especially polygalacturonases, culminates in pulp softening [16,26]. This massive enzyme action naturally modifies insoluble pectin and releases them in the more soluble fraction in the fruit and hydrolyze the long chains into smaller galacturonans chain [16,17]. The interaction of HG segments derived from pectic polysaccharides with PRR and its concomitant health effects have been described elsewhere [27]; but how papaya pectin in the most soluble polysaccharide fraction (WSF), interacts with PRR, has never been studied. In this study, we extracted the highly-purified water-soluble polysaccharide fraction (WSF) from five time points of papaya ripening (unripe to ripe), characterized the polysaccharides and evaluated whether they differentially interact with TLRs and NODs.

The Water-Soluble Fractions of papaya cell wall consists mainly of homogalacturonan

The structural differences between the WSF derived from unripe, intermediate or ripe papaya stages, are the high amount of GalA and the increasing DM and the Mw distribution of the ripe papayas pulp polysaccharides. The less soluble pectin (only soluble in chelate solvent) represented by long chains of galacturonans (HG) with small portions of de-esterified galacturonans attached to each other by calcium bridges is being released during ripening due to activity of cell degrading enzymes [15]. The main enzymes acting in papaya ripening is polygalactunase which cleave the non-esterified HG parts and by lowering the Mw of the calcium bridges pectins made them more soluble. The enrichment of less soluble pectins into the WSF proportionally increases esterified GalA amount of HG (**Table 1**) and decreases the molar proportion of Gal and Glc throughout ripening as described elsewhere [16]. Even with the decreasing in the overall Mw, the higher Mw do not disappear from riper papaya WSF. This could be due to the continuous solubilization of other lesser soluble cell structures (as alkali soluble structures). This happens not only with papayas [24] but also with other fruits and vegetables [28–30]. Strawberries pectin treated with endo-polygalacturonases and evaluated by AFM profile demonstrated similar results than the stated here with papaya ripening. Bigger linear pectin structures and

agglomerates at first, and after the enzymatic treatment a decrease in the chain length and in the agglomerates [31]. The aggregates seen in AFM image can be polymers complexes held together by intermolecular interactions showing pectin heterogeneity and complexity [32]. Pectin mainly formed by GalA, Ara, Rha, and Gal is the papaya WSF composition, and others neutral sugars like Glc could be derived from more soluble hemicelluloses. The FT-IR analysis confirms that the polysaccharides from WSF extracted from papaya pulps are mainly pectins. As papayas become ripen, a more distinct peak for neutral sugar became apparent. These peaks are related not only with the quantity but also with the position and the degree of substitution of the neutral sugars [33].

THP1 reporter cell lines express all TLRs as well as other PRRs such as NOD1 and NOD2. The activation patterns of the pectins was compared with THP1 defMyD88 reporter cells to determine TLR dependent activation. Our data suggest a possible interaction of papaya pectin with different TLR as well as that of NOD1 and/or NOD2. NOD1 and NOD2 was activated in a concentration dependent way only by pectins derived from the ripe papayas (I-WSF, R-1-WSF, and R-2-WSF). Un-2-WSF seems to be less active, but could also activate NOD2 in the highest concentration as it has already been observed for β2→1-fructans [13].

PRR activation by DF has been mainly described for TLR2 and TLR4 [9,10]. Lemon pectin with DM of 74% activated TLR2 and TLR4 with TLR4 being activated to a lesser extent than TLR2 [10]. However lemon pectin with low DM blocked TLR 2/1 instead of activating the receptor [11]. In human dendritic cells, β-glucans synergistically activate TLR4 and Dectin-1 [34]. β2→1-fructans activated TLR2, while TLR4, TLR5, TLR7, TLR8 were mildly activated in reporter HEK cells [13]. Guar gum can activate TLR2 and dectin-1 reducing the inflammation of small intestine epithelium [35]. Fructooligosaccharides, inulin, galactooligosaccharides, and goat's milk oligosaccharides were reported to be TLR4 ligands in intestinal epithelial cells [36] while the bengkoang fiber stimulated macrophages through TLR4 activation [37]. In our study we observed that even with the DM differences TLR2 and TLR4 were activated after treatment with all papaya pectins. However, TLR3, TLR5 and TLR9 were not activated by pectin derived from the unripe papayas (Un-1-WSF and Un-2-WSF) that have as structural characteristics less methylation and higher Mw molecules. The lower HG structures released in the ripe stage with DM higher than 40% and with higher amounts of GalA seems to interact with the cells receptors in a different way than the less esterified and higher Mw WSF from the

unripe papaya. The lower Mw HG structures released in the ripe stage with DM higher than 40% and with higher amounts of GalA seems to interact with the cells receptors in a different way than the less esterified and higher Mw WSF from the unripe papaya. The changes in neutral sugars during the ripening seem to be related with the decreasing size of the chain ramifications, but with higher amount of Rha which could indicate more ramifications with less sugars linked to it, as also observed elsewhere [17].

The non-activation of the HEK TLR reporter cells could be due to long chain papaya pectins (Un-1-WSF and Un-2-WSF) that are not interacting with the receptors (TLR5) or binding but not activating the receptors (TLR3 and TLR9). The pectin extracted from unripe fruit did not bind to TLR5 since reporter cells treatment carrying this TLR did not show any activation after incubation with these pectin fraction.

The Un-1-WSF and Un-2-WSF treatments inhibited TLR 3 and TLR 9 activation as these pectins specifically contains low-esterified and long chain molecules suggesting they are responsible for inhibition of TLR3 and TLR9. This is corroborated by previous findings demonstrating that low-esterified pectins block TLR 2/1 [11], and highly branched citrus pectin suppressed pro-inflammatory interleukin 6 in RAW 264.7 macrophages stimulated with Pam3CSK4 (ligand for TLR1/2), FSL-1 (ligand for TLR2/6), and CpG-ODN (ligand for TLR9) [38].

Our data also suggest that pectins extracted from ripe papayas, with higher esterification and smaller chains, have the ability to interact and to activate all the studied TLR. It also suggests that pectins from unripe papayas, with lower esterification and longer chains have the ability to interact with TLR3 and TLR9 in an irreversible way blocking the agonist activation. The effects shown in our study cannot be explained by possible contaminations with endotoxins since pectin fractions were pre-treated in an affinity column with polymyxin B-agarose extracting possible endotoxins.

During papaya ripening, profound structural changes in pectin structure occur leading to possible differential biological effects [17,24]. Papaya pectins extracted from fruit pulp at different ripening points could interact with different PRR in a ripening-dependent way. This could represent new biological features of papaya pectins besides the anticancer activities [17,24] possibly creating new and cost-effective approaches to extract pectins with desired structural and biological features from ripe papaya fruits.

References

[1] G.R. Gibson, H.M. Probert, J. Van Loo, R.A. Rastall, M.B. Roberfroid, Dietary modulation of the human colonic microbiota: updating the concept of prebiotics, Nutr. Res. Rev. 17 (2004) 259. doi:10.1079/NRR200479.

[2] J.H. Cummings, L.M. Edmond, E.A. Magee, Dietary carbohydrates and health: Do we still need the fibre concept?, Clin. Nutr. Suppl. 1 (2004) 5–17. doi:10.1016/j.clnu.2004.09.003.

[3] K. Minamida, M. Nishimura, K. Miwa, J. Nishihira, Effects of dietary fiber with Bacillus coagulans lilac-01 on bowel movement and fecal properties of healthy volunteers with a tendency for constipation, Biosci. Biotechnol. Biochem. 79 (2015) 300–306. doi:10.1080/09168451.2014.972331.

[4] E. Cario, Bacterial interactions with cells of the intestinal mucosa: Toll-like receptors and NOD2, Gut. 54 (2005) 1182–1193. doi:10.1136/gut.2004.062794.

[5] J.E. Ramberg, E.D. Nelson, R.A. Sinnott, Immunomodulatory dietary polysaccharides: A systematic review of the literature, Nutr. J. 9 (2010) 54. doi:10.1186/1475-2891-9-54.

[6] S.S. Ferreira, C.P. Passos, P. Madureira, M. Vilanova, M.A. Coimbra, Structure-function relationships of immunostimulatory polysaccharides: A review, Carbohydr. Polym. 132 (2015) 378–396. doi:10.1016/j.carbpol.2015.05.079.

[7] T. Shibata, F. Nakashima, K. Honda, Y.J. Lu, T. Kondo, Y. Ushida, K. Aizawa, H. Suganuma, S. Oe, H. Tanaka, T. Takahashi, K. Uchida, Toll-like receptors as a target of food-derived anti-inflammatory compounds, J. Biol. Chem. 289 (2014) 32757–32772. doi:10.1074/jbc.M114.585901.

[8] K. Takeda, S. Akira, Toll-like receptors in innate immunity, Int. Immunol. 17 (2005) 1–14. doi:10.1093/intimm/dxh186.

[9] Z. Jiang, T.W. Mak, G. Sen, X. Li, Toll-like receptor 3-mediated activation of NF-κB and IRF3 diverges at Toll-IL-1 receptor domain-containing adapter inducing IFN-β, 101 (2004) 1–6.

[10] L.M. Vogt, N.M. Sahasrabudhe, U. Ramasamy, D. Meyer, G. Pullens, M.M. Faas, K. Venema, H.A. Schols, P. de Vos, The impact of lemon pectin characteristics on TLR activation and T84 intestinal epithelial cell barrier function, J. Funct. Foods. 22 (2016) 398–407. doi:10.1016/j.jff.2016.02.002.

[11] N.M. Sahasrabudhe, M. Beukema, L. Tian, B. Troost, J. Scholte, E. Bruininx, G.

Bruggeman, M. van den Berg, A. Scheurink, H.A. Schols, M.M. Faas, P. de Vos, Dietary fiber pectin directly blocks toll-like receptor 2-1 and prevents doxorubicin-induced ileitis, Front. Immunol. 9 (2018) 1–19. doi:10.3389/fimmu.2018.00383.

[12] L.M. Vogt, D. Meyer, G. Pullens, M.M. Faas, K. Venema, U. Ramasamy, H.A. Schols, P. de Vos, Toll-Like Receptor 2 Activation by β2→1-Fructans Protects Barrier Function of T84 Human Intestinal Epithelial Cells in a Chain Length-Dependent Manner, J. Nutr. 144 (2014) 1002–1008. doi:10.3945/jn.114.191643.

[13] L. Vogt, U. Ramasamy, D. Meyer, G. Pullens, K. Venema, M.M. Faas, H.A. Schols, P. de Vos, Immune Modulation by Different Types of β2→1-fructans Is Toll-Like Receptor Dependent, PLoS One. 8 (2013) 1–12. doi:10.1371/journal.pone.0068367.

[14] D. Mohnen, Pectin structure and biosynthesis, Curr. Opin. Plant Biol. 11 (2008) 266–277. doi:10.1016/j.pbi.2008.03.006.

[15] J.P. Fabi, B.R. Cordenunsi, G.P. de Ma. Barreto, A.Z. Mercadante, F.M. Lajolo, J.R.O. Do Nascimento, Papaya Fruit Ripening: Response to Ethylene and 1-Methylcyclopropene (1-MCP), J. Food Agric. Food Chem. 55 (2007) 6118–6123.

[16] S.B.R. do Prado, P.R. Melfi, V.C. Castro-Alves, S.G. Broetto, E.S. Araújo, J.R.O. do Nascimento, J.P. Fabi, Physiological Degradation of Pectin in Papaya Cell Walls: Release of Long Chains Galacturonans Derived from Insoluble Fractions during Postharvest Fruit Ripening, Front. Plant Sci. 7 (2016) 1120. doi:10.3389/fpls.2016.01120.

[17] S.B.R. do Prado, G.F. Ferreira, Y. Harazono, T.M. Shiga, A. Raz, N.C. Carpita, J.P. Fabi, Ripening-induced chemical modifications of papaya pectin inhibit cancer cell proliferation, Sci. Rep. 7 (2017) 16564. doi:10.1038/s41598-017-16709-3.

[18] J. Javanmardi, Antioxidant activity and total phenolic content of Iranian Ocimum accessions, Food Chem. 83 (2003) 547–550. doi:10.1016/S0308-8146(03)00151-1.

[19] T.M. Shiga, J.P. Fabi, J.R.O. do Nascimento, C.L.D.O. Petkowicz, L.C. Vriesmann, F.M. Lajolo, B.R. Cordenunsi, Changes in cell wall composition associated to the softening of ripening papaya: evidence of extensive solubilization of large molecular mass galactouronides, J. Agric. Food Chem. 57 (2009) 7064–71. doi:10.1021/jf900073b.

[20] T.M. Shiga, N.C. Carpita, F.M. Lajolo, B.R. Cordenunsi-Lysenko, Two banana cultivars differ in composition of potentially immunomodulatory mannan and arabinogalactan, Carbohydr. Polym. 164 (2017) 31–41.

doi:10.1016/j.carbpol.2017.01.079.

[21] M.M.H. Huisman, A. Oosterveld, H.A. Schols, Fast determination of the degree of methyl esterification of pectins by head-space GC, 18 (2004) 665–668. doi:10.1016/j.foodhyd.2003.11.006.

[22] M. Szymanska-Chargot, A. Zdunek, Use of FT-IR Spectra and PCA to the Bulk Characterization of Cell Wall Residues of Fruits and Vegetables Along a Fraction Process, Food Biophys. 8 (2013) 29–42. doi:10.1007/s11483-012-9279-7.

[23] J. Cybulska, A. Zdunek, A. Koziol, The self-assembled network and physiological degradation of pectins in carrot cell walls, Food Hydrocoll. 43 (2015) 41–50.

[24] S. Prado, G.R. Santos, P. Mourão, J. Fabi, Chelate-soluble pectin fraction from papaya pulp interacts with galectin-3 and inhibits colon cancer cell proliferation, Int. J. Biol. Macromol. 126 (2019) 170–178. doi:10.1016/j.ijbiomac.2018.12.191.

[25] M. Chylinska, B. Kruk, A. Zdunek, Combining FT-IR spectroscopy and multivariate analysis for qualitative and quantitative analysis of the cell wall composition changes during apples development, Carbohydr. Polym. 115 (2015) 93–103. doi:10.1016/j.carbpol.2014.08.039.

[26] J.P. Fabi, S.G. Broetto, S.L.G.L. Da Silva, S. Zhong, F.M. Lajolo, J.R.O. Nascimento, Analysis of Papaya Cell Wall-Related Genes during Fruit Ripening Indicates a Central Role of Polygalacturonases during Pulp Softening, PLoS One. 9 (2014) e105685. doi:10.1371/journal.pone.0105685.

[27] H. Hug, M.H. Mohajeri, G. La Fata, Toll-like receptors: Regulators of the immune response in the human gut, Nutrients. 10 (2018) 11–13. doi:10.3390/nu10020203.

[28] T. Wang, Y.B. Park, D.J. Cosgrove, M. Hong, Cellulose-Pectin Spatial Contacts Are Inherent to Never-Dried Arabidopsis Primary Cell Walls: Evidence from Solid-State Nuclear Magnetic Resonance, Plant Physiol. 168 (2015) 871–884. doi:10.1104/pp.15.00665.

[29] D.J. Cosgrove, Re-constructing our models of cellulose and primary cell wall assembly, Curr. Opin. Plant Biol. 22 (2014) 122–131. doi:10.1016/j.pbi.2014.11.001.

[30] A. Zykwinska, J.F. Thibault, M.C. Ralet, Competitive binding of pectin and xyloglucan with primary cell wall cellulose, Carbohydr. Polym. 74 (2008) 957–961. doi:10.1016/j.carbpol.2008.05.004.

[31] C. Paniagua, A.R. Kirby, A.P. Gunning, V.J. Morris, A.J. Matas, M.A. Quesada, J.A. Mercado, Unravelling the nanostructure of strawberry fruit pectins by atomic

force microscopy, Food Chem. 224 (2017) 4–6. doi:10.1016/j.foodchem.2016.12.049.

[32] S. Posé, A.R. Kirby, J.A. Mercado, V.J. Morris, M.A. Quesada, Structural characterization of cell wall pectin fractions in ripe strawberry fruits using AFM, Carbohydr. Polym. 88 (2012) 882–890. doi:10.1016/j.carbpol.2012.01.029.

[33] M. Kacuráková, P. Capek, V. Sasinková, N. Wellner, A. Ebringerová, FT-IR study of plant cell wall model compounds: Pectic polysaccharides and hemicelluloses, Carbohydr. Polym. 43 (2000) 195–203. doi:10.1016/S0144-8617(00)00151-X.

[34] N.M. Sahasrabudhe, J. Dokter-Fokkens, P. de Vos, Particulate β-glucans synergistically activate TLR4 and Dectin-1 in human dendritic cells, Mol. Nutr. Food Res. 60 (2016) 2514–2522. doi:10.1002/mnfr.201600356.

[35] T. Van Hung, T. Suzuki, Guar gum fiber increases suppressor of cytokine signaling-1 expression via toll-like receptor 2 and dectin-1 pathways, regulating inflammatory response in small intestinal epithelial cells, Mol. Nutr. Food Res. 61 (2017) 1700048. doi:10.1002/mnfr.201700048.

[36] M. Ortega-González, B. Ocón, I. Romero-Calvo, A. Anzola, E. Guadix, A. Zarzuelo, M.D. Suárez, F. Sánchez de Medina, O. Martínez-Augustin, Nondigestible oligosaccharides exert nonprebiotic effects on intestinal epithelial cells enhancing the immune response via activation of TLR4-NFκB, Mol. Nutr. Food Res. 58 (2014) 384–393. doi:10.1002/mnfr.201300296.

[37] I.D. Kumalasari, K. Nishi, A.B.N. Putra, T. Sugahara, Activation of macrophages stimulated by the bengkoang fiber extract through toll-like receptor 4, Food Funct. 5 (2014) 1403–1408. doi:10.1039/c3fo60360a.

[38] K. Ishisono, T. Yabe, K. Kitaguchi, Citrus pectin attenuates endotoxin shock via suppression of Toll-like receptor signaling in Peyer's patch myeloid cells, J. Nutr. Biochem. 50 (2017) 38–45. doi:10.1016/j.jnutbio.2017.07.016.

Supplementary file

Supplementary Table 1. Cell culture specifications and agonists used in reporter cells

Reporter cell line (Invivogen)	Selected antibiotic (Invivogen)	Positive controls - agonists (Invivogen)	Cell density for seeding
Thp1-MD2-CD14	Zeocin (uL x mL CM) 100 ug/mL G418 (uL x mL CM) 100 mg/mL	Escherichia coli K12 lipopolysaccharide-HEK ultrapure (LPS) 10 ng/mL	1 x 10^6 cells/mL
Thp1-DefMyD88	Zeocin (µL x mL CM) 100 µg/mL hygro gold (µLx mL CM) 100 µg/mL	L-ala-γ-d-Glu-mDAP (Tri-DAP) 100 µg/mL	2 x 10^6 cells/mL
HEK-hTLR2	HEK-blue (µL x mL CM) 250X	lipopeptide (FSL-1; TLR2/6) 10 µg/mL Heat-killed Listeria monocytogenes (HKLM) 10^7 cells/mL (TLR2) Pam3CysSerLys4 (PAM3CK4; TLR2/1) 10 ng/mL	2.8 x 10^5 cells/mL
HEK-hTLR3	Zeocin (µL x mL CM) 100 µg/mL Blasticidin (µLx mL CM) 30 µg/mL	Polyinosinic–polycytidylic acid high molecular weight (Poly (I:C) HMW) 5 µg/ml	2.8 x 10^5 cells/mL
HEK-hTLR4	HEK-blue (µL x mL CM) 250X	Escherichia coli K12 lipopolysaccharide-HEK ultrapure (LPS) 10 ng/mL	1.4 x 10^5 cells/mL
HEK-hTLR5	Zeocin (µL x mL CM) 100 µg/mL Blasticidin (µLx mL CM) 30 µg/mL	Flagellin from Salmonella typhymurium (Rec-FLA-ST) 10 ng/mL	1.4 x 10^5 cells/mL
HEK-hTLR9	Zeocin (µL x mL CM) 100 µg/mL Blasticidin (µLx mL CM) 10 µg/mL	Class B CpG oligonucleotide (ODN 2006) 0.25 µM	4.5 x 10^5 cells/mL
HEK-NOD1	Zeocin (µL x mL CM) 100 µg/mL Blasticidin (µLx mL CM) 30 µg/mL	L-ala-γ-d-Glu-mDAP (Tri-Dap) 10 µg/mL	2.8 x 10^5 cells/mL
HEK-NOD2	Zeocin (µL x mL CM) 100 µg/mL Blasticidin (µLx mL CM) 30 µg/mL	MurNAc-L-Ala-γ-D-Glu-mDAP (M-TriDAP) 10 µg/mL	1.4 x 10^5 cells/mL

Chapter 6

Chelate-soluble pectin fraction from papaya pulp interacts with galectin-3 and inhibits colon cancer cell proliferation

Samira Bernardino Ramos do Prado[,], Gustavo R.C. Santos[2], Paulo A.S. Mourão[2], João Paulo Fabi[1,3]

[1]Department of Food Science and Experimental Nutrition, School of Pharmaceutical Sciences, University of São Paulo, São Paulo, SP, Brazil
[2]Institute of Medical Biochemistry, Universidade Federal do Rio de Janeiro, Rio de Janeiro, Brazil
[3]Food Research Center (FoRC), CEPID-FAPESP (Research, Innovation and Dissemination Centers, São Paulo Research Foundation), São Paulo, SP, Brazil

International Journal of Biological Macromolecules, V. 126, p. 170-178, 2019.

Abstract

Colorectal cancer has an overexpression of galectin-3 that is related to cancer progression. A decreased risk of colon cancer can be related to consumption of dietary fibers, but the entire mechanism by which this protection occurs remains unclear. Pectin is a type of dietary fiber that possesses β-galactosides and can bind and inhibit galectin-3–mediated effects. Papaya fruit has a massive cell wall disassembling during ripening that naturally changes its pectin structure. Our work shows that different points in the ripening time of papaya fruit exhibit pectins (chelate-soluble fractions; CSF) that can or cannot inhibit galectin-3. The fraction that inhibits galectin-3 (3CSF) also diminishes the proliferation of colon cancer cell lines, and it is derived from an intermediate point of papaya ripening. Therefore, we related this to a papaya pectin structure-dependent effect, and the papaya fruit seems to have a pectin structure that is promising in decreasing the risk of colon cancer development.

Keywords: papaya pectin, galectin-3, colon cancer

Abbreviations: AFM, Atomic force microscopy; AGII, type II arabinogalactans; Ara, arabinose; ATR, attenuated total reflectance; CSF, chelate-soluble fractions; CRD, β-galactoside–binding domain; DAH; days after harvest; DF, dietary fiber; DMEM, Dulbecco's modified Eagle's medium; FTIR, Fourier Transform-Infrared; Fuc, fucose; Gal, galactose; GalA, galacturonic acid; Glc, glucose; GlcA, glucuronic acid; HG, homogalacturonan; NMR, nuclear magnetic resonance; Man, mannose; MW, molecular weight; RG-I, rhamnogalacturonan type I; RG-I, rhamnogalacturonan type I; RG-II, rhamnogalacturonan type II; Rha, rhamnose; SD, standard deviation; WSF, water-soluble fraction; Xyl, xylose.

Introduction

The lectin galectin-3 is associated with cancer progression and is a biomarker for the development of colorectal cancer, which is the fourth leading cause of cancer-related death worldwide [1–4]. Galectin-3 is highly expressed in colon cancer cells and acts mainly through the interaction of its β-galactoside–binding domain (CRD) with glycans at a cell's surface [4–6]. The CRD-glycan interaction triggers galectin-3 effects in cancer cell growth, adhesion, and differentiation, as well as in tumor progression, angiogenesis, and metastasis [5,7–12]. Therefore, the use of competitive inhibitors targeting the CRD-glycan interaction is a promising tool to inhibit galectin-3–mediated effects in colon cancer therapy [13].

There is a strong relationship between the consumption of dietary fiber (DF)-rich foods and the decreased risk of colon cancer [14]. Since the DF fraction of plant-derived foods can be a source of galactosides, it has been hypothesized that consumption of these DF-rich foods containing galactosides could inhibit galectin-3–induced pro-metastatic effects through competition with the glycans at the cell surface [15].

Pectin is a component of the plant cell wall and is the main source of galactosides in the DF fraction of plant-derived foods. Pectin is composed mainly of homogalacturonan (HG) and rhamnogalacturonan (RG) regions. HG is characterized by galacturonic acid (Gal*p*A) ([→4)-α-D-Gal*p*A-(1→]) residues with varying degrees of acetyl and methyl esterification, whereas RG is composed of repeating units of GalpA and rhamnose (Rha*p*) ([→4)-α-D-Gal*p*A-(1→2)-α-L-Rha*p*-(1→]) that may contain galactosides (galactans and/or arabinogalactans) in the sidechains linked at the O-4 position of the Rha*p* [15,16]. Although extraction using water is the most straightforward method to obtain a pectin-rich fraction, considerable insoluble portions can be linked to other components of the plant cell wall through calcium bridges, thereby remaining associated to the plant cell wall even after extraction using water [17,18]. These fractions are also biologically active since the whole part of DF is ingested. This water-insoluble pectin fraction can be obtained through extraction with a chelate compounds such as oxalate [19]. However, although studies have shown structural differences between the HG and RG regions of the water-soluble and chelate-soluble pectin fractions in the plant cell wall of different fruits [20], the biological effects of chelate-soluble pectin fractions are poorly explored.

Papaya is a climacteric fleshy fruit with a fast ripening time. Recently, it was stated that a massive mobilization of pectin was derived from chelate-insoluble pectic fractions to the water-soluble fraction (WSF) occurring throughout papaya ripening [21]. Notably, these changes in cell wall structure—and therefore in pectin solubility—during distinct ripening-time points of papaya strongly influence the effects of the water-soluble pectin in colon cancer cells [22]. Since the chelate-soluble pectic fraction (CSF) of papaya pulp contains β-galactosides with distinct structure from the water-soluble pectin fraction, the chelate fraction can be a promising source of bioactive polysaccharides that could inhibit galectin-3–mediated effects in colon cancer cells. Thus, in the present study, we obtained and characterized the chelate-soluble fraction from distinct ripening-time points of papaya pulps. Then we tested whether these chelate-soluble fractions interact with galectin-3 and affect the proliferation of colon cancer cells.

Material and Methods

Plant material

Papayas (*Carica papaya* L. cv. "Golden") from two biological replicates were acquired from a producer in Aracruz-Espírito Santo, Brazil (19°47'42.2"S 40°19'09.2"W). After harvesting at the color break to one-fourth yellow, the papayas were allowed to ripen at ambient temperature. The fruits were analyzed daily for respiration (CO_2), ethylene production, and pulp firmness according to Fabi et al. (2007) [23] to determine their ripening-time points. Finally, at least six fruits were selected at each ripening-time point (five points) and were peeled, sliced, frozen in N_2, and stored in -80ºC until analysis.

Extraction of the chelate-soluble pectin fraction (CSF)

The frozen papaya pulp was ground in N_2 and incubated three times in boiling chloroform:methanol (1:1; 15 mins.). The solid residue was further washed in boiling 80% ethanol and acetone and dried at ambient temperature to obtain the papaya's total cell wall. The cell wall was extracted three times with deionized water (20 mins.). Then, the remaining insoluble material was extracted three times with 0.08 M ammonium oxalate (pH 4.5; 30 mins.) accordingly to Prado et al. (2016) [21]. The supernatants from the extraction in ammonium oxalate of each ripening-time point were combined to give the

chelate-soluble pectic fraction, which was dialyzed (MWCO 3.5 kDa, Millipore, Billerica, MA, USA) against cold water for 72 hours and freeze-dried. The CSF obtained on the first until the fifth days after harvest (DAH) were named 1CSF, 2CSF, 3CSF, 4CSF, and 5CSF, respectively. Analysis for ash, starch, proteins and phenolic compounds were done in order to test the purity of CSF extracted from papayas.

Interaction between CSF and galectin-3

The interaction between 1-5CSF and galectin-3 was measured by the ability of pectin fractions to inhibit galectin-3–mediated agglutination, similar to what was described previously [24,25]. Firstly, recombinant galectin-3 was produced (Nangia-Makker, Vitaly, & Avraham, 2012). Then, the minimum amount of recombinant galectin-3 that induces the hemagglutination of a 4% rabbit erythrocytes solution (determined as 4 µg galectin-3 / mL) was determined. Next, a solution of 4% rabbit erythrocytes was added to V-bottom 96 well-plates and mixed with distinct concentrations of 1-5CSF added or not to 4 µg/mL galectin-3. After incubation (90 mins.) at room temperature, the minimum concentration of each pectin fraction that inhibits galectin-3–mediated hemagglutination was determined. PBS or 1% BSA was used instead of galectin-3 as controls. Erythrocytes mixed only with CSF were used to observe distinct effects rather than galectin-3–mediated hemagglutination (results equal to controls). Lactose was used as a positive control to inhibit the galectin-3 hemagglutination (minimum concentration assay). The assay was repeated at least three times to confirm the results.

Effects of CSF on colon cancer cells

Colon cancer cell lines HCT116 and HT29 were purchased from American Type Culture Collection guidelines (ATCC) or Rio de Janeiro Cell Bank (BCRJ, Rio de Janeiro, Brazil). Cells were cultured in Dulbecco's modified Eagle's medium (DMEM) containing penicillin (100 µL/mL) and streptomycin (100 µg/mL) added to 10% fetal bovine serum. Cells were maintained under standard conditions and subcultured when they reached a confluence of 70 to 90%.

Cells (1×10^4 cells/well; 96-well plate) were plated overnight for the MTT assay. Then the medium was replaced, and the cells were treated or not with 2-4CSF (0.05, 0.1 or

0.2%) or lactose (33 or 100 mM) for 24, 48, and 72 hours. The higher concentration was also tested for sucrose (100 mM) and for another type of pectin (citrus pectin by sigma – 1%) to attest that these concentrations did not affect cell proliferation by osmotic effects (**Supplemental Fig. 1**). After incubation, 0.5 mg/mL MTT was added (3 hours, 37°C). Next, the supernatant was removed, and the formazan crystals were solubilized with DMSO. Absorbance at 490 nm was measured in a microplate reader (Bio-Rad, Hercules, CA). The cells' viability at each incubation time was expressed in relation to the untreated cells (control).

Structural characterization of CSF

Homogeneity and molecular weight

Chelate-soluble fractions were analyzed by high-performance size-exclusion chromatography coupled with a refractive index detector (HPSEC-RID). A 1250 Infinity system (Agilent, Santa Clara, CA) was used, equipped with four PL aquagel-OH columns (60, 50, 40, and 30; 429 300 × 7.5 mm) connected in tandem. The eluent was 0.2 M $NaNO_3$/0.02% NaN_3 (0.6 mL/min), and the RID temperature was set at 30°C. Average molecular weight was calculated using a standard curve of dextrans (MW 5–1,800 kDa).

Monosaccharide composition

Monosaccharide composition was performed using a high-performance anion-exchange chromatography coupled with a pulse amperometric detector (HPAEC-PAD) [27,28]. Samples (1mg) were hydrolyzed with 2 M trifluoroacetic acid at 120°C for 90 mins. Then t-butyl alcohol was added, and the mixture was evaporated under N_2 flow, solubilized in water, and filtered. Next, samples were analyzed in a DX 500 system (Dionex, Sunnyvale, CA, USA) equipped with a CarboPac PA10 column (250 × 4 mm). For the analysis of neutral sugars, a post column adjustment with 300 mM NaOH was performed. For the uronic acid analysis, the same system was used with 150 mM NaOH (1 mL/min; 30 mins.) with a 0–220 mM sodium acetate gradient as the eluent. Neutral sugars and uronic acids were used as standards.

Fourier transform infrared (FTIR) attenuated total reflectance ATR

The fourier transform infrared (FTIR) spectroscopy was applied to infer some structure characteristics from papaya pectin and to determine the degree of *O*-methyl esterification [29] using an Alpha FTIR spectrometer (Bruker Optic, Ettlingen, Germany) equipped with a deuterated triglycine sulfate detector and a single-bounce attenuated total reflectance (ATR) accessory (diamond crystal). FTIR–ATR spectra of samples were obtained with a resolution of 4 cm^{-1} and 50 scans. GRAMS/AI 9.1 software (Thermo Scientific) was used for spectra analysis. Methyl esterified and free uronic acids corresponded to bands at 1749 cm^{-1} and 1630 cm^{-1}, respectively. Commercially available pectins with known degrees of *O*-methyl esterification (28%, 64%, 91%) and their mixtures (14%, 46%, 78%) were used to produce a standard curve of *O*-methyl esterification.

Atomic force microscopy (AFM)

Samples diluted in water (2.5 µL/mL) were sonicated, dropped onto freshly cleaved mica, and dried in a vacuum at 30°C for 20 mins. Samples were maintained in a desiccator until analysis. Topography images were obtained in an NX-10 Atomic Force Microscope (Park Systems, Suwon, South Korea) in an acrylic glove box with controlled temperature (~22°C) and humidity (~3%). AFM imaging was acquired on tapping mode using an NCHR probe (NanoWorld) with a spring constant of 42 N/m and 320 kHz resonance frequency. The scan speed and scanning resolution were 0.5 Hz and 512 × 512 points, respectively. For each sample, at least ten images were collected. Image measurements and automatic processing (plane subtraction and row alignment) were performed using Gwyddion 2.47 software (http:// gwyddion.net/).

Nuclear magnetic resonance (NMR)

1D and 2D ^{1}H spectra of 3CSF were recorded using a 500 MHz NMR spectrometer (Bruker Biospin, Rheinstetten, Germany) with a triple resonance probe. Approximately 5 mg of each sample were dissolved in 0.5 mL of 99.9% deuterium oxide (Cambridge Isotope Laboratory, Cambridge, MA). All spectra recorded at 35°C with deuterated water exhibited a peak due to exchange with residual H_2O (HOD), suppressed by presaturation. For 1D ^{1}H NMR (zgpr from Bruker Library) spectra, 64 scans were recorded using an interscan delay

equaling 1s. 2D ^{1}H-^{1}H COSY (cosyphpr from Bruker Library) and ^{1}H-^{1}H TOCSY (mlevphpr from Bruker Library) spectra were recorded using states time proportion phase incrementation for quadrature detection in the indirect dimension. TOCSY spectra were run with 4096 × 512 points with a spin lock field of 10 kHz and a mixing time of 60 ms. The ^{1}H/^{13}C Multiplicity-Edited HSQC (HSQC) spectra were recorded with 1024 x 512 points and 256 scans using an Echo-Antiecho acquisition mode with globally optimized alternating phase rectangular pulses for decoupling. The ^{1}H/^{13}C HMBC spectra were recorded with 2048 x 200 points and 512 scans, with a 50 ms delay for evolution of long-range couplings and set with no decoupling during the acquisition time, a low-pass filter, and a QF magnitude acquisition mode. Chemical shifts were displayed relative to external trimethylsilylpropionic acid at 0 ppm for ^{1}H. The data were processed using TopSpin3.1 (Bruker Biospin) [30].

Statistical analysis

The results were expressed as the mean ± standard deviation (SD), and the significance was set at $P < 0.05$. Data were analyzed using GraphPad Prism 6.0 software (GraphPad, San Diego, CA). One-way ANOVA with Tukey's (to assess differences among all groups) or Dunnett's (to assess differences among the control and two or more groups) were used as post hoc tests.

Results

Definition of ripening-time points of papayas

Papayas were analyzed for pulp softness as well as ethylene and CO_2 production (**Fig. 1**) to define papaya ripening-time points: papayas with 1 and 2DAH had unripe characteristics, as observed by no pulp softening (firmness higher than 2 N.cm^{-2} (10^{-2})) and the low CO_2 and ethylene production (CO_2 lower than 0.25 mL Kg^{-1} h^{-1} and ethylene lower than 0.25 µL Kg^{-1} h^{-1}); papayas with 3DAH had an intermediate ripening-time point (almost ripe), which is marked by the onset of ethylene production and start of pulp softening; papayas with 4 and 5DAH were fully ripe, with high ethylene production (higher than 0.5 µL Kg^{-1} h^{-1}) and a soft pulp (lower than 0.2 N.cm^{-2} (10^{-2})). The WSF and CSF had the yield amounts measured. As expected, the WSF yields increased as the fruit ripened, and the CSF

was a little bit higher on very unripe 1DAH fruit. Ash, starch, proteins and phenolic compounds contents were insignificant in the CSF fractions.

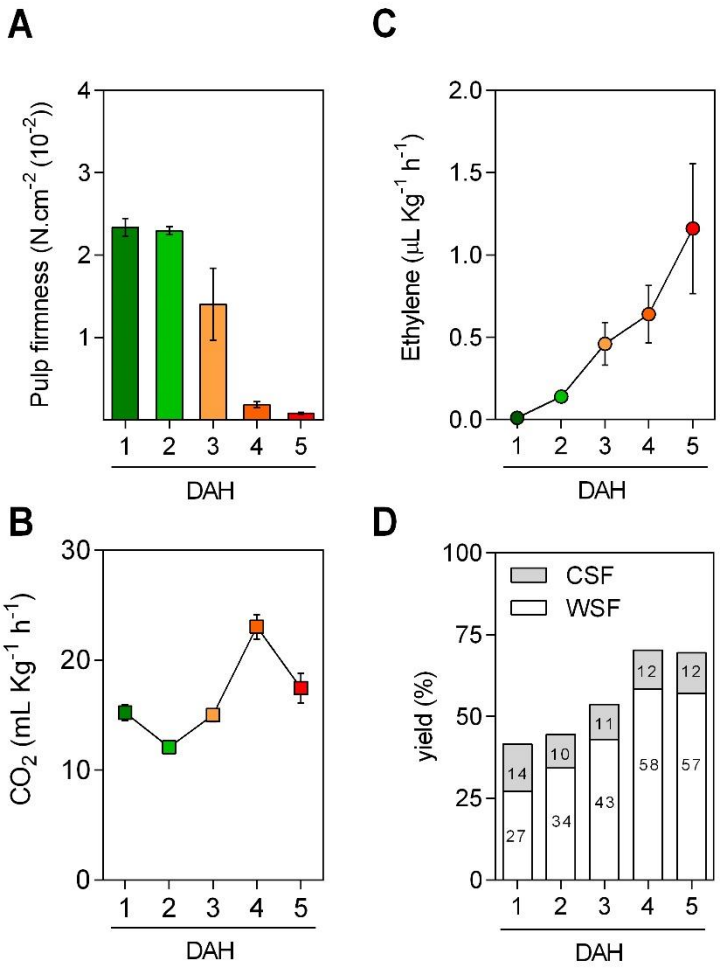

Figure 1. Papaya fruit ripening characterization. A) Papaya pulp firmness. B) Papaya CO_2 production. C) Papaya ethylene production. D) Water-soluble fraction and chelate soluble fraction yield in relation to papaya total cell wall. The results are represented as mean ± standard deviation values (duplicate for each biological replicate, n = 4). DAH: days after harvesting; WSF: water-soluble fraction; CSF: chelate soluble fraction.

3CSF interacts with galectin-3 and inhibits colon cancer cell proliferation

CSF fractions from papayas were tested for galectin-3 interaction through the inhibition of galectin-3–mediated hemagglutination, and the results were compared to lactose inhibition, which is known to interact with galectin-3 CRD. Notably, 3CSF was the

only fraction that inhibited galectin-3–mediated hemagglutination (**Fig. 2**). The other fractions had no apparent inhibitory activity even at relatively high doses. In contrast, 3CSF inhibited galectin-3–mediated hemagglutination at 6 µg/mL, which was similar to that of the positive control (lactose) that had inhibitory effects at 4 µg/mL. After the hemagglutination inhibitory assay, it was tested whether CSF inhibits the proliferation of colon cancer cells. However, only 2-4CSF were tested because of the low yield obtained for 1CSF and the low interaction of 1 and 5CSF to galectin-3. Colon cancer cell lines HCT116 and HT29 both express galectin-3 [6]; however, HCT116 is a $KRAS^{G13D}$ mutation [31] and wild-type for BRAF mutation and HT29 is $BRAF^{V600E}$ mutation and wild-type for KRAS mutation [32,33]. RAS protein activates several downstream signaling cascades that regulate multiple cellular functions including cell proliferation, differentiation, motility, survival, and intracellular trafficking [34]. The BRAF is a serine/threonine kinase that plays a role in cell proliferation, survival, and differentiation [35]. As shown in **Fig. 3A**, CSF fractions affected both HCT116 and HT29 in a concentration-dependent manner. Interestingly, 3CSF was more effective in reducing cell proliferation. Lactose, which is a positive control of galectin-3 inhibition and was used at nontoxic concentrations [36,37], had also reduced HCT116 cell proliferation and sucrose, used as an negative osmotic effect, did not (**Supplemental Fig. 1**).

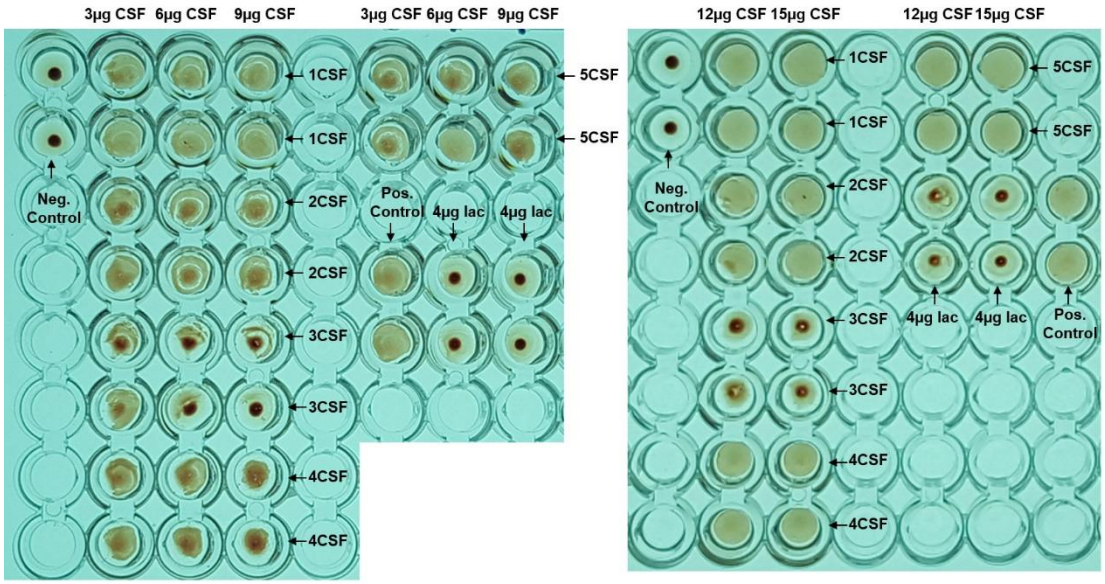

Figure 2. Inhibition of hemagglutination assay. The negative control contains just the erythrocytes; positive control contains the erythrocytes plus galectin-3; and lac (lactose) 4

µg was the minimum quantity that inhibits the hemagglutination. 1CSF: chelate-soluble fraction extracted from papaya with 1 day after harvest; 2CSF: chelate-soluble fraction extracted from papaya with 2 days after harvest; 3CSF: chelate -soluble fraction extracted from papaya with 3 days after harvest; 4CSF: chelate -soluble fraction extracted from papaya with 4 days after harvest; 5CSF: chelate -soluble fraction extracted from papaya with 5 days after harvest.

Since lactose is known to interact with galectin-3 and results have shown that 3CSF also bind to galectin-3, the effects of 3CSF in cells previously treated with lactose were investigated to determine the extension of galectin-3–mediated effects induced by 3CSF. As shown in **Fig. 3B**, the treatment with 3CSF in HCT116 cells previously exposed to lactose did not increase the inhibitory proliferative effect. On the other hand, 3CSF and pre-treated cells with lactose plus the additional inclusion of 3CSF treatment had a strong inhibitory effect on the proliferation of HT29 cells when compared with only lactose, indicating that this CSF fraction also induces galectin-3–independent effects. The differences between the effects of 3CSF in HCT116 and HT29 cells seem to be related to different kinds of mutations in these colon cancer cell lines, as previously reported [22,38]. Besides the differences in mutation types, HT29 has a mutated APC and wild-type β-catenin and HCT116 expresses wild-type APC and a mutant β-catenin [39]. Galectin-3 is a β-catenin important regulator of tumor metastasis [40] and the differences in results presented herein could be derived of these distinct mutations and interaction with galectin-3 and β-catenin. Pectin inhibits β-catenin expression in the colon [41] possibly due to inhibition of galectin-3–β-catenin complex formation [40]. Somehow, in HT29 cell line the 3CSF probably could also interfere in β-catenin expression and reduce the cell viability. Further studies are needed to confirm these mechanisms.

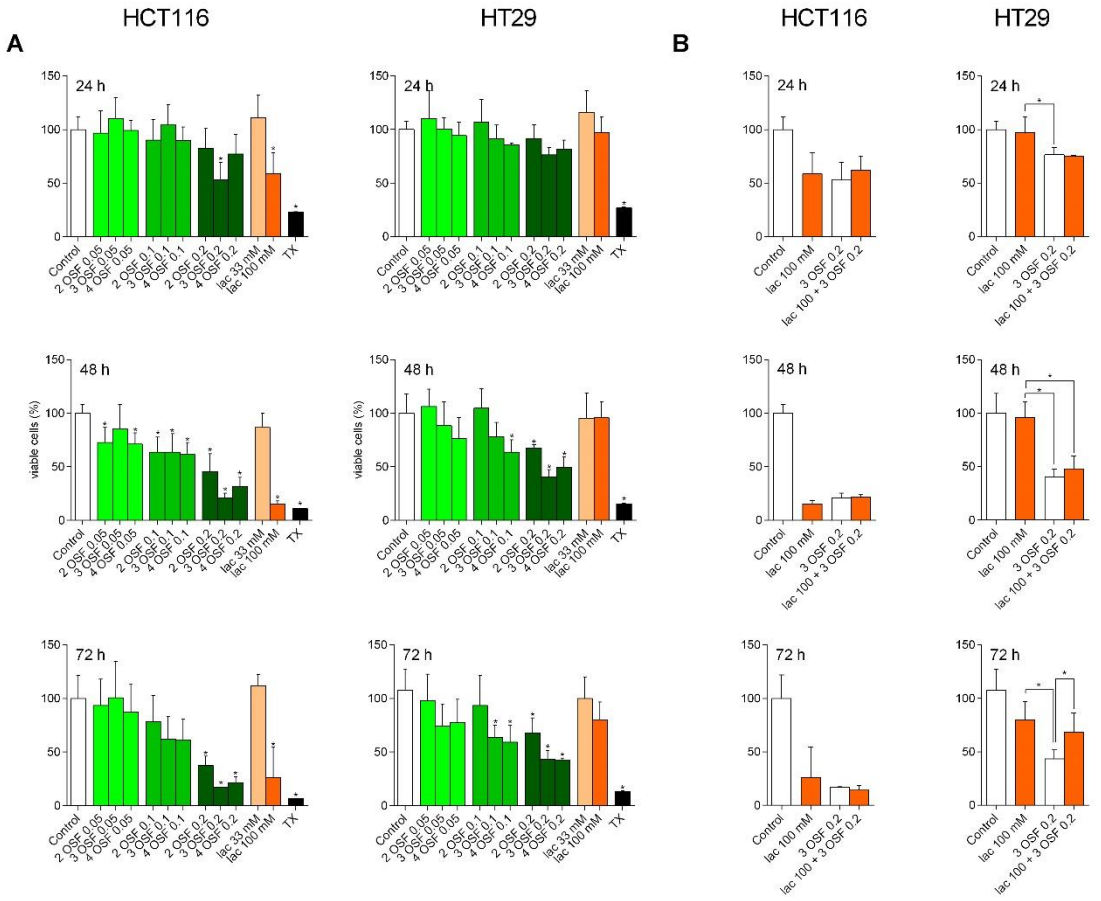

Figure 3. Viability assay by MTT on HCT116 and HT29 cell lines treated with unripe and ripe papaya chelate-soluble fractions. A) Cancer cell lines treated with oxalate-soluble fractions extracted from papaya pulp at diferent ripening points and concentrations (0.05%, 0.1%, 0.2%). B) Viability assay by MTT using lactose and lactose with 3CSF. The results are expressed in percentage of cell viability in comparison with control (no treatment) of the correpondent time. Data were shown as mean ± SD. *P < 0.05 vs control, according to Dunnett's test. The results were from three independent CSF samples (each one performed in technical triplicate) from the biological duplicate (n = 6). 2CSF: chelate-soluble fraction extracted from papaya with 2 days after harvest; 3CSF: chelate-soluble fraction extracted from papaya with 3 days after harvest; 4CSF: chelate-soluble fraction extracted from papaya with 4 days after harvest; 5CSF: chelate-soluble fraction extracted from papaya with 5 days after harvest. TX: triton X-100 0.02%. Lac: lactose.

Structural characterization of CSF fractions indicates that 3CSF has lower molecular weight and more ramifications

Fig. 4A shows that CSF fractions have relatively high molecular weight (between 710 and 1,800 kDa – Void volume); however, the molecular weight decreases along with ripening. Notably, 3CSF had an additional peak between 80 and 410 kDa, indicating an enrichment of lower molecular weight polysaccharides. To visualize changes in size, 3CSF was analyzed through AFM, and results were compared to that of 1 CSF, which is the CSF with the highest molecular weight. As shown in **Fig. 4B**, 3CSF was smaller than 1CSF.

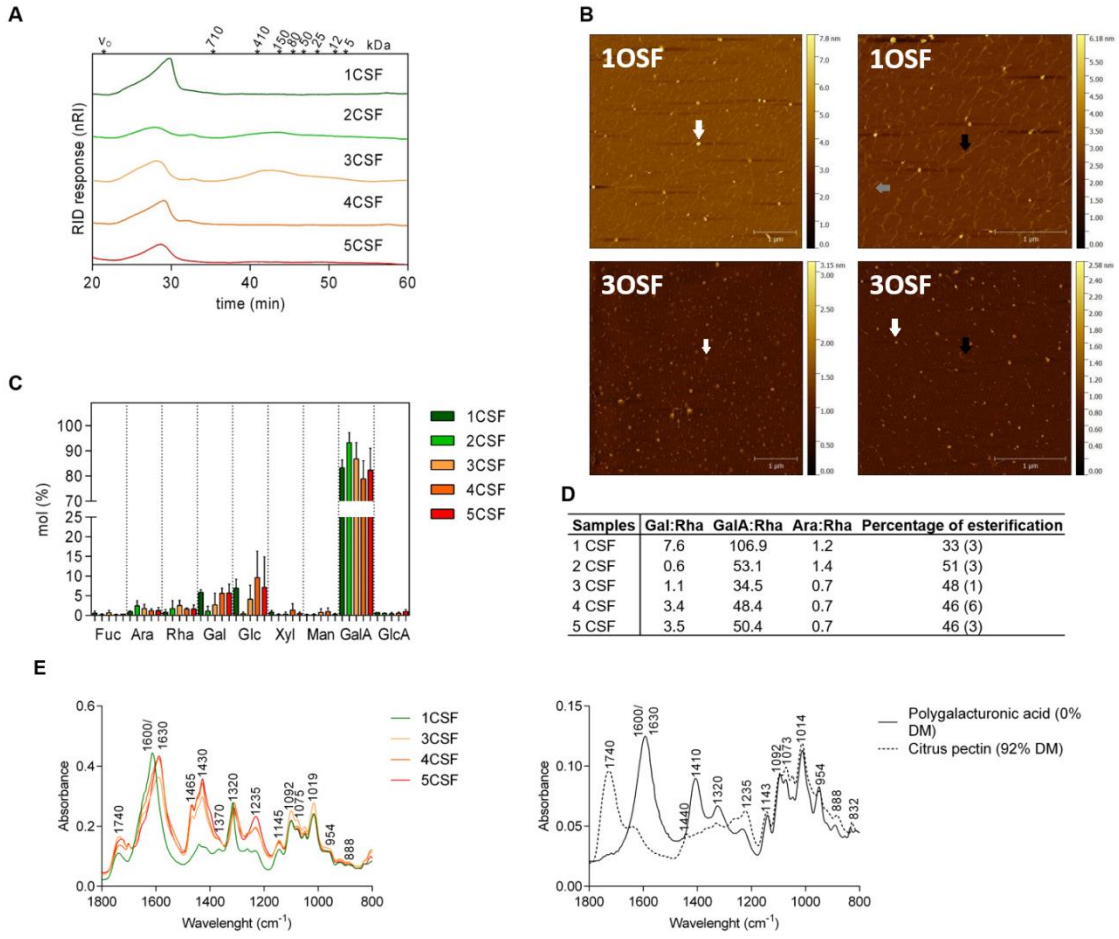

Samples	Gal:Rha	GalA:Rha	Ara:Rha	Percentage of esterification
1 CSF	7.6	106.9	1.2	33 (3)
2 CSF	0.6	53.1	1.4	51 (3)
3 CSF	1.1	34.5	0.7	48 (1)
4 CSF	3.4	48.4	0.7	46 (6)
5 CSF	3.5	50.4	0.7	46 (3)

Figure 4. Characterization of CSF. A) HPSEC-RID elution profile. Vo: void volume (blue dextran elution time). B) Topographical AFM of representative images of papaya chelate-soluble pectins. Black arrows indicate linear structures, white arrows agglomerates and grey arrow ramifications. C) Monosaccharides composition. D) Monosaccharide ratios and percentage of esterification. E) FT-IR spectra of the CSF, polygalacturonic acid and

citrus pectin. 1CSF: chelate-soluble fraction extracted from papaya with 1 day after harvest; 2CSF: chelate-soluble fraction extracted from papaya with 2 days after harvest; 3CSF: chelate-soluble fraction extracted from papaya with 3 days after harvest; 4CSF: chelate-soluble fraction extracted from papaya with 4 days after harvest; 5CSF: chelate-soluble fraction extracted from papaya with 5 days after harvest. Gal: galactose; Ara: arabinose; GalA: galacturonic acid; Man: mannose; Glu: glucose; Xyl: xylose; Rha: rhamnose; GlcA: glucuronic acid; and Fuc: fucose.

Compositional analysis revealed that CSF fractions were composed mainly of GalA, confirming that CSF are HG-rich fractions, with minor amounts of neutral sugars (**Fig. 4C**). The degree of esterification revealed that 1CSF had a smaller degree of esterification (33%) compared to 2-5CSF, which had a degree of esterification around 50% (**Fig. 5D**).

FT-IR spectroscopy were used to calculate the degree of esterification and to identify specific wavenumbers to discriminate different polysaccharides functional groups. Polysaccharides are normally presented in two specific regions: 1,800-1,200 cm^{-1} and 1,200-800 cm^{-1} (**Fig. 4E**). The peaks characteristics from pectin structures were confirmed using polygalacturonic acid (0% DM) and citrus pectin (92% DM). The bands characteristic of pectin structure were similar between the standards and CSF samples: 1740 cm^{-1}, 1600-1630 cm^{-1}, 1320 cm^{-1}, 1235 cm^{-1}, 1143 cm^{-1}, 1092 cm^{-1}, 1019-1014 cm^{-1}, 954 cm^{-1}, 888 cm^{-1} [42]. The peak 1740 cm^{-1} correspond to C═O stretching vibration of alkyl ester (non-esterified pectin), 1600-1630 cm^{-1} to a COO- antisymmetric stretching (pectin ester group) while 1410 cm^{-1} corresponds to COO- symmetric stretching (pectin ester group). The 1320 cm^{-1} peak is pectin ring vibration, the 1235 cm^{-1} a is pectin C─O stretching, the 1143 cm^{-1} is asymmetric stretching of pectin O─C─O, the 1092 cm^{-1} is pectin C─O stretching and C─C stretching, 1014-1019 cm^{-1} are also pectin C─O stretching and C─C stretching and 954 cm^{-1} is CO bending pectin [42]. The peaks 888 cm^{-1} and 1073 cm^{-1} were found in citrus pectin and it seems to be very characteristic of pectin structure, but the peak 1075 cm^{-1} was found only in CSF and it could be a xyloglucan ring C─O stretching and C─C stretching [42]. Other peaks that could be masked in CSF samples are 1465 cm^{-1} (xyloglucan-derived) [43], 1430 cm^{-1} (CH_2 bending vibration) [42] and 1410 cm^{-1} (pectin) [42]. The peak 1370 cm^{-1} observed in CSF samples could be CH_2 bending from xyloglucan and cellulose [42]. It was observed an increment in peaks between 1090 and 1040 cm^{-1} during ripening which

could mean an increment of pectin, hemicellulose and cellulose, and an increase in 1235 cm^{-1} peak coming from the pectin C─O stretching. The bands between 1092 and 1019 cm^{-1} were higher on 3CSF and the area between 1200 and 900 cm^{-1} being indicated by different types of neutral sugars [43].

A more detailed analysis of 3CSF through 1D ^{1}H NMR and 2D ^{13}C-^{1}H HSQC and HMBC clarified its preponderant structure. 1D ^{1}H spectrum (**Fig. 5A**) showed several anomeric signals. Attempts to identify the different spin systems using ^{1}H - ^{1}H COSY and TOCSY spectra failed due to the high complexity of the spectra. We then employed $^{1}H/^{13}C$ HSQC (**Fig. 5B**), which showed a well-defined set of signals, easily assigned by comparison with the chemical shifts reported for a polysaccharide from styrian oil pumpkin [44]. $^{1}H/^{13}C$ HMBC was also employed for a precise assignment of the set of signals. We identified seven sets of signals, named as A → G (**Table 1**). Signals C → F were assigned to α-galacturonic acid units, differing either due to the presence of 6-*O*-methyl ether (E and F) or distinct neighbor units (as in the case of C *vs* D and E *vs* F). In addition to these preponderant signals, we also identified systems assigned to terminal α-arabinofyranosyl (unit A), α-glucopyranosyl (unit B), and β-galactopyranosyl (unit G) residues. The set of well-defined signals observed in the $^{1}H/^{13}C$ HMBC spectrum (**Fig. 5C**) confirms the assignment reported in Table 1, again in agreement with data from literature [44]. The ratio of methylated/non-methylated α-galacturonic acid units is ~1.2 based on integration of signals E5/F5 and C5/D5, which are clearly separated on the $^{1}H/^{13}C$ HSQC spectrum (**Fig. 5B**). These two preponderant units found in the central chain of the polysaccharide are summarized in **Fig. 5D, E, F**.

Table 1. 1H and 13C data for 3CSF.

Code	Sugar type	Linkage	H1/C1	H2/C2	H3/C3	H4/C4	H5/C5	H6/C6	MeO	COO-
A	t-α-Ara*f*-(1→	X	5.28/111.0	4.25/83.0	4.14/79.5	4.17/85.3	-	-	-	-
B	t-α-Glc*p*-(1→	X	4.5/105.2	3.56/73.5	3.71/74.5	3.74/76.4	3.98/78.5	-	-	-
C	→4)-α-Gal*p*A-(1→	C-C	5.15/101.1	3.76/69.9	4.02/69.9	4.5/80.1	4.78/73.4	-	-	-/180
D	→4)-α-Gal*p*A-(1→	D-E	5.12/100.8	3.76/69.9	4.02/69.9	4.46/80.0	4.7/73.2	-	-	-/180
E	→4)-α-6-MeGal*pA*-(1→	E-E	5.00/102.0	3.76/69.9	3.99/70.5	4.49/80.7	5.14/72.3	-	3.83/54.6	-
F	→4)-α-6-MeGal*p*A-(1→	E-C	4.94/101.6	3.76/69.9	3.79/70.5	4.42/80.7	5.08/72.4	-	3.83/54.6	-/180
G	→4)-β-Gal*p*-(1→	X	4.66/97.8	3.28/76.0	3.43/71.5	3.5/77.0	3.7/72.0	3.85-3.73/63	-	-

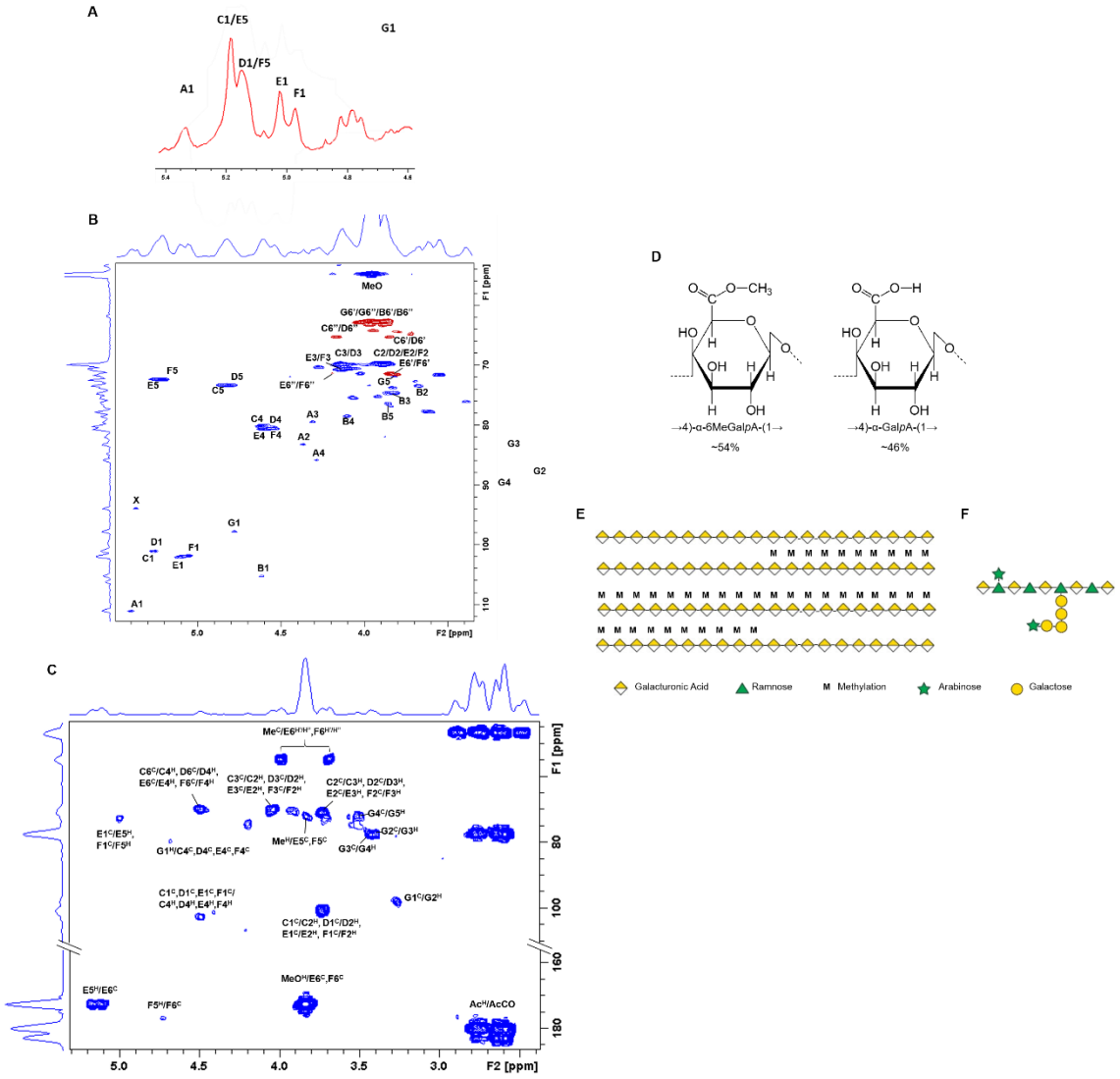

Figure 5. 3CSF structural determination by NMR spectroscopy. A) 1D ^{1}H NMR spectrum. B) ^{13}C-^{1}H HSQC spectrum. C) ^{13}C-^{1}H HMBC spectrum. 3CSF: chelate-soluble fraction extracted from papaya with 3 days after harvest. D) Schematic representation of 3CSF methylated and non-methylated galacturonic acid structure. E) Predominant part of HG not methylated or methylated. F) 3CSF probable presence of RGI fractions enriched by galactans and arabinans.

It is possible that other neutral sugars were not detected by NMR because of their lower abundance, but compositional analysis revealed that 3CSF had decreased GalA:Rha ratio, which suggests an increased proportion of ramifications. Ara, Rha, and Gal seem derived from an RGI structure, which can be composed of AGII, as was previously found in the more soluble pectin WSF extracted from papaya pulp [22]. As during the papaya

ripening the chelate-soluble pectin (CSF) is being solubilized to water-soluble pectin (WSF) [21] we believe that the neutral sugars mentioned before are part of RGI structures as previously stated for papaya pectins (WSF), even if it is in small quantities [21,22]. The Glc seems to be derived from the hemicellulose fraction of cell walls, which is mainly water-insoluble but could be extracted with chelate-solutions [45].

Discussion

Our group has already stated that during papaya ripening, a massive production of enzymes occurs, mainly polygalacturonases and β-galactosidases, and induces solubilization of cell walls and therefore papaya pulp softening [21,46]. The structures of WSF obtained at distinct ripening-time points are remarkably different, and these ripening-induced changes modify the inhibitory effects of pectin in cancer cell proliferation [22]. In the present work, we investigated whether the less soluble pectin fraction, the chelate-soluble one, could also differently affect the proliferation of colon cancer cell lines while interacting with galectin-3. For that, the papaya fruit ripening parameters were accompanied, and the unripe and ripe status of each point was confirmed. In this way, we can focus on studying whether the chelate-soluble pectin (CSF) only modified by the natural ripening (after fruit harvesting) and without any modification (by chemicals or pH or by ion-exchange chromatography) would differently affect cancer cells growth and galectin-3 binding.

Galectin-3 is a pro-metastatic lectin that is overexpressed in some cancer cell lines [6], including in early stages of colon cancer [4]. Both i*n vivo* and *in vitro* studies confirmed that increased galectin-3 expression during cancer progression enhances tumor growth, invasiveness, and metastatic potential, as reviewed previously [47]. The interaction of pectin with galectin-3 CRD prevents galectin-3–mediated effects such as the increase in cells migration and adhesion and the inhibition of cells apoptosis [15]. Lactose is known to bind to the CRD of galectin-3. Furthermore, pectin fragments that contain galactosides, such as arabinogalactan and galactan sidechains in the RGI regions, are also interesting candidates that could interact with the galectin-3 CRD domain [48]. However, while neutral fragments can directly bind on galectin-3 CRD domain, galacturonans might not have a specific binding but instead have a nonspecific charge–charge interaction with galectin-3 [48]. Another study focused on how RG and HG structures bind to galectin-3 suggests that

RG and HG polysaccharides act in concert: their combination in specific proportions enhances galectin-3 activity synergistically [49]. It happens because HG interact with RG promoting increased activity of RG binding to galectin-3, probably by exposing additional galectin-binding sites on the RG [49]. In the present study, we showed that 3CSF was the only papaya chelate-pectin fraction that inhibited galectin-3–mediated hemagglutination. The 3CSF had similar GalA content and degree of esterification from those of other ripening-time points. However, 3CSF had a lower molecular weight peak, which suggests that this CSF is more functional and available to interact with galectin-3 CRD, even with less Gal content since the neutral ramifications could have a molecular size that facilitate the interaction with galectin-3. Besides, the binding to galectin-3 could also occur through nonspecific charge–charge interaction with the smaller HG structures of 3CSF, as previously suggested [48]. The comparisons between the AFM images of 3CSF and 1CSF reveal that samples from unripe papayas possess higher linear and branched structures and possess agglomerates. These branch structures visualized through AFM seemed to be formed by GalA residues and linked via a branched GalA residue [50]. The 3CSF had smaller linear structures in lower amounts, and it was not possible to visualize the branched structures. The most abundant structures in 3CSF are molecules agglomerated with an oval shape. In the chelate-soluble fraction extracted from pears, the long and highly branched structure is visible, and polygalacturonase action induces the formation of spot-like and oval shapes [51]. During papaya ripening, an increase in the activity of polygalacturonases [21,46] may also be responsible for the formation of more agglomerates in 3CSF compared to 1 CSF. The FT-IR analysis also showed that peaks characteristics of neutral sugar was increased in 3CSF and it could be related not only to the amount of neutral substitution but also with the position and the degree of substitution [52]. To summarize, the structure that we have found of 3CSF in **Fig. 5** shows represents its proposal schematic representation.

Analysis of colon cancer cells previously exposed to lactose also reveals that CSF can induce galectin-3–independent cell death. In our previous work, we found that the WSF extracted from papaya pulp induced colon cancer cell necroptosis [22]. Furthermore, previous studies showed that pectin structure composed of RGI and HG inhibits cell adhesion and proliferation by inhibiting ICAM1 protein [53]. Relatively similar pectins also had induced cell cycle arrest [54], autophagy [55], and apoptosis [56] in diverse cancer cells. All these effects are both pectin structurally dependent and cell line–dependent. The effects of 3CSF in colon cancer cell lines and with galectin-3 binding described in this work

reveled a potential anticancer mechanism that still needs to be confirmed. In summary, the smaller molecular weight of pectin from 3CSF seems to be more effective in reducing colon cancer cell proliferation by exposing the neutral sidechains to interact with galectin-3. 3CSF is extracted from an intermediate ripening point, and pectin obtained from later ripening stages that had a continued hydrolyses by cell wall–degrading enzymes had decreased the anticancer activity. As far as we know, papaya is the first fruit described that can naturally modify pectin structures that can interact with galectin-3 having biological benefits if consumed fresh, because usually the pectin has to be extracted and chemically or thermally modified to bind galectin-3 [57].

Conclusions

The innovative character of this study is to explore whether the CSF extracted in different ripening stages have distinct biological effects in colon cancer cells and in binding galectin-3. We have demonstrated that CSF obtained from an intermediate papaya ripening time point (3CSF) is naturally modified by the fruit cell wall–degrading enzymes, and 3CSF has the ability to bind galectin-3, what did not happen with the other fractions (obtained in unripe and ripe stages). The colon cancer cell lines had the proliferation affected by 3CSF treatment probably in a galectin-3 dependent and independent way. The lower molecular weight and the probable more exposed ramifications seem to facilitate the structural interaction with both galectin-3 and cancer cells. Therefore, the consumption of papayas during intermediate ripening time points could be associated with preventive cancer events since they contain pectin structurally compatible to inhibit galectin-3 preventing colon cancer cell proliferation. Further studies have to be conducted in order to isolate the specific carbohydrate structure responsible for the biological effects and the possible interaction with colon cancer cell *in vivo*.

References

[1] M. Arnold, M.S. Sierra, M. Laversanne, I. Soerjomataram, A. Jemal, F. Bray, Global patterns and trends in colorectal cancer incidence and mortality, Gut. 66 (2017) 683–691. doi:10.1136/gutjnl-2015-310912.

[2] M. Jovanovic, N. Gajovic, N. Zdravkovic, M. Jovanovic, M. Jurisevic, D. Vojvodic, V. Maric, A. Arsenijevic, I. Jovanovic, Fecal Galectin-3: A New Promising Biomarker for Severity and Progression of Colorectal Carcinoma, Mediators Inflamm. 2018 (2018) 1–11. doi:10.1155/2018/8031328.

[3] L. Tao, L. Jin, L. Dechun, Y. Hongqiang, K. Changhua, L. Guijun, Galectin-3 expression in colorectal cancer and its correlation with clinical pathological characteristics and prognosis, Open Med. 12 (2017) 226–230. doi:10.1515/med-2017-0032.

[4] K. Endo, S. Kohnoe, E. Tsujita, A. Watanabe, H. Nakashima, H. Baba, Y. Maehara, Galectin-3 expression is a potent prognostic marker in colorectal cancer, Anticancer Res. 25 (2005) 3117–21. http://www.ncbi.nlm.nih.gov/pubmed/16080575.

[5] S.H. Barondes, D.N.W. Cooper, M.A. Gitt, H. Leffler, Galectins: structure and function of a large family of animal lectins, J. Biol. Chem. 269 (1994) 20807–20810. doi:10.1016/j.celrep.2015.02.012.

[6] A. Satelli, P.S. Rao, P.K. Gupta, P.R. Lockman, K.S. Srivenugopal, U.S. Rao, Varied expression and localization of multiple galectins in different cancer cell lines, Oncol. Rep. 19 (2008) 587–594.

[7] R.C. Hughes, Secretion of the galectin family of mammalian carbohydrate-binding proteins, Biochim. Biophys. Acta. 1473 (1999) 172–85. http://www.ncbi.nlm.nih.gov/pubmed/10580137.

[8] P. Nangia-Makker, S. Nakahara, V. Hogan, A. Raz, Galectin-3 in apoptosis, a novel therapeutic target, J. Bioenerg. Biomembr. 39 (2007) 79–84. doi:10.1007/s10863-006-9063-9.

[9] F.T. Liu, R.J. Patterson, J.L. Wang, Intracellular functions of galectins, Biochim. Biophys. Acta - Gen. Subj. 1572 (2002) 263–273. doi:10.1016/S0304-4165(02)00313-6.

[10] A.U. Newlaczyl, L.-G. Yu, Galectin-3--a jack-of-all-trades in cancer, Cancer Lett. 313 (2011) 123–8. doi:10.1016/j.canlet.2011.09.003.

[11] T. Funasaka, A. Raz, P. Nangia-Makker, Galectin-3 in angiogenesis and

metastasis, Glycobiology. 24 (2014) 886–891. doi:10.1093/glycob/cwu086.

[12] S. Nakahara, N. Oka, A. Raz, On the role of galectin-3 in cancer apoptosis, Apoptosis. 10 (2005) 267–75. doi:10.1007/s10495-005-0801-y.

[13] K. Wdowiak, T. Francuz, E. Gallego-Colon, N. Ruiz-Agamez, M. Kubeczko, I. Grochoła, J. Wojnar, Galectin targeted therapy in oncology: Current knowledge and perspectives, Int. J. Mol. Sci. 19 (2018) 1–21. doi:10.3390/ijms19010210.

[14] A.T. Kunzmann, H.G. Coleman, W.-Y. Huang, C.M. Kitahara, M.M. Cantwell, S.I. Berndt, Dietary fiber intake and risk of colorectal cancer and incident and recurrent adenoma in the Prostate, Lung, Colorectal, and Ovarian Cancer Screening Trial, Am J Clin Nutr. 102 (2015) 881–890. doi:10.3945/ajcn.115.113282.1.

[15] E.G. Maxwell, N.J. Belshaw, K.W. Waldron, V.J. Morris, Pectin – An emerging new bioactive food polysaccharide, Trends Food Sci. Technol. 24 (2012) 64–73. doi:10.1016/j.tifs.2011.11.002.

[16] D. Mohnen, Pectin structure and biosynthesis, Curr. Opin. Plant Biol. 11 (2008) 266–277. doi:10.1016/j.pbi.2008.03.006.

[17] D. a. Brummell, Cell wall disassembly in ripening fruit, Funct. Plant Biol. 33 (2006) 103. doi:10.1071/FP05234.

[18] R.R. Selvendran, Developments in the chemistry and biochemistry of pectic and hemicellulosic polymers, J. Cell Sci. Suppl. 2 (1985) 51–88. doi:10.1242/jcs.1985.Supplement_2.4.

[19] E. Taboada, P. Fisher, R. Jara, E. Zúñiga, M. Gidekel, J.C. Cabrera, E. Pereira, A. Gutiérrez-Moraga, R. Villalonga, G. Cabrera, Isolation and characterisation of pectic substances from murta (Ugni molinae Turcz) fruits, Food Chem. 123 (2010) 669–678. doi:10.1016/j.foodchem.2010.05.030.

[20] C. Paniagua, S. Posé, V.J. Morris, A.R. Kirby, M.A. Quesada, J.A. Mercado, Fruit softening and pectin disassembly: An overview of nanostructural pectin modifications assessed by atomic force microscopy, Ann. Bot. 114 (2014) 1375–1383. doi:10.1093/aob/mcu149.

[21] S.B.R. do Prado, P.R. Melfi, V.C. Castro-Alves, S.G. Broetto, E.S. Araújo, J.R.O. do Nascimento, J.P. Fabi, Physiological Degradation of Pectin in Papaya Cell Walls: Release of Long Chains Galacturonans Derived from Insoluble Fractions during Postharvest Fruit Ripening, Front. Plant Sci. 7 (2016) 1120. doi:10.3389/fpls.2016.01120.

[22] S.B.R. do Prado, G.F. Ferreira, Y. Harazono, T.M. Shiga, A. Raz, N.C. Carpita, J.P. Fabi, Ripening-induced chemical modifications of papaya pectin inhibit cancer cell proliferation, Sci. Rep. 7 (2017) 16564. doi:10.1038/s41598-017-16709-3.

[23] J.P. Fabi, B.R. Cordenunsi, G.P. de Ma. Barreto, A.Z. Mercadante, F.M. Lajolo, J.R.O. Do Nascimento, Papaya Fruit Ripening: Response to Ethylene and 1-Methylcyclopropene (1-MCP), J. Food Agric. Food Chem. 55 (2007) 6118–6123.

[24] T.P. Nowak, P.L. Haywood, S.H. Barondes, Developmentally regulated lectin in embryonic chick muscle and a myogenic cell line, Biochem. Biophys. Res. Commun. 68 (1976) 650–657.

[25] J. Ochieng, D. Platt, L. Tait, V. Hogan, T. Raz, P. Carmi, a Raz, Structure-function relationship of a recombinant human galactoside-binding protein., Biochemistry. 32 (1993) 4455–60. http://www.ncbi.nlm.nih.gov/pubmed/8476870.

[26] P. Nangia-Makker, B. Vitaly, R. Avraham, Galectin-3-Binding and Metastasis, Methods Mol. Biol. 878 (2012) 241–250. doi:10.1007/978-1-61779-854-2.

[27] T.M. Shiga, J.P. Fabi, J.R.O. do Nascimento, C.L.D.O. Petkowicz, L.C. Vriesmann, F.M. Lajolo, B.R. Cordenunsi, Changes in cell wall composition associated to the softening of ripening papaya: evidence of extensive solubilization of large molecular mass galactouronides, J. Agric. Food Chem. 57 (2009) 7064–71. doi:10.1021/jf900073b.

[28] T.M. Shiga, N.C. Carpita, F.M. Lajolo, B.R. Cordenunsi-Lysenko, Two banana cultivars differ in composition of potentially immunomodulatory mannan and arabinogalactan, Carbohydr. Polym. 164 (2017) 31–41. doi:10.1016/j.carbpol.2017.01.079.

[29] G.D. Manrique, F.M. Lajolo, FT-IR spectroscopy as a tool for measuring degree of methyl esterification in pectins isolated from ripening papaya fruit, Postharvest Biol. Technol. 25 (2002) 99–107. doi:10.1016/S0925-5214(01)00160-0.

[30] G.R.C. Santos, B.F. Glauser, L.A. Parreiras, E. Vilanova, P.A.S. Mourão, Distinct structures of the α-fucose branches in fucosylated chondroitin sulfates do not affect their anticoagulant activity, Glycobiology. 25 (2015) 1043–1052. doi:10.1093/glycob/cwv044.

[31] J.Y. Guo, H.Y. Chen, R. Mathew, J. Fan, A.M. Strohecker, G. Karsli-Uzunbas, J.J. Kamphorst, G. Chen, J.M.S. Lemons, V. Karantza, H.A. Coller, R.S. DiPaola, C. Gelinas, J.D. Rabinowitz, E. White, Activated Ras requires autophagy to maintain oxidative metabolism and tumorigenesis, Genes Dev. 25 (2011) 460–470.

doi:10.1101/gad.2016311.

[32] S. Benlloch, A. Payá, C. Alenda, X. Bessa, M. Andreu, R. Jover, A. Castells, X. Llor, F.I. Aranda, B. Massutí, Detection of BRAF V600E mutation in colorectal cancer: Comparison of automatic sequencing and real-time chemistry methodology, J. Mol. Diagnostics. 8 (2006) 540–543. doi:10.2353/jmoldx.2006.060070.

[33] H. Davies, G.R. Bignell, C. Cox, P. Stephens, S. Edkins, S. Clegg, J. Teague, H. Woffendin, M.J. Garnett, W. Bottomley, N. Davis, E. Dicks, R. Ewing, Y. Floyd, K. Gray, S. Hall, R. Hawes, J. Hughes, V. Kosmidou, A. Menzies, S. Hooper, R. Wilson, H. Jayatilake, B.A. Gusterson, M.R. Stratton, P.A. Futreal, Mutations of the BRAFgene in human cancer, (2002) 949–954. doi:10.1038/nature00766.

[34] G. Poulogiannis, F. Luo, M.J. Arends, RAS signalling in the colorectum in health and disease, Cell Commun. Adhes. 19 (2012) 1–9. doi:10.3109/15419061.2011.649380.

[35] C. Hertzman Johansson, S. Egyhazi Brage, BRAF inhibitors in cancer therapy, Pharmacol. Ther. 142 (2014) 176–182. doi:10.1016/j.pharmthera.2013.11.011.

[36] H. Inohara, A. Raz, Functional Evidence that Cell Surface Galectin-3 Mediates Homotypic Cell Adhesion, Cancer Res. 55 (1995) 3267–3271.

[37] P. Mina-Osorio, I. Soto-Cruz, E. Ortega, A role for galectin-3 in CD13-mediated homotypic aggregation of monocytes, Biochem. Biophys. Res. Commun. 353 (2007) 605–610. doi:10.1016/j.bbrc.2006.12.081.

[38] H. Tabusa, T. Brooks, A.J. Massey, Knockdown of PAK4 or PAK1 Inhibits the Proliferation of Mutant KRAS Colon Cancer Cells Independently of RAF / MEK / ERK and PI3K / AKT Signaling, Mol. Cancer Res. 11 (2013) 109–121. doi:10.1158/1541-7786.MCR-12-0466.

[39] M. El-Bahrawy, S.R. Poulsom, A.J. Rowan, I.T. Tomlinson, M.R. Alison, Characterization of the E-cadherin/catenin complex in colorectal carcinoma cell lines, Int. J. Exp. Pathol. 85 (2004) 65–74. doi:10.1111/j.0959-9673.2004.0371.x.

[40] T. Shimura, Y. Takenaka, S. Tsutsumi, V. Hogan, A. Kikuchi, A. Raz, Galectin-3, a novel binding partner of β-catenin, Cancer Res. 64 (2004) 6363–6367. doi:10.1158/0008-5472.CAN-04-1816.

[41] S. Umar, A.P. Morris, F. Kourouma, J.H. Sellin, Dietary pectin and calcium inhibit colonic proliferation in vivo by differing mechanisms, Cell Prolif. 36 (2003) 361–375. doi:10.1046/j.1365-2184.2003.00291.x.

[42] M. Szymanska-Chargot, A. Zdunek, Use of FT-IR Spectra and PCA to the Bulk Characterization of Cell Wall Residues of Fruits and Vegetables Along a Fraction Process, Food Biophys. 8 (2013) 29–42. doi:10.1007/s11483-012-9279-7.

[43] J. Cybulska, A. Zdunek, A. Koziol, The self-assembled network and physiological degradation of pectins in carrot cell walls, Food Hydrocoll. 43 (2015) 41–50.

[44] Z. Koˇ, Z. Hromádková, A. Ebringerová, Structural diversity of pectins isolated from the Styrian oil-pumpkin (Cucurbita pepo var . styriaca) fruit, 93 (2013) 163–171. doi:10.1016/j.carbpol.2012.05.017.

[45] D.J. Cosgrove, Growth of the plant cell wall, Nat. Rev. Mol. Cell Biol. 6 (2005) 850–861. doi:10.1038/nrm1746.

[46] J.P. Fabi, S.G. Broetto, S.L.G.L. Da Silva, S. Zhong, F.M. Lajolo, J.R.O. Nascimento, Analysis of Papaya Cell Wall-Related Genes during Fruit Ripening Indicates a Central Role of Polygalacturonases during Pulp Softening, PLoS One. 9 (2014) e105685. doi:10.1371/journal.pone.0105685.

[47] M. Farhad, A.S. Rolig, W.L. Redmond, The role of Galectin-3 in modulating tumor growth and immunosuppression within the tumor microenvironment, Oncoimmunology. 7 (2018) 1–8. doi:10.1080/2162402X.2018.1434467.

[48] V.J. Morris, A. Gromer, A.R. Kirby, R.J.M. Bongaerts, A. Patrick Gunning, Using AFM and force spectroscopy to determine pectin structure and (bio) functionality, Food Hydrocoll. 25 (2011) 230–237. doi:10.1016/j.foodhyd.2009.11.015.

[49] T. Zhang, M.C. Miller, Y. Zheng, Z. Zhang, H. Xue, D. Zhao, J. Su, K.H. Mayo, Y. Zhou, G. Tai, Macromolecular assemblies of complex polysaccharides with galectin-3 and their synergistic effects on function, Biochem. J. 474 (2017) 3849–3868. doi:10.1042/BCJ20170143.

[50] A.N. Round, N.M. Rigby, A.J. MacDougall, S.G. Ring, V.J. Morris, Investigating the nature of branching in pectin by atomic force microscopy and carbohydrate analysis, Carbohydr. Res. 331 (2001) 337–342. doi:10.1016/S0008-6215(01)00039-8.

[51] A. Kozioł, J. Cybulska, P.M. Pieczywek, A. Zdunek, Changes of pectin nanostructure and cell wall stiffness induced in vitro by pectinase, Carbohydr. Polym. 161 (2017) 197–207. doi:10.1016/j.carbpol.2017.01.014.

[52] M. Kacuráková, P. Capek, V. Sasinková, N. Wellner, A. Ebringerová, FT-IR study of plant cell wall model compounds: Pectic polysaccharides and hemicelluloses, Carbohydr. Polym. 43 (2000) 195–203. doi:10.1016/S0144-8617(00)00151-X.

[53] E.G. Maxwell, I.J. Colquhoun, H.K. Chau, A.T. Hotchkiss, K.W. Waldron, V.J. Morris, N.J. Belshaw, Rhamnogalacturonan I containing homogalacturonan inhibits colon cancer cell proliferation by decreasing ICAM1 expression, Carbohydr. Polym. 132 (2015) 546–553. doi:10.1016/j.carbpol.2015.06.082.

[54] H. Cheng, Z. Zhang, J. Leng, D. Liu, M. Hao, X. Gao, G. Tai, Y. Zhou, The inhibitory effects and mechanisms of rhamnogalacturonan I pectin from potato on HT-29 colon cancer cell proliferation and cell cycle progression, Int. J. Food Sci. Nutr. 64 (2013) 36–43. doi:10.3109/09637486.2012.694853.

[55] L. Leclere, M. Fransolet, F. Cote, P. Cambier, T. Arnould, P. Van Cutsem, C. Michiels, Heat-Modified Citrus Pectin Induces Apoptosis-Like Cell Death and Autophagy in HepG2 and A549 Cancer Cells, PLoS One. 10 (2015) e0115831. doi:10.1371/journal.pone.0115831.

[56] C.L. Jackson, T.M. Dreaden, K. Theobald, N.M. Tran, T.L. Beal, M. Eid, M.Y. Gao, R.B. Shirley, T. Stoffel, M.V. Kumar, D. Mohnen, L.K. Theobald, N.M. Tran, T.L. Beal, M. Eid, M.Y. Gao, R.B. Shirley, M.T. Stoffel, M.V. Kumar, D. Mohnen, K. Theobald, T. Stoffel, Pectin induces apoptosis in human prostate cancer cells: correlation of apoptotic function with pectin structure, Glycobiology. 17 (2007) 805–19. doi:10.1093/glycob/cwm054.

[57] H. Inohara, A. Raz, Identification of human melanoma cellular and secreted ligands for galectin-3, Biochem. Biophys. Res. Commun. 201 (1994) 1366–1375.

Supplementary files

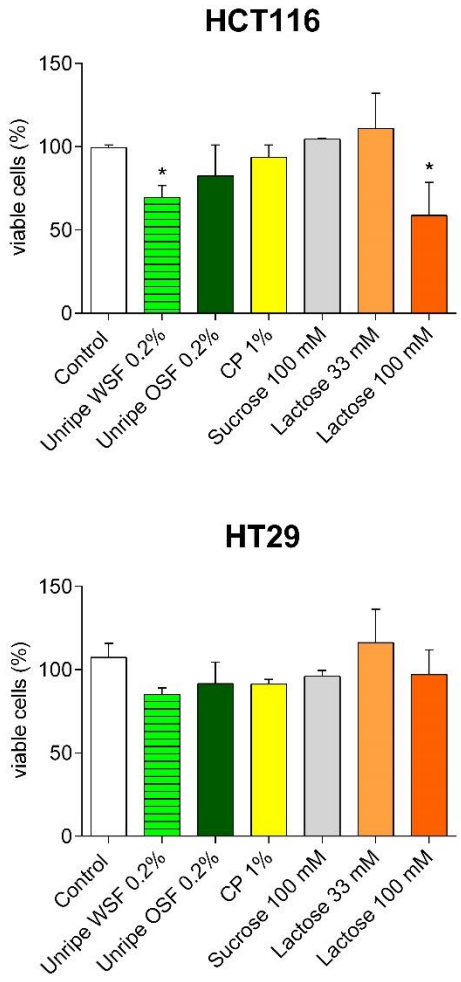

Supplemental Fig. 1. Viability assay by MTT on HCT116 and HT29 cell lines treated with different compounds for 24 h. Unripe WSF: polysaccharides extracted from total plant cell wall after water treatment and using papayas from the 2nd ripening point (unripe fruits) at 2 mg/mL (0.2%). Unripe OSF: polysaccharides extracted from total plant cell wall after oxalate treatment and using papayas from the 2nd ripening point (unripe fruits) at 2 mg/mL (0.2%). CP: Citrus Pectin. The results are expressed in percentage of cell viability in comparison with control (no treatment) of the correspondent time. Data were shown as mean ± SD. *P < 0.05 vs control, according to Dunnett's test. The results were from three independent WSF or CSF samples (each one performed in technical triplicate) from the biological duplicate (n = 6).

Chapter 7

Dietary fiber from unripe and ripe papaya differentially regulate microbiota composition: Evidence from an *in vitro* colonic fermentation study

Samira Bernardino Ramos do Prado[1], Beatriz Toledo Minguzzi[1], Christian Hoffmann[1], João Paulo Fabi[1,2,3]

[1]Department of Food Science and Experimental Nutrition, School of Pharmaceutical Sciences, University of São Paulo, São Paulo, SP, Brazil
[2]Food and Nutrition Research Center (NAPAN), University of São Paulo, São Paulo, SP, Brazil.
[3]Food Research Center (FoRC), CEPID-FAPESP (Research, Innovation and Dissemination Centers, São Paulo Research Foundation), São Paulo, SP, Brazil.

Abstract

Dietary fibers (DF) consumption is recommended because of the healthy and protective effects in decreasing the risk of diseases, such as colon cancer. DF have complexes structures that is determinant for their biological effects that includes the indirect effects of SCFA, and the effects of DF on the modulation of the microbiota profile. In the present study, we explore the biological effects of DF from unripe and ripe papaya using colonic *in vitro* fermentation. These effects include the utilization of the DF by the fecal inoculum, the production of SCFA, and the microbiota profile that was characterized by 16S sequencing. Results shown that DF from unripe and ripe papaya induces a similar production of SCFA, characterized by increased levels of acetate, propionate and butyrate, compared to apple pectin and lactulose, which were also used as fermentation substrates. Besides the similar results concerning the SCFA, the DF utilization by the bacteria showed a distinct profile. The DF from unripe papayas had a slow bacteria utilization than the DF from ripe papayas, and the latter had a faster oligosaccharide degradation by the microorganisms. Furthermore, weighted UniFrac distances matrix analysis revealed significant changes in the bacteria profile after 24 h of fermentation compared to the initial time of fermentation (0 h), the differences were between both the DF from unripe and ripe papayas and the apple pectin and lactulose at 24 h of fermentation. Notably, although DF from unripe and ripe papaya induces similar results concerning the levels of SCFA, the colonic fermentation of these DF induces distinct changes in the bacteria profile. Fermentation of DF from unripe papaya increased the abundance of *Clostridiaceae 02d06*, *Coprabacilus*, *Bulleidia* and *Slackia* genera, and both unripe and ripe papayas DF showed an enhancement of *Clostridium* and *Bacteroides*. Therefore, the DF utilization from papaya by the bacteria is dependent of the carbohydrate structure, resulting in distinct changes in bacteria profile. However, besides their differences in the carbohydrate structure and therefore on the induction of a distinct bacterial profile, DF from unripe and ripe papaya similarly increased the production of acetate, propionate and butyrate, demonstrating the possible benefits of ingesting both types of DF.

Key-words: *in vitro* fermentation; dietary fiber; pectin; papaya; microbiota.

Abbreviations: Ara, arabinose; DF, dietary fibers; Gal, galactose; GalA, galacturonic acid; Glc, glucose; HG, homogalacturonan; RGI, rhamnogalacturonan I; SCFA, short chain fatty acids; Xyl, xylose.

Introduction

Dietary fibers (DF) consumption has been associated with several health benefits including the reducing both postprandial glucose levels and the reabsorption of bile acids [1], as well increasing satiety and stool bulk [2] and effects resulting from both the direct interaction with cells (intestinal epithelial cells and immune cells) [3] and fermentation-related effects [4]. The DF fermentation process lead to the production of substrates including short chain fatty acids (SCFA) such as acetate, propionate and butyrate [5,6]. The increase in SCFA levels help in lowering the intestinal pH thus favoring the environment for healthy associated bacteria, thereby reducing the establishment of pathogenic bacteria [7]. Butyrate is used as a primary source of energy for intestinal epithelial cells, stimulating both the growth of these cells and the production of cytokines that act protecting the epithelial integrity [8,9]. Acetate is usually the SCFA produced in higher amounts during DF fermentation [10] and is absorbed and metabolized in muscle, kidney, heart, and brain tissues [11]. Propionate is metabolized in the liver, and appears to suppress cholesterol synthesis in addition to enhance the antiproliferative properties of butyrate in cancer cells [12].

Some intestinal bacteria have a repertoire of carbohydrate-active enzymes that can hydrolyze specific glycosidic linkages from DF [13]. Thus, the knowledge of DF structures are crucial to establish a relationship between the effect of a specific DF structure and changes in the fermentation profile by the gut microbiota. The fruit cell wall is a complex structure composed mainly by cellulose, hemicellulose and pectin, which are composed mostly by DF [14]. Cellulose is a structure composed by 1,4-β-D-glucose (Glc) residues [15] and hemicellulose is composed by a range of structural polymers such as xyloglucan [16], which consist in a backbone of 1,4-β-D-Glc residues such as cellulose, but containing 1,6-α-D-xylose (Xyl) side chains [17]. The most abundant structure in pectin is homogalacturonan (HG), which is a linear structure comprised of α-1,4-α-D-galacturonic acid (GalA) residues with varying degrees of acetyl and methyl esterification. Pectin also contain ramified structures such as rhamnogalacturonan I (RGI), which have a backbone with repeating units of GalA (1,4-α-D-GalpA) and rhamnose (1,2-α-L-Rhap), usually containing side chains of arabinose (Ara) and galactose (Gal) [18,19].

Papaya (*Carica* papaya L.) is a climacteric fruit with a fast ripening after harvesting with a concomitant change in cell wall structure that leads also to a fast pulp softening. Just around 3 to 5 days after harvesting green papayas, the fruit pulp become completely soft and ready for human consumption [20]. Polygalacturonases are ethylene-controlled enzymes that act hydrolyzing papaya cell wall in just a few days, making the papaya pulp soft by turning the insoluble pectin into water-soluble pectin by decreasing the molecular weight of these less soluble pectin [21,22]. Despite the structural changes that occur in papaya cell wall during ripening, it is unknown whether these differences in DF structure of unripe and ripe papayas influences their fermentation profile. As DF are not digested by the human enzymes and reach the colon where they are fermented by the gut microbiota, it is important not just know their whole structure and utilization by the microbiota but also the growth profile of the bacteria that are being favored. Thus, in this study, we used an *in vitro* colonic fermentation approach to explore the utilization of DF from unripe and ripe papaya by intestinal bacteria, as well as the effects of these DF on SCFA production and modulation of the bacteria profile by 16S sequencing.

Material and methods

Plant material

Papaya (*Carica papaya* L. cv. "Golden") from two biological replicates were acquired from a producer in Aracruz (Espírito Santo, Brazil; 19°47′42.2″S, 40°19′09.2″W) as described in Prado et al. (2018), in which the same fruit sampling was used [23].

Dietary fiber extraction from papayas

The frozen papaya pulp was ground in N_2 and incubated three times in boiling chloroform:methanol (1:1; 15 min) in order to get rid of the proteins, lipids and pigments. The solid residue was further washed in boiling 80% (three times) ethanol to extract the remaining soluble sugars and then in acetone. After washing, the residue was dried at ambient temperature to obtain the total cell wall (DF) of papaya pulp.

Batch colonic *in vitro* fermentation

Feces of three volunteers were used to make a pool, which was used to prepare the fermentation inoculum. For that, three health volunteers with no history of antibiotics usage on the last three months were recruited after Ethics Committee approval (School of Pharmaceutical Sciences, University of São Paulo; Number #1.089.446). The feces were collected in a sterile container and immediately put on ice until the sample delivery, which was done at the same day. The *in vitro* fermentation assay was based on previously described methods [24,25]. Briefly, after receiving the fecal samples, the inoculum was immediately prepared.

After pooling the feces, they were diluted in anaerobic and sterile 0.9% NaCl solution in a ratio of 1:6 (w/v). The material was homogenized and filtered (Miracloth, EMD Millipore), resulting in the inoculum, which was put in a CO_2-filled container for anaerobic condition maintenance. The fermentation medium prepared contained basal solution (76%), vitamins/phosphate buffer solution (1%), bicarbonate buffer (1%) and reducing agent (4%) as described in Williams et al. (2005). All bottles and containers used were sterile and the bottles with the medium and the inoculum were continually flushed with CO_2, as described in the original methods.

The steps of the *in vitro* fermentation assay are summarized in **Figure 1**. The carbohydrates used as substrate were unripe papayas DF, ripe papayas DF, apple pectin (Sigma, 76282), and lactulose (Sigma, L7877). Each fermentation bottle was added 100 mg of a specific carbohydrate, 24 mL of fermentation medium and 1.5 mL of the inoculum. The CO_2 was flushed inside the screw capped bottles and they were incubated in a water bath at 39 °C. A blank control was used, without the addition of any kind of DF. A bottle with just the fermentation medium was also used as negative control of medium sterility. A duplicate of each treatment was used for the analysis each fermentation time (0 h, 8 h, 16 h and 24 h).

The pH and pressure were evaluated at each fermentation time point as an indicator that fermentation is occurring. The fermentation content was gently centrifugated and aliquots of the supernatant were separated for the analysis of SCFA and carbohydrates (Monosaccharide analysis, homogeneity and average molecular size, and oligosaccharide

analysis). The precipitates were immediately frozen using N2 and storage at –80 ºC until DNA analysis.

Monosaccharide analysis

High-performance anion-exchange chromatography coupled with a pulse amperometric detector (HPAEC-PAD) was used to analyze the monosaccharide composition [26,27]. DF from unripe and ripe papayas (1 mg) were hydrolyzed using 2 M trifluoroacetic acid at 120 °C for 90 min. *T*-butyl alcohol was added in the mixture and the hydrolysate was evaporated under N_2 flow, solubilized in water, and filtered. An DX 500 system (Dionex) equipped with a CarboPac PA10 column (250 × 4 mm; Dionex) was used to analyze the samples. For the analysis of neutral sugars, the eluent was 150 mM NaOH (1 mL/min; 30 min), and a post column adjustment with 300 mM NaOH was used. For the uronic acid analysis, the same system was used but a 0–220 mM sodium acetate was used as gradient eluent. Neutral sugars and uronic acids (Sigma) were used as standards.

Homogeneity and average molecular size

Supernatant (1 mL) from the fermentation time points were filtered (0.22 µm) and analyzed through high-performance size-exclusion chromatography coupled with a refractive index detector (HPSEC-RID). In a 1250 Infinity system (Agilent, Santa Clara, CA). The system was equipped with four PL aquagel-OH columns (60, 50, 40, and 30; 429,300 × 7.5 mm; Agilent) connected in tandem. The eluent was 0.2 M NaNO3/0.02% NaN3 (0.6 mL/min), and the RID temperature was set at 30 °C. An external curve of dextran (MW 5–1800 kDa; Sigma) was used as size standards.

Oligosaccharide analysis

Supernatants (1 mL) from the fermentation time points were analyzed using a DX 500 HPAEC-PAD system (Dionex) as described by Jonathan et al. (2012). The samples were filtered (0.22 µm) and analyzed in a CarboPac PA- 1 column (2 mm × 250 mm; Dionex). Oligomers derived from neutral sugars were eluted (0.3 mL/min) with a linear gradient of 0.02–0.05 M NaOH for 3 min and 0.05–0.075 M NaOH for 10 min, followed by isocratic elution of 0.1 M NaOH for 2 min. Oligomers derived from uronic acids were

eluted with a gradient of 0–1 M NaOAc in 0.1 M NaOH for 50 min. Finally, the column was washed with 1 M NaOAc in 0.1 M NaOH for 7 min followed by 0.1 M NaOH for 3 min. Equilibration was done by eluting 0.02 M NaOH for 20 min.

Bacterial DNA extraction and 16 s sequencing

The fermentation precipitate containing the inoculum bacteria had the DNA extracted using the kit PSP® Spin Stool DNA Kit (Stratec Molecular) and lysis beads (Lysing matrix E, MP Biomedicals) following the manufacturer's instructions. The 16S rRNA gene was amplified using primer pairs, BSF8 (27F) e BSR357 (338R), targeting the V1 and V2 hypervariable region. AMPure XP (Beckman Coulter) was used to purify the PCR products, according to the manufacturer's instructions. Amplicons were generated according to the Illumina MiSeq 16S Metagenomic Sequencing Library. Samples were prepared using the Nextera XT Index kit (Illumina) and the quality of libraries was assessed and quantified using Bioanalyzer (Agilent) and Qubit (Life Technologies), respectively. The 16S amplicon sequencing was performed at the Core Facility for Scientific Research of the University of São Paulo (CEFAP/ICB-USP). Prepared libraries were pooled and then sequenced in a paired-end 2x300bp format on an Illumina MiSeq platform. Quantitative Insights Into Microbial Ecology (Qiime) analysis was done by Tau GC Bioinformatics. Paired end sequence experiments had read pairs joined with PEAR (v0.9.10) using default settings (p:0.01,v:10,m:0,n:50,t:1,q:0,u:1,g:1,e,s:2,b:33,c:40). Sequence analysis was done using the Qiime package version 1.9.1 and enclosed reference Greengenes database from August 2013. OTU picking and taxonomic assignment was done using pick_de_novo_otus.py script with default parameters, i.e.: 97% sequence identity, first (seed) representative sequence and consensus taxonomy assigned using uclust (v1.2.22q); alignment with PyNAST (v1.2.2) removed all gaps positions and mask non-conserved positions; representative OTU sequence tree building with FastTree (v2.1.3). The unrarefied Weighted UniFrac distance matrices were used. OTU networks were generated using Qiime´s make_otu_network.py script. Taxonomy summaries figures were done without count normalization (collapse_samples.py). Alpha diversity was done with rarefaction (alpha_rarefaction.py) using 10 steps of both the median number of sequences between samples and 5000 sequences. Beta diversity was calculated with jackknifing for both weighted and unweighted UniFrac (v1.5.3) (jackknifed_beta_diversity.py). The abundance percentage and heatmaps were made using the OTU table, taxonomy table and

the metadata file with MicrobiomeAnalyst tools (https://www.microbiomeanalyst.ca/faces/home.xhtml).

Statistics

The results were expressed as the mean ± standard deviation (SD), and the significance was set at $p < 0.05$. Data were analyzed using GraphPad Prism 6.0 software (GraphPad, San Diego, CA). One-way ANOVA with Tukey's (to assess differences among all groups) was used as post hoc test.

Results and Discussion

The colonic *in vitro* fermentation was performed at 0, 8, 16 and 24 h using DF extracted and isolated from unripe and ripe papayas as substrate. Furthermore, a commercial apple pectin was used as a standard type of DF, and lactulose as a disaccharide that is completely fermentable. A control blank with inoculum without any DF was used in order to visualize any alteration from the possible fermentable substrates that come from the volunteers feces, and another control with only medium was also used to demonstrate the sterility of the inoculum, that resulted in no fermentation and no alteration in any studied parameter, such as medium pH and flask pressure.

The DF from unripe and ripe papaya differs in the amount and composition of their soluble DF. The main changes in papaya cell wall (mainly formed by DF) during ripening is caused by the action of polygalacturonases, a pectinase that are produced after ethylene triggering during the fruit climacteric with a huge impact on the degradation of papaya cell wall [21,22]. The papaya fruit enzymes act not just mobilizing the insoluble pectins to water-soluble pectins but also degrading the soluble pectins into a smaller molecular size [21,22,26,28]; therefore, the main change in papayas DF during the ripening is in the pectin structure. It can be easily confirmed by measuring the yield of the DF that is water-soluble obtained from unripe and ripe papayas. Previous study using the same sampling revealed that the yield of the most soluble pectin (water-soluble fraction) extracted from unripe papaya was 34%, whereas the yield of the same fraction from ripe papaya was 57% [23]. The difference on DF solubility and pectin composition is probably the reason why the DF from unripe or ripe papayas present different effects on fermentation describe herein.

Besides that, using the whole DF and not just the most soluble part, it was proposed here to determine a most reliable simulation of human digestion, and how these DF from papaya pulp could be bio-transformed by the intestinal bacteria.

The monosaccharide composition of DF from unripe and ripe papaya showed that the latter has lower amounts of GalA, Gal and Glc, and increased Rha levels (**Figure 2**). These monosaccharides residues are usually associated with pectin structure, that in papaya is formally mostly by HG and RGI. The increased amount of Rha indicates the presence of more ramified RGI, even with less extend branching – as Gal and Ara are diminished – thereby indicating that arabinans and arabinogalactans are probably smaller than in unripe papayas DF [28]. Other components of the fruit cell wall are also present in papaya pulp, as cellulose that is formed by Glc residues, and hemicellulose that is composed by Xyl, Glc, Man and/or Gal residues.

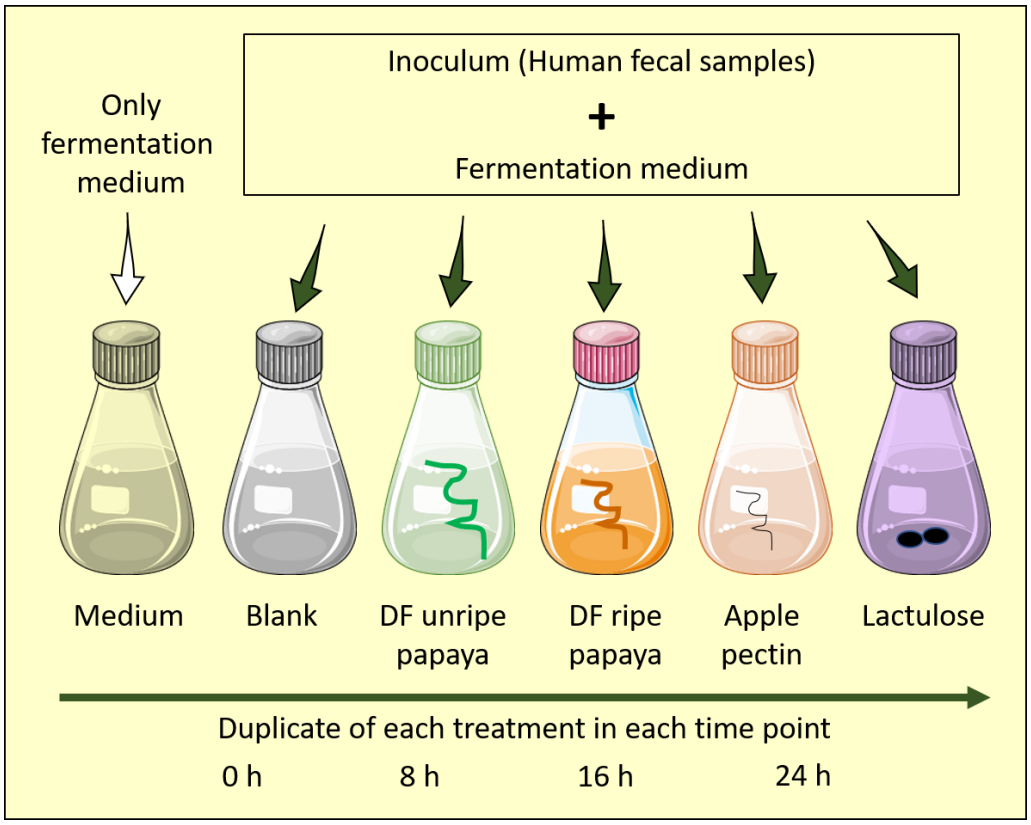

Figure 1. Schematic representation of the *in vitro* batch colonic fermentation designed for this study.

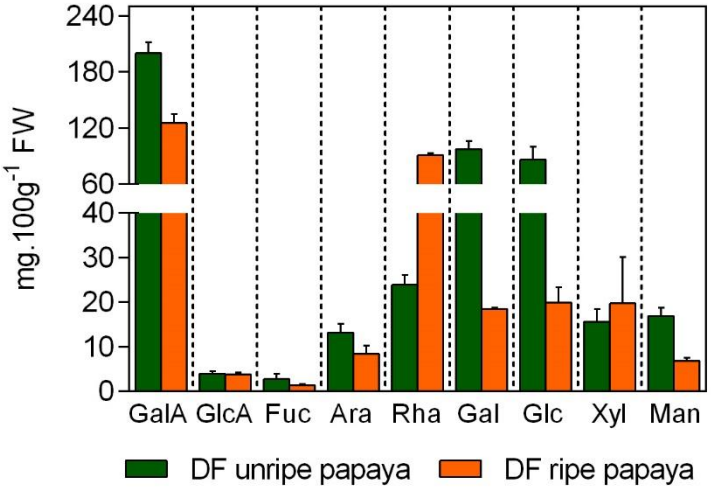

Figure 2. Monosaccharide composition of DF from unripe and ripe papaya.

The pH and pressure were used to indicate that the fermentation is normally occurring in the samples. According to **Figure 3A**, DF from unripe papaya showed a rapid increase in pressure and reach pressure levels similar to that of lactulose at 24 h. Lactulose is largely referred as a control of fermentation and its pH after fermentation is commonly associated to the lowest values [29–31], as we observed in our experiments (**Figure 3B**). The resulted pH of both DF from unripe and ripe papayas and the apple pectin showed lower values than the blank (only the inoculum). The pH of 0 h and 24 h were 7.61 and 6.11 for the blank, 7.38 and 5.51 for lactulose group, 7.04 and 6.05 for apple pectin group, 7.73 and 6.09 for DF from unripe papaya, and 7.8; and 6.13 for ripe papya. Therefore, the differences between the pH on the beginning and the final of fermentation were 1.50, 1.87, 0.98, 1.64 and 1.67 for blank, lactulose, apple pectin, and DF from unripe and ripe papaya, respectively. Thus, although lactulose have the highest reduction in pH the value during the fermentation, the DF from both unripe and ripe papaya also showed a higher decrease compared to the blank and to apple pectin.

In accordance with pH levels, the SCFA production were observed as the highest levels after 24 h of fermentation (**Figure 4**). Acetate showed the greatest accumulation mainly for DF from unripe and ripe papayas and for lactulose. Acetate is normally the main product of DF fermentations [32,33], and is associated with effects on lipid metabolism, whereas propionate is associated with reduced synthesis of fatty acids in both liver and

plasma [34]. Butyrate was significantly increased in DF from unripe and ripe papayas compared to other treatments. Butyrate is related to maintain integrity of intestinal cells and reduces pro-inflammatory signaling [35,36]. The *in vitro* fermentation of citrus pectin also increase acetate and butyrate levels [37]. Recently, it was shown that inulin, fructooligosaccharides, native pectin from citrus (10–12 kDa and 100–800 kDa) and sunflower (100–800 kDa), and modified pectin from sunflower (12.5 kDa) and artichole (80–300 kDa) were used as substrate for *in vitro* fermentation, and results suggests that neither the degree of methoxylation nor the molecular weight of these pectin influences SCFA production, as all samples showed similar levels of acetate, propionate and butyrate [38]. One interesting question is why the pH of lactulose was the lowest one, but the sum of the SCFA was not the highest one. This could be explained by the fact that the fermentation of lactulose will produce high amounts of lactic acid with low transformation in acetate thus lowering the pH [30]. We did not perform this analysis since pectin fermentation, in general, did not result in high amounts of lactic acid [39], and the beneficial effects for human health is related to the SCFA produced and studied in this work, especially the butyrate.

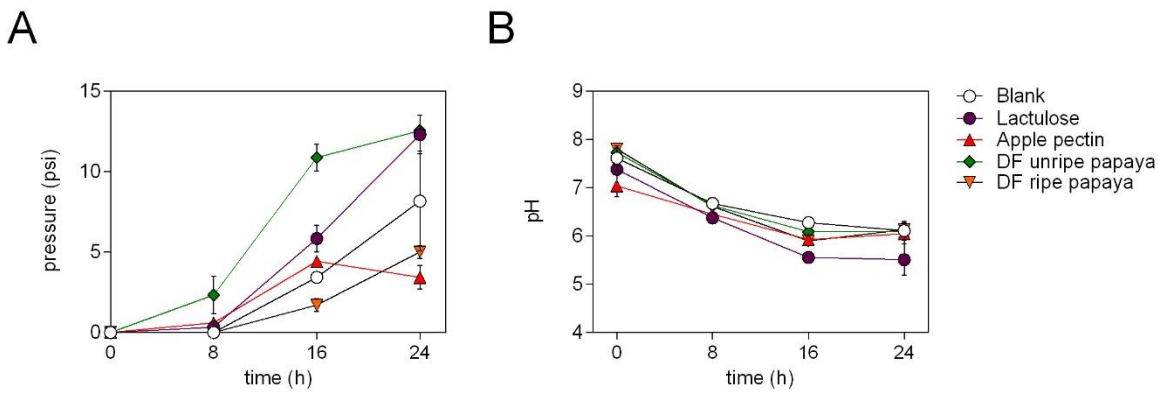

Figure 3. Pressure and pH of *in vitro* colonic fermentation time points.

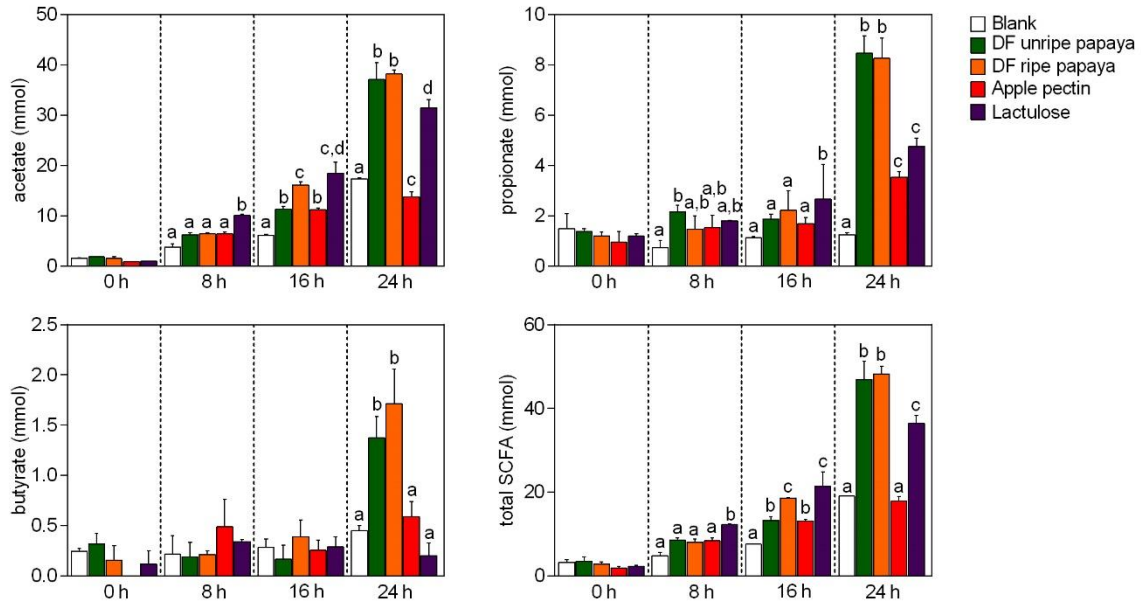

Figure 4. Short chain fatty acid production: acetate, propionate, butyrate and total SCFA (the sum of acetate, propionate and butyrate). Data were shown as mean ± SD. Tukey's test (*p < 0.05) was performed. Different letters represent significant differences between the treatments of each time.

The carbohydrates degradation caused by fermentation were evaluated by homogeneity and average molecular weight and oligosaccharide analysis. In the earliest fermentation time-points it can be seen higher molecular weight structures for unripe and ripe papayas DF, and for apple pectin, with peaks eluted around 5 and 150 kDa of equivalent dextran (**Figure 5**). The blank (without DF as substrate) do not have signals detected equivalent to 5 and 150 kDa of equivalent dextran molecular weight (**Supplementary Figure S1**). Peaks eluted around 59 – 63 min could be due to fermentation medium interference, as seen in **Figure S1** with only the medium being detected in HPSEC. However, on the later times of fermentation it is possible to see a higher peak eluted around 63 min for ripe papayas DF and lactulose, indicating that ripe papayas DF fermentation have a different pattern than DF from unripe papayas. The peaks eluted after 65 min were considered interference of lower molecules as monosaccharide and organic acids [40]. The smaller fermentation products can be better visualized and separated through the oligosaccharide analysis (**Figure 6**). The peaks that eluted before 5 min were considered as monosaccharides and interferences, but after 5 min a distinct oligosaccharide patterns can

be observed to the samples. The blank, which contains only the fermentation medium showed lower signals. Apple pectin had increased detection of polymers, and lactulose showed less signals as expected for a disaccharide. DF from unripe and ripe papaya did not showed signals at 0 h of fermentation, and peaks derived from ripe papaya appeared at early fermentation times compared with DF from unripe papayas. At 16 h of fermentation the DF from ripe papaya presented higher signal compared to DF from unripe papaya, and the peaks of the first seem disappear at 24 h of fermentation, indicating a higher consumption of oligosaccharides after 24 h of the fermentation. Others studies showed that different lengths of isomalto/malto-polysaccharides showed distinct utilization and fermentation ratio [40]. Ensiled chicory root pulp (more soluble) had higher utilization by fermentation than native chicory root pulp (less soluble). These differences appear to be associated with an increased levels of soluble pectin (HG and RGI) and probably to a more open structure that is more accessible for the enzymatic degradation [41]. *In vitro* fermentation of linear arabino-oligosaccharides and debranched (linear) sugar beet arabinans showed that the former were slowly fermented than the last [42]. Thus, the abovementioned studies indicate that changes in carbohydrate structure (size and composition) influences the utilization of DF by the microbiota, and possibly changes in the bacteria profile.

The bacteria profile was evaluated throughout the distance between the bacterial profile from blank (0 h fermentation) to the treatments at 24 h, calculated using Weighted UniFrac distances matrix (**Figure 6A**). The closer to the number 0 on y axis means that the sample is more similar to the blank (0 h), and the higher the value on y axis means that the sample is more different to the blank (0 h). Lactulose and apple pectin on 24 h of fermentation were significantly different from DF extracted from unripe and ripe papayas. No statistical difference was observed between the DF from unripe and ripe papayas, meaning that both are more distant of blank 0 h than the other substrates, but not necessarily meaning that these DF have the same changes in bacteria profile. To evaluate the types of bacteria that could have changed over the fermentation, a percentage of phylum and family abundance is shown in **Figure 6 B and Figure C**, respectively. The phylum data suggests that at 8 h of fermentation Bacteroidetes decrease and the Proteobacteria increase. The enhancement of Proteobacteria at 8 h can be explained by the initial process of *in vitro* fermentation that inevitable has more oxygen, even though the anaerobic condition was provided. At 24 h of fermentation the Bacteroidetes increase again, and for DF from unripe and ripe papaya the Bacteroidetes abundance seem to be equal or higher at 24 h compared

to 0 h. The bacteria composition of the Bacteroidetes Phyla at 0 h is mainly composed by *Prevotellacaeae* and *Paraprevotellaceae*, and at 24 h for DF from ripe papaya the *Bacteroidaceae* family is prevalent.

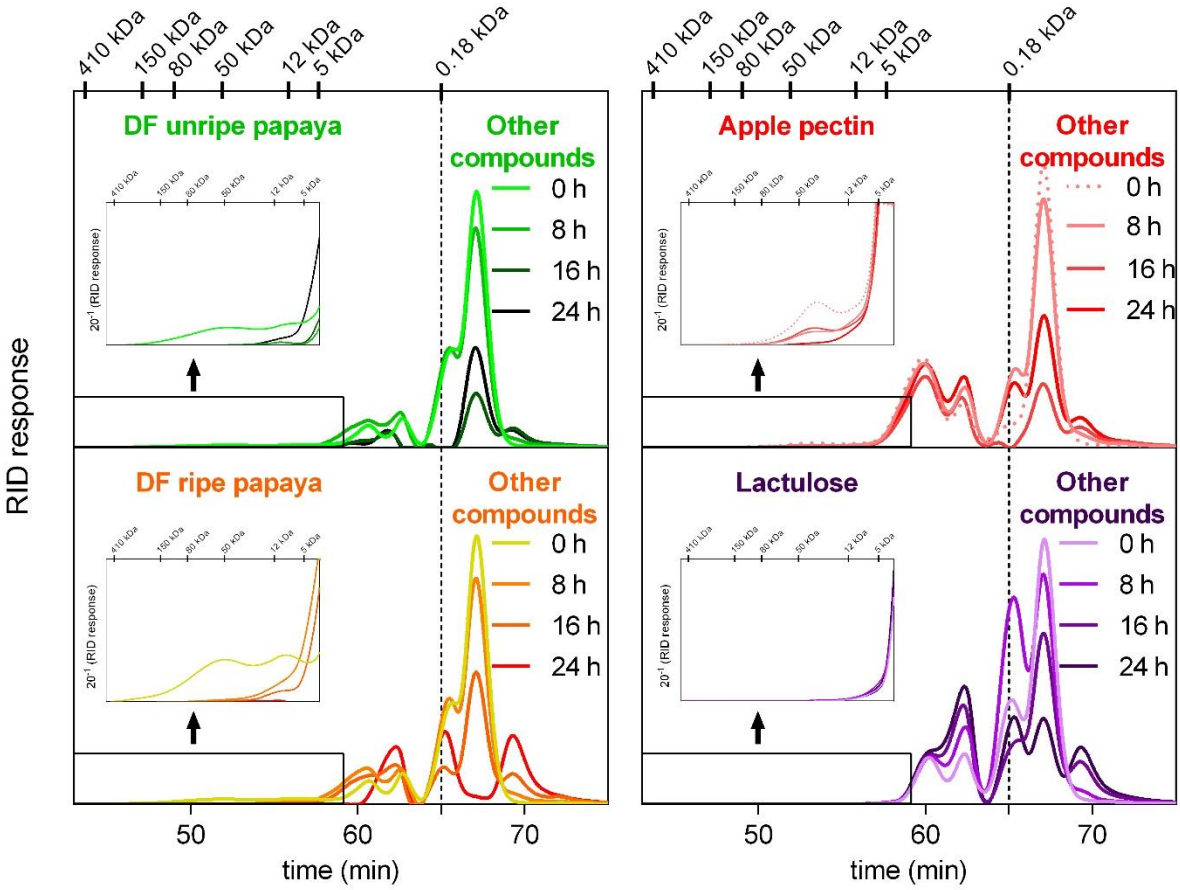

Figure 5. HPSEC of colonic *in vitro* fermentation aliquots. The inside boxes represent a zoom on the marked area. Above to the graphs are indicated the standards dextran sizes and glucose (0.18 kDa).

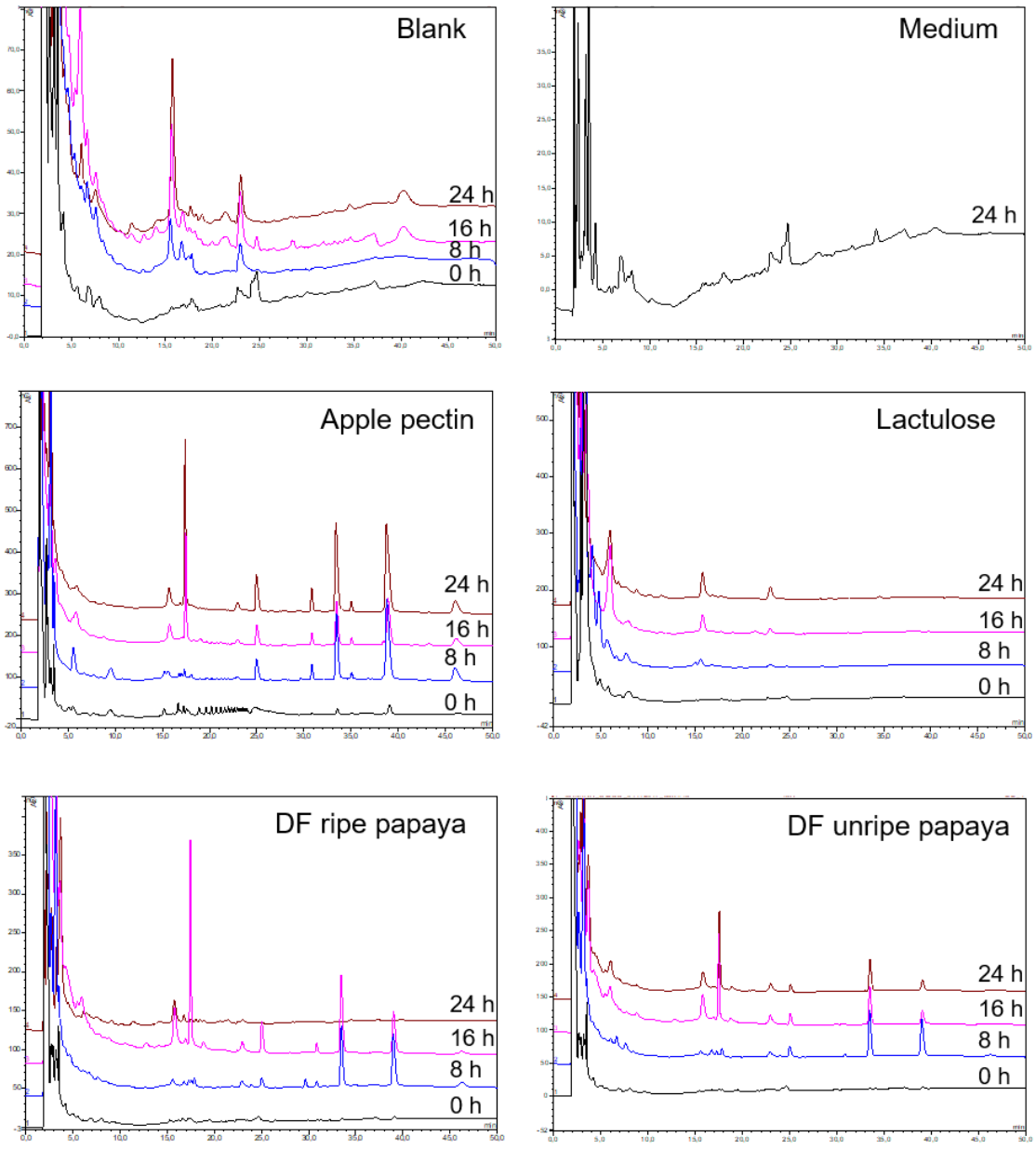

Figure 6. Oligosaccharide of colonic *in vitro* fermentation aliquots.

DF from unripe and ripe papaya had the Weighted UniFrac distances matrix significantly different from the others carbohydrate treatments at 24 h of fermentation, so we decided to evaluate what could be changing in the bacteria profile focusing on DF from unripe and ripe papaya. As lactulose also significantly increased acetate and butyrate production, we focused on the analysis of the blank at 0 h, as well as lactulose and DF from unripe and ripe papaya after 24 h of fermentation. In this way, the differences between these groups can be assigned.

On the operational taxonomic unit (OUT) heatmap we can clearly see changes on the abundance of microorganism sequences and the DF extracted from both unripe and ripe papaya seems to present a distinct bacterial profile compared to the other groups (**Figure 7A**). At the genus level *Clostridium* and *Bacteroides* were the main difference assigned between the fermentation of DF from (unripe and ripe) papaya compared with the blank at 0 h and lactulose at 24 h (**Figure 7B**). *Bacteroides* may produce acetic acid and propionic acid from carbohydrates [39], and *Clostridium* is usually assigned as a producer of butyrate, specifically the *Clostridium XIVa* sp. [41]. This later specie was not identified in the samples, but a considerable increase in *Clostridium* genus was seen after fermentation of DF from papaya, especially for DF from ripe papaya. Furthermore, *Clostridiaceae 02d06* sp. was found increased in the batch incubated with DF from unripe papaya, and this *Clostridiaceae* is usually regarded as a species that uses DF for fermentation and is an indicator of a healthy microbial balance [43,44].

Interestingly, *Prevotella*, which was diminished after fermentation of lactulose and DF from ripe papaya, was still abundant after fermentation of unripe papaya. *Prevotella* (along with *Bacteroides*) is considered a versatile saccharolytic microorganism, being one of the responsible for polysaccharide digestion in the human large intestine [45]. There are others butyrate producers bacteria including *Lachnospiracea incertae sedis* sp., *Faecalibacterium* sp., and *Butyricicoccus* sp. [41]; however, these bacteria were not enhanced after 24 h of fermentation. It is already known that butyrate is not a major end product of *Bifidobacteria* or *Lactobacilli* as believed before, as it appears that *Clostridium* and *Eubacterium* are the main producers of this SCFA [41,46,47].

Furthermore, *Enterococcus* increase during the fermentation of DF from papaya. *Enterococcus* is a commensal bacterial commonly found in the human intestinal tract that has been related with the production of lactic acid, which can be a precursor of SCFA such as acetate [48,49]. *Bulledia* and *Slackia* only increased after the fermentation of DF from unripe papayas. An enrichment of *Bulledia* was reported for a fecal microbiota of growing pigs fed with extrusion of barley and also with a resistant starch-rich diet [50,51]. As far as we known, it is unknown whether *Slackia* have a role in polysaccharide fermentation, but it has been shown that *Slackia* acts transforming secondary bioactive compounds from plants, such as daidzein from soy and trans-resveratrol from grape vine [52,53].

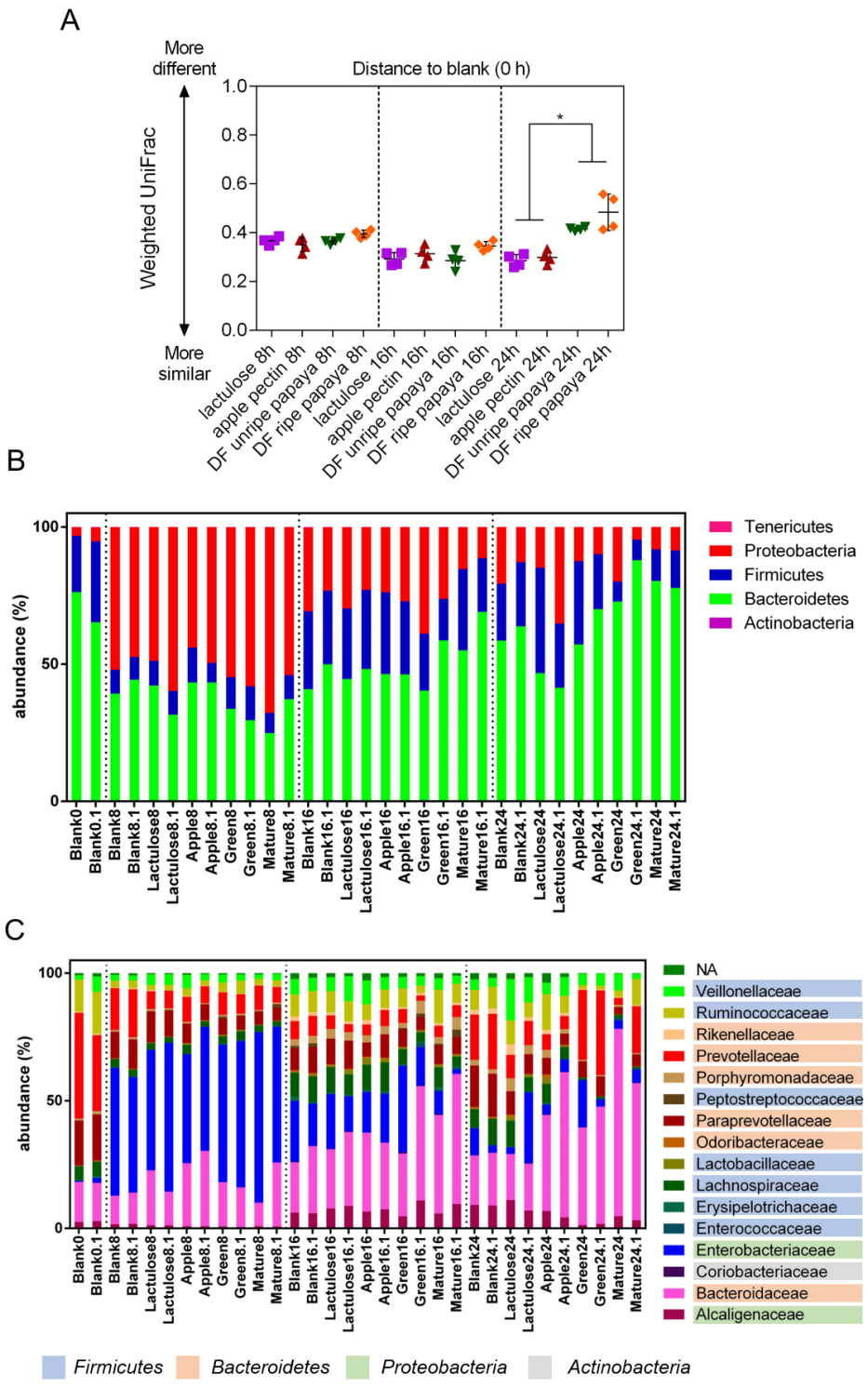

Figure 7. Bacteria profile of different colonic *in vitro* fermentation time points. A) Weighted pairwise UniFrac distances between corresponding to the different carbohydrates used in colonic *in vitro* fermentation. Statistic was calculated: one-way Anova Bonferroni's multiple comparisons test. * $p<0.05$. B) Bacteria percental of abundance at family level.

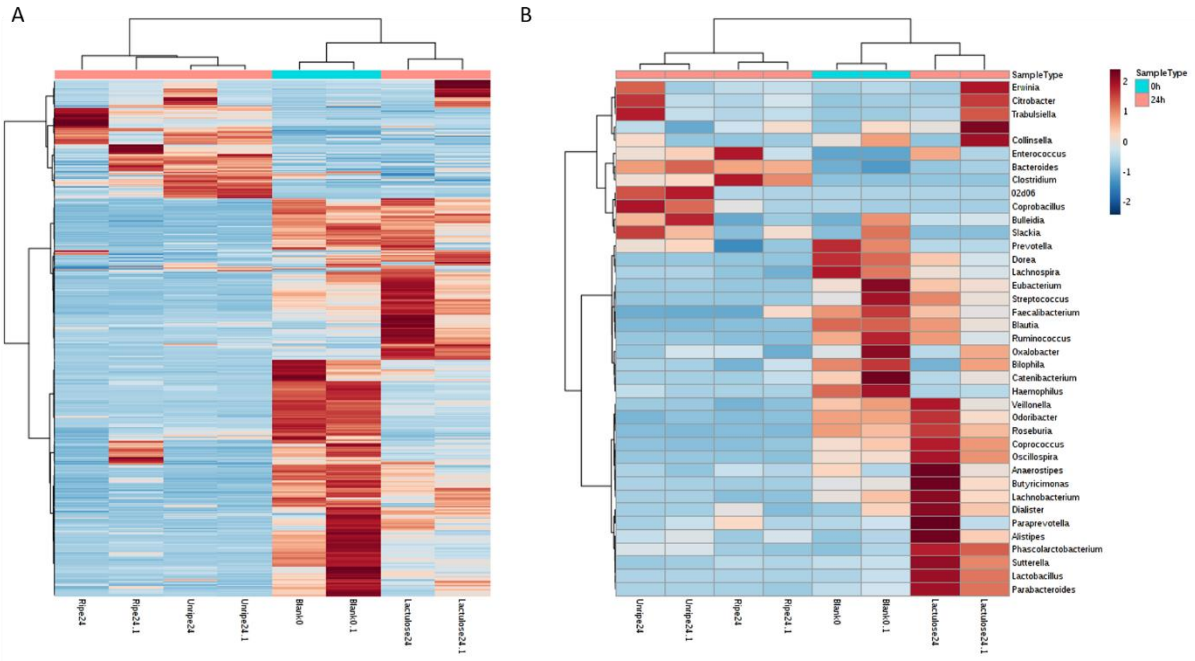

Figure 8. Heatmap of blank 0 h and lactulose, DF from unripe and ripe papayas at 24 h of fermentation. A) OTU heatmap. B) Genus heatmap.

Acetate producing bacteria are *Bifidobacterium* and *Lactobacillus* and also associated with lactulose fermentation [30]. *Lactobacillus* increased for lactulose after 24 h of fermentation; however, no *Bifidobacterium* was found. In another study, no effect on *Lactobacillus* was reported for lactulose fermentation, but for *Bifidobacterium*, *Alistipes*, *Parabacteroides*, *Parasutterella*, and *Anaerostipes* [32]. In our study we also observed after lactulose fermentation an increase in *Alistipes*, *Parabacteroides*, and *Anaerostipes* besides *Lactobacillus*. *Roseburia* was also enhanced for lactulose and it is normally associated with butyrate production, but no pronounced increase in butyrate was observed. This can be explained by a few anaerobes bacteria that can produce not just butyrate but also propionate, such as *Roseburia inulinivorans* and *Coprococcus catus* [5] , thereby explaining why the propionate production was increased and not butyrate.

In summary, besides the similarities between the fermentation profile of lactulose and DF from unripe and ripe papaya, differences in the bacterial profile after fermentation can be easily pointed out. The differences in the structure (and solubility) of DF from unripe and ripe papaya that are dependent of the ripening appears to be the main reasons why the bacteria profile at different time points are different. Even that the increase in SCFA was

seen for DF from both unripe and ripe papaya, the distinct bacterial profile can also influence on the possible health effects.

Conclusions

In this work, the fermentation profile of DF from unripe and ripe papaya were explored in terms of carbohydrate utilization, SCFA production, and effects on the bacterial profile. The DF from ripe papaya seem to be degraded faster than the DF from the unripe papaya, probably by their higher amount of soluble pectin with lower molecular weight of the first. The bacteria profile evaluated by 16s sequencing show similarities as the increase in the abundance of *Clostridium* and *Bacteroides* at genus level. However, DF from unripe papayas appears to induce a specific growth of *Clostridiaceae 02d06*, *Coprabacilus*, *Bulleidia* and *Slackia.* Besides differences on both carbohydrate utilization during fermentation and bacteria profile, the production of SCFA was high after the fermentation of DF from both unripe and ripe papaya compared to other DF, which show that DF from papaya have promising fermentation-related effects.

References

[1] M.M.-L. Grundy, C.H. Edwards, A.R. Mackie, M.J. Gidley, P.J. Butterworth, P.R. Ellis, Re-evaluation of the mechanisms of dietary fibre and implications for macronutrient bioaccessibility, digestion and postprandial metabolism., Br. J. Nutr. 116 (2016) 816–33. doi:10.1017/S0007114516002610.

[2] K. Logan, A.J. Wright, H.D. Goff, Correlating the structure and in vitro digestion viscosities of different pectin fibers to in vivo human satiety, Food Funct. 6 (2015) 62–70. doi:10.1039/C4FO00543K.

[3] F. Fransen, N.M. Sahasrabudhe, M. Elderman, M. Bosveld, S. El Aidy, F. Hugenholtz, T. Borghuis, B. Kousemaker, S. Winkel, C. van der Gaast-de Jongh, M.I. de Jonge, M. V. Boekschoten, H. Smidt, H.A. Schols, P. de Vos, β2→1-Fructans Modulate the Immune System In Vivo in a Microbiota-Dependent and -Independent Fashion, Front. Immunol. 8 (2017). doi:10.3389/fimmu.2017.00154.

[4] H. Zeng, D. Lazarova, M. Bordonaro, Mechanisms linking dietary fiber, gut microbiota and colon cancer prevention, World J. Gastrointest. Oncol. 6 (2014) 41. doi:10.4251/wjgo.v6.i2.41.

[5] P. Louis, G.L. Hold, H.J. Flint, The gut microbiota, bacterial metabolites and colorectal cancer, Nat. Rev. Microbiol. 12 (2014) 661–672. doi:10.1038/nrmicro3344.

[6] K. Willson, C. Situ, Systematic Review on Effects of Diet on Gut Microbiota in Relation to Metabolic Syndromes, J. Clin. Nutr. Metab. 3 (2017) 1–2.

[7] J.M. Laparra, Y. Sanz, Interactions of gut microbiota with functional food components and nutraceuticals, Pharmacol. Res. 61 (2010) 219–225. doi:10.1016/j.phrs.2009.11.001.

[8] U. Kalina, N. Koyama, T. Hosoda, H. Nuernberger, K. Sato, D. Hoelzer, F. Herweck, T. Manigold, M.V. Singer, S. Rossol, U. Böcker, Enhanced production of IL-18 in butyrate-treated intestinal epithelium by stimulation of the proximal promoter region, Eur. J. Immunol. 32 (2002) 2635–2643. doi:10.1002/1521-4141(200209)32:9<2635::AID-IMMU2635>3.0.CO;2-N.

[9] Y. Zhao, F. Chen, W. Wu, M. Sun, A.J. Bilotta, S. Yao, Y. Xiao, X. Huang, T.D. Eaves-Pyles, G. Golovko, Y. Fofanov, W. D'Souza, Q. Zhao, Z. Liu, Y. Cong, GPR43 mediates microbiota metabolite SCFA regulation of antimicrobial peptide expression in intestinal epithelial cells via activation of mTOR and STAT3, Mucosal Immunol. 11 (2018) 752–762. doi:10.1038/mi.2017.118.

[10] S.H. Duncan, G. Holtrop, G.E. Lobley, A.G. Calder, C.S. Stewart, H.J. Flint, Contribution of acetate to butyrate formation by human faecal bacteria, Br. J. Nutr. 91 (2004) 915. doi:10.1079/BJN20041150.

[11] R. Campos-Vega, R. Reynoso-Camacho, G. Pedraza-Aboytes, J. a Acosta-Gallegos, S.H. Guzman-Maldonado, O. Paredes-Lopez, B.D. Oomah, G. Loarca-Piña, Chemical composition and in vitro polysaccharide fermentation of different beans (Phaseolus vulgaris L.)., J. Food Sci. 74 (2009) T59-65. doi:10.1111/j.1750-3841.2009.01292.x.

[12] B.L. Pool-Zobel, G. Jahreis, C. Persin, E. Hartmann, R. Hughes, R. Schubert, M. Glei, G. Beyer-Sehlmeyer, V. Böhm, Butyrate is only one of several growth inhibitors produced during gut flora-mediated fermentation of dietary fibre sources, Br. J. Nutr. 90 (2003) 1057. doi:10.1079/bjn20031003.

[13] H.J. Flint, K.P. Scott, S.H. Duncan, P. Louis, E. Forano, Microbial degradation of complex carbohydrates in the gut, (2012) 289–306.

[14] N.C. Carpita, D.M. Gibeaut, Structural models of primary cell walls in flowering plants: consistency of molecular structure with the physical properties of the walls during growth, Plant J. 3 (1993) 1–30.

[15] D. a. Brummell, Cell wall disassembly in ripening fruit, Funct. Plant Biol. 33 (2006) 103. doi:10.1071/FP05234.

[16] G. Tucker, X. Yin, A. Zhang, M. Wang, Q. Zhu, X. Liu, X. Xie, K. Chen, D. Grierson, Ethylene† and fruit softening, Food Qual. Saf. 1 (2017) 253–267. doi:10.1093/fqsafe/fyx024.

[17] H.V. Scheller, P. Ulvskov, Hemicelluloses, Annu. Rev. Plant Biol. 61 (2010) 263–289. doi:10.1146/annurev-arplant-042809-112315.

[18] E.G. Maxwell, N.J. Belshaw, K.W. Waldron, V.J. Morris, Pectin – An emerging new bioactive food polysaccharide, Trends Food Sci. Technol. 24 (2012) 64–73. doi:10.1016/j.tifs.2011.11.002.

[19] D. Mohnen, Pectin structure and biosynthesis, Curr. Opin. Plant Biol. 11 (2008) 266–277. doi:10.1016/j.pbi.2008.03.006.

[20] J.P. Fabi, B.R. Cordenunsi, G.P. de Ma. Barreto, A.Z. Mercadante, F.M. Lajolo, J.R.O. Do Nascimento, Papaya Fruit Ripening: Response to Ethylene and 1-Methylcyclopropene (1-MCP), J. Food Agric. Food Chem. 55 (2007) 6118–6123.

[21] S.B.R. do Prado, P.R. Melfi, V.C. Castro-Alves, S.G. Broetto, E.S. Araújo, J.R.O. do Nascimento, J.P. Fabi, Physiological Degradation of Pectin in Papaya Cell

Walls: Release of Long Chains Galacturonans Derived from Insoluble Fractions during Postharvest Fruit Ripening, Front. Plant Sci. 7 (2016) 1120. doi:10.3389/fpls.2016.01120.

[22] J.P. Fabi, S.G. Broetto, S.L.G.L. Da Silva, S. Zhong, F.M. Lajolo, J.R.O. Nascimento, Analysis of Papaya Cell Wall-Related Genes during Fruit Ripening Indicates a Central Role of Polygalacturonases during Pulp Softening, PLoS One. 9 (2014) e105685. doi:10.1371/journal.pone.0105685.

[23] S. Prado, G.R. Santos, P. Mourão, J. Fabi, Chelate-soluble pectin fraction from papaya pulp interacts with galectin-3 and inhibits colon cancer cell proliferation, Int. J. Biol. Macromol. 126 (2019) 170–178. doi:10.1016/j.ijbiomac.2018.12.191.

[24] B. a. Williams, M.W. Bosch, H. Boer, M.W. a. Verstegen, S. Tamminga, An in vitro batch culture method to assess potential fermentability of feed ingredients for monogastric diets, Anim. Feed Sci. Technol. 123–124 (2005) 445–462. doi:10.1016/j.anifeedsci.2005.04.031.

[25] M.C. Jonathan, J.J.G.C. van den Borne, P. van Wiechen, C. Souza da Silva, H. a. Schols, H. Gruppen, In vitro fermentation of 12 dietary fibres by faecal inoculum from pigs and humans, Food Chem. 133 (2012) 889–897. doi:10.1016/j.foodchem.2012.01.110.

[26] T.M. Shiga, J.P. Fabi, J.R.O. do Nascimento, C.L.D.O. Petkowicz, L.C. Vriesmann, F.M. Lajolo, B.R. Cordenunsi, Changes in cell wall composition associated to the softening of ripening papaya: evidence of extensive solubilization of large molecular mass galactouronides, J. Agric. Food Chem. 57 (2009) 7064–71. doi:10.1021/jf900073b.

[27] T.M. Shiga, N.C. Carpita, F.M. Lajolo, B.R. Cordenunsi-Lysenko, Two banana cultivars differ in composition of potentially immunomodulatory mannan and arabinogalactan, Carbohydr. Polym. 164 (2017) 31–41. doi:10.1016/j.carbpol.2017.01.079.

[28] S.B.R. do Prado, G.F. Ferreira, Y. Harazono, T.M. Shiga, A. Raz, N.C. Carpita, J.P. Fabi, Ripening-induced chemical modifications of papaya pectin inhibit cancer cell proliferation, Sci. Rep. 7 (2017) 16564. doi:10.1038/s41598-017-16709-3.

[29] P. Delgado-Fernández, N. Corzo, S. Lizasoain, A. Olano, F.J. Moreno, Fermentative properties of starter culture during manufacture of kefir with new prebiotics derived from lactulose, Int. Dairy J. (2019). doi:10.1016/j.idairyj.2019.01.014.

[30] M.K. Bothe, A.J.H. Maathuis, S. Bellmann, J.M.B.M. van der Vossen, D. Berressem, A. Koehler, S. Schwejda-Guettes, B. Gaigg, A. Kuchinka-Koch, J.F. Stover, Dose-dependent prebiotic effect of lactulose in a computer-controlled in vitro model of the human large intestine, Nutrients. 9 (2017). doi:10.3390/nu9070767.

[31] F. van den Berg, S. Nielsen, M. Wiese, H. Sørensen, D.S. Nielsen, B. Khakimov, CoMiniGut—a small volume in vitro colon model for the screening of gut microbial fermentation processes , PeerJ. 6 (2018) e4268. doi:10.7717/peerj.4268.

[32] M. Aguirre, D.M.A.E. Jonkers, F.J. Troost, G. Roeselers, K. Venema, In vitro characterization of the impact of different substrates on metabolite production, energy extraction and composition of gut microbiota from lean and obese subjects, PLoS One. 9 (2014) 1–23. doi:10.1371/journal.pone.0113864.

[33] C. Liu, T. Li, S. Wu, Z. Wang, J. Chen, R. Liang, W. Liu, Pectic-oligosaccharides prepared by dynamic high-pressure microfluidization and their in vitro fermentation properties, Carbohydr. Polym. 91 (2012) 175–182. doi:10.1016/j.carbpol.2012.08.021.

[34] Y. Zaïr, H. Piloquet, E. Pouteau, M. Krempf, V. Ferchaud-Roucher, Colonic fermentation from lactulose inhibits lipolysis in overweight subjects, Am. J. Physiol. Metab. 289 (2005) E716–E720. doi:10.1152/ajpendo.00430.2004.

[35] M.E. Rodríguez-Cabezas, J. Gálvez, M.D. Lorente, A. Concha, D. Camuesco, S. Azzouz, A. Osuna, L. Redondo, A. Zarzuelo, Dietary Fiber Down-Regulates Colonic Tumor Necrosis Factor α and Nitric Oxide Production in Trinitrobenzenesulfonic Acid-Induced Colitic Rats, J. Nutr. 132 (2002) 3263–3271. http://dx.doi.org/10.1093/jn/132.11.3263.

[36] J. Jang, Y. Jung, Y. Kim, E.-H. Jho, Y. Yoon, LPS-induced inflammatory response is suppressed by Wnt inhibitors, Dickkopf-1 and LGK974, Sci. Rep. 7 (2017) 41612. doi:10.1038/srep41612.

[37] S.-J. Bang, G. Kim, M.Y. Lim, E.-J. Song, D.-H. Jung, J.-S. Kum, Y.-D. Nam, C.-S. Park, D.-H. Seo, The influence of in vitro pectin fermentation on the human fecal microbiome, AMB Express. 8 (2018). doi:10.1186/s13568-018-0629-9.

[38] A. Ferreira-Lazarte, V. Kachrimanidou, M. Villamiel, R.A. Rastall, F.J. Moreno, In vitro fermentation properties of pectins and enzymatic-modified pectins obtained from different renewable bioresources, Carbohydr. Polym. 199 (2018) 482–491. doi:10.1016/j.carbpol.2018.07.041.

[39] B. Gómez, B. Gullón, R. Yáñez, H. Schols, J.L. Alonso, Prebiotic potential of pectins and pectic oligosaccharides derived from lemon peel wastes and sugar beet pulp: A comparative evaluation, J. Funct. Foods. 20 (2016) 108–121. doi:10.1016/j.jff.2015.10.029.

[40] F. Gu, K. Borewicz, B. Richter, P.H. van der Zaal, H. Smidt, P.L. Buwalda, H.A. Schols, In Vitro Fermentation Behavior of Isomalto/Malto-Polysaccharides Using Human Fecal Inoculum Indicates Prebiotic Potential, Mol. Nutr. Food Res. 62 (2018). doi:10.1002/mnfr.201800232.

[41] U.S. Ramasamy, K. Venema, H.A. Schols, H. Gruppen, Effect of Soluble and Insoluble Fibers within the in Vitro Fermentation of Chicory Root Pulp by Human Gut Bacteria, J. Agric. Food Chem. (2014).

[42] J.S. Moon, S.Y. Shin, H.S. Choi, W. Joo, S.K. Cho, L. Li, J.H. Kang, T.J. Kim, N.S. Han, In vitro digestion and fermentation properties of linear sugar-beet arabinan and its oligosaccharides, Carbohydr. Polym. 131 (2015) 50–56. doi:10.1016/j.carbpol.2015.05.022.

[43] M.A. Azcarate-Peril, S. Amzazi, A. Astudillo, P.I. Marron, I. Allali, S. Delgado, J.J. Yeh, T. Keku, H. Ghazal, Gut microbiome compositional and functional differences between tumor and non-tumor adjacent tissues from cohorts from the US and Spain, Gut Microbes. 6 (2015) 161–172. doi:10.1080/19490976.2015.1039223.

[44] L. Chatellard, E. Trably, H. Carrère, The type of carbohydrates specifically selects microbial community structures and fermentation patterns, Bioresour. Technol. 221 (2016) 541–549. doi:10.1016/j.biortech.2016.09.084.

[45] N. Salazar, P. Ruas-Madiedo, S. Kolida, M. Collins, R. Rastall, G. Gibson, C.G. de los Reyes-Gavilán, Exopolysaccharides produced by Bifidobacterium longum IPLA E44 and Bifidobacterium animalis subsp. lactis IPLA R1 modify the composition and metabolic activity of human faecal microbiota in pH-controlled batch cultures, Int. J. Food Microbiol. 135 (2009) 260–267. doi:10.1016/j.ijfoodmicro.2009.08.017.

[46] S.E. Pryde, S.H. Duncan, G.L. Hold, C.S. Stewart, H.J. Flint, The microbiology of butyrate formation in the human colon, FEMS Microbiol Lett. 217 (2002). doi:10.1111/j.1574-6968.2002.tb11467.x.

[47] M. Rajilić-Stojanović, W.M. de Vos, The first 1000 cultured species of the human gastrointestinal microbiota, FEMS Microbiol. Rev. 38 (2014) 996–1047.

doi:10.1111/1574-6976.12075.

[48] S.H. Duncan, P. Louis, H.J. Flint, Lactate-Utilizing Bacteria , Isolated from Human Feces , That Produce, Appl. Environ. Microbiol. 70 (2004) 5810–5817. doi:10.1128/AEM.70.10.5810.

[49] S. Macfarlane, G.T. Macfarlane, Regulation of short-chain fatty acid production, Proc. Nutr. Soc. 62 (2003) 67–72. doi:10.1079/pns2002207.

[50] B. Moen, I. Berget, I. Rud, A.S. Hole, N.P. Kjos, S. Sahlstrøm, Extrusion of barley and oat influence the fecal microbiota and SCFA profile of growing pigs, Food Funct. 7 (2016) 1024–1032. doi:10.1039/c5fo01452b.

[51] Ö.C.O. Umu, J.A. Frank, J.U. Fangel, M. Oostindjer, C.S. Da Silva, E.J. Bolhuis, G. Bosch, W.G.T. Willats, P.B. Pope, D.B. Diep, Resistant starch diet induces change in the swine microbiome and a predominance of beneficial bacterial populations, Microbiome. 3 (2015) 1–15. doi:10.1186/s40168-015-0078-5.

[52] L.M. Bode, B. Diana, H. Melanie, C. Gyu-Sung, R. Denise, B. Mirko, B. Achim, C.M.A.P. Franz, S.E. Kulling, In vivo and in vitro metabolism of trans-resveratrol by human gut microbiota., Am. J. Clin. Nutr. 97 (2013) 295–309. doi:10.3945/ajcn.112.049379.INTRODUCTION.

[53] C. Schröder, A. Matthies, W. Engst, M. Blaut, A. Braune, Identification and expression of genes involved in the conversion of daidzein and genistein by the equol-forming bacterium slackia isoflavoniconvertens, Appl. Environ. Microbiol. 79 (2013) 3494–3502. doi:10.1128/AEM.03693-12.

Supplementary files

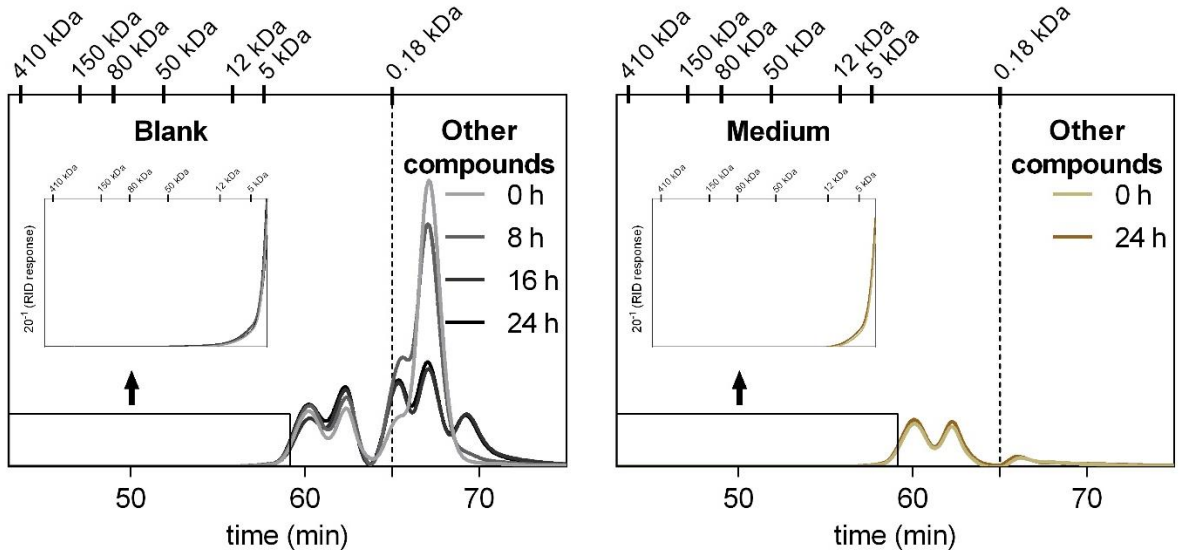

Figure S1. HPSEC from colonic in vitro fermentation: blank and medium treatments.

Chapter 8

Structure-dependent chemopreventive effects of dietary fiber from papaya in rats with colon pre-neoplastic lesions

Samira Bernardino Ramos do Prado[1,3], Rodrigo Invernort[1], Renato Heidor[1], Fernando Salvador Moreno[1], João Paulo Fabi[1,2,3]

[1]Department of Food Science and Experimental Nutrition, School of Pharmaceutical Sciences, University of São Paulo, São Paulo, SP, Brazil
[2]Food and Nutrition Research Center (NAPAN), University of São Paulo, São Paulo, SP, Brazil.
[3]Food Research Center (FoRC), CEPID-FAPESP (Research, Innovation and Dissemination Centers, São Paulo Research Foundation), São Paulo, SP, Brazil.

Abstract

The consumption of dietary fibers (DF) is for a long time related to beneficial intestinal health habits and with decreasing the risk of colon cancer development. However, DF have a very complex and heterogenous group of molecules, which can differently impact on the decrease in the risk of colon cancer. The naturally modified pectin from papaya fruit has been shown fermentation-related effects and direct effects on colon cancer that are structure-dependent, but until now the *in vivo* results regarding the consumption of DF from papaya is unknown. This study aims to evaluate whether DF from unripe and ripe papaya differently affect the colon lesions development in rats. Chemically-induced animals fed with the DF from ripe papaya showed a significantly decrease in aberrant crypt foci (ACF) formation in the intestine, specially ACF with less than 4 foci. Besides that, the location of ACF inhibition seem to be closer to the proximal colon part than to the distal part. The DF from ripe papayas probably had a different fermentation pattern than the DF from unripe papayas, resulting in distinct interaction with the intestinal cells and microbiota profile. Therefore, the structural differences of DF from papayas – depending on the fruit ripening stage – changes their biological effects, and the ripe DF seem to be more effective as a chemopreventive agent.

Key-words: aberrant crypt foci; azoxymethane; cell wall; colon cancer, dietary fiber; papaya.

Abbreviations: AOM, azoxymethane; ACF, aberrant crypt foci; CRC, colorectal cancer; DF, dietary fibers; DMH, 1,2-dimethylhydrazine; GalA, galacturonic acid; HG, homogalacturonan; IEC, intestinal epithelial cells; Rha, rhamnogalacturonan; SD, standard deviation; TUNEL (Terminal deoxynucleotidyl transferase (TdT) mediated dUTP Nick End Labeling).

Introduction

The consumption of dietary fiber (DF) from plant sources are related to decrease in the incidence of colorectal cancer (CRC) development [1–4]. DF are comprised mainly by carbohydrates that are not hydrolyzed by the gastrointestinal enzymes, but some intestinal bacteria produce the enzymes that can cleave the glycosidic linkages of DF [5]. As result of the fermentation of the DF in the gut, some metabolites are produced including the short chain fatty acids (SCFA) that are associated with the decrease of intestinal pH, as well as with healthy effects such as being energy source for the intestinal epithelial cells (IEC) and promoting benefits that includes the maintenance of the intestinal epithelial barrier integrity [6,7].

The DF from fruits consist mainly of cell wall components including cellulose, hemicellulose, and pectin [8]. Papaya (*C. papaya* L. cv. 'Golden') is a fleshy fruit that usually have a massive pulp softening in just a few days after harvest. The texture of papaya fruit pulp appears to be determined mainly by its cell wall structure, which quickly changes in terms of structure during the ripening. The main fraction of the papaya cell wall that changes after harvest appears to be the pectic fraction, because polygalacturonases and galactanases are the main enzymes that act hydrolyzing the cell wall during papaya ripening [9,10]. Pectin is a complex polysaccharide composed mainly by linear α-(1,4)-linked galacturonic acid (GalA) residues (homogalacturonan, HG) with varying degree of methyl and acetyl esterification [11]. The pectic fraction also consists of branched structures named type I rhamnogalacturonan (RGI), that is the second major pectic fraction of papaya fruit and consists of a backbone of alternate α-(1,4)-GalA and α-(1,2)-rhamnose (Rha) residues [12]. During papaya ripening, polygalacturonases hydrolyze mainly the less soluble pectic fraction, which contains a higher degree of esterification to that of water-soluble pectin. This increase in the activity of polygalacturonases during ripening results in an increased amount of more soluble and more esterified pectin in ripe papaya [10,13,14]. These changes in the DF structure can influence the biological effects of DF and are being pointed out as essential to determine fermentation-related effects that are associated to a decrease risk of colon cancer [15–18].

Among the animal models of chemically induced colorectal cancer models, 1,2 dimethylhydrazine (DMH) and azoxymethane (AOM) are the carcinogens most frequently

used [19]. DMH is an AOM metabolite and both are widely used agents for the induction of colorectal carcinogenesis in rodents [20], which depending on the experimental design can be used to evaluate cancer initiation, promotion and/or metastasis [21]. DMH/AOM-induced colon carcinogenesis may thus be inhibited or enhanced by substances that are administered during the initiation stage. The chemopreventive treatment can begin before exposure to the carcinogen and during the initiation phase, the promotion phase, or through both phases [20]. Aberrant crypt foci (ACF) formation is an early preneoplastic marker of colon tumorigenesis in rats particularly at the promotion stage [22].

The DF from papaya is naturally modified during fruit ripening and different fermentation-related effects and durect effects in colon cancer cells has been related to these structures [13,14]; However, it is unknown whether these DF from unripe and ripe papaya induces *in vivo* effects. In the present study, we incorporate DF from unripe or ripe papaya in the diet of rats and then chemically induce these animals with AOM to develop ACF. In this way, the measurement of the ACF development in animals receiving different diets could indicate a protective effect regarding the inhibition of pre-neoplastic lesions by these diets. Furthermore, as the DF are a food component that should be constantly present in a diet, we continue to incorporate DF from unripe or ripe papaya in the animals diet at both the initiation and the promotion phase after induction with AOM.

Material and methods

Papayas sampling and characterization

Approximately 150 papaya fruits harvested in Bahia (Brazil) were acquired in a commercial fruit market in São Paulo (Brazil), and the ripening were monitored through analysis of internal pulp firmness and peel color according to Fabi et al. (2007) [23]. In addition to the internal pulp firmness, the measurement of the external (whole) pulp was assessed by compression of the fruit with a cylindric probe (4 cm diameter) and analysis using a TA XTplus Texture analyzer (Stable Microsystems). This latter method was used to measure the whole papaya firmness without causing any bruise in the fruit. In this way, we aimed to correlate the external (whole) papaya firmness with the internal (pulp) firmness – this latter is measured on fruit pulp slices. After defining a correlation between the internal pulp firmness and the external fruit firmness it was possible classify the fruits as “unripe”

or “not unripe” without slice the fruits. The fruits classified as “unripe” after measurement of the external fruit firmness were sliced, immediately freeze in liquid nitrogen, and storage in a freezer to further extraction of DF from unripe papaya. Fruits that were determined as “not unripe” were allowed to ripe in a room with controlled temperature (22 ± 0.5 ºC) until they were fully ripe. These ripe fruits were sliced, immediately freeze in liquid nitrogen, and storage in a freezer to further extraction of DF from ripe papaya.

Dietary fiber extraction

Unripe and ripe papaya pulp were freeze-dried and then grinded on a M 20 Universall mill (IKA-Werke GmbH). The powder was further incubated with methanol:chloroform (1:1 v/v) under reflux for 2 h at 70 °C to extract lipids, inactivate enzymes and remove pigments. The solid residue was then washed with 80% boiling ethanol for 1 h under reflux twice for monosaccharide removal and were also washed with three volumes of acetone for drying purposes. Finally, the residue was dried at ambient temperature, resulting in the total cell wall (DF) from papaya.

***In vivo* experiment**

The experiment was done after the approval of the Ethics Committee for Animal Research of the School of Pharmaceutical Sciences at the University of São Paulo (protocol #543). Males Wistar rats with six weeks and weighing 60–80 g were obtained from the colony of the Biomedical Institute at the University of São Paulo. The animals were maintained inside cages containing 4 animals each at a controlled temperature of 22.0 ± 0.5 °C with 12 h light–dark cycle and receiving water and standard commercial AIN-93G diet *ad libitum*. After 1 week of acclimatization, two groups of animals had the dietary fiber of the AIN-93G totally substituted by the DF from unripe or ripe papaya. Four groups were used in the study: Rats not treated with AOM and feed with standard AIN-93G diet (negative control; n = 4), AOM-induced rats feed with standard AIN-93G (AOM control; n =8), and AOM-induced rats feed with AIN-93G but with the DF substituted by DF from unripe or ripe papaya (unripe papaya DF group and ripe papaya DF group; each group with n = 8). Therefore, except for the negative control, all rats received two doses of azoxymethane (AOM; 15 mg/kg body weight; **Figure 1**) on the second week after receiving the diet [24]. After 11 weeks of the first AOM treatment (13 weeks after receiving the diet)

the animals were euthanized and the colon portion – after cecum until the most distal colon part – was resected and washed with sterilized saline solution. The feces and the cecal content were collected and immediately frozen in liquid N_2 and stored at −80 °C. The intestine was longitudinal divided, and half part was immersed in 70% ethanol at 4 ºC. The other half part of the intestine had the mucosa scraped, which was immediately frozen in liquid N_2 and stored at −80 °C.

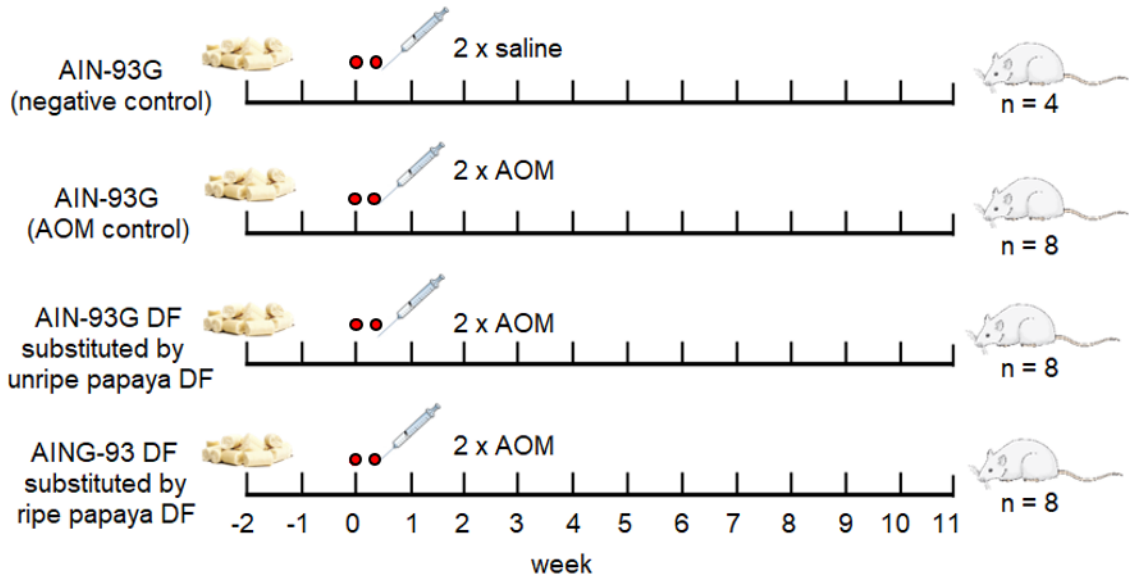

Figure 1. Experimental design of the study.

Aberrant crypt foci (ACF)

The hemicolon segments fixed in 70% ethanol were stained for 5 min with 0.02% methylene blue in phosphate-buffered saline (PBS; 2.7 mM KCl, 8.1 mM Na_2PO_4, 1.5 mM KH_2PO_4, 0.14 M NaCl, pH 7.6). The ACF were analyzed as previously described [25,26] with an inverted microscope (Axiovert 40C, Carl Zeiss Microscopy GmbH, Jena, Germany) at 40× magnification. The total number of ACF and ACF multiplicity in each focus (number of crypts/ACF) was recorded. Data were expressed as ACF/hemicolon segment area (ACF/cm^2).

Statistical analysis

The results were expressed as the mean ± standard deviation (SD). Parametric distribution of data was tested using Shapiro-Wilk normality test. Data were analyzed using GraphPad Prism 6.0 software (GraphPad Software, San Diego, CA). One-way ANOVA with Tukey's (to assess differences between all groups) or Dunnett's or Dunn's multiple comparisons test (to assess differences between the control and two or more groups) were used as post hoc tests. Student's t-test was applied to analyze the differences between two groups. Significance was set at $p < 0.001$***, $p < 0.01$** and $p < 0.05$*.

Results and Discussion

Our group has been intensely studying the structure of DF from unripe and ripe papayas, and one of the challenges regarding this matter is the obtention was how we could obtain the DF from of the unripe papaya, since the fruit ripening occurs very fast. Papaya is harvest unripe (~ ¼ yellow color in the peel) and after 1-2 days the fruit starts the softening process of the pulp from inside to outside because of the increased ethylene production [23], it is unfeasible to go to the field and harvest more than 140 fruits for a study since papaya in Brazil is normally cultivated in the state of Bahia and Espírito Santo – which is at least at 800 km of distance from the laboratory. Therefore, we decided to acquire fruits in São Paulo market where they were used to receive papaya with 1-2 days after harvest after and it was transported refrigerated (~ 15 ^{o}C). The analysis of pulp texture is a destructive method in which the fruit is cut in a half and using a texturometer with a determined probe, it is possible to measure the internal pulp firmness. Since de quantity of papayas were higher than we were used to work in the *in vitro* experiments, we needed a methodology that indicated the ripening without being destructive. Therefore, we decided to determine whether the measurement of the external papaya firmness by pressuring the fruit with a specific larger probe could be correlated to the internal pulp texture thus indicating the onset of ripening. For the unripe papayas, the external firmness above to 40 N was correspondent to the papayas with internal firmness around 20 N, a firmness represented by the "crisp" appearance of the pulp, and thus showing no or little influence by the pectinases. For the ripe papayas, the external firmness between to 30 and 10 N were correspondent to the papayas with internal firmness below 10 N, a firmness represented by

the ideal consumption, since the pulp could be eaten by a spoon but not soften. These values were established as the cut-off for this study (**Figure 2A**). The values of internal texture achieved were in accordance with the literature [9,10,23]. Therefore, with the cut-off determined, the papayas were acquired in batches of a maximum of 25 fruits/day as soon as the market received the stock. For each papaya fruit acquired it was determined the external texture and defined whether the papaya was classified as unripe or whether the papaya was classified as not unripe. Unripe papayas were sliced, and then frozen, and the not unripe papaya were left to ripe until the appropriate cut-off of the external texture for a ripe fruit (**Figure 2B**). At least 25% of the fruits had also their internal firmness measured after slicing, confirming the correlation between the external and internal texture previously determined (not shown). At total, 74 fruits classified as unripe and 74 fruits classified as fully ripe were obtained and used DF extraction. Unripe papayas had 47 kg at total, being 35 kg of pulp, whereas ripe papaya had 41 kg, being 32 kg of pulp. The hue color was also measured (**Figure 2C**). The papayas peels were greener at unripe fruits as expected, and for the riper fruit the peel were more heterogenous, with parts of the fruit varying from yellow to orange color. Besides that, the water-soluble fraction extracted from the DF of unripe papaya showed a yield of 17%, whereas the ripe papaya had a yield of 30%. These results were in agreement with analysis of the water-soluble fraction yield for unripe and ripe papaya obtained from previous studies [13,14,27], thereby confirming that the fruits were appropriately selected according to their ripening stage.

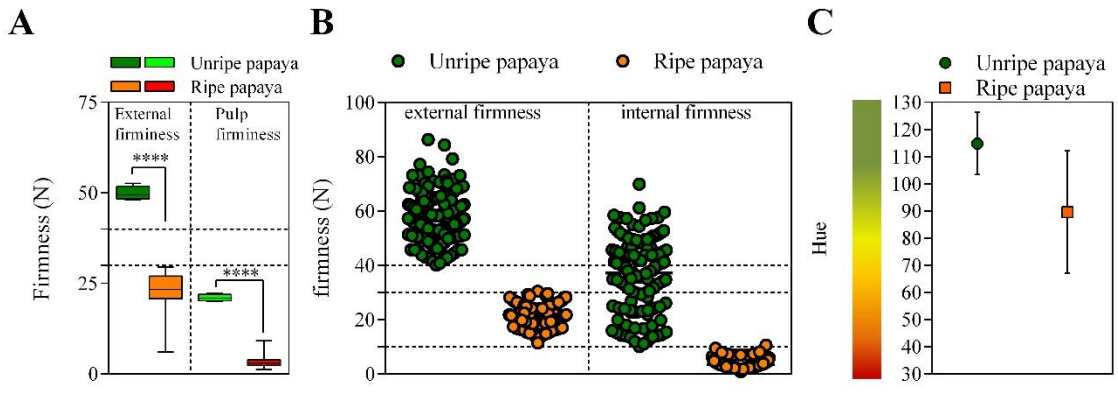

Figure 2. Characterization of papaya ripening. (A) Cut-off definition of external firmness related to unripe and ripe papaya (defined by internal firmness values; n = 29 papayas). (B) External and internal firmness of papaya used as source for DF extraction in the present study. Cut-off definition: external firmness for unripe papaya ≥ 40 N; external

firmness for ripe papaya ≤ 30 N ≥ 10 N. (C) Hue color of papaya used as source for DF extraction in the present study (at least 105 and 187 measurements were performed in unripe and ripe papaya). **** p value < 0.0001 according Student's t-test.

After defining the ripening stage and the papayas sampling, the DF extracted from unripe and ripe papaya and were incorporated to the AIN-93G standard chow by substituting the amount of standard DF (5% w/w of the chow) for DF from unripe or ripe papaya fruit. After two weeks of the maintenance of the standard diet (negative and AOM group) or substitution of the DF by DF from unripe or ripe papaya, the animals were treated with two injection of intraperitonially saline (control) or AOM (15 mg/kg body weight) in a 3-day interval (**Figure 1**). All animals started with an initial weight of 76.69 ± 6.74 g and reach in the final of experiment with a final weight of 365.94 ± 30.22 g (**Figure 3A**). The differences between the initial and final weight among groups were not significantly.

After the second week that the rats were already receiving the chow with or without DF from papaya (weeks –2 and –1), they receive two dosages of saline solution or AOM solution. The rats that received AOM solution tended to maintain or lose weight between the first and second dose, but after three days of the injection they return to increase the weight. The negative control group that only received injection of saline solution had the tendency of gain more weight throughout the experiment compared to the groups that were treated with AOM, because they do not have an impact of receive a carcinogen. Besides that, on the second week, the animals that received AOM solution consumed less chow than the control group and consequently are less prone to gain weight (**Figure 3B**). However, considering the whole experiment duration, the average chow consumption per kg of each animal had no significant difference between the groups. Therefore, the animals weight gain and chow consumption, did not differ between the groups.

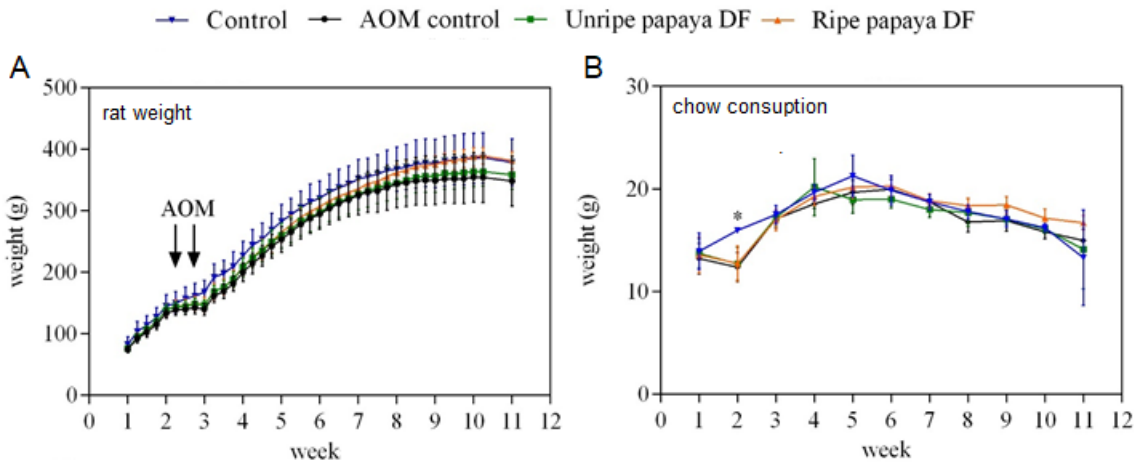

Figure 3. Rat weight and chow weight during the experiment. (A) Rats weight. (B) Avarege chow weight calculated per rat. Data were shown as mean ± SD. *p < 0.05 according to Dunnett's test (all groups compared with the control).

The rat colon was analyzed regarding the ACF quantity, the most proximal part analyzed was the part of the colon next to the cecum, whereas the most distal part of the colon analyzed was the one closer to the rectum. There were significant differences between the total percentage of ACF found in the group that received DF from ripe papaya compared with the AOM control group (**Figure 4A**). The main differences observed was in the more proximal part of the colon and not in the more distal part. Besides that, when we segregated the ACF by their number of foci, we can observe a significant difference for the total ACF counting with less than 4 focus. This difference seems to be mostly associated with the proximal colon part (**Figure 4B**).

In another studies using *in vivo* models with AOM or DMH [20] – different effects regarding DF are seen. Galacto-oligosaccharides had a protective effect against the development of colorectal tumors in rats using AOM model [15]. Slowly fermentable fibers such as wheat bran and oat bran were more protective than rapidly fermentable fibers such as fructooligosaccharides in AOM rat model in reducing the formation of colon tumors [17]. Rats fed with DF source from pectin do not showed a decreased ACF formation [31]; however the pectin source and characterization was not provided, being difficult to establish an structural-dependent effect. Apple pectin reduced the occurrence of colon cancer induced by AOM or DMH [32,33]. Dietary long-chain inulin suppresses AOM-induced ACF formation [34] and even comparing the short-chain inulin with long-chain

inulin, the last showed better effects in inhibits AOM formation [35]. DF from cooked common beans (*P. vulgaris* L., cv Negro 8025) inhibited colon carcinogenesis at an early stage by inducing cell cycle arrest [36,37]. DF of barley reduced the incidence the AOM-induced aberrant crypt foci development [38]. In AOM treated A/J Min/$^{+}$ mice fed with inulin, cellulose or brewers spent grain showed that the type of DF may play a pivotal role in the development of CRC, since just inulin suppressed colonic tumorigenesis [39]. Thus, specific DF structure should be studied in order to establish the specific effects of each DF, especially pectins, since their results in the literature can be very contradictories – probably because of their different structures that is not always characterized.

According to our data, one could speculate that the ripe DF were more active in inhibiting the ACF formation and/or propagation mostly in the proximal part of the intestine. This could be due to the higher quantities of soluble fibers the ripe DF have, since the ripening process transform insoluble to water-soluble pectin, as it has already stated before [10,13,28]. Besides that, the high and low-esterified pectin have different patterns of fermentation in the cecum – being the high-methyl esterified pectin fermented less efficiently than the low-methyl esterified pectin [29,30]. Recently it was shown that rats feed with a high-methyl esterified pectin diet made others DF including arabinoxylans and cellulose shifted the location of fermentation from the cecum to the colon, and this shift not happens when rats were feed with a low-methyl esterified pectin diet [29]. These results from the literature showed differences in pectin structures that affects the fermentation pattern, reinforcing that the papaya pectin modifications during the ripening can affect the pectin structure and the consequent biological effect. Therefore, the biological activity of the ripe DF in the proximal colon could be answered by raising two hypotheses. The first would be the direct effects of the soluble pectins, in which they could interact with IEC, such as activating some toll-like receptors and even inhibiting the galectin-3, thus decreasing the formation and/or propagation of ACF. The other one would be the fermentation process that occurred in a better way in the ripe DF, since there are more soluble DF, and thus facilitating the microbiota fermentation and SCFA production, such as butyrate which has an established anti-cancer effect. The biological samples (feces and cecum content and scrapped mucosa) are stocked in -80 ^{o}C and the paraffined colon sections are stored in order to further studies be done to establish whether these suppositions can be confirmed. The next steps could include molecular biology studies of

scrapped mucosa, histological studies of the colon sections, the microbiota composition of the feces and cecum content besides their DF colonic composition.

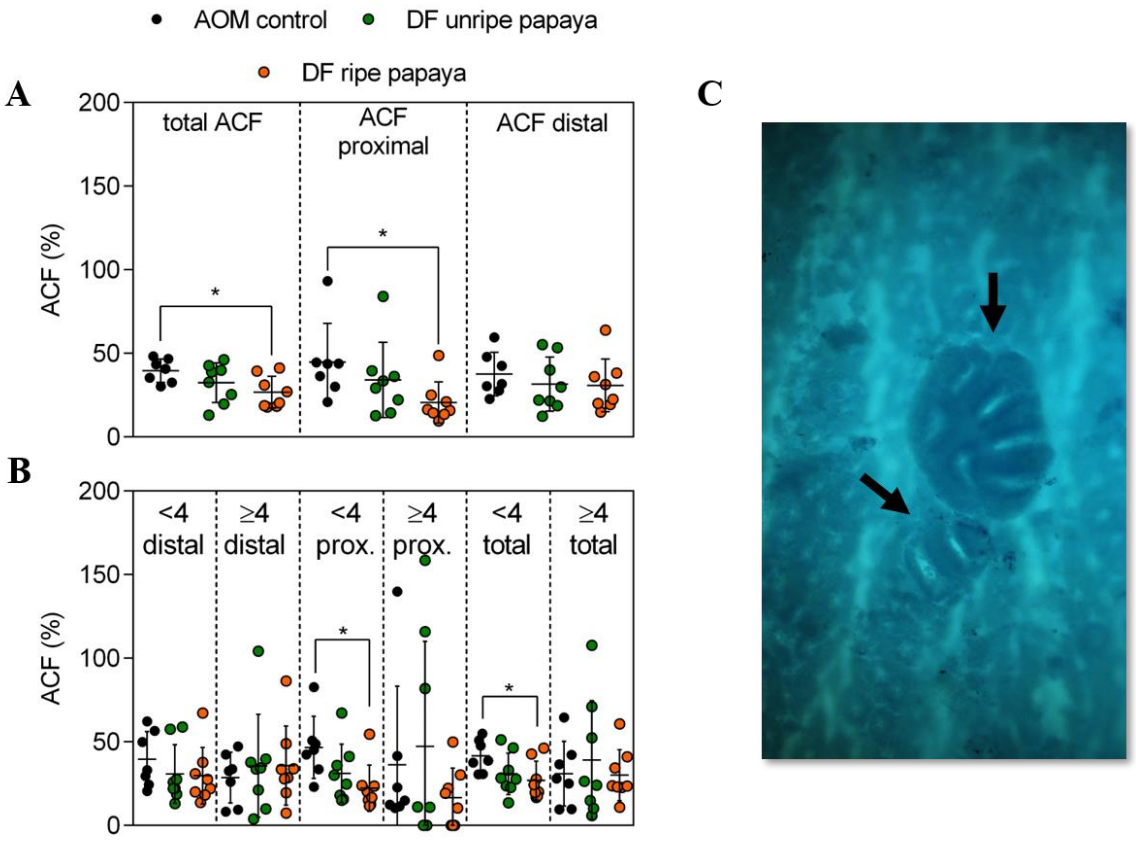

Figure 4. Aberrant crypt foci percentages and representative image. A) Total ACF percentage into more distal or more proximal part of the colon. B) Percentage of ACF with higher or lesser than 4 focus into more distal or more proximal part of the colon. C) Representative of ACF image. The first black arrow indicates an ACF with six focus and the second arrow indicates an ACF with two focus. Data were shown as mean ± SD. Dunn's test, *$p < 0.05$. ACF: aberrant crypt foci.

Conclusions

The papayas ripening challenges regarding the sampling of the unripe papayas were well resolved. We could obtain enough papayas to extract their DF from unripe and ripe fruits and insert theses DF in rats chow. The difference into the animal's diet was just in the DF structure, while all groups received 5% of DF, composed by cellulose (from AIN-

93G), or DF from unripe papaya or DF from ripe papaya. The rats were chemically induced by AOM to develop ACF lesions and the rats fed with ripe papaya DF showed an inhibition of ACF mainly in more proximal colon part. The main change in papayas DF structure is on the pectin structure, since during the ripening the polygalacturonases enzymes are strongly acting and degrading the fruit cell wall [9,10]. The ripe papaya DF may present best results because of the higher quantities of soluble fibers, especially pectins, that could directly act in IEC or be highly fermented by the intestinal microbiota thus producing butyrate. More studies regarding the cecum and colon carbohydrates composition could elucidate whether the utilization of the DF is really happening as hypothesized in this study, together with some molecular biology studies and with the SCFA production and the microbiota composition.

References

[1] R.A. Torres Stone, M.E. Waring, S.L. Cutrona, C.I. Kiefe, J. Allison, C.A. Doubeni, The association of dietary quality with colorectal cancer among normal weight, overweight and obese men and women: A prospective longitudinal study in the USA, BMJ. 7 (2017) 1–11. doi:10.1136/bmjopen-2016-015619.

[2] K.E. Bradbury, P.N. Appleby, T.J. Key, Fruit, vegetable, and fiber intake in relation to cancer risk: findings from the European Prospective Investigation into Cancer and Nutrition (EPIC), Am. J. Clin. Nutr. 100 (2014) 394S–398S. doi:10.3945/ajcn.113.071357.394S.

[3] M. Leenders, P.D. Siersema, K. Overvad, A. Tjønneland, A. Olsen, M.C. Boutron-Ruault, N. Bastide, G. Fagherazzi, V. Katzke, T. Kühn, H. Boeing, K. Aleksandrova, A. Trichopoulou, P. Lagiou, E. Klinaki, G. Masala, S. Grioni, M. Santucci De Magistris, R. Tumino, F. Ricceri, P.H.M. Peeters, E. Lund, G. Skeie, E. Weiderpass, J.R. Quirõs, A. Agudo, M.J. Sánchez, M. Dorronsoro, C. Navarro, E. Ardanaz, B. Ohlsson, K. Jirström, B. Van Guelpen, M. Wennberg, K.T. Khaw, N. Wareham, T.J. Key, I. Romieu, I. Huybrechts, A.J. Cross, N. Murphy, E. Riboli, H. Bueno-De-Mesquita, Subtypes of fruit and vegetables, variety in consumption and risk of colon and rectal cancer in the European Prospective Investigation into Cancer and Nutrition, Int. J. Cancer. 137 (2015) 2705–2714. doi:10.1002/ijc.29640.

[4] F. Turati, M. Rossi, C. Pelucchi, F. Levi, C. La Vecchia, Fruit and vegetables and cancer risk: A review of southern European studies, Br. J. Nutr. 113 (2015) S102–S110. doi:10.1017/S0007114515000148.

[5] H.J. Flint, K.P. Scott, S.H. Duncan, P. Louis, E. Forano, Microbial degradation of complex carbohydrates in the gut, (2012) 289–306.

[6] P. Louis, G.L. Hold, H.J. Flint, The gut microbiota, bacterial metabolites and colorectal cancer, Nat. Rev. Microbiol. 12 (2014) 661–672. doi:10.1038/nrmicro3344.

[7] K. Willson, C. Situ, Systematic Review on Effects of Diet on Gut Microbiota in Relation to Metabolic Syndromes, J. Clin. Nutr. Metab. 3 (2017) 1–2.

[8] N.C. Carpita, D.M. Gibeaut, Structural models of primary cell walls in flowering plants: consistency of molecular structure with the physical properties of the walls during growth, Plant J. 3 (1993) 1–30.

[9] J.P. Fabi, S.G. Broetto, S.L.G.L. Da Silva, S. Zhong, F.M. Lajolo, J.R.O.

Nascimento, Analysis of Papaya Cell Wall-Related Genes during Fruit Ripening Indicates a Central Role of Polygalacturonases during Pulp Softening, PLoS One. 9 (2014) e105685. doi:10.1371/journal.pone.0105685.

[10] S.B.R. do Prado, P.R. Melfi, V.C. Castro-Alves, S.G. Broetto, E.S. Araújo, J.R.O. do Nascimento, J.P. Fabi, Physiological Degradation of Pectin in Papaya Cell Walls: Release of Long Chains Galacturonans Derived from Insoluble Fractions during Postharvest Fruit Ripening, Front. Plant Sci. 7 (2016) 1120. doi:10.3389/fpls.2016.01120.

[11] D. Mohnen, Pectin structure and biosynthesis, Curr. Opin. Plant Biol. 11 (2008) 266–277. doi:10.1016/j.pbi.2008.03.006.

[12] J.-P. Ele-Ekouna, C. Pau Roblot, B. Courtois, J. Courtois, Chemical characterization of pectin from green tea (Camellia sinensis), 2011. doi:10.1016/j.carbpol.2010.09.028.

[13] S.B.R. do Prado, G.F. Ferreira, Y. Harazono, T.M. Shiga, A. Raz, N.C. Carpita, J.P. Fabi, Ripening-induced chemical modifications of papaya pectin inhibit cancer cell proliferation, Sci. Rep. 7 (2017) 16564. doi:10.1038/s41598-017-16709-3.

[14] S. Prado, G.R. Santos, P. Mourão, J. Fabi, Chelate-soluble pectin fraction from papaya pulp interacts with galectin-3 and inhibits colon cancer cell proliferation, Int. J. Biol. Macromol. 126 (2019) 170–178. doi:10.1016/j.ijbiomac.2018.12.191.

[15] M.V.W. Wijnands, H.C. Schoterman, J.P. Bruijntjes, V.M.H. Hollanders, R.A. Woutersen, Effect of dietary galacto-oligosaccharides on azoxymethane- induced aberrant crypt foci and colorectal cancer in Fischer 344 rats and their colon was removed for scoring ACF . Half of the diet (L / HGOS) and half of those in the HGOS group to an, Carcinogenesis. 22 (2001) 127–132.

[16] L. Tian, G. Bruggeman, K. Borewicz, A.J.W. Scheurink, E. Bruininx, P. De Vos, H. Smidt, H.A. Schols, H. Gruppen, Effects of pectin on fermentation characteristics, carbohydrate utilization, and microbial community composition in the gastrointestinal tract of weaning pigs, Mol. Nutr. Food Res. 61 (2016) 1–10. doi:10.1002/mnfr.201600186.

[17] J. Raju, J. Roberts, Q. Chen, S.A. Aziz, D. Caldwell, R.P. Bird, K.A. Scoggan, S.P.J. Brooks, Fermentable Carbohydrates Differentially Affect Colon Tumor Formation in Azoxymethane-Induced Male Fischer 344 Rats, J. Nutr. 146 (2016) 737–744. doi:10.3945/jn.115.214833.an.

[18] A.T. Kunzmann, H.G. Coleman, W.-Y. Huang, C.M. Kitahara, M.M. Cantwell,

S.I. Berndt, Dietary fiber intake and risk of colorectal cancer and incident and recurrent adenoma in the Prostate, Lung, Colorectal, and Ovarian Cancer Screening Trial, Am J Clin Nutr. 102 (2015) 881–890. doi:10.3945/ajcn.115.113282.1.

[19] D.E. Corpet, F. Pierre, How good are rodent models of carcinogenesis in predicting efficacy in humans ? A systematic review and meta-analysis of colon chemoprevention in rats , mice and men, Eur. J. Cancer. 41 (2005) 1911–1922. doi:10.1016/j.ejca.2005.06.006.

[20] M. Perše, A. Cerar, Morphological and molecular alterations in 1,2 dimethylhydrazine and azoxymethane induced colon carcinogenesis in rats, J. Biomed. Biotechnol. 2011 (2011). doi:10.1155/2011/473964.

[21] P.C. Muzzio, E. Cobos, M. Chiriva-Internati, A. Di Ieva, C. Russo, E.E. Frezza, F. Grizzi, Cancer initiation and progression: an unsimplifiable complexity, Theor. Biol. Med. Model. 3 (2006) 1–6. doi:10.1186/1742-4682-3-37.

[22] R.P. Bird, C.K. Good, The significance of aberrant crypt foci in understanding the pathogenesis of colon cancer, Toxicol. Lett. 113 (2000) 395–402.

[23] J.P. Fabi, B.R. Cordenunsi, G.P. de Ma. Barreto, A.Z. Mercadante, F.M. Lajolo, J.R.O. Do Nascimento, Papaya Fruit Ripening: Response to Ethylene and 1-Methylcyclopropene (1-MCP), J. Food Agric. Food Chem. 55 (2007) 6118–6123.

[24] M.J. Wargovich, A. Jimenez, K. McKee, V.E. Steele, M. Velasco, J. Woods, R. Price, K. Gray, G.J. Kelloff, Efficacy of potential chemopreventive agents on rat colon aberrant crypt formation and progression, Carcinogenesis. 21 (2000) 1149–1155. doi:10.1093/carcin/21.6.1149.

[25] A. Vieira, R. Heidor, M.T. Cardozo, C. Scolastici, E. Purgatto, T.M. Shiga, L.F. Barbisan, T.P. Ong, F.S. Moreno, Efficacy of geraniol but not of β-ionone or their combination for the chemoprevention of rat colon carcinogenesis, Brazilian J. Med. Biol. Res. 44 (2011) 538–545. doi:10.1590/S0100-879X2011007500037.

[26] R.P. Bird, Observation and Quantification of Aberrant Crypts in the Murine Colon Treated With a Colon Carcinogen: Preliminary findings, Cancer Lett. 37 (1987) 147–151.

[27] T.M. Shiga, J.P. Fabi, J.R.O. do Nascimento, C.L.D.O. Petkowicz, L.C. Vriesmann, F.M. Lajolo, B.R. Cordenunsi, Changes in cell wall composition associated to the softening of ripening papaya: evidence of extensive solubilization of large molecular mass galactouronides, J. Agric. Food Chem. 57 (2009) 7064–71.

doi:10.1021/jf900073b.

[28] S.B.R. do Prado, G.R.C. Santos, P.A.S. Mourão, J.P. Fabi, Chelate-soluble pectin fraction from papaya pulp interacts with galectin-3 and inhibits colon cancer cell proliferation, Int. J. Biol. Macromol. 126 (2019) 170–178. doi:https://doi.org/10.1016/j.ijbiomac.2018.12.191.

[29] L. Tian, J. Scholte, K. Borewicz, B. van den Bogert, H. Smidt, A.J.W. Scheurink, H. Gruppen, H.A. Schols, Effects of pectin supplementation on the fermentation patterns of different structural carbohydrates in rats, Mol. Nutr. Food Res. 60 (2016) 2256–2266. doi:10.1002/mnfr.201600149.

[30] G.D. of M.I. the D. of P. in the I.T. of R. and I.V. 1 Dongowski, A. Lorenz, The Degree of Methylation Influences the Degradation of Pectin in the Intestinal Tract of Rats and In Vitro, Nutr. Metab. (2002) 1935–1944.

[31] S.U. Nurdin, R.K. Le Leu, A. Aburto-Medina, G.P. Young, J.C.R. Stangoulis, A.S. Ball, C.A. Abbott, Effects of dietary fibre from the traditional Indonesian food, green cincau (Premna oblongifolia merr.) on preneoplastic lesions and short chain fatty acid production in an azoxymethane rat model of colon cancer, Int. J. Mol. Sci. 19 (2018) 1–18. doi:10.3390/ijms19092593.

[32] K. Ohno, S. Narushima, S. Takeuchi, K. Itoh, T. Mitsuoka, H. Nakayama, T. Itoh, K. Hioki, T. Nomura, Inhibitory effect of apple pectin and culture condensate of Bifidobacterium longum on colorectal tumors induced by 1,2-dimethylhydrazine in transgenic mice harboring human prototype c-Ha-ras genes., Exp. Anim. 49 (2000) 305–7. http://www.ncbi.nlm.nih.gov/pubmed/11109558.

[33] H. Ohkami, K. Tazawa, I. Yamashita, T. Shimizu, K. Murai, K. Kobashi, M. Fujimaki, Effects of apple pectin on fecal bacterial enzymes in Azoxymethane-induced Rat Colon Carcinogenesis, Japanese J. Cancer Res. 86 (1995) 523–529.

[34] M. Verghese, D.R. Rao, C.B. Chawan, L.L. Williams, L. Shackelford, Dietary inulin suppresses azoxymethane-induced aberrant crypt foci and colon tumors at the promotion stage in young Fisher 344 rats, J Nutr. 132 (2002) 2809–2813. http://www.ncbi.nlm.nih.gov/entrez/query.fcgi?cmd=Retrieve&db=PubMed&dopt=Citation&list_uids=12221250.

[35] T. Pattananandecha, S. Sirilun, Y. Duangjitcharoen, B.S. Sivamaruthi, P. Suwannalert, S. Peerajan, C. Chaiyasut, Hydrolysed inulin alleviates the azoxymethane-induced preneoplastic aberrant crypt foci by altering selected intestinal microbiota in Sprague–Dawley rats, Pharm. Biol. 54 (2016) 1596–1605.

doi:10.3109/13880209.2015.1110597.

[36] G.F. Vergara-Castañeda, H.A.; Guevara-González, R.G.; Guevara-Olvera, B.L.; Oomah, B.D.; Loarca-Piña, Non-digestible fraction of beans (Phaseolus vulgaris L.) modulates signalling pathway genes at an early stage of colon cancer in Sprague-Dawley rats., Br. J. Nutr. 108 Suppl (2012) S145-54. doi:10.1017/S0007114512000785.

[37] A.A. Feregrino-Perez, C. Pi??ol-Felis, X. Gomez-Arbones, R.G. Guevara-Gonz??lez, R. Campos-Vega, J. Acosta-Gallegos, G. Loarca-Pi??a, A Non-digestible Fraction of the Common Bean (Phaseolus vulgaris L.) Induces Cell Cycle Arrest and Apoptosis During Early Carcinogenesis, Plant Foods Hum. Nutr. (2014) 248–254. doi:10.1007/s11130-014-0428-7.

[38] L. Lahouar, P. Pochart, H. Ben Salem, M. El Felah, M. Mokni, F. Magne, I. Mangin, A. Suau, E. Pereira, M. Hammami, L. Achour, Effect of dietary fibre of barley variety ‘Rihane’ on azoxymethane-induced aberrant crypt foci development and on colonic microbiota diversity in rats, Br. J. Nutr. (2012) 1–9. doi:10.1017/S0007114512000219.

[39] B. Moen, K. Henjum, I. M??ge, S.H. Knutsen, I. Rud, R.B. Hetland, J.E. Paulsen, Effect of dietary fibers on cecal microbiota and intestinal tumorigenesis in azoxymethane treated A/J Min/+ mice, PLoS One. 11 (2016) 1–20. doi:10.1371/journal.pone.0155402.

Concluding remarks and perspectives

Dietary fibers consumption has been related to improving some health effects, as they can increase the stool bulk by gel-forming properties, water holding capacity while having the ability of bind to other organic compounds thus decreasing the cholesterol reabsorption and helping to control the glycemic response. Besides the physical properties, the dietary fibers are also fermented by the intestinal microbiota helping to modulate the bacteria diversity and increasing the beneficial metabolites production, such as short chain fatty acids. The effects of the dietary fibers by the direct interaction with the epithelial intestinal cells or with the immune cells can also occur (**Chapter 3**). However, most of these effects are dependent on the polysaccharide structure with a lack in understanding this structure–function relationship between dietary fibers and the human health effects. In this work, we contribute to increase the knowledge about the fruit dietary fibers, mainly derived from papayas obtained in different ripening time points. Our innovated idea was to try to establish the relationship between the papaya changes in the cell wall during the ripening phenomenon with the structural–dependent effects on cancer cells, on cells pattern recognition receptors, on *in vitro* fermentation, and on *in vivo* experiment. As part of this thesis, we also contributed to the dietary fiber field studying the modified citrus pectin, which was separated into different molecular sizes and their structure–dependent effects on cancer cells were investigated (**Chapter 4-part I)**.

In the **Chapters 1 and 2** we concluded that the fast softening of papaya fruit during ripening is a process caused by a coordinated action of several enzymes in the polysaccharide structure that forms the plant cell wall. The pectinases, mainly endopolygalacturonases and galactanases, were responsible for the mobilization of high molecular size pectins from less soluble to more soluble in water fractions. The solubilized pectins were especially the pectins tightly bound to cellulose/hemicellulose and to each other by calcium bridges.

The dietary fibers from unripe to ripe papayas were extracted and the pectins were directly tested on cancer cells. In **Chapter 4-part II**, we stated that the papaya pectin structure is indeed affected by the coordinated action of several pectinolytic enzymes during fruit ripening. The pectin derived from intermediate papaya ripening time point increased the anti-cancer activity when compared to pectin isolated from other ripening stages. This intermediate papaya ripening time point pectin had smaller homogalacturonans

chains, smaller type I rhamnogalacturonans side-groups, and type II arabinogalactans associated with type I rhamnogalacturonans. The anti-cancer different mechanisms of cell death and migration were dependent on both the dietary fiber structure and the cancer cells mutation. Similar experiments were conducted to the very known pectin – the thermally modified citrus pectin – on **Chapter 4-part I**. The modified citrus pectin fractionated by molecular size resulted in diverse effects on cancer cell proliferation, migration, and aggregation. Those effects were size–, structure–, and cell line–dependent. The smaller sizes showed the strongly anti-cancer effects, and structurally one of these molecules had an enrichment of type I arabinogalactans and another had both fewer branched structures (type I rhamnogalacturonans and type I arabinogalactans) and more de-esterified homogalacturonans oligomers.

The investigation of the papaya pectin interaction with pattern recognition receptors showed in **Chapter 5** suggests that pectin fractions from ripe papayas that have higher degree of esterification and smaller chains, interact and activate all the studied TLR (TLR2, TLR3, TLR4, TLR5 and TLR9). Pectin from unripe papayas that have lower degree of esterification and longer homogalacturonan chains interact with TLR3 and TLR9 in an irreversible way blocking the agonist activation. One more time, it was concluded that the ripening process altered the pectin structures thus altering some biological effects. Besides the water-soluble fraction of the papaya dietary fiber, it was investigated the chelate-soluble fraction, if one could argue during papaya consumption, all fractions of the plant cell wall will be ingested. The chelate fraction is marked for being formed by pectin tightly bound to each other by "egg-boxes" resulted from calcium chelation. In **Chapter 6**, the chelate-soluble fraction obtained from an intermediate papaya ripening time point showed the ability to bind the pro-metastatic protein galectin-3 and to inhibit the colon cancer cell lines proliferation, probably in a galectin-3 dependent and independent way. This chelate-soluble fraction obtained from intermediate papaya ripening had a lower molecular size, and probably the more exposed ramifications could have facilitated the structural interaction with both galectin-3 and cancer cells.

So far, the more soluble dietary fiber from papaya pulp was related to the direct effects to cancer cells, to galectin-3 inhibition and to cells expressing specific pattern recognition receptors. These effects were mainly dependent of the dietary fiber structures and of the papayas ripening stages. The main fraction that presented the best biological

activity was the pectin fraction, and despite the fact the water soluble and the chelate soluble fractions were studied, there might be other fractions that could have some biological effects after being altered by the intestinal microbiota. These fractions include the insoluble pectin (the ones cross-linked to hemicelluloses and to the cellulose microfibrils) and the hemicellulose and cellulose fractions, themselves. The total unripe and ripe papaya dietary fibers were used as substrate for a human colonic *in vitro* fermentation described in **Chapter 7**. The total dietary fibers from ripe papaya was degraded faster than the dietary fibers from the unripe papaya due to the probable easier accessibility of bacteria to higher amounts of soluble polysaccharides with lower molecular weight from the ripe papaya dietary fibers. Besides the differences on carbohydrate utilization by fermentation and bacteria profile, the production of SCFA was the same for both unripe and ripe papaya dietary fibers, but both being higher than lactulose and apple pectin, two standard substances of colonic fermentation. The papaya dietary fibers were also incorporated in AIN-93G chow to evaluate their consumption by rats that were chemically induced to develop pre-neoplastic lesions in the colon (**Chapter 8**). The animals fed with dietary fibers from ripe papayas showed a significantly inhibition in aberrant crypt foci development, mainly localized at the more proximal colon region (near to cecum). Since during the papaya ripening the polygalacturonases enzymes are strongly acting and degrading the fruit cell wall, the main changes in papaya dietary fibers structure is related to pectin solubilization. Thus, the higher quantities of soluble fibers (mainly the pectins) may facilitate the bacteria accessibility increasing the fermentation and could also have some effects acting directly with the intestinal epithelial cells.

Therefore, in this thesis we determined the main changes in papaya cell wall during the ripening, the structural characterization of papaya dietary fibers and the distinct biological effects that are structural–ripening–dependent. During papaya ripening, profound structural changes, mainly in pectin structure, occur leading to different pectin structures that presented differential biological effects. The changes in the structure of the papaya pectin driven by natural ripening provide promising clues regarding the structures of bioactive fruit compounds, especially bioactive polysaccharides that are found in fleshy fruit. Besides that, the results of this thesis could be used as basis to create new and cost-effective approaches to extract and to create pectins with desired structural and biological features.

Further studies are needed to standardize a high-throughput method for the dietary fibers optimal structure isolation, in which structures could have specific target effects in specific groups or for generical beneficial effects for the population. The screening of optimal dietary fibers structure can be done using cell-based assay, using epithelial, immune and transformed cells to study the specific receptor structure interaction. More studies in animals and in humans should be done, in order to be able to identify and pinpoint how the dietary fiber structures influence human heath, by evaluating for example, the gut microbiota, the stimuli of specific immune responses and whether it can improve intestinal barrier function. In this way, it could be possible to select the dietary fiber structures to specific cases allowing a tailored nutrition products development and/or specific food source recommendation. Furthermore, the dietary fiber daily recommendation should be restructured based on different dietary fibers structures, since the effects of its consumption could be completely different.

Appendices

UNIVERSIDADE DE SÃO PAULO

FACULDADE DE CIÊNCIAS FARMACÊUTICAS
Comissão de Ética no Uso de Animais - CEUA

CEUA/FCF 44.**2017-P543**

CERTIFICADO

Certificamos que a proposta intitulada **Efeito da pectina de mamões no tratamento de células de câncer colorretal e em modelo in vivo de carcinogênese**, registrada com o nº **543**, sob a responsabilidade do(a) pesquisador(a) **Samira Bernardino Ramos do Prado**, sob orientação do(a) **Prof. Dr. João Paulo Fabi** – que envolve produção ou manutenção ou utilização de animais pertencentes ao filo Chordata, subfilo Vertebrata (exceto humanos), para fins de pesquisa científica – encontra-se de acordo com os preceitos da Lei Federal nº 11.794, de 8 de outubro de 2008, do Decreto Federal nº 6.899, de 15 de julho de 2009, e das normas editadas pelo Conselho Nacional de Controle de Experimentação Animal (CONCEA), e foi aprovada pela Comissão de Ética no Uso de Animais (CEUA) da Faculdade de Ciências Farmacêuticas da Universidade de São Paulo (FCF/USP), em reunião de **04 de agosto de 2017**.

Finalidade	Pesquisa Científica
Vigência da autorização	04/08/2017 a 31/12/2019
Espécie/linhagem/raça	*Rato / Wistar*
Número de animais	28
Peso/Idade	100g; 6 semanas
Sexo	Macho
Origem	Biotério - USP

Conforme a legislação vigente, deverá ser apresentado, no encerramento do projeto de pesquisa, o respectivo **relatório final**.

São Paulo, 04 de agosto de 2017.

Profa. Dra. Neuza Mariko Aymoto Hassimotto
Vice-Coordenadora da CEUA/FCF/USP

Av. Prof. Lineu Prestes, 580, Bloco 13 A, Cidade Universitária, CEP 05508-900, São Paulo, SP
Telefone: (11) 3091 3622 - e-mail: ceuafcf@usp.br

PARECER CONSUBSTANCIADO DO CEP

DADOS DO PROJETO DE PESQUISA

Título da Pesquisa: Fermentação in vitro das pectinas extraídas de mamões
Pesquisador: JOÃO PAULO FABI
Área Temática:
Versão: 1
CAAE: 43129115.7.0000.0067
Instituição Proponente: Faculdade de Ciências Farmacêuticas da Universidade de São Paulo
Patrocinador Principal: Financiamento Próprio

DADOS DO PARECER

Número do Parecer: 1.089.446
Data da Relatoria: 27/04/2015

Apresentação do Projeto:
O surgimento de doenças crônicas não transmissíveis, como o câncer, pode ser influenciado por hábitos pouco saudáveis como uma alimentação com baixo consumo de frutas. A ingestão de fibras alimentares solúveis presentes nas frutas, com destaque para as pectinas, pode contribuir para uma alteração desse panorama. Dentre os vários efeitos benéficos dessa ingestão, atualmente destacam-se a diminuição da incidência do
surgimento e da evolução (metástase) do câncer. Quando as pectinas são metabolizadas pela microbiota intestinal (fermentação colônica), os metabólitos produzidos podem inibir determinados mecanismos de surgimento do câncer. Devido ao fato do mamão papaia ser um fruto carnoso, com grandes quantidades de pectinas solúveis ricas em galactanos, o objetivo do presente trabalho é avaliar os efeitos biológicos das pectinas de mamão extraídas em diferentes tempos de amadurecimento na fermentação colônica in vitro e seus metabólitos tem efeito contra células de câncer. Dessa forma, os resultados obtidos poderão contribuir para o estabelecimento de uma relação entre as transformações bioquímicas das pectinas de mamões decorrentes do amadurecimento e os prováveis efeitos biológicos de sua ingestão, podendo servir de auxílio para o incentivo do consumo dessa fruta ou para o desenvolvimento de alimentos funcionais derivados das pectinas de frutas.

Endereço: Av. Prof. Lineu Prestes, 580, Bloco 13A, sala 112
Bairro: Butantã **CEP:** 05.508-000
UF: SP **Município:** SAO PAULO
Telefone: (11)3091-3622 **Fax:** (11)3031-8986 **E-mail:** cepfcf@usp.br

Objetivo da Pesquisa:

Avaliação dos efeitos biológicos do tratamento de células de câncer colorretal com os metabólitos resultantes da fermentação colônica in vitro das fibras alimentares de mamões verdes e maduros.

Avaliação dos Riscos e Benefícios:

Riscos mínimos, serão fornecidas amostras de fezes, portanto material obtido de forma não invasiva.

Benefícios: Trará maior conhecimento sobre possível ação de componentes de frutas na redução do risco de câncer retal.

Comentários e Considerações sobre a Pesquisa:

A pesquisa pretende demonstrar que alguns componentes presentes em frutos poderiam contribuir para a redução dos riscos de DCNT. Está muito bem elaborada, e certamente os resultados serão muito interessantes. Uma vez comprovada a hipótese poderá trazer ganhos para a população.

Considerações sobre os Termos de apresentação obrigatória:

Adequada.

Recomendações:

Sem recomendações.

Conclusões ou Pendências e Lista de Inadequações:

Não há pendências.

Situação do Parecer:

Aprovado

Necessita Apreciação da CONEP:

Não

Considerações Finais a critério do CEP:

Este CEP entende que o projeto pode ser aprovado.

SAO PAULO, 01 de Junho de 2015

Assinado por:
Mauricio Yonamine
(Coordenador)

Endereço: Av. Prof. Lineu Prestes, 580, Bloco 13A, sala 112
Bairro: Butantã **CEP:** 05.508-000
UF: SP **Município:** SAO PAULO
Telefone: (11)3091-3622 **Fax:** (11)3031-8986 **E-mail:** cepfcf@usp.br

INSTITUTO NACIONAL DA PROPRIEDADE INDUSTRIAL

09/01/2019 870190002478 12:05

29409161812680421

Outras petições

Número do Processo: BR 10 2018 074786 0

Dados do Depositante (71)

Depositante 1 de 1

Nome ou Razão Social: UNIVERSIDADE DE SÃO PAULO - USP
Tipo de Pessoa: Pessoa Jurídica
CPF/CNPJ: 63025530000104
Nacionalidade: Brasileira
Qualificação Jurídica: Instituição de Ensino e Pesquisa
Endereço: Rua da Reitoria, 374 - Butantã
Cidade: São Paulo
Estado: SP
CEP: 05508220
País: Brasil
Telefone: (11) 3091.4474
Fax:
Email: pidireto@usp.br

Referência Petição

Pedido : BR102018074786-0

Documentos anexados

Tipo Anexo	Nome
Autorizações dos inventores	Autorizações inventores.pdf
Declaração de divulgação	Declaração divulgação Pectina de mamões.pdf
Esclarecimento	Esclarecimento complemento documentos BR 10 2018 074786-0.pdf
Comprovante de pagamento	GRU e comprovante complemento.pdf

PETICIONAMENTO ELETRÔNICO

Esta solicitação foi enviada pelo sistema Peticionamento Eletrônico em 09/01/2019 às 12:05, Petição 870190002478

Declaração de veracidade

☑ Declaro, sob as penas da lei, que todas as informações acima prestadas são completas e verdadeiras.

Janus - Sistema Administrativo da Pós-Graduação

Universidade de São Paulo
Faculdade de Ciências Farmacêuticas
Documento sem validade oficial

FICHA DO ALUNO

9131 - 8213944/1 - Samira Bernardino Ramos do Prado

Email:	samiraprado@usp.br
Data de Nascimento:	17/07/1990
Cédula de Identidade:	RG - 8.972.733-2 - PR
Local de Nascimento:	Estado do Paraná
Nacionalidade:	Brasileira
Graduação:	Bacharel em Nutrição - Centro Universitário de Maringá - Paraná - Brasil - 2012
Mestrado:	Mestra em Ciências - Área: Nutrição Experimental - Faculdade de Ciências Farmacêuticas - Universidade de São Paulo - São Paulo - Brasil - 2014

Curso:	Doutorado
Programa:	Ciência dos Alimentos
Área:	Bromatologia
Data de Matrícula:	28/11/2014
Início da Contagem de Prazo:	28/11/2014
Data Limite para o Depósito:	28/03/2019
Orientador:	Prof(a). Dr(a). João Paulo Fabi - 28/11/2014 até o presente. Email: jpfabi@usp.br
Proficiência em Línguas:	Inglês, Aprovado em 28/11/2014
Prorrogação(ões):	120 dias Período de 28/11/2018 até 28/03/2019
Data de Aprovação no Exame de Qualificação:	Aprovado em 16/12/2016
Estágio no Exterior:	Universitair Medisch Centrum Groningen, Holanda - Período de 01/11/2017 até 31/01/2018
Data do Depósito do Trabalho:	
Título do Trabalho:	
Data Máxima para Aprovação da Banca:	
Data de Aprovação da Banca:	
Data Máxima para Defesa:	
Data da Defesa:	
Resultado da Defesa:	
Histórico de Ocorrências:	Primeira Matrícula em 28/11/2014 Prorrogação em 29/10/2018

Aluno matriculado no Regimento da Pós-Graduação USP (Resolução nº 6542 em vigor de 20/04/2013 até 28/03/2018).
Última ocorrência: Matrícula de Acompanhamento em 04/02/2019
Impresso em: 16/03/2019 22:18:58

Janus - Sistema Administrativo da Pós-Graduação

Universidade de São Paulo
Faculdade de Ciências Farmacêuticas
Documento sem validade oficial

FICHA DO ALUNO

9131 - 8213944/1 - Samira Bernardino Ramos do Prado

Sigla	Nome da Disciplina	Início	Término	Carga Horária	Cred.	Freq.	Conc.	Exc.	Situação
FBA5899-2/4	Biodisponibilidade de Nutrientes e de Substâncias Bioativas em Alimentos e Dietas	02/03/2015	12/04/2015	90	6	100	A	N	Concluída
FBT5700-3/2	Preparo de Artigos Científicos na Área de Tecnologia Bioquímico-Farmacêutica	08/05/2015	09/07/2015	90	6	100	A	N	Concluída
FBC5734-3/1	Aplicações da Citometria de Fluxo em Modelos Experimentais	03/08/2015	09/08/2015	30	2	100	A	N	Concluída
FBC5719-3/2	Trato Gastrointestinal: Imunomodulação da Colonização e Infecção Bacteriana	10/08/2015	22/11/2015	90	6	93	A	N	Concluída
Atividade do Programa	Participou da Etapa de Estágio Supervisionado em Docência do Programa de Aperfeiçoamento de Ensino junto à Disciplina FBA0413 Química de Alimentos, ministrada aos alunos de graduação do curso de Farmácia e Bioquímica da Faculdade de Ciências Farmacêuticas da Universidade de São Paulo (1)	01/02/2016	30/06/2016	-	3	-	-	-	-
Atividade do Programa	Trabalho Publicado no periódico Frontiers in Plant Science, com o trabalho intitulado: "Papaya Cell Walls: Release of Long Chains Galacturonans Derived from Insoluble Fractions during Postharvest Fruit Ripening", páginas 7-11, Lausanne, Switzerland - 2016 (2)	27/07/2016	27/07/2016	-	2	-	-	-	-
FBA5712-6/3	Fisiologia da Nutrição I	02/03/2017	12/04/2017	90	6	90	A	N	Concluída
FBA5897-3/2	Nutrigenômica do Câncer	19/02/2018	25/02/2018	30	2	100	A	N	Concluída

	Créditos mínimos exigidos		Créditos obtidos
	Para exame de qualificação	Para depósito de tese	
Disciplinas:	0	20	33
Estágios:			
Total:	0	20	33

Créditos Atribuídos à Tese: 172

Observações:

1) Créditos atribuídos de acordo com o disposto na Portaria GR-3588 e GR-4391 - PAE, de 31.08.09 e aprovados pela Comissão de Pós-Graduação, em Sessão de 07/06/2017.

2) Créditos atribuídos de acordo com o Artigo 64 do Regimento de Pós-Graduação e aprovados pela Comissão de Pós-Graduação, em Sessão de 07/06/2017.

Conceito a partir de 02/01/1997:

A - Excelente, com direito a crédito; B - Bom, com direito a crédito; C - Regular, com direito a crédito; R - Reprovado; T - Transferência.

Um(1) crédito equivale a 15 horas de atividade programada.

Última ocorrência: Matrícula de Acompanhamento em 04/02/2019

Impresso em: 16/03/2019 22:18:58

Samira Bernardino Ramos do Prado

Endereço para acessar este CV: http://lattes.cnpq.br/1233421864475330
Última atualização do currículo em 08/03/2019

Possui graduação em Nutrição pelo Centro Universitário de Maringá - UniCesumar (2008-2011) e Mestrado em Ciência dos Alimentos pela Universidade de São Paulo (USP). Durante o Mestrado estabeleceu novas ferramentas e realizou a avaliação comparativa do perfil nutricional de alimentos processados, bem como propôs a sistematização de alimentos prioritários para atualização de base de dados de composição de alimentos. Atualmente está finalizando o doutorado em Ciência dos Alimentos pela Faculdade de Ciências Farmacêuticas (USP), vinculado ao Food Research Center (FoRC/CEPID/Fapesp) e com período sanduíche na University Medical Center Groningen (UMCG, Holanda). Atualmente investiga a relação estrutura-dependente de fibras alimentares com efeitos benéficos à saúde. **(Texto informado pelo autor)**

Identificação

Nome Samira Bernardino Ramos do Prado
Nome em citações bibliográficas PRADO, S. B. R.;DO PRADO, SAMIRA BERNARDINO RAMOS;PRADO, SAMIRA BERNARDINO RAMOS DO;PRADO, SAMIRA B. R. DO

Endereço

Endereço Profissional Universidade de São Paulo, Faculdade de Ciências Farmacêuticas, Departamento de Alimentos e Nutrição Experimental.
Av. Prof Lineu Prestes
Cidade Universitária
05508-000 - Sao Paulo, SP - Brasil
Telefone: (11) 30913624

Formação acadêmica/titulação

2014 Doutorado em andamento em Ciências dos Alimentos (Conceito CAPES 7).
Universidade de São Paulo, USP, Brasil.
com **período sanduíche** em University Medical Center Groningen (Orientador: Prof. Dr. Paul de Vos).
Título: Estudo dos efeitos do tratamento de células de câncer colorretal com pectinas de mamões e com seus metabólitos resultantes da fermentação in vitro,
Orientador: Prof. Dr. João Paulo Fabi.
Bolsista do(a): Conselho Nacional de Desenvolvimento Científico e Tecnológico, CNPq, Brasil.

2012 - 2014 Mestrado em Ciências dos Alimentos (Conceito CAPES 7).
Universidade de São Paulo, USP, Brasil.
Título: Alimentos processados: avaliação comparativa do perfil nutricional e sistematização do processo de categorização de alimentos prioritários para atualização de bases de dados,Ano de Obtenção: 2014.
Orientador: Prof. Dra. Elizabete Wenzel de Menezes.
Bolsista do(a): Coordenação de Aperfeiçoamento de Pessoal de Nível Superior, CAPES, Brasil.

2008 - 2011 Graduação em Nutrição.
Centro de Ensino Superior de Maringá, CESUMAR, Brasil.
Título: ASPECTOS SOCIOECONÔMICOS, DEMOGRÁFICOS E CONSUMO ALIMENTAR DE IDOSOS PARTICIPANTES DA UNIVERSIDADE ABERTA À TERCEIRA IDADE (UNATI) NA CIDADE DE MARINGÁ PARANÁ.
Orientador: Gersislei Antônia Salado.

2005 - 2007 Ensino Médio (2º grau).
Colégio Santa Cruz, SANTA CRUZ, Brasil.

Atuação Profissional

Universidade de São Paulo, USP, Brasil.

Vínculo institucional
2014 - Atual Vínculo: Bolsista, Enquadramento Funcional: Bolsista GD-CNPq, Carga horária: 40, Regime: Dedicação exclusiva.

Vínculo institucional
2016 - 2016 Vínculo: Bolsista, Enquadramento Funcional: Bolsista PAE/USP, Carga horária: 6

Vínculo institucional
2012 - 2014 Vínculo: Bolsista, Enquadramento Funcional: Bolsista Capes, Carga horária: 40, Regime: Dedicação exclusiva.

Vínculo institucional
2013 - 2013 Vínculo: Bolsista, Enquadramento Funcional: Bolsista PAE/USP, Carga horária: 6

Universidade Estadual de Maringá, UEM, Brasil.

Vínculo institucional
2011 - Atual Vínculo: Estágio, Enquadramento Funcional: Estágio de Iniciação Científica, Carga horária: 12

Centro de Ensino Superior de Maringá, CESUMAR, Brasil.

Vínculo institucional
2009 - Atual Vínculo: Integrante bolsista, Enquadramento Funcional: Integrante, Carga horária: 12

Projetos de extensão

2010 - 2011 CENTRO DE REFERENCIA EM AGRICULTURA URBANA E PERIURBANA
Descrição: Tem o objetivo de promover assistência técnica e extensão rurbana e viabilizar ferramentas necessária para os dos atores envolvidos nos programas de Agricultura Urbana e Periurbana na Região Metropolitana de Maringá-PR alcancem a Segurança Alimentar e Nutricional..
Situação: Em andamento; Natureza: Extensão.
Alunos envolvidos: Graduação: (8) .

Integrantes: Samira Bernardino Ramos do Prado - Integrante / Ednaldo Michellon - Coordenador.
Financiador(es): Ministério do Desenvolvimento Social - Outra.

Outros Projetos

2013 - 2013 DESENVOLVIMENTO DE PRODUTO TIPO SHAKE COM ALTO CONTEÚDO DE AMIDO RESISTENTE
Descrição: Projeto interdisciplinar desenvolvido para "Olimpíadas do Conhecimento" da Universidade de São Paulo, o qual apresentou como objetivo desenvolver uma bebida tipo shake com farinha de banana verde e realizar análise sensorial para verificação da aceitação do produto..
Situação: Concluído; Natureza: Outra.
Alunos envolvidos: Graduação: (4) / Mestrado acadêmico: (5) / Doutorado: (4) .

Integrantes: Samira Bernardino Ramos do Prado - Coordenador / Eliana Bistriche Giuntini - Integrante / Juliana de Almeida Egas Negrini - Integrante / Elizabete Wenzel de Menezes - Integrante / Fabiana Andréa Hoffmann Sardá - Integrante / Carmem Cecília Tadini - Integrante / Ana Carolina da Silva Mouratório - Integrante / Camila Pereira da Mata - Integrante / Fernanda Neres Ribeiro de Lima - Integrante / Gabriela Feltre - Integrante / Gustavo César Dacanal - Integrante / Lílian de Cássia Santos Victorino - Integrante / Lívia Chaguri e Carvalho - Integrante / Luciana Tiemi Caraça - Integrante / Mariana Sanchez Pereira - Integrante / Verônica Pereira Flammia - Integrante.

Áreas de atuação

1. Grande área: Ciências Agrárias / Área: Ciência e Tecnologia de Alimentos / Subárea: Ciência de Alimentos.

Idiomas

Inglês	Compreende Bem, Fala Bem, Lê Bem, Escreve Bem.
Espanhol	Compreende Razoavelmente, Fala Razoavelmente, Lê Razoavelmente, Escreve Razoavelmente.
Português	Compreende Bem, Fala Bem, Lê Bem, Escreve Bem.

Prêmios e títulos

2018	Menção Honrosa em Apresentação de Pôster na categoria de Doutorado, XXIII Semana Farmacêutica de Ciência e Tecnologia, FCF/USP.
2018	1º lugar em apresentação oral na categoria de Doutorado, XXIII Semana Farmacêutica de Ciência e Tecnologia.

Produções

Produção bibliográfica

Artigos completos publicados em periódicos

Ordenar por

Ordem Cronológica ▼

1. ★ **PRADO, SAMIRA BERNARDINO RAMOS DO**; SANTOS, GUSTAVO R.C. ; MOURÃO, PAULO A.S. ; FABI, JOÃO PAULO . Chelate-soluble pectin fraction from papaya pulp interacts with galectin-3 and inhibits colon cancer cell proliferation. INTERNATIONAL JOURNAL OF BIOLOGICAL MACROMOLECULES JCR, v. 126, p. 170-178, 2019.

2. ★ **PRADO, S. B. R.**; SHIGA, TÂNIA MISUZU ; HARAZONO, YOSUKE ; HOGAN, V. A. ; RAZ, AVRAHAM ; CARPITA, NICHOLAS C. ; FABI, JOÃO P. . Migration and proliferation of cancer cells in culture are differentially affected by molecular size of modified citrus pectin. CARBOHYDRATE POLYMERS JCR, p. 141, 2019.

3. ★ **PRADO, SAMIRA BERNARDINO RAMOS DO**; FERREIRA, GABRIELLE FERNANDEZ ; HARAZONO, YOSUKE ; SHIGA, TÂNIA MISUZU ; RAZ, AVRAHAM ; CARPITA, NICHOLAS C. ; FABI, JOÃO PAULO . Ripening-induced chemical modifications of papaya pectin inhibit cancer cell proliferation. Scientific Reports JCR, v. 7, p. 16564, 2017.

4. MENEZES, ELIZABETE WENZEL DE ; GRANDE, Fernanda ; GIUNTINI, ELIANA BISTRICHE ; LOPES, TÁSSIA DO VALE CARDOSO ; DAN, MILANA CARA TANASOV ; **PRADO, SAMIRA BERNARDINO RAMOS DO** ; FRANCO, BERNADETTE DORA GOMBOSSY DE MELO ; CHARRONDIÈRE, U. RUTH ; LAJOLO, FRANCO MARIA . Impact of dietary fiber energy on the calculation of food total energy value in the Brazilian Food Composition Database. Food Chemistry JCR, v. 193, p. 128-133, 2016.

Citações: SCOPUS 5

5. ★ **PRADO, SAMIRA B. R. DO**; MELFI, PAULO R. ; CASTRO-ALVES, VICTOR C. ; BROETTO, SABRINA G. ; ARAÚJO, ELIAS S. ; NASCIMENTO, JOÃO R. O. DO ; FABI, JOÃO P. . Physiological Degradation of Pectin in Papaya Cell Walls: Release of Long Chains Galacturonans Derived from Insoluble Fractions during Postharvest Fruit Ripening. Frontiers in Plant Science JCR, v. 7, p. 1120, 2016.

Citações: WEB OF SCIENCE℠ 17

6. **PRADO, SAMIRA BERNARDINO RAMOS DO**; GIUNTINI, ELIANA BISTRICHE ; GRANDE, Fernanda ; MENEZES, ELIZABETE WENZEL DE . Techniques to evaluate changes in the nutritional profile of food products. Journal of Food Composition and Analysis (Print) JCR, v. 53, p. 1-6, 2016.

Resumos expandidos publicados em anais de congressos

1. Longo, G Z ; GRAVENA, A. A. F. ; **PRADO, S. B. R.** ; GARBUGIO, T. L. S. . PREVALÊNCIA DE ALEITAMENTO MATERNO EXCLUSIVO E SEUS DETERMINANTES EM CRIANÇAS MENORES DE SEIS MESES EM MARINGÁ-PR. In: V MOSTRA INTERNA DE TRABALHOS DE INICIAÇÃO CIENTÍFICA DO CESUMAR, 2009, MARINGÁ. PREVALÊNCIA DE ALEITAMENTO MATERNO EXCLUSIVO E SEUS DETERMINANTES EM CRIANÇAS MENORES DE SEIS MESES EM MARINGÁ-PR, 2009.

Resumos publicados em anais de congressos

1.

PRADO, S. B. R.; GRANDE, F. ; GIUNTINI, E. B. ; NEGRINI, J. A. E. ; MENEZES, E. W. . Variação de energia, fibra alimentar e gordura total no decorrer de 10 anos em alimentos processados. In: 12º Congresso Nacional da Sociedade Brasileira de Alimentação e Nutrição, 2013, Foz do Iguaçú. Variação de energia, fibra alimentar e gordura total no decorrer de 10 anos em alimentos processados, 2013.

2. MENEZES, E. W. ; GRANDE, F. ; GIUNTINI, E. B. ; **PRADO, S. B. R.** ; CORDENUNSI, B. R. ; FRANCO, B. G. M. ; LAJOLO, F. M. ; CHARRONDIERE, Ruth U. . Impacto da energia da fibra alimentar na estimativa do valor energético em base de dados de alimentos. In: 12º Congresso Nacional da Sociedade Brasileira de Alimentação e Nutrição, 2013, Foz do Iguaçú. Impacto da energia da fibra alimentar na estimativa do valor energético em base de dados de alimentos, 2013.
3. **PRADO, S. B. R.**; SOUZA, G. S. ; SARDA, F. A. H. ; GIUNTINI, E. B. ; MENEZES, E. W. . Utilização do Gastrointestinal Symptom Rating Scale na avaliação do funcionamento intestinal após consumo regular de inulina. In: 12º Congresso Nacional da Sociedade Brasileira de Alimentação e Nutrição, 2013, Foz do Iguaçú. Utilização do Gastrointestinal Symptom Rating Scale na avaliação do funcionamento intestinal após consumo regular de inulina, 2013.
4. MENEZES, Elizabete W. ; GIUNTINI, Eliana B. ; **PRADO, S. B. R.** ; FISBERG, R. ; BASTOS, Deborah H. M. ; MARCHIONI, Dirce M. L. ; CHARRONDIERE, Ruth U. ; CORDENUNSI, Beatriz R. ; LAJOLO, Franco M. . UPDATE ON FOOD COMPOSITION DATA: BRASILFOODS AND NAPAN INTEGRATED PROJECT. In: XVI SLAN Congresso Latinoamericano de Nutrición, 2012, La Habana. UPDATE ON FOOD COMPOSITION DATA: BRASILFOODS AND NAPAN INTEGRATED PROJECT, 2012.
5. MENEZES, Elizabete W. ; GIUNTINI, Eliana B. ; MELO, Alexandra T. ; GRANDE, Fernanda ; LOPES, Tássia V. C. ; MAZZINI, Eliana ; **PRADO, S. B. R.** ; LAJOLO, Franco M. . BRASILFOODS REFERENCE ELECTRONIC REGISTER (RER): A TOOL TO FACILITATE COMPILATION OF FOOD COMPOSITION DATA. In: XVI SLAN Congresso Latinoamericano de Nutrición, 2012, La Habana. BRASILFOODS REFERENCE ELECTRONIC REGISTER (RER): A TOOL TO FACILITATE COMPILATION OF FOOD COMPOSITION DATA, 2012.
6. MICHELLON, E. ; GONÇALVES, E. ; **PRADO, S. B. R.** ; SALOMÃO, V. A. . HORTAS ESCOLARES COMO FERRAMENTA PREVENTIVA NA QUALIDADE DE VIDA. In: 9º FÓRUM DE EXTENSÃO E CULTURA UEM, 2011, MARINGÁ. HORTAS ESCOLARES COMO FERRAMENTA PREVENTIVA NA QUALIDADE DE VIDA, 2011.
7. MICHELLON, E. ; **PRADO, S. B. R.** ; SALOMÃO, V. A. . SEGURANÇA ALIMENTAR E NUTRICIONAL EM HORTAS COMUNITÁRIAS NO PONTO DE VISTA DA EDUCAÇÃO NUTRICIONAL. In: I MOSTRA REGIONAL DE TRABALHOS EM AGROECOLOGIA, ECONOMIA SOLIDÁRIA, SEGURANÇA ALIMENTAR E NUTRICIONAL UEM, 2011, MARINGÁ. SEGURANÇA ALIMENTAR E NUTRICIONAL EM HORTAS COMUNITÁRIAS NO PONTO DE VISTA DA EDUCAÇÃO NUTRICIONAL, 2011.
8. MICHELLON, E. ; ROSSI, W. ; **PRADO, S. B. R.** ; SALOMÃO, V. A. . AVALIAÇÃO NUTRICIONAL DE BENEFICIÁRIOS EM HORTAS COMUNITÁRIAS DE MARINGÁ. In: VII MOSTRA DE TRABALHOS CIENTÍFICOS EM AGRONOMIA, 2010, MARINGÁ. AVALIAÇÃO NUTRICIONAL DE BENEFICIÁRIOS EM HORTAS COMUNITÁRIAS DE MARINGÁ, 2010.
9. MICHELLON, E. ; GRAVENA, A. A. F. ; GONÇALVES, E. ; **PRADO, S. B. R.** ; SALOMÃO, V. A. . EDUCAÇÃO NUTRICIONAL PARA PARTICIPANTES DE HORTAS COMUNITÁRIAS NA REGIÃO METROPOLITANA DE MARINGÁ. In: VII MOSTRA DE TRABALHOS CIENTÍFICOS EM AGRONOMIA, 2010, MARINGÁ. EDUCAÇÃO NUTRICIONAL PARA PARTICIPANTES DE HORTAS COMUNITÁRIAS NA REGIÃO METROPOLITANA DE MARINGÁ, 2010.

Apresentações de Trabalho

1. MENEZES, Elizabete W. ; GRANDE, F. ; GIUNTINI, E. B. ; LOPES, Tássia V. C. ; **PRADO, S. B. R.** ; CORDENUNSI, Beatriz R. ; FRANCO, B. G. M. ; CHARRONDIERE, Ruth U. ; LAJOLO, F. M. . Impact of dietary fiber energy on foods composition database. 2013. (Apresentação de Trabalho/Congresso).

Eventos

Participação em eventos, congressos, exposições e feiras

1. Aula Inaugural do PPG Nutrição e Alimentos, Unisinos.O efeito das fibras alimentares na saúde: estudo de caso do mamão papaia. 2018. (Outra).
2. Health Perspectives of Bioactive Non-Disgestible Oligos and Polysaccharides.Structural-dependent effects of dietary fibers in colon cancer. 2018. (Simpósio).
3. I International Symposium on Citrus Bioactive compounds and health benefits. 2018. (Simpósio).
4. I Simpósio do Programa de Pós-Graduação em Ciência dos Alimentos: Ensino e Pesquisa para uma Alimentação Saudável. 2018. (Simpósio).
5. XXIII Semana Farmacêutica de Ciência e Tecnologia.Structure-function relationship between dietary fiber from papayas and their effects on colon cancer development: in vitro and in vivo approaches. 2018. (Simpósio).
6. 23º Simpósio Internacional de Iniciação Científica e Tecnológica da USP - SIICUSP.Avaliador. 2015. (Simpósio).
7. 12º Congresso Nacional da Sociedade Brasileira de Alimentação e Nutrição. Variação de energia, fibra alimentar e gordura total no decorrer de 10 anos em alimentos processados. 2013. (Congresso).

Organização de eventos, congressos, exposições e feiras

1. **PRADO, SAMIRA BERNARDINO RAMOS DO**; FABI, JOÃO P. ; NASCIMENTO, JOÃO R. O. DO ; ONG, Thomas Prates . I Simpósio do Programa de Pós-Graduação em Ciência dos Alimentos: Ensino e Pesquisa para uma Alimentação Saudável. 2018. (Outro).
2. **PRADO, S. B. R.**; CASTRO-ALVES, V. C. ; GOMES, B. L. ; TOBARUELA, E. C. ; H S, G. . I Jornada CiênciAlimenta. 2016. (Outro).

Outras informações relevantes

Representante discente Suplente na Comissão de Pesquisa (CoPesq) da Faculdade de Ciências Farmacêuticas/USP (2015). Representante discente Titular na Comissão Coordenadora do Programa de Pós-Graduação em Ciência dos Alimentos (FCF/USP) (2016-2018).

Página gerada pelo Sistema Currículo Lattes em 24/03/2019 às 15:05:47

Imprimir currículo